

# *Sinocyclocheilus longicornus* (Cypriniformes, Cyprinidae), a new species of microphthalmic hypogean fish from Guizhou, Southwest China

Cheng Xu<sup>1\*</sup>, Tao Luo<sup>2\*</sup>, Jia-Jun Zhou<sup>3,4\*</sup>, Li Wu<sup>1</sup>,  
Xin-Rui Zhao<sup>1</sup>, Hong-Fu Yang<sup>5</sup>, Ning Xiao<sup>6</sup>, Jiang Zhou<sup>1</sup>

**1** School of Karst Science, Guizhou Normal University, Guiyang 550001, Guizhou, China **2** School of Life Sciences, Guizhou Normal University, Guiyang 550025, Guizhou, China **3** Zhejiang Forest Resource Monitoring Center, Hangzhou 310020, Zhejiang, China **4** Zhejiang Forestry Survey Planning and Design Company Limited, Hangzhou 310020, Zhejiang, China **5** Fishery Administration of Qiubei County, Qiubei 663200, Yunnan, China **6** Guiyang Healthcare Vocational University, Guiyang 550081, Guizhou, China

Corresponding author: Jiang Zhou ([zhoujiang@ioz.ac.cn](mailto:zhoujiang@ioz.ac.cn))

Academic editor: Sven Kullander | Received 10 August 2022 | Accepted 12 December 2022 | Published 17 January 2023

<https://zoobank.org/B816E2E2-3841-4433-9CFC-8BF350BEDA97>

**Citation:** Xu C, Luo T, Zhou J-J, Wu L, Zhao X-R, Yang H-F, Xiao N, Zhou J (2023) *Sinocyclocheilus longicornus* (Cypriniformes, Cyprinidae), a new species of microphthalmic hypogean fish from Guizhou, Southwest China. ZooKeys 1141: 1–28. <https://doi.org/10.3897/zookeys.1141.91501>

## Abstract

*Sinocyclocheilus longicornus* **sp. nov.** is described from the Pearl River basin in Hongguo Town, Panzhou City, Guizhou Province, Southwest China. Based on the presence of the long horn-like structure on the back of the head, *Sinocyclocheilus longicornus* **sp. nov.** is assigned to the *Sinocyclocheilus angularis* species group. *Sinocyclocheilus longicornus* **sp. nov.** is distinguished from its congeners by a combination of morphological characters: (1) presence of a single, relatively long horn-like structure on the back of the head; (2) pigmentation absent; (3) reduced eyes; (4) dorsal-fin rays, ii, 7; (5) pectoral-fin rays, i, 13; (6) anal-fin rays, iii, 5; (7) pelvic-fin rays, i, 7; (8) lateral line pores 38–49; (9) gill rakers well developed, nine on first gill arch; and (10) tip of adpressed pelvic fin not reaching anus.

## Keywords

cave fish, morphology, taxonomy, phylogeny

\* These authors contributed equally to this paper.

## Introduction

The golden-line fish genus *Sinocyclocheilus* Fang, 1936, is endemic to China, and is mainly distributed in the karst areas of Southwest China, including Guangxi, Guizhou, Yunnan, and Hubei provinces (Zhao and Zhang 2009; Jiang et al. 2019). The narrow distribution, morphological similarities, and morphological adaptations to cave environments, such as the degeneration or loss of eyes and body scales, have made classification of the genus difficult and often controversial (Chu and Cui 1985; Shan and Yue 1994; Wang et al. 1995; Wang and Chen 1998; Wang et al. 1999; Wang and Chen 2000; Xiao et al. 2005; Mao et al. 2021, 2022; Wen et al. 2022). A phylogenetic study based on the mitochondrial cytochrome b gene (Cyt *b*) showed that all members of *Sinocyclocheilus* clustered as a monophyletic group, divided into four species groups, namely the *S. jii*, *S. angularis*, *S. cyphotergous*, and *S. tingi* groups (Zhao and Zhang 2009). However, phylogenetic studies based on restriction site-associated DNA sequencing and mitochondrial genome reconstruction suggest that the *S. angularis* and *S. cyphotergous* species groups are not monophyletic (Xiang 2014; Liu 2018; Mao et al. 2021, 2022; Wen et al. 2022). *Sinocyclocheilus* comprises 76 valid species, of which 71 species are grouped into five species groups (Table 1).

**Table 1.** List of 76 currently recognized species of the genus *Sinocyclocheilus* endemic to China and references. Recognized species modified from Jiang et al. (2019).

ID	Species	Species group	Province	River	Reference
1	<i>S. altishoulderus</i> (Li & Lan, 1992)	<i>S. angularis</i> group	Guangxi	Hongshuihe River	Li and Lan 1992
2	<i>S. anatrostris</i> Lin & Luo, 1986	<i>S. angularis</i> group	Guangxi	Hongshuihe River	Lin and Luo 1986
3	<i>S. angularis</i> Zheng & Wang, 1990	<i>S. angularis</i> group	Guizhou	Nanpanjiang River	Zheng and Wang 1990
4	<i>S. aquihornes</i> Li & Yang, 2007	<i>S. angularis</i> group	Yunnan	Nanpanjiang River	Li et al. 2007
5	<i>S. bicornutus</i> Wang & Liao, 1997	<i>S. angularis</i> group	Guizhou	Beipanjiang River	Wang and Liao 1997
6	<i>S. brevibarbatus</i> Zhao, Lan & Zhang, 2009	<i>S. angularis</i> group	Guangxi	Hongshuihe River	Zhao et al. 2009
7	<i>S. broadihornes</i> Li & Mao, 2007	<i>S. angularis</i> group	Yunnan	Nanpanjiang River	Li and Mao 2007
8	<i>S. convexiforeheadus</i> Li, Yang & Li, 2017	<i>S. angularis</i> group	Yunnan	Nanpanjiang River	Yang et al. 2017
9	<i>S. hyalinus</i> Chen & Yang, 1994	<i>S. angularis</i> group	Yunnan	Nanpanjiang River	Chen et al. 1994
10	<i>S. juxuensis</i> Li & Lan, 2003	<i>S. angularis</i> group	Guangxi	Hongshuihe River	Li et al. 2003c
11	<i>S. flexuodorsalis</i> Zhu & Zhu, 2012	<i>S. angularis</i> group	Guangxi	Hongshuihe River	Zhu and Zhu 2012
12	<i>S. furcodorsalis</i> Chen, Yang & Lan, 1997	<i>S. angularis</i> group	Guangxi	Hongshuihe River	Chen et al. 1997
13	<i>S. mashanensis</i> Wu, Liao & Li, 2010	<i>S. angularis</i> group	Guangxi	Hongshuihe River	Wu et al. 2010
14	<i>S. rhinocerosus</i> Li & Tao, 1994	<i>S. angularis</i> group	Yunnan	Nanpanjiang River	Li and Tao 1994
15	<i>S. simengensis</i> Li, Wu, Li & Lan, 2018	<i>S. angularis</i> group	Guangxi	Hongshuihe River	Wu et al. 2018
16	<i>S. tianensis</i> Li, Xiao & Luo, 2003	<i>S. angularis</i> group	Guangxi	Hongshuihe River	Li et al. 2003d
17	<i>S. tianlinensis</i> Zhou, Zhang, He & Zhou, 2004	<i>S. angularis</i> group	Guangxi	Nanpanjiang River	Zhou et al. 2004
18	<i>S. tileihornes</i> Mao, Lu & Li, 2003	<i>S. angularis</i> group	Yunnan	Nanpanjiang River	Mao et al. 2003
19	<i>S. zhenfengensis</i> Liu, Deng, Ma, Xiao & Zhou, 2018	<i>S. angularis</i> group	Guizhou	Beipanjiang River	Liu et al. 2018
20	<i>S. anshuiensis</i> Gan, Wu, Wei & Yang, 2013	<i>S. microphthalmus</i> group	Guangxi	Hongshuihe River	Gan et al. 2013
21	<i>S. microphthalmus</i> Li, 1989	<i>S. microphthalmus</i> group	Guangxi	Hongshuihe River	Li 1989
22	<i>S. aluensis</i> Li & Xiao, 2005	<i>S. tingi</i> group	Yunnan	Nanpanjiang River	Li et al. 2005; Zhao and Zhang 2013
23	<i>S. angustiporus</i> Zheng & Xie, 1985	<i>S. tingi</i> group	Guizhou; Yunnan	Beipanjiang River; Nanpanjiang River	Zheng and Xie 1985
24	<i>S. anophthalmus</i> Chen & Chu, 1988	<i>S. tingi</i> group	Yunnan	Nanpanjiang River	Chen et al. 1988a Zhao and Zhang 2009
25	<i>S. grahami</i> (Regan, 1904)	<i>S. tingi</i> group	Yunnan	Jinshajiang River	Regan 1904; Zhao and Zhang 2009

ID	Species	Species group	Province	River	Reference
26	<i>S. guishanensis</i> Li, 2003	<i>S. tingi</i> group	Yunnan	Nanpanjiang River	Li et al. 2003a
27	<i>S. huaningensis</i> Li, 1998	<i>S. tingi</i> group	Yunnan	Nanpanjiang River	Li et al. 1998
28	<i>S. huizeensis</i> Cheng, Pan, Chen, Li, Ma & Yang, 2015	<i>S. tingi</i> group	Yunnan	Niulanjiang River	Cheng et al. 2015
29	<i>S. bannaensis</i> Li, Li & Chen, 2019	<i>S. tingi</i> group	Yunnan	Luosuojiang River	Li et al. 2019
30	<i>S. maculatus</i> Li, 2000	<i>S. tingi</i> group	Yunnan	Nanpanjiang River	Zhao and Zhang 2009
31	<i>S. maitianheensis</i> Li, 1992	<i>S. tingi</i> group	Yunnan	Nanpanjiang River	Li 1992
32	<i>S. malacopterus</i> Chu & Cui, 1985	<i>S. tingi</i> group	Yunnan	Nanpanjiang River	Chu and Cui 1985
33	<i>S. longifinus</i> Li, 1998	<i>S. tingi</i> group	Yunnan	Nanpanjiang River	Li et al. 1998
34	<i>S. longshanensis</i> Li & Wu, 2018	<i>S. tingi</i> group	Yunnan	Nanpanjiang River	Li et al. 2018
35	<i>S. macrocephalus</i> Li, 1985	<i>S. tingi</i> group	Yunnan	Nanpanjiang River	Li 1985
36	<i>S. lateristriatus</i> Li, 1992	<i>S. tingi</i> group	Yunnan	Nanpanjiang River	Li 1992
37	<i>S. purpureus</i> Li, 1985	<i>S. tingi</i> group	Yunnan	Nanpanjiang River	Li 1985
38	<i>S. qiubeiensis</i> Li, 2002	<i>S. tingi</i> group	Yunnan	Nanpanjiang River	Li et al. 2002b
39	<i>S. qujingensis</i> Li, Mao & Lu, 2002	<i>S. tingi</i> group	Yunnan	Nanpanjiang River	Li et al. 2002c
40	<i>S. robustus</i> Chen & Zhao, 1988	<i>S. tingi</i> group	Guizhou	Nanpanjiang River	Chen et al. 1988b
41	<i>S. wumengshanensis</i> Li, Mao, Lu & Yan, 2003	<i>S. tingi</i> group	Yunnan	Niulanjiang River	Li et al. 2003a
42	<i>S. sichouensis</i> Pan, Li, Yang & Chen, 2013	<i>S. tingi</i> group	Yunnan	Panlonghe River	Pan et al. 2013
43	<i>S. tingi</i> Fang, 1936	<i>S. tingi</i> group	Yunnan	Nanpanjiang River	Fang, 1936; Zhao and Zhang 2009
44	<i>S. yangzongensis</i> Chu & Chen, 1977	<i>S. tingi</i> group	Yunnan	Nanpanjiang River	Wu 1977; Zhao and Zhang 2009
45	<i>S. yimenensis</i> Li & Xiao, 2005	<i>S. tingi</i> group	Yunnan	Yuanjiang River	Li et al. 2005
46	<i>S. oxycephalus</i> Li, 1985	<i>S. tingi</i> group	Yunnan	Nanpanjiang River	Li 1985
47	<i>S. brevis</i> Lan & Chen, 1992	<i>S. cyphotergous</i> group	Guangxi	Liujiang River	Chen and Lan 1992
48	<i>S. cyphotergous</i> (Dai, 1988)	<i>S. cyphotergous</i> group	Guizhou	Hongshuihe River	Dai 1988; Huang et al. 2017
49	<i>S. donglanensis</i> Zhao, Watanabe & Zhang, 2006	<i>S. cyphotergous</i> group	Guangxi	Hongshuihe River	Zhao et al. 2006
50	<i>S. dongtangenensis</i> Zhou, Liu & Wang, 2011	<i>S. cyphotergous</i> group	Guizhou	Liujiang River	Zhou et al. 2011
51	<i>S. huanjiangensis</i> Wu, Gan & Li, 2010	<i>S. cyphotergous</i> group	Guangxi	Liujiang River	Wu et al. 2010
52	<i>S. hugeibarbus</i> Li, Ran & Chen, 2003	<i>S. cyphotergous</i> group	Guizhou	Liujiang River	Li et al. 2003b
53	<i>S. gracilicaudatus</i> Zhao & Zhang, 2014	<i>S. cyphotergous</i> group	Guangxi	Liujiang River	Wang et al. 2014
54	<i>S. lingyunensis</i> Li, Xiao & Lu, 2000	<i>S. cyphotergous</i> group	Guangxi	Hongshuihe River	Li et al. 2000
55	<i>S. longibarbus</i> Wang & Chen, 1989	<i>S. cyphotergous</i> group	Guizhou; Guangxi	Liujiang River	Wang and Chen 1989
56	<i>S. luopingensis</i> Li & Tao, 2002	<i>S. cyphotergous</i> group	Yunnan	Nanpanjiang River	Li et al. 2002a
57	<i>S. macrolepis</i> Wang & Chen, 1989	<i>S. cyphotergous</i> group	Guizhou; Guangxi	Liujiang River	Wang and Chen 1989
58	<i>S. macropthalmus</i> Zhang & Zhao, 2001	<i>S. cyphotergous</i> group	Guangxi	Hongshuihe River	Zhang and Zhao 2001
59	<i>S. macroscalus</i> Li, 1992	<i>S. tingi</i> group	Yunnan	Nanpanjiang River	Li 1992
60	<i>S. multipunctatus</i> (Pellegriin, 1931)	<i>S. cyphotergous</i> group	Guizhou; Guangxi	Wujiang River; Liujiang River; Hongshuihe River	Pellegriin 1931; Zhao and Zhang 2009
61	<i>S. punctatus</i> Lan & Yang, 2017	<i>S. cyphotergous</i> group	Guizhou; Guangxi	Liujiang River; Hongshuihe River	Lan et al. 2017
62	<i>S. ronganensis</i> Luo, Huang & Wen, 2016	<i>S. cyphotergous</i> group	Guangxi	Liujiang River	Luo et al. 2016
63	<i>S. xunlensis</i> Lan, Zhan & Zhang, 2004	<i>S. cyphotergous</i> group	Guangxi	Liujiang River	Lan et al. 2004
64	<i>S. yaolanensis</i> Zhou, Li & Hou, 2009	<i>S. cyphotergous</i> group	Guizhou	Liujiang River	Zhou et al. 2009
65	<i>S. yishanensis</i> Li & Lan, 1992	<i>S. cyphotergous</i> group	Guangxi	Liujiang River	Li and Lan 1992
66	<i>S. sanxiaensis</i> Jiang, Li, Yang & Chang, 2019	<i>S. cyphotergous</i> group	Hubei	Yangtze River	Jiang et al. 2019
67	<i>S. brevifinus</i> Li, Li & Maiden, 2014	<i>S. jii</i> group	Guangxi	Hejiang River	Li et al. 2014
68	<i>S. guanyangensis</i> Chen, Peng & Zhang, 2016	<i>S. jii</i> group	Guangxi	Guijiang River	Chen et al. 2016
69	<i>S. guilinensis</i> Ji, 1985	<i>S. jii</i> group	Guangxi	Guijiang River	Zhou 1985; Zhao and Zhang 2009
70	<i>S. huangtianensis</i> Zhu, Zhu & Lan, 2011	<i>S. jii</i> group	Guangxi	Hejiang River	Zhu et al. 2011
71	<i>S. jii</i> Zhang & Dai, 1992	<i>S. jii</i> group	Guangxi	Guijiang River	Zhang and Dai 1992
72	<i>S. gracilis</i> Li & Li, 2014	No assignment	Guangxi	Guijiang River	Li and Li 2014
73	<i>S. pingshanensis</i> Li, Li, Lan & Wu, 2018	No assignment	Guangxi	Liujiang River	Wu et al. 2018
74	<i>S. wenshanensis</i> Li, Yang, Li & Chen, 2018	No assignment	Yunnan	Panlonghe River	Yang et al. 2018
75	<i>S. wui</i> Li & An, 2013	No assignment	Yunnan	Mingyihe River	Li and An 2013
76	<i>S. luolouensis</i> Lan, 2013	No assignment	Guangxi	Hongshuihe River	Lan et al. 2013

Species of *Sinocyclocheilus* have variably developed eyes and horn-like structures on the back of the head. Eye morphology includes normal, microphthalmic, and anophthalmic conditions (Mao et al. 2021). Normal-eyed and microphthalmic species are distributed from eastern Guangxi through southern Guizhou to eastern Yunnan, and eyeless species are mainly distributed in the Hongshuihe river basin in northern Guangxi and the Nanpanjiang river basin in eastern Yunnan (Mao et al. 2021). It may be absent, short, long, or single and forked. The horn-like structure is present mainly in species of the *S. angularis* and *S. microphthalmus* species groups (Zhao and Zhang 2009; Mao et al. 2021; Wen et al. 2022). These horned species are distributed in the Nanpanjiang, Beipanjiang, and Hongshuihe river basins of the upper Pearl River (Fig. 1).

We collected specimens of a horned, scaleless, and unpigmented species of *Sinocyclocheilus* in a completely dark cave in southwestern Guizhou Province in China. Molecular phylogenetic analyses and morphological comparisons showed that these specimens represented an undescribed species of *Sinocyclocheilus*. Here, we provide the formal description of that species as *Sinocyclocheilus longicornus* sp. nov.

## Materials and methods

### Specimen sampling

During a cavefish diversity survey in southern China in May 2021, 32 specimens of the genus *Sinocyclocheilus* were collected in southwestern Guizhou Province. Among

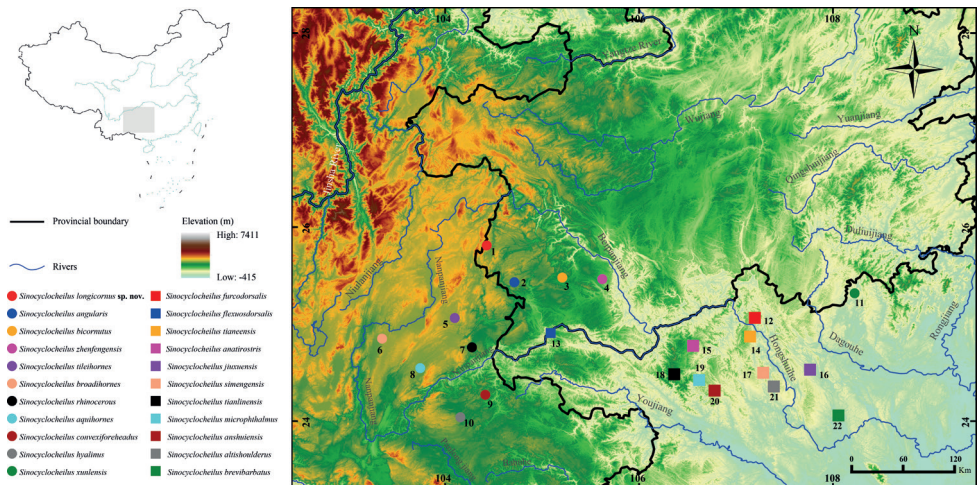


**Figure 1.** Sampling collection localities and distribution of the *Sinocyclocheilus longicornus* sp. nov. and 21 species of the *S. angularis* and *S. microphthalmus* species groups of the genus *Sinocyclocheilus* in Southwest China. 1. Hongguo Town, Panzhou City, Guizhou Province. 2. Baotian Town, Panzhou City, Guizhou Province. 3. Xinlongchang Town, Xingren City, Guizhou Province. 4. Zhexiang Town, Zhenfeng County, Guizhou Province. 7. Huancheng Town, Luoping County, Yunnan Province. 5–6, 8–22 is detailed in Suppl. material 1. The maps are from Standard Map Service website (<http://bzdt.ch.mnr.gov.cn/index.html>).

these, 15 specimens represented an undescribed species, subject of this, paper from Hongguo Town in Panzhou City; seven were *S. angularis* from Baotian Town in Panzhou; two were *S. bicornutus* from Xiashan Town in Xingren City; and eight were *S. zhenfengensis* from Zhexiang Town in Zhenfeng County (Fig. 1). Gill muscle tissues used for molecular analysis were preserved in 95% alcohol at  $-20^{\circ}\text{C}$ . All specimens were fixed in 10% buffered formalin and later transferred to 75% ethanol for long term preservation. All specimens were deposited in Guizhou Normal University, Guiyang City, Guizhou Province, China.

## DNA Extraction, PCR amplification, and sequencing

Genomic DNA was extracted from muscle tissues using a DNA extraction kit from Tiangen Biotech Co., Ltd. (Beijing, China). Because the most used molecular markers in *Sinocyclocheilus* are fragments of the mitochondrial cytochrome b (*Cyt b*) and NADH dehydrogenase subunit 4 (*ND4*) genes, we selected these fragments for amplification and sequencing. Primers used for *Cyt b* were L14737 (5'-CCACCGTTGTTAATTCAACTAC-3') and H15915 (5'-CTCCGATCTCCGGATTA-CAAGAC-3'), following Xiao et al. (2005). Primers used for *ND4* were L11264 (5'-ACGGGACTGAGCGATTAC-3') and H12346 (5'-TCATCATATTGGGT-TAG-3'), following Xiao et al. (2005). PCR amplifications were performed in a 25- $\mu\text{l}$  reaction volume with the following cycling conditions: an initial denaturing step at  $95^{\circ}\text{C}$  for 3 min; 35 cycles of denaturing at  $94^{\circ}\text{C}$  for 50 s, annealing at  $52^{\circ}\text{C}$  (for *Cyt b* and *ND4*) for 1 min and extension at  $72^{\circ}\text{C}$  for 1 min, and a final extension step of  $72^{\circ}\text{C}$  for 10 min. The PCR products were sequenced on an ABI Prism 3730 automated DNA sequencer at Chengdu TSING KE Biological Technology Co. Ltd. (Chengdu, China). All sequences were deposited in GenBank (Table 2).

## Phylogenetic analyses

We used a total of 108 mitochondrial gene sequences for molecular analyses (55 *Cyt b* sequences and 53 *ND4* sequences). Four samples of muscle tissues from *S. Sinocyclocheilus angustiporus*, *S. angularis*, and *Sinocyclocheilus longicornus* sp. nov. were sequenced for two mitochondrial genes and 100 sequences from 45 species of *Sinocyclocheilus* were downloaded from GenBank. Following Wen et al. (2022), we selected *Carassius auratus*, *Cyprinus carpio*, *Garra orientalis*, *Neolissochilus hexagonolepis*, *Schizothorax yunnanensis*, *Barbus barbuis*, *Onychostoma simum*, *Pethia ticto*, *Myxocyprinus asiaticus*, and *Danio rerio* as outgroup (Table 2).

All sequences were assembled and aligned using the MUSCLE (Edgar 2004) module in MEGA 7.0 (Kumar et al. 2016) with default settings. Alignment results were checked by eye. Phylogenetic trees were constructed with both maximum likelihood (ML) and Bayesian inference (BI) methods. The ML was conducted in IQ-TREE 2.0.4 (Nguyen et al. 2015) with 2000 ultrafast bootstrap (UBP) replicates (Hoang et al. 2018) and was performed until a correlation coefficient of at least 0.99 was reached.

The BI was performed in MrBayes 3.2.1 (Ronquist et al. 2012), and the best-fit model was obtained based on the Bayesian information criterion computed with Partition-Finder 2.1.1 (Lanfear et al. 2017). In this analysis, the first, second and third codons of both *Cyt b* and *ND4* genes were defined.

The analysis suggested the best partition scheme for each codon position of *Cyt b* and *ND4* genes. GTR+I+G, HKY+I+G, and TRN+I+G were selected for first, second, and third codons, respectively for both *Cyt b* and *ND4* genes. Two independent runs were conducted in BI analysis, each of which was performed for  $2 \times 10^7$  generations and sampled every 1000 generations. The first 25% of the samples were discarded as burn-in, resulting in a potential scale reduction factor of  $< 0.01$ . Nodes in the trees were considered well supported when Bayesian posterior probabilities (BPP) were  $\geq 0.95$  and the ML ultrafast bootstrap value (UBP) was  $\geq 95\%$ . Uncorrected *p*-distances (1000 replicates) based on *Cyt b* and *ND4* genes were calculated in MEGA 7.0 (Kumar et al. 2016).

**Table 2.** Localities, voucher information, and GenBank numbers for all samples used.

ID	Species	Locality (* type localities)	Voucher number	GenBank accession No.	
				<i>Cyt b</i>	<i>ND4</i>
1	<i>Sinocyclocheilus huizeensis</i>	Leye Town, Huize County, Yunnan, China	hrfri2018046	MH982229	MH982229
2	<i>Sinocyclocheilus qiubeiensis</i>	Songming, Yunnan, China	IHB:2006624	EU366188	EU366182
3	<i>Sinocyclocheilus yimenensis</i>	Yimen, Yunnan, China	IHB:2006646	EU366191	EU366180
4	<i>Sinocyclocheilus grahami</i>	Haikou, Kunming City, Yunnan, China	–	GQ148557	GQ148557
5	<i>Sinocyclocheilus tingi</i>	Fuxian Lake, Yunnan, China	YNUST201406180002	MG323567	MG323567
6	<i>Sinocyclocheilus wumengshanensis</i>	Xuanwei County, Yunnan, China	YNUMS20160817008	MG021442	MG021442
7	<i>Sinocyclocheilus anophthalmus</i>	Jiuxiang, Yiliang County, Yunnan, China	XH3001	AY854715	AY854772
8	<i>Sinocyclocheilus maculatus</i>	Yiliang, Yunnan, China	IHB:2006632	EU366193	EU366183
9	<i>Sinocyclocheilus maitianbeensis</i>	Jiuxiang, Yiliang County, Yunnan, China	XH2301	AY854710	AY854767
10	<i>Sinocyclocheilus lateristriatus</i>	Maojiachong, Zhanyi County, Yunnan	XH1102	AY854703	AY854760
11	<i>Sinocyclocheilus qujingensis</i>	Huize County, Yunnan, China	hrfri2018044	MH937706	MH937706
12	<i>Sinocyclocheilus guishanensis</i>	Guishan, Shilin County, Yunnan, China	XH5401	AY854722	AY854779
13	<i>Sinocyclocheilus huaniangensis</i>	Huaniang County, Yunnan, China	XH3701	AY854718	AY854775
14	<i>Sinocyclocheilus oxycephalus</i>	Heilongtan, Shilin County, Yunnan, China	XH0201	AY854685	AY854742
15	<i>Sinocyclocheilus macrocephalus</i>	Heilongtan, Shilin County, Yunnan	XH0103	AY854683	AY854740
16	<i>Sinocyclocheilus malacopterus</i>	Wulonghe, Shizong County, Yunnan, China	XH0901	AY854697	AY854754
17	<i>Sinocyclocheilus purpureus</i>	Luoping County, Yunnan, China	IHB:2006638	EU366189	EU366178
18	<i>Sinocyclocheilus angustiporus</i>	Xinlongchnag Town, Xingren City, Guizhou, China	GZNU20210322002	MZ636515	MZ636515
19	<i>Sinocyclocheilus yangzongensis</i>	Yangzonghai Lake, Yunnan, China	XH6101	AY854725	AY854782
20	<i>Sinocyclocheilus multipunctatus</i>	Huishui County, Guizhou, China	–	MG026730	MG026730
21	<i>Sinocyclocheilus sanxiaensis</i>	Guojiaba Town, Zigui County, Hubei, China*	KNHM 2019000001	MN106258	–
22	<i>Sinocyclocheilus cyphotergous</i>	Dongdang township, Luodian County, Guizhou, China*	GZNU20150819010	MW024370	MW024370
23	<i>Sinocyclocheilus punctatus</i>	Dongtang Township, Libo County, Guizhou, China	GZNU20150811002	MW014318	MW014318
24	<i>Sinocyclocheilus macrolepis</i>	Nandan County, Guangxi, China	XH8201	AY854729	AY854786
25	<i>Sinocyclocheilus brevis</i>	–	GX0155	MT373105	MW548424
26	<i>Sinocyclocheilus huanjiangensis</i>	–	GX0124	MT373103	MW548429
27	<i>Sinocyclocheilus longibarbatous</i>	Dongtang Township, Libo County, Guizhou, China*	GZNU20150809004	MW024372	MW024372

ID	Species	Locality (* type localities)	Voucher number	GenBank accession No.	
				Cyt <i>b</i>	ND4
28	<i>Sinocyclocheilus xunlensis</i>	Huanjiang, Guangxi, China	IHB:04050268	EU366187	EU366184
29	<i>Sinocyclocheilus donglanensis</i>	Hongshuihe River, Donglan County, Guangxi, China	CA139	AB196440	MW548425
30	<i>Sinocyclocheilus lingyunensis</i>	Shadong, Lingyun County, Guangxi, China	XH0502	AY854691	AY854748
31	<i>Sinocyclocheilus hugeibarbus</i>	Xiaoqikong Town, Libo County, Guizhou, China*	GZNU20150120005	MW014319	MW014319
32	<i>Sinocyclocheilus macrophthalmus</i>	Xiao, Duan County, Guangxi, China	XH8401	AY854733	AY854790
33	<i>Sinocyclocheilus yishanensis</i>	Liujiang County, Guangxi, China	–	MK387704	MK387704
34	<i>Sinocyclocheilus ronganensis</i>	Rong'an County, Guangxi, China	–	KX778473	KX778473
35	<i>Sinocyclocheilus furcadorsalis</i>	Tian'e County, Guangxi, China	–	GU589570	GU589570
36	<i>Sinocyclocheilus tianlinensis</i>	–	GX0087-L17-16	MT373102	MW548431
37	<i>Sinocyclocheilus anatirostris</i>	Leye County, Guangxi, China	XH1901	AY854708	AY854765
38	<i>Sinocyclocheilus anshuiensis</i>	Lingyun County, Guangxi, China	–	KR069120	KR069120
39	<i>Sinocyclocheilus microphthalmus</i>	Lingyun County, Guangxi, China	NNNU201712001	MN145877	MN145877
40	<i>Sinocyclocheilus altishoulderus</i>	Mashan County, Guangxi, China	–	FJ984568	FJ984568
41	<i>Sinocyclocheilus mashanensis</i>	–	GX0026-L18-12	MT373107	MW548430
42	<i>Sinocyclocheilus brevibarbus</i>	–	GX0064-L20-13	MT373106	MW548423
43	<i>Sinocyclocheilus jiuxuensis</i>	Jiuxu Town, Hechi City, Guangxi, China	XH8501	AY854736	AY854793
44	<i>Sinocyclocheilus angularis</i>	Baotian Town, Panzhou City, Guizhou, China*	GZNU20210322001	MZ636514	MZ636514
45	<i>Sinocyclocheilus zhenfengensis</i>	Zhexiang Town, Zhenfeng County, Guizhou, China*	GZNU20150112021	MW014317	MW014317
46	<i>Sinocyclocheilus bicornutus</i>	Xinlongchnag Town, Xingren City, Guizhou, China*	–	KX528071	KX528071
47	<i>Sinocyclocheilus longicornus</i> sp. nov.	Hongguo Town, Panzhou City, Guizhou, China*	GZNU20210503016	MZ634123	MZ634125
48	<i>Sinocyclocheilus longicornus</i> sp. nov.	Hongguo Town, Panzhou City, Guizhou, China*	GZNU20210503017	MZ634124	MZ634126
49	<i>Sinocyclocheilus hyalinus</i>	Alugudong, Luxi County, Yunnan, China	XH4701	AY854721	AY854778
50	<i>Sinocyclocheilus rhinoceros</i>	Luoping County, Yunnan, China	–	KR069119	KR069119
51	<i>Sinocyclocheilus guanyangensis</i>	–	GX0173	MT373108	MW548426
52	<i>Sinocyclocheilus jii</i>	Gongcheng County, Guangxi, China	YNUSJ201308060038	MF100765	MF100765
53	<i>Sinocyclocheilus huangtianensis</i>	–	GX0175	MT373109	MW548428
54	<i>Sinocyclocheilus guilinensis</i>	–	GX0073-L17-2	MT373104	MW548427
55	<i>Carassius auratus</i>	–	–	AB111951	AB111951
56	<i>Cyprinus carpio</i>	–	–	JN105357	JN105357
57	<i>Garra orientalis</i>	–	–	JX290078	JX290078
58	<i>Neolissochilus hexagonolepis</i>	–	–	KU380329	KU380329
59	<i>Schizothorax yunnanensis</i>	–	–	KR780749	KR780749
60	<i>Barbus barbatus</i>	–	–	AB238965	AB238965
61	<i>Onychostoma simum</i>	–	–	KF021233	KF021233
62	<i>Pethia ticto</i>	–	–	AB238969	AB238969
63	<i>Mxocyprinus asiaticus</i>	–	–	AY526869	AY526869
64	<i>Danio rerio</i>	–	–	KM244705	KM244705

## Morphological comparisons

Morphometric data were collected from 44 well-preserved specimens of *Sinocyclocheilus* (Suppl. material 1). A total of 31 measurements were recorded to the nearest 0.1 mm with digital calipers following the protocol of Zhao et al. (2006) and Zhao and Zhang (2009). The following measurements were taken:

<b>TL</b>	total length (from the tip of snout to the end of the caudal-fin);
<b>SL</b>	standard length (from the tip of the upper jaw to the position of the last half-centrum);
<b>BD</b>	body depth (from the insertion of the dorsal fin vertically to the ventral midline);
<b>PL</b>	predorsal length (from the tip of the upper jaw to the origin of the dorsal-fin);
<b>DFL</b>	dorsal-fin depth (from the origin of the dorsal-fin to the tip of the longest ray);
<b>DBL</b>	dorsal-fin length (from the origin to the insertion of dorsal-fin base);
<b>PAL</b>	preanal length (from the tip of the upper jaw to the origin of the anal-fin);
<b>ABL</b>	anal-fin base length (from the origin to the insertion of anal-fin base);
<b>AFL</b>	anal-fin depth (from the origin of the anal-fin to the tip of the longest ray);
<b>PPTL</b>	prepectoral length (from the tip of the upper jaw to the base of anterior pectoral-fin ray);
<b>PTBL</b>	pectoral-fin base length (from the anterior to posterior end of pectoral-fin base);
<b>PTFL</b>	pectoral-fin length (from the base of the first pectoral-fin ray to the tip of the longest ray);
<b>PPVL</b>	prepelvic length (from the tip of the upper jaw to the base of the first pelvic-fin ray);
<b>PVBL</b>	pelvic-fin base length (from the anterior to the posterior end of the pelvic-fin base);
<b>PVFL</b>	pelvic-fin length (from the base of the first pelvic-fin ray to the tip of the longest ray);
<b>CPL</b>	caudal peduncle length (from the anal-fin insertion to the position of the last centrum);
<b>CPD</b>	caudal peduncle depth (depth at the narrowest part of the caudal peduncle);
<b>HL</b>	head length (from the tip of the upper jaw to the posteriormost point of the operculum);
<b>HD</b>	head depth at nape;
<b>HW</b>	head width (widest distance between the two gill covers);
<b>SNL</b>	snout length (from tip of snout to the anterior corner of the eye);
<b>ED</b>	eye diameter (diameter of the exposed portion of the eyeball);
<b>IOD</b>	interorbital distance (minimum distance between the eyes);
<b>IPND</b>	prenostril distance (the tip of the upper jaw to the anterior margin of the anterior nostril);
<b>POND</b>	distance between posterior nostrils (the shortest distance between posterior nostrils);
<b>UJL</b>	upper jaw length (from the tip of the upper jaw (the symphysis of the pre-maxilla) to the corner of the mouth);
<b>LJL</b>	lower jaw length (from the symphysis of the dentary to the corner of the mouth);
<b>MW</b>	mouth width (the distance between the two corners of the mouth);
<b>RBL</b>	rostral barbel length;
<b>MBL</b>	maxillary barbel length;
<b>FHL</b>	forehead horn length;
<b>PPFVL</b>	distance from the pectoral-fin insertion to the ventral-fin origin; and
<b>PVAFL</b>	distance from the insertion of the pelvic fin to the origin of the anal-fin.

We compared the morphological characters of the new species with literature data for 21 other species in the *S. angularis* and *S. microphthalmus* species groups (Table 3). We also examined the type and/or materials from the type-localities of *S. angularis*, *S. bicornutus*, *S. hyalinus*, *S. rhinoceros*, and *S. zhenfengensis* (Appendix 1). Principal component analyses (PCAs) of size-corrected measurements and simple bivariate scatterplots were used to explore and characterize the morphometric differences between the new species and *S. rhinoceros* and *S. hyalinus*. Mann–Whitney *U* tests were used to determine the significance of differences in morphometric characters between the new species and similar species, i.e., *S. angularis*, *S. bicornutus*, and *S. rhinoceros*. All statistical analyses were performed using SPSS 21.0 (SPSS, Inc., Chicago, IL, USA), and differences were considered statistically significant at  $P < 0.05$ . PCAs of morphological data were performed after logarithmic transformation and under conditions of no rotation. In addition, as reported by other researchers (Parsons and Jones 2000; Polaszek et al. 2010), canonical discriminant analysis (CDA, George and Paul 2010) was used to classify individuals into different groups, where *a priori* membership was determined based on specimens belonging to different species. All pre-processing of morphological data was performed in Microsoft Excel (Microsoft Corporation 2016).

## Results

### Phylogenetic analyses and genetic divergence

ML and BI phylogenies were constructed based on two concatenated mitochondrial gene sequences, including 1140 bp Cyt *b* and 1380 bp *ND4*. The ML and the BI phylogenetic trees showed identical topology (Fig. 2). The monophyly of the genus *Sinocyclocheilus* was strongly supported by both phylogenetic analyses but the monophyly of the *S. angularis* and *S. cyphotergous* species groups was rejected (Fig. 2). In both analyses, the *S. longicornus* sp. nov. formed a highly supported clade (0.99 in BI and 96% in ML) with *S. hyalinus* and *S. rhinoceros*.

The smallest *p*-distances between *S. longicornus* sp. nov. and other species of *Sinocyclocheilus* were 6.0% in Cyt *b* (with *S. rhinoceros*) and 5.6% in *ND4* (with *S. bicornutus*). These levels of divergence were similar to those between pairs of other recognized species. For example, the Cyt *b* *p*-distance was 2.4% between *S. anatirostris* and *S. angularis*, 3.4% between *S. bicornutus* and *S. brevibarbatus*, while the *ND4* *p*-distance was 2.7% between *S. anatirostris* and *S. angularis* and 2.6% between *S. bicornutus* and *S. anatirostris* (Suppl. materials 2, 3).

### Morphological analyses

Mann–Whitney *U* tests showed that the *Sinocyclocheilus longicornus* sp. nov. differed from *S. angularis*, *S. bicornutus*, and *S. rhinoceros* in several morphological characters (Table 4). This was specially most obvious comparing *S. longicornus* sp. nov. and *S. rhinoceros*, in which 87% of the morphometric characters were significantly different ( $p = 0.00–0.03$ ) (Table 3).

**Table 3.** Comparison of the diagnostic features of the new species described here with those selected for the 21 species of the *S. angularis* and *S. microphthalmus* species groups within the genus *Simocyclocheilus*. Grey shading indicates clear difference in character compared to that of *Simocyclocheilus longicornus* sp. nov.

Species	Horn length (2), single (1), indistinct (0)	Horn shape: forked (2), single (1), absent or indistinct (0)	Eyes: normal (2), reduced (1), absent (0)	Dorsal-fin rays	Pectoral-fin rays	Anat-fin rays	Pelvic-fin rays	Lateral-line scales/pores	Body scales	Gill rakers	Pelvic-fin rays reaches backward
<i>S. longicornus</i> sp. nov.	Long	1	1/0	ii, 7	ii, 13	iii, 5	i, 7	38–49	Absent	9	Tips of the pelvic-fin rays without reaches to the anus
<i>S. althouldersi</i>	Absent	0	1	iv, 4–7	i, 16	ii, 3–5	i, 8	54–58	Body covered with thin scale	10–12	Tips of the pelvic-fin rays reaches to or beyond the anus
<i>S. anatrostris</i>	Short	1	0	iii, 8	i, 12–13	iii, 6	i, 6–8	33–42	Absent	8–12	Tips of the pelvic-fin rays without reaches to the anus
<i>S. angularis</i>	Short	1	1	iii, 7	i, 15–18	iii, 5	i, 8	37–39	Absent	7	Tips of the pelvic-fin rays without reaches to the anus
<i>S. anshutensis</i>	Short	1	0	iii, 7	i, 11–12	ii, 5	i, 7	34–38	Body covered with thin scale	14	Tips of the pelvic-fin rays without reaches to the anus
<i>S. aquihornes</i>	Short	1	0	iii, 7	i, 9	ii, 5	i, 6	36	Absent	8	Tips of the pelvic-fin rays reaches to the anus
<i>S. bicornutus</i>	Short	2	1/0	iii, 7	i, 13–15	iii, 5	i, 7–9	36–40	Body covered with thin scale	7–9	Tips of the pelvic-fin rays reaches to the anus
<i>S. brevisbarbatus</i>	Absent	0	2	iii, 7	i, 14–15	iii, 5	i, 8–9	49–51	Body covered with thin scale	8–9	Tips of the pelvic-fin rays without reaches to the anus
<i>S. broadihornes</i>	Short	1	1	iii, 6–7	i, 12–13	ii, 5	i, 5–6	35–37	Absent	4–6	Tips of the pelvic-fin rays reaches to or beyond the anus
<i>S. comexiforeheadus</i>	Short	1	0	iii, 7	i, 9	ii, 5	i, 6	/	Absent	/	Tips of the pelvic-fin rays without reaches to the anus
<i>S. flexuosodorsalis</i>	Short	1	1	iii, 8	i, 12–13	iii, 5	i, 7	37–41	Body covered with thin scale	10	Tip of the pelvic-fin beyond the anus
<i>S. fircadororsalis</i>	Short	2	0	iii, 7	i, 14–15	ii, 5	i, 7	40–46	Body covered with thin scale	8–10	Tips of the pelvic-fin rays reaches to the anus
<i>S. hyalinus</i>	Long	1	0	iii, 7	i, 12–13	iii, 5	ii, 6–7	35–37	Absent	7–9	Tips of the pelvic-fin rays reaches to the anus
<i>S. jincuenensis</i>	Absent	0	1	iii, 7	ii, 12–14	ii, 5	i, 8	47–49	Body covered with thin scale	7–9	Tips of the pelvic-fin rays without reaches to the anus
<i>S. mshanensis</i>	Absent	0	2	iii, 7	i, 9–11	ii, 5	i, 7–8	47–50	Body covered with thin scale	7–9	Tips of the pelvic-fin rays reaches to the anus
<i>S. microphthalmus</i>	Absent	0	1	iii, 8	i, 12	iii, 5	i, 7	48–57	Absent	10–12	Tips of the pelvic-fin rays reaches to the anus
<i>S. rhinacernus</i>	Long	1	1	iii, 7	i, 12	iii, 5	i, 6	37–45	Absent	8	Tips of the pelvic-fin rays without reaches to the anus
<i>S. sinuogensis</i>	Short	1	2	iii, 7	i, 13–15	ii, 5	i, 7	56–57	Body covered with thin scale	9–10	Tips of the pelvic-fin rays without reaches to the anus
<i>S. tianlinensis</i>	Short	1	0	iii, 8	i, 12	iii, 5	i, 7	Absent	Absent	10	Tips of the pelvic-fin rays nearly reaches to the anus
<i>S. tianmensis</i>	Short	2	0	iii, 7	i, 9–11	ii, 5	i, 6	35–39	Body covered with thin scale	7–9	Tips of the pelvic-fin rays reaches to the anus
<i>S. tiki-hornes</i>	Long	2	1	iii, 7	i, 12–14	iii, 5	ii, 6–7	35–37	Absent	6–8	Tips of the pelvic-fin rays reaches to the anus or to the origin of the anal fin rays
<i>S. zhenfengensis</i>	Absent	0	2	iii, 6–7	i, 13–15	iii, 5	i, 7	36–41	Body covered with thin scale	7–9	Tips of the pelvic-fin rays nearly reaches to the anus

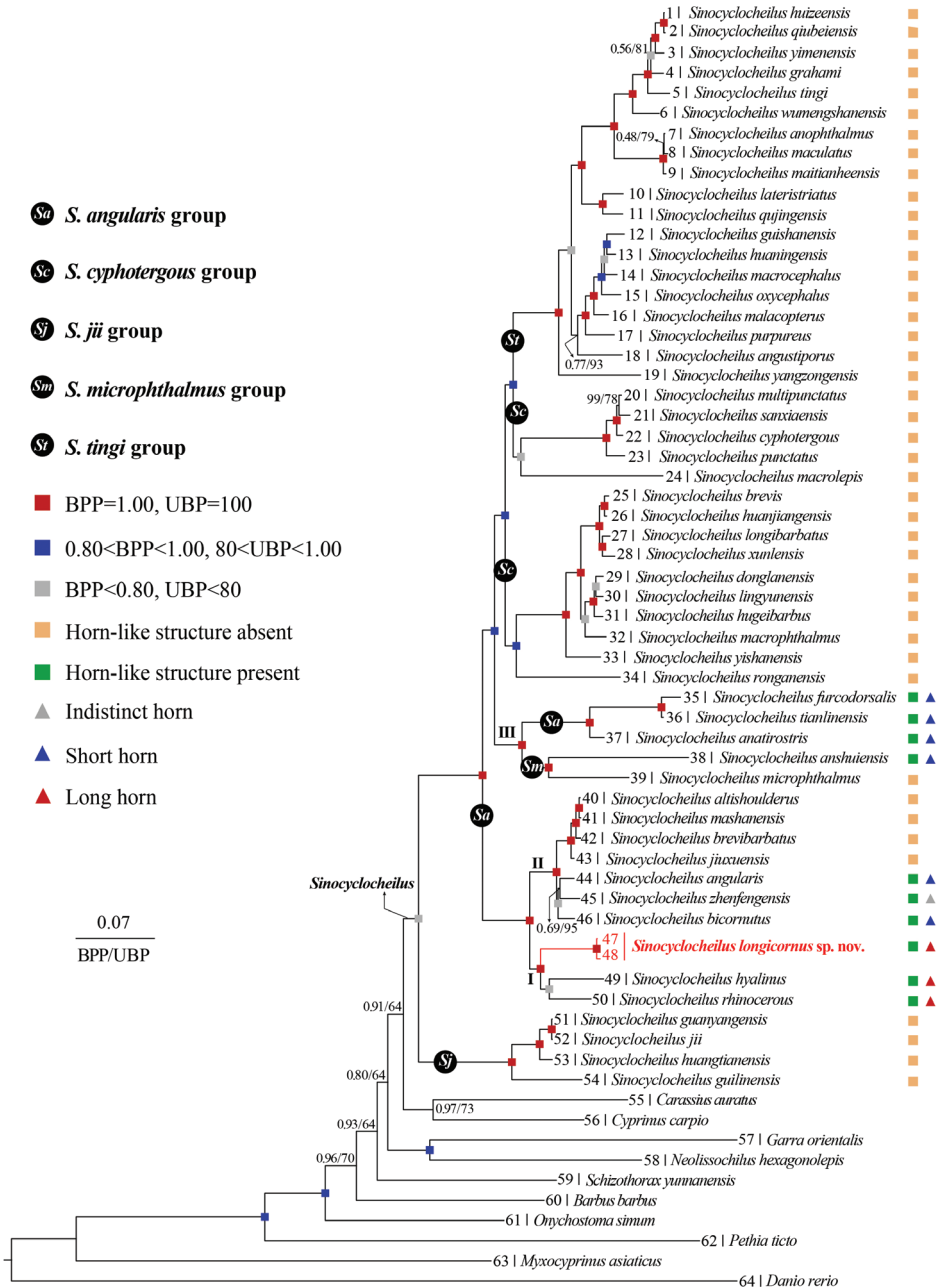


**Figure 2.** Phylogenetic tree based on mitochondrial Cyt *b* + *ND4* genes. In this phylogenetic tree, ultrafast bootstrap supports (UBP) from ML analyses/Bayesian posterior probabilities (BPP) from BI analyses were noted beside nodes. The scale bar represents 0.07 nucleotide substitutions per site. The numbers at the tip of branches corresponds to the ID numbers in Table 2. Different colored rectangular and triangular boxes in addition to the nodes denote the different states of the presence of horn-like structures of species within the genus *Sinocyclocheilus*.



Measurements	<i>S. longicornis</i> sp. nov. (N = 15)			<i>S. angularis</i> (N = 7)			<i>S. bicornutus</i> (N = 2)			<i>S. rhinoceros</i> (N = 11)			<i>S. zhenfengensis</i> (N = 8)			<i>S. byadinus</i> (N = 1)			<i>P</i> -value from Mann-Whitney U test			
	Range	Mean ± SD		Range	Mean ± SD		Range	Mean ± SD		Range	Mean ± SD		Range	Mean ± SD		Range	Mean ± SD		SL vs. SA	SL vs. SB	SL vs. SR	SL vs. SZ
PVAFL	13.2-22.9	18.6 ± 2.8		14.1-22.8	18.8 ± 3.0		21.8-23.3	22.6 ± 1.1		7.0-14.3	9.8 ± 2.1		12.4-19.9	15.2 ± 2.7		12.6	0.891	0.059	0.000	0.000	0.000	0.013
SL/TL	0.79-0.83	0.81 ± 0.01		0.80-0.83	0.81 ± 0.01		0.78-0.79	0.78 ± 0.01		0.80-0.85	0.82 ± 0.02		0.79-0.82	0.80 ± 0.01		0.81	0.332	0.015	0.266	0.015	0.266	0.325
SL/BD	2.98-3.66	3.24 ± 0.19		3.18-3.60	3.31 ± 0.15		3.82-4.22	4.02 ± 0.28		3.76-4.59	3.96 ± 0.24		1.95-3.97	3.34 ± 0.61		4.27	0.267	0.015	0.000	0.000	0.000	0.056
SL/HL	3.12-3.70	3.49 ± 0.14		3.33-3.72	3.50 ± 0.14		3.23-3.24	3.24 ± 0.01		2.93-3.17	3.06 ± 0.08		1.86-3.52	3.14 ± 0.53		2.90	0.945	0.059	0.000	0.000	0.000	0.003
SL/CP/L	4.18-6.72	4.85 ± 0.69		4.83-6.66	5.31 ± 0.78		5.68-6.12	5.90 ± 0.31		4.28-5.72	5.05 ± 0.50		2.58-5.88	4.67 ± 0.99		5.53	0.032	0.088	0.238	0.088	0.238	0.776
SL/CP/D	8.04-9.84	8.95 ± 0.63		7.69-8.69	8.25 ± 0.36		9.58-11.61	10.60 ± 1.44		8.62-13.27	10.61 ± 1.42		4.59-9.15	8.14 ± 1.49		14.58	0.056	0.059	0.003	0.059	0.003	0.131
SL/PL	1.77-2.00	1.87 ± 0.06		1.78-1.98	1.87 ± 0.07		1.85-1.88	1.87 ± 0.02		1.72-1.87	1.79 ± 0.04		1.06-1.94	1.74 ± 0.28		1.68	0.783	1.000	0.001	1.000	0.001	0.213
SL/PP/L	3.06-3.46	3.25 ± 0.12		3.19-3.43	3.32 ± 0.09		3.14-3.31	3.22 ± 0.12		2.77-2.96	2.83 ± 0.06		1.68-3.80	3.20 ± 0.64		2.71	0.185	1.000	0.000	1.000	0.000	0.169
SL/PP/VL	1.87-2.06	1.97 ± 0.05		1.83-1.99	1.92 ± 0.06		1.86-1.93	1.89 ± 0.05		1.91-2.08	1.99 ± 0.05		0.96-1.97	1.80 ± 0.34		1.73	0.066	0.088	0.184	0.088	0.184	0.028
SL/PAL	1.36-1.48	1.42 ± 0.04		1.32-1.42	1.38 ± 0.03		1.31-1.44	1.37 ± 0.09		1.37-3.99	1.68 ± 0.77		0.74-1.46	1.32 ± 0.23		1.35	0.106	0.441	0.023	0.441	0.023	0.238
CP/L/CP/D	1.25-2.35	1.88 ± 0.27		1.15-1.78	1.58 ± 0.22		1.69-1.90	1.79 ± 0.15		1.72-2.71	2.11 ± 0.30		1.45-1.89	1.76 ± 0.17		2.64	0.011	0.618	0.066	0.618	0.066	0.149
HL/SNL	2.04-2.55	2.32 ± 0.13		2.25-2.67	2.45 ± 0.14		2.46-2.84	2.65 ± 0.27		2.31-2.78	2.51 ± 0.15		2.27-3.54	2.67 ± 0.39		2.15	0.066	0.059	0.008	0.059	0.008	0.002
HL/HW	1.79-2.34	2.06 ± 0.14		2.04-2.26	2.11 ± 0.10		1.87-2.19	2.03 ± 0.23		2.19-2.67	2.43 ± 0.16		1.82-2.08	1.97 ± 0.08		2.41	0.581	0.824	0.000	0.824	0.000	0.131
HL/HD	1.43-1.78	1.61 ± 0.10		1.60-1.92	1.76 ± 0.10		1.47-1.98	1.73 ± 0.36		1.77-2.16	1.96 ± 0.11		1.54-1.85	1.67 ± 0.09		1.73	0.007	0.824	0.000	0.824	0.000	0.149
HL/RBL	1.47-2.46	1.88 ± 0.27		1.88-2.91	2.30 ± 0.37		1.78-1.79	1.79 ± 0.00		2.34-5.55	3.79 ± 1.04		1.90-2.41	2.20 ± 0.18		7.29	0.017	0.529	0.000	0.529	0.000	0.007
HL/MBL	1.77-2.75	2.05 ± 0.26		1.93-3.15	2.56 ± 0.47		1.65-1.77	1.71 ± 0.08		2.31-6.19	3.82 ± 1.32		1.92-2.59	2.20 ± 0.24		8.39	0.007	0.015	0.000	0.015	0.000	0.131
HL/PPND	6.20-9.59	7.37 ± 0.88		5.97-10.35	7.06 ± 1.51		5.50-7.94	6.72 ± 1.72		5.73-14.77	10.45 ± 2.55		4.98-6.51	5.47 ± 0.53		7.10	0.210	0.529	0.012	0.529	0.012	0.000
HL/PPND	2.07-3.06	2.56 ± 0.25		2.41-2.96	2.63 ± 0.21		2.45-3.26	2.86 ± 0.57		1.84-2.45	2.10 ± 0.19		2.39-2.88	2.65 ± 0.20		/	0.630	0.618	0.000	0.618	0.000	0.466
PTEL/PPFVL	1.09-1.40	1.24 ± 0.08		1.00-1.27	1.13 ± 0.11		1.22-1.45	1.33 ± 0.17		1.20-1.62	1.43 ± 0.13		0.81-1.71	1.07 ± 0.29		1.45	0.066	0.368	0.003	0.368	0.003	0.007
PVEL/PVAFL	0.74-2.14	0.94 ± 0.34		0.61-0.88	0.76 ± 0.10		0.82-1.04	0.93 ± 0.15		0.72-1.40	1.06 ± 0.17		0.79-1.34	0.95 ± 0.18		0.91	0.056	0.721	0.021	0.721	0.021	0.392
HW/IOD	1.68-2.64	2.01 ± 0.29		1.51-1.86	1.66 ± 0.15		2.72-2.81	2.76 ± 0.06		1.04-2.53	2.07 ± 0.39		1.61-2.07	1.89 ± 0.16		/	0.004	0.015	0.186	0.015	0.186	0.728

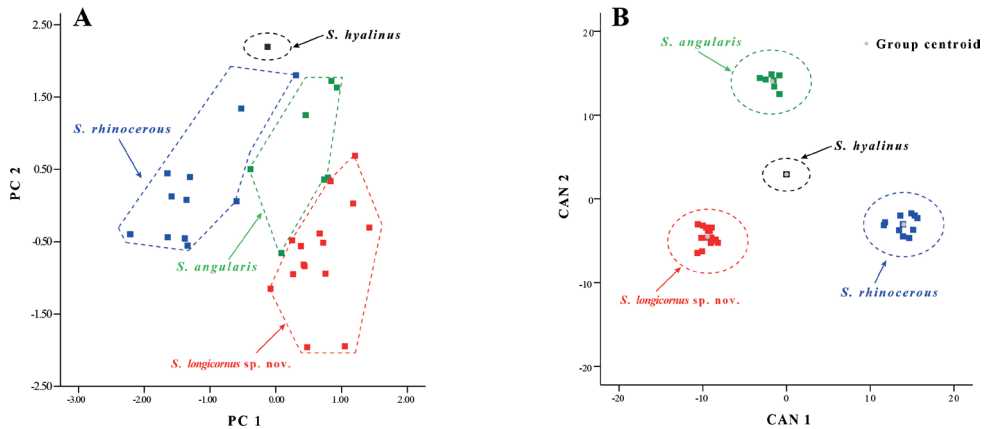


**Figure 3.** Plots of principal component analysis, and canonical discriminant analysis scores of *Sinocyclocheilus longicornus* sp. nov., *S. angularis*, *S. rhinoceros*, and *S. hyalinus* based on morphological characters.

Based on PCA of the morphological data, two principal component factors with eigenvalues greater than two were extracted. These accounted for a total of 89.86% of the total variation (Suppl. material 4). The first principal component (PC1) accounted for 83.37% of the variation and was positively correlated with all variables (eigenvalue = 27.22), thus reflecting the morphological differences between *S. longicornus* sp. nov. and similar species. The second principal component (PC2) accounted for 4.85% of the variation and was dominated by the length of the lower jaw (LJL), length of the upper jaw (UJL), and length of the head (HL) (eigenvalue = 0.44). On the two-dimensional plots of PC1 and PC2, *S. longicornus* sp. nov. can be clearly distinguished from *S. angularis*, *S. rhinoceros*, and *S. hyalinus*, and can be almost separated from *S. angularis* (Fig. 3A). A total of 29 characters were loaded on the PC 1 axis and were mainly influenced by body length, head, and fin ray characteristics (Suppl. material 4). CDA correctly classified 100% of the individuals in the initial grouping case for the four sample groups ( $N = 36$ ). Canonical axes (CAN) 1–3 explained 59.8%, 30.6%, and 9.6% of the total variation, respectively (Fig. 3B; Suppl. material 5). Therefore, based on PCA and CDA, the 15 specimens of *S. longicornus* sp. nov. regions in the space of morphological characters compared to four similar species.

## Taxonomic account

### *Sinocyclocheilus longicornus* Luo, Xu, Wu, Zhou & Zhou, sp. nov.

<https://zoobank.org/F447A6B3-1304-4734-BC57-B46E32034451>

Figs 4, 5, Suppl. material 1

**Material examined. Holotype.** GZNU20210503002, 135.9 mm total length (TL), 109.8 mm standard length (SL), adult male collected by Jia-Jun Zhou and Tao Luo on May 6, 2021 in Hongguo Town, Panzhou City, Guizhou Province, China (25.6576°N, 104.4044°E; ca. 1852 m a.s.l.). **Paratypes.** Fourteen adult male specimens from the

same locality as the holotype: GZNU20210503001, GZNU20210503003–03013, GZNU20210503015–503016, 84.3–116.4 mm SL, collected by Tao Luo, Jia-Jun Zhou, and Xing-Liang Wang on May 6, 2021.

**Diagnosis.** *Sinocyclocheilus longicornus* sp. nov. can be distinguished from all other congeners by the following combination of characters: (1) having a single, relatively long horn-like structure on the back of the head; (2) body scaleless, albinotic body without pigmentation; (3) reduced eyes; (4) dorsal-fin rays, ii, 7; (5) pectoral-fin rays, i, 13; (6) anal-fin rays, iii, 5; (7) pelvic-fin rays, i, 7; (8) lateral line pores 38–49; (9) gill rakers well developed, 9 on first gill arch; (10) tip of the pelvic-fin rays not reaching the anus when pelvic-fin rays extended backward.

**Description.** Body moderately elongate and compressed. Dorsal profile convex from nape to dorsal-fin; greatest body depth at dorsal-fin insertion; ventral profile slightly concave, tapering gradually toward the caudal-fin; greatest body depth slightly anterior to dorsal-fin insertion.

Head short, compressed laterally, length longer than maximum head width, depth longer than maximum head width. large and long anterior horn-like structure present on back of head not forked at tip, at about 45° angle to horizontal and curved downward at tip. Reduced eyes present in upper half of head; eye diameter less than interorbital distance; interorbital distance larger than distance between posterior nostrils. Snout short, U-shaped, and projecting beyond lower jaw in dorsal view, less than half head length.

Mouth subterminal, with slightly projecting upper jaw. Two pairs of nostrils, anterior and posterior nostrils neighboring, nares at 1/3 between snout tip and anterior margin of eye; anterior nares possessing an anterior rim with a posterior fleshy flap forming a half-tube. Two pairs of barbels; rostral barbels long, insertion of rostral barbel in front of anterior nostril, not reaching anterior edge of operculum when rostral bent backward; maxillary barbel slightly shorter compared to rostral barbel, tip surpassing eye but not reaching anterior edge of operculum when bent backward. Gill opening large, opercular membranes connected at isthmus, gill rakers well developed, nine on first gill arch. Pharyngeal teeth in three rows with counts of 2, 3, 5–5, 3, 2; pharyngeal teeth strong and well developed, with curved and pointed tips.

Dorsal fin with two unbranched and seven branched rays; last unbranched dorsal-fin ray hard at base, softening toward tip, with strong serrations along posterior edge; distal margin slightly concave, origin slightly anterior to, or superior to, pelvic-fin insertion and closer to caudal-fin base than to snout tip. Pectoral fin long with one unbranched and 13 branched rays; tip of depressed fin extending about midway between pectoral fin and pelvic-fin insertion; extending from posterior to pelvic-fin insertion and reaching to 35.44% of pelvic-fin length. Pelvic-fin long with one unbranched and seven branched rays, insertion slightly in front of dorsal-fin insertion, tip of the pelvic-fin rays not reaching the anus when pelvic-fin rays extended backward. Anus closer to anal-fin insertion than pelvic-fin insertion; anal fin with three unbranched and five branched rays; tip of anal-fin not reaching to caudal-fin base. Caudal fin with 17 branched rays and 14 unbranched rays, strongly forked; upper and lower lobes broadly pointed, unequal in length and shape.



**Figure 4.** Lateral view of adult male holotype GZNU20210503002 of *Sinocyclocheilus longicornus* sp. nov. in preservative. **A** left side view **B** right side view.

Lateral line complete, slightly straight, curved upward at the anus position, originating from posterior margin of operculum and extending to end of caudal peduncle. Body scaleless, lateral line pores 38–49.

**Coloration of holotype.** In life, body overall white, slightly pink posterior to dorsal fin; barbels and gills red (Fig. 5); with white granular nuptial organs on dorsal surfaces of horn-like structure on back of head and snout (Fig. 5). In 10% formalin, body overall light yellow; posterior part of operculum and all fins partially transparent (Fig. 4).

**Comparative morphology.** *Sinocyclocheilus longicornus* sp. nov. is assigned to the *Sinocyclocheilus angularis* species group based on phylogenetic analysis and the shared presence of the anterior horn-like structure on the back of the head (Fig. 2; Zhao and Zhang 2009). Comparative data of *Sinocyclocheilus longicornus* sp. nov. with the 21 recognized species in the *S. angularis* and *S. microphthalmus* species groups are given in Table 3.

*Sinocyclocheilus longicornus* sp. nov. differs from 55 species in the *S. cyphotergous*, *S. jii*, and *S. tingi* species groups by the presence of a horn-like structure on the back of the head (vs. absent). From the 21 species in the *S. angularis* and *S. microphthalmus*



**Figure 5.** Live adult male paratype of *Sinocyclocheilus longicornus* sp. nov.

species groups, *Sinocyclocheilus longicornus* sp. nov. can be distinguished from *S. altishoulderus*, *S. jiuxuensis*, *S. brevibarbatus*, *S. microphthalmus*, *S. zhenfengensis*, and *S. mashanensis* by having a long horn-like structure on the back of the head (vs. absent or indistinct), further distinguished from *S. brevibarbatus*, *S. mashanensis*, *S. simengensis*, *S. zhenfengensis* by reduced eyes (vs. normal); differs from *S. furcodorsalis*, *S. hyalinus*, *S. anatirostris*, *S. aquihornes*, *S. tianlinensis*, *S. anshuiensis*, *S. convexiforeheadus*, and *S. tianeensis* by reduced eyes (vs. absent).

*Sinocyclocheilus longicornus* sp. nov. differs from *S. angularis* by having a relatively long horn-like structure ( $14.7 \pm 1.5$  mm vs.  $10.6 \pm 1.9$  mm;  $p$ -value  $< 0.01$ , Table 4), long rostral and maxillary barbels ( $p$ -value  $< 0.05$ , Table 4), two unbranched dorsal-fin rays (vs. three), pectoral-fin rays (ii, 13 vs. i, 15–18), pelvic-fin rays (i, 7 vs. i, 8–10), gill rakers (nine vs. seven), and body scaleless (vs. body covered with thin scales); from *S. bicornutus* by single horn-like structure on the back of the head (vs. forked), dorsal fin rays (ii, 7 vs. iii, 7), pectoral-fin rays (ii, 13 vs. i, 15–18), body scaleless (vs. body covered with thin scales), and tip of the pelvic-fin rays not reaching the anus when pelvic-fin rays extended backward (vs. beyond the anus); from *S. broadihornes* and *S. simengensis* by dorsal fin rays (ii, 7 vs. iii, 6–7), anal-fin rays (iii, 5 vs. ii, 5), and lateral line pores (38–49 vs. 35–37 in *S. broadihornes* and 56–57 in *S. simengensis*); from *S. flexuosdorsalis* by having a relatively long horn-like structure (vs. short), dorsal-fin rays (ii, 7 vs. iii, 8), pectoral fin rays (ii, 13 vs. i, 12–13), snout length to standard length ratio is small (12.4% vs. 14.4%), body scaleless (vs. body covered with scales),

and tip of the pelvic-fin rays not reaching the anus when pelvic-fin rays extended backward (vs. beyond the anus); from *S. tileihornesy* by dorsal-fin rays (ii, 7 vs. iii, 7), anal-fin rays (iii, 5 vs. ii, 5), pelvic-fin rays (i, 7 vs. ii, 6–7), pectoral fin rays (ii, 13 vs. i, 12–15), pelvic fin rays (i, 7 vs. i, 6), lateral line pores (38–49 vs. 35–37), gill rakers (9 vs. 6–8), and tip of the pelvic-fin rays not reaching the anus when pelvic-fin rays extended backward (vs. beyond the anus).

*Sinocyclocheilus longihornes* can be morphologically distinguished from its close relatives *S. rhinoceros* and *S. hyalinus*. *Sinocyclocheilus longicornus* sp. nov. differs from *S. hyalinus* by eyes small and degenerate (vs. absent), dorsal-fin rays (ii, 7 vs. iii, 7), pelvic-fin rays (i, 7 vs. ii, 6–7), lateral line pores (39–45 vs. 35–37), and tip of the pelvic-fin rays not reaching the anus when pelvic-fin rays extended backward (vs. beyond the anus). *Sinocyclocheilus longicornus* sp. nov. differs from *S. rhinoceros* by having a large body size ( $123.3 \pm 11.3$  mm vs.  $76.5 \pm 12.3$  mm;  $p = 0.00$ , Table 3), long horn-like structure ( $14.7 \pm 1.5$  mm vs.  $9.4 \pm 2.1$  mm;  $p = 0.00$ , Table 3), dorsal-fin rays (ii, 7 vs. iii, 7), pectoral-fin rays (ii, 13 vs. i, 12), pelvic-fin rays (i, 7 vs. i, 6), gill rakers (9 vs. 8), and a relatively long, single horn-like structure on the back of the head ( $14.7 \pm 1.5$  mm vs.  $9.4 \pm 2.1$  mm;  $p < 0.01$ , Table 4). In addition, except for morphological characteristics (eye diameter, mouth width) and some ratios, such as the SL to TL ratio, SL to CPL ratio, SL to PPVL ratio, and HW to IOD ratio, the remaining morphometric values and ratios of *Sinocyclocheilus longicornus* sp. nov. are significantly greater than those of *S. rhinoceros*.

**Geographical distribution and habitat.** *Sinocyclocheilus longicornus* sp. nov. is only known from the type locality, a vertical cave some distance from Hongguo Town, Panzhou city, Guizhou, China at an elevation of 2276 m. There was no light inside the cave. Individuals of *S. longicornus* sp. nov. were located in a small pool ~ 25 m from the cave entrance. The pool was ~ 1.8 m wide and 80 cm deep, with a water temperature of ~ 16 °C at collection time and a water pH of 7.4. The 15 specimens collected on 3 May 2021 were all adult males. Therefore, we believe that the breeding period started from mid-April. Within this cave, *Sinocyclocheilus longicornus* sp. nov. co-occurred with *Triplophysa* sp., and *Sinocyclocheilus* sp. Outside the cave, the arable land was farmed to produce maize, wheat, and potatoes.

**Etymology.** The specific epithet *longicornus* is an invariable noun in apposition, derived from the Latin words *longus*, meaning long, and *cornu* or *cornus*, meaning horn of the forehead, in reference to the presence of a long horn-like structure on the forehead of the species. We propose the English common name Long-Horned Golden-lined Fish and the Chinese common name Cháng Jiǎo Jīn Xiàn Bā (长角金线鲃).

## Discussion

Morphological comparison and phylogenetic analysis support the generic assignment and separate species status of *Sinocyclocheilus longicornus* sp. nov. The genetic

differences between the new species and its close relatives, *S. hyalinus* and *S. rhinocerosus*, were greater than the known genetic distances between other species (Suppl. materials 3, 4). *Sinocyclocheilus longicornus* sp. nov. the number of species of *Sinocyclocheilus* to 77, of which 13 species are recorded from Guizhou Province, China.

The genus *Sinocyclocheilus* is recognized as monophyletic, but there is no consensus on the classification of species groups (Zhao and Zhang 2009; Xiang 2014; Liu 2018; Mao et al. 2021, 2022; Wen et al. 2022). Initially, *Sinocyclocheilus* was divided into four species groups, *S. jii*, *S. angularis*, *S. cyphotergous*, and *S. tingi*, based on mitochondrial *Cyt b* and morphological differences (Zhao and Zhang 2009). Phylogenetic trees reconstructed using mitochondrial *ND4* and *Cyt b*, mitochondrial genome, and restriction site-associated DNA sequencing supported monophyly of the *S. jii* and *S. tingi* species groups and rejected monophyly of the *S. angularis* and *S. cyphotergous* species groups (Xiang 2014; Liu 2018; Mao et al. 2021, 2022; Wen et al. 2022; this study). These studies proposed new classification schemes, such as two new clades (Clades E and F) from Mao et al. (2022) and a new species group (*S. microphthalmus* group) from Wen et al. (2022). Inconsistent topological differences may be related to molecular marker types, number of species and evolutionary models. For example, a phylogenetic tree reconstructed by Mao et al. (2021) for 49 species of *Sinocyclocheilus* using the GTR+I+G model for both mitochondrial *ND4* and *Cyt b* rejected monophyly of the *S. cyphotergous* group. We reanalyzed their data for codon partitioning and found that the monophyly of both *S. angularis* and *S. cyphotergous* species groups was rejected. Different genes and different codons may have different evolutionary rates (Degnan and Rosenberg 2009), so the analysis may produce conflicting results when the same untested model is applied to different gene segments. Therefore, to resolve classification disagreements among species groups, the use of genomic data and a sufficient number of species is needed for future studies.

Variable or specialized morphological characters of *Sinocyclocheilus* are closely related to the orogeny producing dark cave environments (Yang et al. 2016; Mao et al. 2021, 2022; Wen et al. 2022). For example, horn-like structures (single or forked, long or short) or bulges on the back of the head, and degeneration or loss of eyes (Zhao and Zhang 2009). *Sinocyclocheilus longicornus* sp. nov. has a relatively long, unforked horn-like structure on the forehead, and small, degenerated eyes. It clustered with eight species of the *S. angularis* species group on the phylogenetic tree and could be divided into Clade I and Clade II. (Fig. 2). Long and short/indistinct horn-like structures are present in Clade I and Clade II, respectively (Fig. 2). Based on the present study and previous phylogenetic trees (Mao et al. 2021, 2022; Wen et al. 2022), we hypothesize that the evolution of the forehead horn may have occurred in at least two independent formations, one weakening event and one loss event (Fig. 2). As for the eye, no corresponding clade was found within the *S. angularis* species group, and variable eye phenotypes were also reported within *S. bicornutus* (in press), which may be related to the reduction of eye size during evolution or to the abundance and deprivation of food resources during growth and development, as well as related gene mutations (Ma et al. 2020; Mao et al. 2021).

## Acknowledgements

This research was supported by the programs of the Strategic Priority Research Program B of the Chinese Academy of Sciences (CAS) (No. XDB31000000), the National Animal Collection Resource Center, China (No. 2005DKA21402), the Guizhou Normal University Academic Emerging Talent Fund Project (Qianshi Xin Miao [2021] 20), and the Postgraduate Education Innovation Programme of Guizhou Province (No. Qianjiaohu YJSKYJJ [2021] 091). We thank Gao-Kui Feng, Xing-Liang Wang, Ya-Li Wang, Wei Li, and Chang-Ting Lan for help with specimen collection. We thank LetPub ([www.letpub.com](http://www.letpub.com)) for its linguistic assistance during manuscript preparation.

## References

- Chen JX, Lan JH (1992) Description of a new genus and three new species of fishes from Guangxi, China (Cypriniformes: Cyprinidae, Cobitidae). *Acta Zootaxonomica Sinica* 17(1): 104–109. [In Chinese]
- Chen YR, Chu XL, Luo ZY, Wu JY (1988a) A new blind Cyprinid fish from Yunnan, China with a reference to the evolution of its characters. *Acta Zootaxonomica Sinica* 34(1): 64–70. [In Chinese]
- Chen JX, Zhao ZF, Zheng JZ, Li DJ (1988b) Description of three new barbine species from Guizhou, China (Cypriniformes, Cyprinidae). *Acta Academiae Medicinae Zunyi* 11(1): 1–4 [92–93]. [In Chinese]
- Chen YR, Yang JX, Zhu CG (1994) A new fish of the genus *Sinocyclocheilus* from Yunnan with comments on its characteristic adaptation (Cypriniformes: Cyprinidae). *Acta Zootaxonomica Sinica* 19(2): 246–252. [In Chinese]
- Chen YR, Yang JX, Lan JH (1997) One new species of blind cavefish from Guangxi with comments on its phylogenetic status (Cypriniformes: Cyprinidae: Barbinae). *Acta Zootaxonomica Sinica* 22(2): 219–223. [In Chinese]
- Chen YQ, Peng CL, Zhang E (2016) *Sinocyclocheilus guanyangensis*, a new species of cavefish from the Li-Jiang basin of Guangxi, China (Teleostei: Cyprinidae). *Ichthyological Exploration of Freshwaters* 27(1): 1–8.
- Cheng C, Pan XF, Chen XY, Li JY, Ma L, Yang JX (2015) A new species of the genus *Sinocyclocheilus* (Teleostei: Cypriniformes), from Jinshajiang Drainage, Yunnan, China. *Cave Research* 2(4): 1–4.
- Chu XL, Cui GH (1985) A revision of Chinese cyprinid genus *Sinocyclocheilus* with reference to the interspecific relationships. *Acta Zootaxonomica Sinica* 10(4): 435–441. [In Chinese]
- Dai DR (1988) Un nouveau poisson cavernicole. In: Guizhou expe '86: Première expedition speleologique franco-chinoise dans le centre et le sud de la Province du Guizhou. Federation Française de Spéléologie, Paris, 88–89 pp.
- Degnan JH, Rosenberg NA (2009) Gene tree discordance, phylogenetic inference and the multispecies coalescent. *Trends in Ecology and Evolution* 24(6): 332–340. <https://doi.org/10.1016/j.tree.2009.01.009>

- Edgar RC (2004) MUSCLE: Multiple sequence alignment with high accuracy and high throughput. *Nucleic Acids Research* 32(5): 1792–1797. <https://doi.org/10.1093/nar/gkh340>
- Fang PW (1936) *Sinocyclocheilus tingi*, a new genus and species of Chinese barboid fishes from Yunnan. *Sinensia* 7: 588–593.
- Gan X, Wu TJ, Wei ML, Yang J (2013) A new blind barboid species, *Sinocyclocheilus anshuiensis* sp. nov. (Cypriniformes: Cyprinidae) from Guangxi, China. *Zoological Research* 34(5): 459–463. <https://doi.org/10.11813/j.issn.0254-5853.2013.5.0459> [In Chinese]
- George D, Paul M (2010) SPSS for Windows step by step: A Simple study guide and reference, 18.0 Update (11<sup>th</sup> edn.). Prentice Hall, New Jersey, USA.
- Hoang DT, Chernomor O, von Haeseler A, Minh BQ, Vinh LS (2018) UFBoot2: Improving the ultrafast bootstrap approximation. *Molecular Biology and Evolution* 35(2): 518–522. <https://doi.org/10.1093/molbev/msx281>
- Huang J, Gluesenkamp A, Fenolio D, Wu Z, Zhao Y (2017) Neotype designation and redescription of *Sinocyclocheilus cyphotergous* (Dai) 1988, a rare and bizarre cavefish species distributed in China (Cypriniformes: Cyprinidae). *Environmental Biology of Fishes* 100(11): 1483–1488. <https://doi.org/10.1007/s10641-017-0658-2>
- Jiang WS, Li J, Lei XZ, Wen ZR, Han YZ, Yang JX, Chang JB (2019) *Sinocyclocheilus sanxiaensis*, a new blind fish from the Three Gorges of Yangtze River provides insights into speciation of Chinese cavefish. *Zoological Research* 40(6): 552–557. <https://doi.org/10.24272/j.issn.2095-8137.2019.065>
- Kumar S, Stecher G, Tamura K (2016) MEGA7: Molecular evolutionary genetics analysis version 7.0 for bigger datasets. *Molecular Biology and Evolution* 33(7): 1870–1874. <https://doi.org/10.1093/molbev/msw054>
- Lan JH, Zhang CG, Zhao YH (2004) A new species of the genus *Sinocyclocheilus* from China (Cypriniformes, Cyprinidae, Barbinae). *Acta Zootaxonomica Sinica* 29(2): 377–380. [In Chinese]
- Lan JH, Gan X, Wu TJ, Yang J (2013) Cave Fishes of Guangxi, China. Science Press, Beijing.
- Lan YB, Qin XC, Lan JH, Xiu LH, Yang J (2017) A new species of the genus *Sinocyclocheilus* (Cypriniformes, Cyprinidae) from Guangxi, China. *Journal of Xinyang Normal University* 30(1): 97–101. <https://doi.org/10.3969/j.issn.1003-0972.2017.01.021> [Natural Science Edition] [In Chinese]
- Lanfear R, Frandsen PB, Wright AM, Senfeld T, Calcott B (2017) PartitionFinder 2: New methods for selecting partitioned models of evolution for molecular and morphological phylogenetic analyses. *Molecular Biology and Evolution* 34(3): 772–773. <https://doi.org/10.1093/molbev/msw260>
- Li WX (1985) Four species of *Sinocyclocheilus* from Yunnan. *Zoological Research* 6(4): 423–427.
- Li GL (1989) On a new fish of the genus *Sinocyclocheilus* from Guangxi China (Cypriniformes: Cyprinidae: Barbinae). *Acta Zootaxonomica Sinica* 14(1): 123–126. [In Chinese]
- Li WX (1992) Description on three species of *Sinocyclocheilus* from Yunnan, China. *Acta Hydrobiologica Sinica* 16(1): 57–61. [In Chinese]
- Li WX, An L (2013) A new species of *Sinocyclocheilus* from Kunming, Yunnan—*Sinocyclocheilus wui* sp. nov. *Journal of Jishou University* 34(1): 82–84. <https://doi.org/10.3969/j.issn.1007-2985.2013.01.019> [Natural Science Edition] [In Chinese]
- Li WX, Lan JH (1992) A new genus and three new species of Cyprinidae from Guangxi, China. *Journal of Zhanjiang Fisheries College* 12(2): 46–51. [In Chinese]

- Li J, Li XH (2014) *Sinocyclocheilus gracilis*, a new species of hypogean fish from Guangxi, South China (Teleostei: Cypriniformes: Cyprinidae). *Ichthyological Exploration of Freshwaters* 24(3): 249–256.
- Li WX, Mao WN (2007) A new species of the genus *Sinocyclocheilus* living in cave from Shilin, Yunnan, China (Cypriniformes, Cyprinidae). *Acta Zootaxonomica Sinica* 32(1): 226–229.
- Li WX, Tao JN (1994) A new species of Cyprinidae from Yunnan—*Sinocyclocheilus rhinoceros*, sp. nov. *Journal of Zhanjiang Fisheries College* 14(1): 1–3. [In Chinese]
- Li WX, Wu DF, Chen AL (1998) Two new species of *Sinocyclocheilus* from Yunnan, China. (Cypriniformes: Cyprinidae). *Journal of Zhanjiang Ocean University* 18(4): 1–5. [In Chinese]
- Li WX, Xiao H, Zan RG, Luo ZF, Li HM (2000) A new species of *Sinocyclocheilus* from Guangxi, China. *Zoological Research* 21(2): 155–157. [In Chinese]
- Li WX, Mao WN, Lu ZM, Tao JN (2002a) Two new species of Cyprinidae from Yunnan. *Journal of Yunnan University* 24(5): 385–387. [In Chinese]
- Li WX, Liao YP, Yang HF (2002b) Two new species of *Sinocyclocheilus* from Eastern Yunnan, China. *Journal of Yunnan Agricultural University* 17(2): 161–163. [In Chinese]
- Li WX, Mao WL, Lu ZM (2002c) A new species of *Sinocyclocheilus* from Yunnan' China. *Journal of Zhanjiang Ocean University* 22(3): 1–2. [In Chinese]
- Li WX, Mao WN, Lu ZM, Yan WZ (2003a) The two new species of *Sinocyclocheilus* from Yunnan, China. *Journal of Jishou University* 24(2): 63–65. [Natural Science Edition] [In Chinese]
- Li WX, Ran JC, Chen HM (2003b) A new species of cave *Sinocyclocheilus* in Guizhou and its adaptation comment. *Journal of Jishou University* 24(4): 61–63. [Natural Sciences Edition] [In Chinese]
- Li WX, Lan JC, Chen XY (2003c) A new species of cave *Sinocyclocheilus* from Guangxi—*Sinocyclocheilus jiuxuensis* Li et Ran, sp. nov. *Journal of Guangxi Normal University* 21(4): 83–85. [In Chinese]
- Li WX, Xiao H, Zan RG, Luo ZY, Ban CH, Fen JB (2003d) A new species of *Sinocyclocheilus* from caves in Guangxi. *Journal of Guangxi Normal University* 21(3): 80–81. [In Chinese]
- Li WX, Xiao H, Jin XL, Wu DJ (2005) A new species of *Sinocyclocheilus* from Yunnan, China. *Xi Nan Nong Ye Xue Bao* 18(1): 90–91. [In Chinese]
- Li WX, Yang HF, Han F, Tao CP, Hong Y, Chen H (2007) A new species in cave of blind *Sinocyclocheilus* from Yunnan, China (Cypriniformes: Cyprinidae). *Journal of Guangdong Ocean University* 27(4): 1–3. [In Chinese]
- Li J, Li XH, Mayden RL (2014) *Sinocyclocheilus brevifinus* (Teleostei: Cyprinidae), a new species of cavefish from Guangxi, China. *Zootaxa* 3873(1): 37–48. <https://doi.org/10.11646/zootaxa.3873.1.3>
- Li GH, Wu JJ, Leng Y, Zhou R, Pan XF, Han F, Li SY, Liang X (2018) A new species *Sinocyclocheilus longshanensis* sp. nov. from Yunnan. *Zhongguo Nongxue Tongbao* 34(5): 153–158. [In Chinese]
- Li WX, Li QQ, Chen HY (2019) A new species of *Sinocyclocheilus* from Yunnan, China: *Sinocyclocheilus bannaensis*. *Journal of Jishou University* 40(1): 61–63. <http://doi.org/10.13438/j.cnki.jdzk.2019.01.015> [Natural Science Edition] [In Chinese]
- Lin RD, Luo ZF (1986) A new blind barboid fish (Pisces, Cyprinidae) from subterranean water in Guangxi, China. *Acta Hydrobiologica Sinica* 10(4): 380–382.

- Liu T (2018) Molecular Phylogenetic Relationships among 30 *Sinocyclocheilus* species Based on RAD-seq Technology. Yunnan University. Master Thesis. [In Chinese]
- Liu T, Deng HQ, Ma L, Xiao N, Zhou J (2018) *Sinocyclocheilus zhenfengensis*, a new cyprinid species (Pisces: Teleostei) from Guizhou Province, Southwest China. *Journal of Applied Ichthyology* 34(4): 945–953. <https://doi.org/10.1111/jai.13629>
- Luo FG, Huang J, Liu X, Luo T, Wen YH (2016) *Sinocyclocheilus ronganensis* Luo, Huang et Wen sp. nov., a new species belonging to *Sinocyclocheilus* Fang from Guangxi (Cypriniformes: Cyprinidae). *Journal of Southern Agriculture* 47(4): 650–655. <https://doi.org/10.3969/j.issn.2095-1191.2016.04.650> [In Chinese]
- Ma L, Zhao Y, Yang JX (2019) Cavefish of China. In *Encyclopedia of caves*. Academic Press, USA. <http://doi.org/10.1016/B978-0-12-814124-3.00027-3>
- Ma L, Gore AV, Castranova D, Shi J, Ng M, Tomins KA, van der Weele CM, Weinstein BM, Jeffery WR (2020) A hypomorphic cystathionine  $\beta$ -synthase gene contributes to cavefish eye loss by disrupting optic vasculature. *Nature Communications* 11(1): 1–15. <https://doi.org/10.1038/s41467-020-16497-x>
- Mao WN, Lu ZM, Li WX, Ma HB, Huang G (2003) A new species of *Sinocyclocheilus* (Cyprinidae) from cave of Yunnan, China. *Journal of Zhanjiang Ocean University* 23(3): 1–2. [In Chinese]
- Mao TR, Liu YW, Meegaskumbura M, Yang J, Ellepola G, Senevirathne G, Fu CH, Gross JB, Pie MR (2021) Evolution in *Sinocyclocheilus* cavefish is marked by rate shifts, reversals, and origin of novel traits. *BMC Ecology and Evolution* 21(1): 1–14. <https://doi.org/10.1186/s12862-021-01776-y>
- Mao T, Liu Y, Vasconcellos MM, Pie MR, Ellepola G, Fu C, Meegaskumbura M (2022) Evolving in the darkness: Phylogenomics of *Sinocyclocheilus* cavefishes highlights recent diversification and cryptic diversity. *Molecular Phylogenetics and Evolution* 168: 107400. <https://doi.org/10.1016/j.ympev.2022.107400>
- Microsoft Corporation (2016) Microsoft Excel. <https://office.microsoft.com/excel>
- Nguyen LT, Schmidt HA, Von HA, Minh BQ (2015) IQ-TREE: A fast and effective stochastic algorithm for estimating maximum-likelihood phylogenies. *Molecular Biology and Evolution* 32(1): 268–274. <https://doi.org/10.1093/molbev/msu300>
- Pan XF, Li L, Yang JX, Chen XY (2013) *Sinocyclocheilus xichouensis*, a new species of golden-line fish from the Red River drainage in Yunnan, China (Teleostei: Cypriniformes). *Zoological Research* 34(4): 368–373. <https://doi.org/10.11813/j.issn.0254-5853.2013.4.0368> [In Chinese]
- Parsons S, Jones G (2000) Acoustic identification of twelve species of echolocating bat by discriminant function analysis and artificial neural networks. *The Journal of Experimental Biology* 203(17): 2641–2656. <https://doi.org/10.1242/jeb.203.17.2641>
- Pellegrin J (1931) Description de deux Cyprinidés nouveaux de Chine appartenant au genre *Schizothorax* Heckel. *Bulletin de la Société Zoologique de France* 56: 145–149, 289.
- Polaszek A, Manzari S, Quicke DLJ (2010) Morphological and molecular taxonomic analysis of the *Encarsia meritoria* species complex (Hymenoptera, Aphelinidae), parasitoids of whiteflies (Hemiptera, Aleyrodidae) of economic importance. *Zoologica Scripta* 33(5): 403–421. <https://doi.org/10.1111/j.0300-3256.2004.00161.x>
- Regan C T (1904) On a collection of fishes made by Mr. John Graham at Yunnan Fu. *Annals and Magazine of Natural History [Series 7]* 13(75): 190–194.

- Ronquist F, Teslenko M, Van DMP, Ayres DL, Darling A, Höhna S, Larget B, Liu L, Suchard MA, Huelsenbeck JP (2012) MrBayes 3.2: Efficient Bayesian phylogenetic inference and model choice across a large model space. *Systematic Biology* 61(3): 539–542. <https://doi.org/10.1093/sysbio/sys029>
- Shan XH, Yue PQ (1994) The study on phylogeny of the *Sinocyclocheilus* fishes (Cypriniformes: Cyprinidae: Barbinae). *Zoological Research* 15(Supplement): 36–44. [In Chinese]
- Wang DZ, Chen YY (1989) Descriptions of three new species of Cyprinidae from Guizhou Province, China (Cypriniformes: Cyprinidae). *Academiae Medicinae Zunyi* 12(4): 29–34. [In Chinese]
- Wang DZ, Chen YY (1998) On the diagnosis of *Sinocyclocheilus* and the taxonomic position of its closely related genus *Anchicyclocheilus* (Cypriniformes: Cyprinidae: Barbinae). *Acta Zootaxonomica Sinica* 23(1): 101–104. [In Chinese]
- Wang DZ, Chen YY (2000) The origin and adaptive evolution of the genus *Sinocyclocheilus*. *Acta Hydrobiologica Sinica* 24(6): 630–634.
- Wang DZ, Liao JW (1997) A new species of *Sinocyclocheilus* from Guizhou, China (Cypriniformes: Cyprinidae: Barbinae). *Acta Academiae Medicinae Zunyi* 20(2/3): 1–3. [In Chinese]
- Wang DZ, Huang Y, Liao JW, Zheng JZ (1995) Taxonomic revision of the genus *Gibbibarbus* Dai. *Acta Academiae Medicinae Zunyi* 18(3): 166–168. [In Chinese]
- Wang DZ, Chen YY, Li XY (1999) Molecular phylogeny of *Sinocyclocheilus*. *Acta Academiae Medicinae Zunyi* 22(1): 1–6. [In Chinese]
- Wang D, Zhao YH, Yang JX, Zhang CG (2014) A new cavefish species from Southwest China, *Sinocyclocheilus gracilicaudatus* sp. nov. (Teleostei: Cypriniformes: Cyprinidae). *Zootaxa* 3768(5): 583–590. <https://doi.org/10.11646/zootaxa.3768.5.5>
- Wen H, Luo T, Wang Y, Wang S, Liu T, Xiao N, Zhou J (2022) Molecular phylogeny and historical biogeography of the cave fish genus *Sinocyclocheilus* (Cypriniformes: Cyprinidae) in southwest China. *Integrative Zoology* 17(2): 311–325. <https://doi.org/10.1111/1749-4877.12624>
- Wu HW (1977) The cyprinid fishes of China [Zhongguo like yulei zhi]. Volume 2. People's Press, Shanghai. [In Chinese]
- Wu TJ, Liao ZP, Gan X, Li WX (2010) Two new species of *Sinocyclocheilus* in Guangxi, China (Cypriniformes, Cyprinidae). *Journal of Guangxi Normal University* 28(4): 116–120. <https://doi.org/10.16088/j.issn.1001-6600.2010.04.008> [Natural Science Edition]
- Wu ZL, Li CQ, Lan C, Li WX (2018) Two new species of *Sinocyclocheilus* from Guangxi, China. *Journal of Jishou University* 39(3): 55–59. <https://doi.org/10.13438/j.cnki.jdzk.2018.03.012> [Natural Science Edition] [In Chinese]
- Xiang XH (2014) Estimation of divergence times and detection of selection pressure for representative species of the genus *Sinocyclocheilus* based on the mitochondrial genome. Yunnan University. Master Thesis. [In Chinese]
- Xiao H, Chen SY, Liu ZM, Zhang RD, Li WX, Zan RG, Zhang YP (2005) Molecular phylogeny of *Sinocyclocheilus* (Cypriniformes: Cyprinidae) inferred from mitochondrial DNA sequences. *Molecular Phylogenetics and Evolution* 36(1): 67–77. <https://doi.org/10.1016/j.ympev.2004.12.007>
- Yang JX, Chen XL, Bai J, Fang DM, Qiu Y, Jiang WS, Yuan H, Bian C, Lu J, He Y, Pan XF, Zhang YL, Wang XA, You XX, Wang YS, Sun Y, Mao DQ, Liu Y, Fan GY, Zhang H, Chen XY, Zhang XH, Zheng LP, Wang JT, Cheng L, Chen JM, Ruan ZQ, Li J, Yu H, Peng C,

- Ma XY, Xu JM, He Y, Xu ZF, Xu P, Wang J, Yang HM, Wang J, Whitten T, Xu X, Shi Q (2016) The *Sinocyclocheilus* cavefish genome provides insights into cave adaptation. BMC Biology 14(1): 1–13. <https://doi.org/10.1186/s12915-015-0223-4>
- Yang HF, Li QQ, Li WX (2017) A new species cave blind fish of the *Sinocyclocheilus* from Yunnan Province: *Sinocyclocheilus convexiforeheadus*. Journal of Jishou University 38(2): 58–60. <https://doi.org/10.13438/j.cnki.jdzk.2017.02.011> [Natural Science Edition] [In Chinese]
- Yang HF, Li CQ, Chen YY, Li WX (2018) A new species of *Sinocyclocheilus* from Yunnan: *Sinocyclocheilus wenshanensis*. Journal of Yunnan University 39(3): 507–512. <https://doi.org/10.7540/j.ynu.20160534> [Natural Science Edition] [In Chinese]
- Zhang CG, Dai DY (1992) A new species of the *Sinocyclocheilus* from Guangxi, China (Cypriniformes: Cyprinidae). Acta Zootaxonomica Sinica 17(3): 377–380. [In Chinese]
- Zhang CG, Zhao YH (2001) A new fish of *Sinocyclocheilus* from Guangxi, China with a comment on its some biological adaptation (Cypriniformes: Cyprinidae). Acta Zootaxonomica Sinica 26(1): 102–107. [In Chinese]
- Zhang CG, Zhao YH, Xing YC, Zhou W, Tang WQ (2016) Species diversity and distribution of inland fishes in China. Science Press, Beijing. [In Chinese]
- Zhao YH, Zhang CG (2009) Endemic fishes of *Sinocyclocheilus* (Cypriniformes: Cyprinidae) in China species diversity, cave adaptation, systematics and zoogeography. Science Press, Beijing. [In Chinese]
- Zhao YH, Zhang CG (2013) Validation and re-description of *Sinocyclocheilus aluensis* Li et Xiao, 2005 (Cypriniformes: Cyprinidae). Zoological Research 34(4): 374–378. <https://doi.org/10.11813/j.issn.0254-5853.2013.4.0374> [In Chinese]
- Zhao YH, Watanabe K, Zhang CG (2006) *Sinocyclocheilus donglanensis*, a new cavefish (Teleostei: Cypriniformes) from Guangxi, China. Ichthyological Research 53(2): 121–128. <https://doi.org/10.1007/s10228-005-0317-z>
- Zhao YH, Lan JH, Zhang CG (2009) A new cavefish species, *Sinocyclocheilus brevibarbatus* (Teleostei: Cypriniformes: Cyprinidae), from Guangxi, China. Environmental Biology of Fishes 86(1): 203–209. <https://doi.org/10.1007/s10641-008-9338-6>
- Zheng JZ, Wang J (1990) Description of a new species of the genus *Sinocyclocheilus* from China (Cypriniformes: Cyprinidae). Acta Zootaxonomica Sinica 15(2): 251–254. [In Chinese]
- Zheng CY, Xie JH (1985) One new carp of the genus *Sinocyclocheilus* (Barbinae, Cyprinidae) from Guizhou Province, China. Transactions of the Chinese Ichthyological Society 4: 123–126.
- Zheng H, Xiu L, Yang J (2013) A new species of Barbine genus *Sinocyclocheilus* (Teleostei: Cyprinidae) from Zuojiang river drainage in Guangxi, China. Environmental Biology of Fishes 96(6): 747–751. <https://doi.org/10.1007/s10641-012-0068-4>
- Zhou J (1985) Fishes in Karst caves of Guangxi. Carsologica Sinica 4: 377–386. [In Chinese]
- Zhou J, Zhang CG, He AY (2004) A new species of the genus *Sinocyclocheilus* from Guangxi, China (Cypriniformes, Cyprinidae). Acta Zootaxonomica Sinica 29(3): 591–594. [In Chinese]
- Zhou J, Li XZ, Hou XF, Sun ZL, Gao L, Zhao T (2009) A new species of *Sinocyclocheilus* in Guizhou, China. Sichuan Journal of Zoology 28(3): 321–323. [In Chinese]
- Zhou J, Liu Q, Wang HX, Yang LJ, Zhao DC, Zhang TH, Hou XF (2011) Description on a new species of *Sinocyclocheilus* in Guizhou. Sichuan. Journal of Zoology 30(3): 387–389. <https://doi.org/10.3969/j.issn.1000-7083.2011.03.019> [In Chinese]

- Zhu DG, Zhu Y (2012) A new species of the genus *Sinocyclocheilus* (Cypriniformes, Cyprinidae) from Guangxi, China. *Acta Zootaxonomica Sinica* 37(1): 222–226. [In Chinese]
- Zhu DG, Zhu Y, Lan JH (2011) Description of a new species of Barbinae, *Sinocyclocheilus huangtianensis* from China (Teleostei: Cyprinidae). *Zoological Research* 32(2): 204–207. <https://doi.org/10.3724/SP.J.1141.2011.02204> [In Chinese]

## Appendix I

### Specimens examined

- Sinocyclocheilus angularis* ( $N = 7$ ): China: Guizhou Province: Panzhou City: Baotian Town, (type locality): GZNU 20210505001–05004, GZNU 20210505006–05007, GZNU 0505001, collected by Tao Luo, Jiajun Zhou and Xingliang Wang on 5 May 2021. These specimens are stored at the Guizhou Normal University, Yunyan District, Guiyang City, Guizhou Province, China.
- Sinocyclocheilus bicornutus* ( $N = 2$ ): China: Guizhou Province: Xingren City: Xishan Town, Gaowu Village (type locality): GZNU 20210506001–06002, collected by Tao Luo, Jiajun Zhou and Xingliang Wang on 6 May 2021. These specimens are stored at the Guizhou Normal University, Yunyan District, Guiyang City, Guizhou Province, China.
- Sinocyclocheilus hyalinus* ( $N = 1$ ): China: Yunnan Province: Luxi County: Alu Ancient Cave (type locality): KIZ 916001 (type locality). Currently preserved in Kunming Institute of Zoology, Chinese Academy of Sciences, China.
- Sinocyclocheilus rhinoceros* ( $N = 11$ ): China: Yunnan Province: Luoping County: Huancheng Township, Xiaomingzhai Group (type locality): FWOQB199309001–09006, collected by Weixian Li and Jinneng Tao in September 1993; Yunnan Province: Shizong County: Wulong Township, Huaga Village (topotype locality): FWOQB20180322001–22005, collected by Hongfu Yang on 22 March 2018. Currently these specimens are stored by Yang Hongfu at the fisheries workstation in Qubei County, Yunnan Province, China.
- Sinocyclocheilus zhenfengensis* ( $N = 8$ ): China: Guizhou Province: Zhenfeng County: Zhexiang Town, Shuangrufeng Scenic Area (type locality): GZNU20120701001 (Holotype), GZNU20190707001–07003, GZNU20210619001–19004. These specimens are stored at the Guizhou Normal University, Yunyan District, Guiyang City, Guizhou Province, China.

## Supplementary material 1

### **Measurements of the adult specimens of *Sinocyclocheilus longicornus* sp. nov.**

Authors: Cheng Xu, Tao Luo, Jia-Jun Zhou, Li Wu, Xin-Rui Zhao, Hong-Fu Yang, Ning Xiao, Jiang Zhou

Data type: table (word document).

Copyright notice: This dataset is made available under the Open Database License (<http://opendatacommons.org/licenses/odbl/1.0/>). The Open Database License (ODbL) is a license agreement intended to allow users to freely share, modify, and use this Dataset while maintaining this same freedom for others, provided that the original source and author(s) are credited.

Link: <https://doi.org/10.3897/zookeys.1141.91501.suppl1>

## Supplementary material 2

### **Uncorrected *p*-distance (%) between 53 species of the genus *Sinocyclocheilus* based on mitochondrial *Cyt b* sequences**

Authors: Cheng Xu, Tao Luo, Jia-Jun Zhou, Li Wu, Xin-Rui Zhao, Hong-Fu Yang, Ning Xiao, Jiang Zhou

Data type: table (excel document).

Copyright notice: This dataset is made available under the Open Database License (<http://opendatacommons.org/licenses/odbl/1.0/>). The Open Database License (ODbL) is a license agreement intended to allow users to freely share, modify, and use this Dataset while maintaining this same freedom for others, provided that the original source and author(s) are credited.

Link: <https://doi.org/10.3897/zookeys.1141.91501.suppl2>

## Supplementary material 3

### **Uncorrected *p*-distance (%) between 52 species of the genus *Sinocyclocheilus* based on mitochondrial *ND4* sequences**

Authors: Cheng Xu, Tao Luo, Jia-Jun Zhou, Li Wu, Xin-Rui Zhao, Hong-Fu Yang, Ning Xiao, Jiang Zhou

Data type: table (excel document).

Copyright notice: This dataset is made available under the Open Database License (<http://opendatacommons.org/licenses/odbl/1.0/>). The Open Database License (ODbL) is a license agreement intended to allow users to freely share, modify, and use this Dataset while maintaining this same freedom for others, provided that the original source and author(s) are credited.

Link: <https://doi.org/10.3897/zookeys.1141.91501.suppl3>

## Supplementary material 4

### **Variable loadings for principal components with Eigenvalues greater than 2, from morphometric characters corrected by SL**

Authors: Cheng Xu, Tao Luo, Jia-Jun Zhou, Li Wu, Xin-Rui Zhao, Hong-Fu Yang, Ning Xiao, Jiang Zhou

Data type: table (word document).

Copyright notice: This dataset is made available under the Open Database License (<http://opendatacommons.org/licenses/odbl/1.0/>). The Open Database License (ODbL) is a license agreement intended to allow users to freely share, modify, and use this Dataset while maintaining this same freedom for others, provided that the original source and author(s) are credited.

Link: <https://doi.org/10.3897/zookeys.1141.91501.suppl4>

## Supplementary material 5

### **Parameters in the canonical discriminant analysis (CDA)**

Authors: Cheng Xu, Tao Luo, Jia-Jun Zhou, Li Wu, Xin-Rui Zhao, Hong-Fu Yang, Ning Xiao, Jiang Zhou

Data type: table (word document).

Copyright notice: This dataset is made available under the Open Database License (<http://opendatacommons.org/licenses/odbl/1.0/>). The Open Database License (ODbL) is a license agreement intended to allow users to freely share, modify, and use this Dataset while maintaining this same freedom for others, provided that the original source and author(s) are credited.

Link: <https://doi.org/10.3897/zookeys.1141.91501.suppl5>

# New subgeneric names for the most commercially important shrimp genus *Penaeus* Fabricius, 1798 (Crustacea, Decapoda, Penaeidae)

Tin-Yam Chan<sup>1</sup>

<sup>1</sup> Institute of Marine Biology and Center of Excellence for the Oceans, National Taiwan Ocean University, Keelung 202301, R.O.C., Taiwan

Corresponding author: Tin-Yam Chan ([tychan@mail.ntou.edu.tw](mailto:tychan@mail.ntou.edu.tw))

---

Academic editor: L. E. Bezerra | Received 9 November 2022 | Accepted 23 December 2022 | Published 17 January 2023

---

<https://zoobank.org/5E821334-8E05-4736-9D58-CE27C132C80C>

---

**Citation:** Chan T-Y (2023) New subgeneric names for the most commercially important shrimp genus *Penaeus* Fabricius, 1798 (Crustacea, Decapoda, Penaeidae). ZooKeys 1141: 29–40. <https://doi.org/10.3897/zookeys.1141.97349>

---

## Abstract

Although a recent comprehensive molecular phylogenetic study on *Penaeus* Fabricius, 1798 reinstated a single genus for these economically important shrimps, several clades in the molecular phylogenetic tree do not have formal names. Subgeneric names are given herein to five of these clades if *Penaeus* is to be split. A key to the subgenera in *Penaeus* is also provided.

## Keywords

Key, marine invertebrates, new subgenus, nomenclature, stability, taxonomy

## Introduction

The most comprehensive study to date on the phylogenetic relationships amongst the members of the genus *Penaeus* s.l. Fabricius, 1798 was by Yang et al. (2023), which suggested that a single genus should be reinstated for these commercially important shrimps. Their study also proposes that if those molecular clades revealed in the phylogenetic tree of *Penaeus* s.l. (Yang et al. 2023: fig. 3) are recognized as taxonomic groups, the use of subgenera is preferable; the use of this rank would also reduce confusion and maintain stability for non-taxonomists who use the name.

In their phylogenetic study, Yang et al. (2023: fig. 3) showed that up to 11 sub-generic-level clades can be recognized. While many of these clades have been named in the past, five of them, however, remain un-named. In the interest of nomenclatural stability and consistency in discussing their systematics, I here propose to apply formal names for them. This action is justified especially if the peculiar taxon *Marsupenaeus* Tirmizi, 1971, which has a very specialized pouch-like thelycum, is to be maintained.

A key to these 11 subgenera is also provided even though all important characters used have already been proved to be neither synapomorphic nor evolutionary informative in Yang et al. (2023).

## Systematic account

### *Penaeus* (*Penaeus*) Fabricius, 1798

**Type species.** *Penaeus monodon* Fabricius, 1798.

**Gender of subgenus.** Masculine.

**Diagnosis.** Rostrum generally armed with 3 ventral teeth. Median sulcus on postrostral carina shallow to indistinct. Adrostral sulcus extending posteriorly more or less to level of epigastric tooth. Gastrofrontal carina absent. Cervical carina with dorsal end a distance from dorsal carapace. Hepatic carina distinct, nearly horizontal. First pereopod with distinct ischial spine. Fifth pereopod without exopod. Sixth abdominal somite completely lacking dorsolateral sulcus. Telson without lateral spines. Thelycum closed.

**Species included.** *Penaeus* (*Penaeus*) *monodon* Fabricius, 1798, *Penaeus* (*Penaeus*) *simplex* Chan, Muchlisin & Hurzaid, 2021.

**Remarks.** Although this is the nominotypical subgenus of *Penaeus*, it is unusual in lacking an epipod on the fifth pereopod; the subgenus contains only two of the 32 recognized species in the genus.

### *Penaeus* (*Melicertus*) Rafinesque, 1814

**Type species.** *Melicertus tigrinus* Rafinesque, 1814 (= *Cancer kerathurus* Forskål, 1775).

**Gender of subgenus.** Masculine.

**Diagnosis.** Rostrum usually bearing 1 ventral tooth. Median sulcus at postrostral carina deep, long, about half carapace length. Adrostral sulcus as wide as postrostral carina, extending to near posterior margin of carapace. Gastrofrontal carina distinct and with posterior end turning anterodorsally. Cervical carina long, extending almost to dorsal carapace. Hepatic carina distinct. First pereopod with ischial spine small to absent. Fifth pereopod bearing exopod. Sixth abdominal somite completely lacking dorsolateral sulcus. Telson with 3 pairs of lateral spines. Thelycum closed.

**Species included.** *Penaeus* (*Melicertus*) *kerathurus* (Forskål, 1775).

**Remarks.** Amongst the members of *Penaeus*, only this subgenus has a geographical distribution in the eastern Atlantic and the Mediterranean. This subgenus is also unique in the genus by having a long cervical carina which has the dorsal end almost reaching the dorsal carapace.

### *Penaeus (Fenneropenaeus) Pérez Farfante, 1969*

**Type species.** *Penaeus indicus* H. Milne Edwards, 1837.

**Gender of subgenus.** Masculine.

**Diagnosis.** Rostrum generally bearing 2–5 ventral teeth. Postrostral carina without median sulcus, sometimes with pits or sunken areas. Adrostral sulcus extending posteriorly more or less to epigastric tooth. Gastrofrontal carina absent. Cervical carina with dorsal end a distance from dorsal carapace. Hepatic carina often absent, if present, ill-defined. First pereopod with small to minute ischial spine. Fifth pereopod bearing exopod. Sixth abdominal somite completely lacking dorsolateral sulcus. Telson without lateral spines. Thelycum closed.

**Species included.** *Penaeus (Fenneropenaeus) chinensis* (Osbeck, 1765), *Penaeus (Fenneropenaeus) indicus* H. Milne Edwards, 1837, *Penaeus (Fenneropenaeus) merguensis* De Man, 1888, *Penaeus (Fenneropenaeus) penicillatus* Alcock, 1905, *Penaeus (Fenneropenaeus) silasi* Muthu & Motoh, 1979.

**Remarks.** This subgenus is unique in the genus by lacking a distinct hepatic carina. Only *P. (Fenneropenaeus) chinensis* bears an ill-defined hepatic carina while all other species of *Penaeus (Fenneropenaeus)* lack a hepatic carina. As mentioned in Ma et al. (2011) and Yang et al. (2023), *Fenneropenaeus konkani* Chanda & Bhattacharya, 2003 is very likely to be an invalid taxon with a deformed rostrum and a synonym of a known species of *Penaeus (Fenneropenaeus)*.

### *Penaeus (Litopenaeus) Pérez Farfante, 1969*

**Type species.** *Penaeus vannamei* Boone, 1931.

**Gender of subgenus.** Masculine.

**Diagnosis.** Rostrum usually bearing 2–4 ventral teeth. Postrostral carina without median sulcus, only sometimes with pits or sunken areas. Adrostral sulcus extending posteriorly more or less to epigastric tooth. Gastrofrontal carina absent. Cervical carina with dorsal end a distance from dorsal carapace. Hepatic carina distinct. First pereopod with distinct ischial spine. Fifth pereopod bearing exopod. Sixth abdominal somite bearing weak to distinct dorsolateral sulcus. Telson without lateral spines. Thelycum open.

**Species included.** *Penaeus (Litopenaeus) occidentalis* Streets, 1871; *Penaeus (Litopenaeus) schmitti* Burkenroad, 1936; *Penaeus (Litopenaeus) setiferus* (Linnaeus, 1767); *Penaeus (Litopenaeus) stylirostris* Stimpson, 1871; *Penaeus (Litopenaeus) vannamei* Boone, 1931.

**Remarks.** This subgenus is unique in the genus by having an open thelycum.

***Penaeus (Marsupenaeus) Tirmizi, 1971***

**Type species.** *Penaeus canaliculatus* var. *japonicus* Bate, 1888.

**Gender of subgenus.** Masculine.

**Diagnosis.** Rostrum generally armed with 1 ventral tooth. Median sulcus at postrostral carina deep, long, about half carapace length. Adrostral sulcus extending to near posterior margin of carapace, posterior part somewhat narrower than postrostral carina. Gastrofrontal carina distinct, with posterior end turning anterodorsally. Cervical carina with dorsal end a distance from dorsal carapace. Hepatic carina distinct. First pereopod with ischial spine minute or absent. Fifth pereopod bearing exopod. Sixth abdominal somite completely lacking dorsolateral sulcus. Telson with 3 pairs of lateral spines. Thelycum pouch-like.

**Species included.** *Penaeus (Marsupenaeus) japonicus* Bate, 1888, *Penaeus (Marsupenaeus) pulchricaudatus* Stebbing, 1914.

**Remarks.** Although this subgenus is unique in the genus by having a highly specialized pouch-like thelycum, males and juveniles are morphologically very similar to those of the subgenus *Penaeus (Oleopenaeus)* subgen. nov., except for coloration [see “Remarks” under *Penaeus (Oleopenaeus)* subgen. nov.].

***Penaeus (Farfantepeneus) Burukovsky, 1972***

**Type species.** *Penaeus brasiliensis* var. *aztecus* Ives, 1891.

**Gender of subgenus.** Masculine.

**Diagnosis.** Rostrum usually bearing 2 ventral teeth. Median sulcus at postrostral carina generally distinct, long. Adrostral sulcus extending to near posterior margin of carapace. Gastrofrontal carina distinct, with posterior end not turning anteriorly. Cervical carina with dorsal end a distance from dorsal carapace. Hepatic carina distinct. First pereopod with strong ischial spine. Fifth pereopod bearing exopod. Sixth abdominal somite with distinct dorsolateral sulcus. Telson without lateral spines. Thelycum closed.

**Species included.** *Penaeus (Farfantepeneus) aztecus* Ives, 1891, *Penaeus (Farfantepeneus) brasiliensis* Latreille, 1817, *Penaeus (Farfantepeneus) brevirostris* Kingsley, 1878, *Penaeus (Farfantepeneus) californiensis* Holmes, 1900, *Penaeus (Farfantepeneus) duorarum* Burkenroad, 1939, *Penaeus (Farfantepeneus) isabellae* Tavares & Gusmão, 2016, *Penaeus (Farfantepeneus) notialis* Pérez Farfante, 1967, *Penaeus (Farfantepeneus) paulensis* Pérez Farfante, 1967, *Penaeus (Farfantepeneus) subtilis* Pérez Farfante, 1967.

**Remarks.** This subgenus together with *Penaeus (Litopenaeus)* are often called the American *Penaeus*. Morphologically these two subgenera are markedly different from each other and had long been thought to be evolutionary far apart (see Burkenroad 1934; Kubo 1949; Pérez Farfante 1969; Dall et al. 1990; von Sternberg and Motoh 1995; Pérez Farfante and Kensley 1997; von Sternberg 1997). They are, however, very closely related genetically (see Yang et al. 2023). At present only one morphological character, the sixth abdominal somite with dorsolateral sulcus, is found to separate the

American *Penaeus* from other congeneric species. Recent molecular analysis has suggested that *P. (Farfantepenaeus) notialis*, originally described as a subspecies of *P. (Farfantepenaeus) duorarum*, may not be distinct at the species level (Timm et al. 2019).

***Penaeus (Altiopeneaus) subgen. nov.***

<https://zoobank.org/594460D1-98BB-4C4B-9902-068EB4E1DEBA>

**Type species.** *Penaus marginatus* Randall, 1840.

**Gender of subgenus.** Masculine.

**Diagnosis.** Rostrum usually armed with 2 ventral teeth. Postrostral carina lacking median sulcus. Adrostral sulcus as wide as postrostral carina, extending to near posterior margin of carapace. Gastrofrontal carina distinct, with posterior end turning anterodorsally. Cervical carina with dorsal end a distance from dorsal carapace. Hepatic carina distinct. First pereopod with strong ischial spine. Fifth pereopod bearing exopod. Sixth abdominal somite completely lacking dorsolateral sulcus. Telson with 3 pairs of lateral spines. Thelycum closed.

**Etymology.** The name *Altiopeneaus* (from the Latin *altio* for deeper) alluding to members of this subgenus which have a deeper vertical (depth) distribution than other *Penaeus*.

**Species included.** *Penaus (Altiopeneaus) marginatus* Randall, 1840

**Remarks.** This taxon corresponds to “gen. nov. 5” in the 11-genus scheme of fig. 3 in Yang et al. (2023). This subgenus is unusual in the genus in inhabiting deeper waters (see Chan 1998). It is also unique amongst the “grooved” species by completely lacking a median sulcus on the postrostral carina.

***Penaus (Eopenaeus) subgen. nov.***

<https://zoobank.org/4BBD630C-8CB8-4AEE-89F0-949C019DFFAB>

**Type species.** *Penaus semisulcatus* De Haan, 1844.

**Gender of subgenus.** Masculine.

**Diagnosis.** Rostrum generally bearing 3 or 4 ventral teeth. Median sulcus on postrostral carina present or absent. Adrostral sulcus extending posteriorly more or less to level of epigastric tooth. Gastrofrontal carina absent. Cervical carina with dorsal end a distance from dorsal carapace. Hepatic carina distinct and usually sloping anteroventrally. First pereopod with distinct ischial spine. Fifth pereopod bearing exopod. Sixth abdominal somite completely lacking dorsolateral sulcus. Telson without lateral spines. Thelycum closed.

**Etymology.** The name *Eopenaeus* (from the Greek *Eos* for others) refers to this subgenus being morphologically close to the nominotypical subgenus of *Penaus* while the molecular data revealed that this subgenus is actually more derived than *Penaus* (*Penaus*) (Yang et al. 2023).

**Species included.** *Penaus (Eopenaeus) esculentus* Haswell, 1879, *Penaus (Eopenaeus) semisulcatus* De Haan, 1844.

**Remarks.** This taxon corresponds to “gen. nov.1” in the 11-genus scheme of fig. 3 in Yang et al. (2023). Morphologically this subgenus is similar to *Penaeus* (*Litopenaeus*). Other than having different types of thelycum, these two subgenera can be distinguished by the body coloration [banded in *Penaeus* (*Eopenaeus*) subgen. nov. but not banded in *Penaeus* (*Litopenaeus*)] and the development of the dorsolateral sulcus on the sixth abdominal somite [weak to distinct in *Penaeus* (*Litopenaeus*) but completely absent in *Penaeus* (*Eopenaeus*) subgen. nov.]. Pérez Farfante (1969) and Pérez Farfante and Kensley (1997) also pointed out that there are differences in the shape of the petasma between these two subgenera, with the ventral costa reaching or not reaching the distal margin of the lateral lobe in *Penaeus* (*Eopenaeus*) subgen. nov. and *Penaeus* (*Litopenaeus*), respectively.

***Penaeus* (*Ischiopenaeus*) subgen. nov.**

<https://zoobank.org/716AD2C7-AEDE-4549-94B3-65378708E2DB>

**Type species.** *Penaeus longistylus* Kubo, 1943.

**Gender of subgenus.** Masculine.

**Diagnosis.** Rostrum generally armed with 1 ventral tooth. Median sulcus at postrostral carina deep but distinctly shorter than half carapace length. Adrostral sulcus somewhat wider than postrostral carina and extending to near posterior margin of carapace. Gastrofrontal carina distinct and with posterior end turning anterodorsally. Cervical carina with dorsal end a distance from dorsal carapace. Hepatic carina distinct. First pereopod with strong ischial spine. Fifth pereopod bearing exopod. Sixth abdominal somite completely lacking dorsolateral sulcus. Telson with 3 pairs of lateral spines. Thelycum closed.

**Etymology.** The name *Ischiopenaeus* alludes to the presence of a strong ischial spine at the first pereopod in this subgenus of *Penaeus*.

**Species included.** *Penaeus* (*Ischiopenaeus*) *longistylus* Kubo, 1943

**Remarks.** This taxon corresponds to “gen. nov. 4” in the 11-genus scheme of fig. 3 in Yang et al. (2023). This subgenus differs from almost all the non-American “grooved” species in the first pereopod bearing a strong ischial spine (vs. small to absent). Another non-American “grooved” species with a strong ischial spine at the first pereopod is *P.* (*Altiopenaeus*) *marginatus*, which lacks a median sulcus on the postrostral carina and generally has two ventral rostral teeth. Thus, the enigmatic *Melicertus similis* Chanda & Bhattacharya, 2002 described from the Andaman Sea likely represents juveniles of *P.* (*Ischiopenaeus*) *longistylus* as its original description and figures (Chanda and Bhattacharya 2002: figs 1, 6) indicated the presence of postrostral sulcus, only one ventral rostral tooth and the first pereopod bearing a strong ischial spine. The “absence” of lateral spines on the telson in *Melicertus similis* is likely evidence that Chanda and Bhattacharya’s (2002) material are juveniles (total length including rostrum less than 80 mm) as juveniles of *Penaeus* generally have the lateral spines on the telson rather small and can be easily detached or overlooked.

***Penaeus (Oleopenaeus)* subgen. nov.**

<https://zoobank.org/12C57BB8-B27D-4AD7-B3C3-2AD35708E4EC>

**Type species.** *Penaeus latisulcatus* Kishinouye, 1896.

**Gender of subgenus.** Masculine.

**Diagnosis.** Rostrum generally armed with 1 ventral tooth. Median sulcus at postrostral carina deep, long, about half carapace length. Adrostral sulcus as wide as postrostral carina, extending to near posterior margin of carapace. Gastrofrontal carina distinct, with posterior end turning anterodorsally. Cervical carina with dorsal end a distance from dorsal carapace. Hepatic carina distinct. First pereopod with ischial spine minute or absent. Fifth pereopod bearing exopod. Sixth abdominal somite completely lacking dorsolateral sulcus. Telson with 3 pairs of lateral spines. Thelycum closed.

**Etymology.** The name *Oleopenaeus* (from the Latin *olea* for olive coloured) refers to the more or less uniform greenish-yellow body coloration of this group of *Penaeus* shrimps.

**Species included.** *Penaeus (Oleopenaeus) hathor* Burkenroad, 1959, *Penaeus (Oleopenaeus) latisulcatus* Kishinouye, 1896, *Penaeus (Oleopenaeus) plebejus* Hess, 1865.

**Remarks.** This taxon corresponds to “gen. nov. 3” in the 11-genus scheme of fig. 3 in Yang et al. (2023). Except for the shape of the thelycum and body coloration, this subgenus is morphologically very similar to *Penaeus (Marsupenaeus)* (see Chan 1998; Tsoi et al. 2014). The thelycum is of the normal closed type in *Penaeus (Oleopenaeus)* subgen. nov. but pouch-like in *Penaeus (Marsupenaeus)*. With regards to the colour in life, the body is not banded in *Penaeus (Oleopenaeus)* subgen. nov. but is covered with thick cross bands in *Penaeus (Marsupenaeus)*. The taxonomic status of *P. (O.) hathor* is still uncertain if it merely represents a subspecies of *P. (O.) latisulcatus* or even a synonym of the latter, as both morphological and genetic differences between these two taxa are rather minor (Holthuis 1980; Miquel 1984; Chan 1998; Ma et al. 2011; 0.8% sequence divergence in COIb 512 bp, Yang et al. 2023: table 1).

***Penaeus (Plagosopenaeus)* subgen. nov.**

<https://zoobank.org/B5F2E1F8-8B97-402E-AC9A-57B8AFCC43EB>

**Type species.** *Palaemon canaliculatus* Olivier, 1811.

**Gender of subgenus.** Masculine.

**Diagnosis.** Rostrum generally bearing 1 ventral tooth. Median sulcus at postrostral carina deep, long, about half carapace length. Adrostral sulcus as wide as postrostral carina, extending to near posterior margin of carapace. Gastrofrontal carina distinct, posterior end turning anterodorsally. Cervical carina with dorsal end a distance from dorsal carapace. Hepatic carina distinct. First pereopod with ischial spine minute or absent. Fifth pereopod bearing exopod. Sixth abdominal somite completely lacking dorsolateral sulcus. Telson without lateral spines. Thelycum closed.

**Etymology.** The name *Plagosopenaeus* (from the Latin *plagosus* for banded) refers to this subgenus of *Penaeus*, which has a very striking banded body coloration.

**Species included.** *Penaeus (Plagosopenaeus) canaliculatus* (Olivier, 1811).

**Remarks.** This taxon corresponds to “gen. nov. 2” in the 11-genus scheme of fig. 3 in Yang et al. (2023). Morphologically, including coloration, this subgenus is extremely similar to *Penaeus (Marsupenaeus)* (see Yu and Chan 1986; Chan 1998) and such close affinity is also supported by the molecular data (Yang et al. 2023: figs 2, 3). *Penaeus (Plagosopenaeus)* subgen. nov. only differs from *Penaeus (Marsupenaeus)* in lacking lateral spines on the telson (vs. bearing three pairs of lateral spines), the thelycum not pouch-like and the last transverse band on the sixth abdominal somite not interrupted (Chan 1998).

### Key to subgenera in *Penaeus*

- 1 Adrostral sulcus and carina long, reaching near posterior margin of carapace; gastrofrontal carina present ..... **2**
- Adrostral sulcus and carina short, extending posteriorly at most to mid-carapace around level of epigastric tooth; gastrofrontal carina absent..... **8**
- 2 Gastrofrontal carina not turning anteriorly at posterior end; sixth abdominal tergite with well-defined dorsolateral sulcus .....  
..... *Penaeus (Farfantepenaeus) Burukovsky, 1972*
- Gastrofrontal carina turning anterodorsally at posterior end; sixth abdominal tergite without dorsolateral sulcus..... **3**
- 3 Telson lacking lateral spines ..... *Penaeus (Plagosopenaeus) subgen. nov.*
- Telson armed with 3 pairs of movable lateral spines ..... **4**
- 4 Postrostral carina without median sulcus; usually 2 ventral rostral teeth.....  
..... *Penaeus (Altiopenaeus) subgen. nov.*
- Postrostral carina bearing median sulcus; usually 1 ventral rostral tooth..... **5**
- 5 Median sulcus at postrostral carina distinctly shorter than half carapace length; first pereopod armed with strong ischial spine.....  
..... *Penaeus (Ischiopenaeus) subgen. nov.*
- Median sulcus at postrostral carina more or less as long as half carapace length; first pereopod with ischial spine minute or absent..... **6**
- 6 Cervical carina with dorsal end almost reaching dorsal carapace.....  
..... *Penaeus (Melicertus) Rafinesque, 1814*
- Cervical carina with dorsal end a distance from dorsal carapace ..... **7**
- 7 Thelycum pouch-like; posterior part of adrostral sulcus somewhat narrower than postrostral carina; body banded .....  
..... *Penaeus (Marsupenaeus) Tirmizi, 1971*
- Thelycum closed but not pouch-like; adrostral sulcus as wide as postrostral carina; body not banded ..... *Penaeus (Oleopenaeus) subgen. nov.*
- 8 Hepatic carina absent or ill-defined.....  
..... *Penaeus (Fenneropenaeus) Pérez Farfante, 1969*
- Hepatic carina distinct..... **9**

- 9 Fifth pereopod without exopod; hepatic carina nearly horizontal .....  
 ..... *Penaeus (Penaeus) Fabricius, 1798*
- Fifth pereopod bearing exopod; hepatic carina usually sloping anteroventrally ..... **10**
- 10 Thelycum open; dorsolateral sulcus, though sometimes rather weak, present on sixth abdominal somite ..... *Penaeus (Litopenaeus) Pérez Farfante, 1969*
- Thelycum closed; dorsolateral sulcus completely absent on sixth abdominal somite ..... *Penaeus (Eopenaeus) subgen. nov.*

## Acknowledgements

Sincerely thanks are extended to L. Corbari and P. R. Moreno-Martin-Lefèvre and S. Faninoz of the Muséum national d'Histoire naturelle, Paris for allowing the author to examine the exceptionally rich *Penaeus* collection in their museum; Peter K.L. Ng of the University of Singapore for his comments on the new subgenus names. This work was supported by grants from the National Science and Technology Council, Taiwan, R.O.C. and the Center of Excellence for the Oceans (National Taiwan Ocean University), which is financially supported from The Featured Areas Research Center Program within the framework of the Higher Education Sprout Project by the Ministry of Education (MOE) in Taiwan, R.O.C.

## References

- Alcock A (1905) A revision of the "Genus" *Penaeus*, with diagnoses of some new species and varieties. *Annals & Magazine of Natural History* 16(7): 508–532. <https://doi.org/10.1080/03745480509443078>
- Bate CS (1888) Report on the Crustacea Macrura Collected by HMS Challenger During the Years 1873–1876, Zoology. Neill and Company, Edinburgh, 942 pp. [pls 1–157]
- Boone L (1931) A collection of anomuran and macruran Crustacea from the Bay of Panama and the fresh waters of the Canal Zone. *Bulletin of the American Museum of Natural History* 63: 137–189.
- Burkenroad MD (1934) Littoral Penaeidea chiefly from the Bingham Oceanographic Collection, with a revision of *Penaeopsis* and descriptions of two new genera and eleven new American species. *Bulletin of the Bingham Oceanographic Collection* 4: 1–109.
- Burkenroad MD (1936) A new species of *Penaeus* from the American Atlantic. *Anais da Academia Brasileira de Ciências* 8: 315–318.
- Burkenroad MD (1939) Further observations on Penaeidae of the northern Gulf of Mexico. *Bulletin of the Bingham Oceanographic Collection* 6(6): 1–62.
- Burkenroad MD (1959) Decapoda Macrura I. Penaeidae. Mission Robert Ph. Dollfus Egypte XXV. Mission Robert Ph. Dollfus Égypte. *Résultats Scientifique* 3: 67–92.

- Burukovsky RN (1972) Some problems of the systematics and distribution of shrimps of the genus *Penaeus*. Trudy AtlantNIRO, Kaliningrad 2: 3–21. [in Russian]
- Chan TY (1998) Shrimps and prawns. In: Carpenter KE, Niem VH (Eds) FAO Species Identification Guide for Fishery Purposes. The Living Marine Resources of the Western Central Pacific. Food and Agriculture Organization of the United Nations, Rome, 851–971.
- Chan TY, Muchlisin ZA, Hurzaid A (2021) Verification of a pseudocryptic species in the commercially important tiger prawn *Penaeus monodon* Fabricius, 1798 (Decapoda: Penaeidae) from Aceh Province, Indonesia. Journal of Crustacean Biology 41(1): 1–10. <https://doi.org/10.1093/jcabi/ruaa096>
- Chanda A, Bhattacharya T (2002) *Melicertus similis*, a new species of prawn, Decapoda: Penaeidae, from India. Journal of the Bombay Natural History Society 99: 495–498.
- Chanda A, Bhattacharya T (2003) *Fenneropenaeus konkani*, a new species of prawn (Decapoda: Penaeidae) from Indian Coast. Science & Culture 69: 229–230.
- Dall W, Hill BJ, Rothlisberg NW, Staples DJ (1990) The biology of Penaeidae. Advances in Marine Biology 27: 1–484.
- de Haan W (1833–1850) Crustacea. In: von Siebold PF (Ed.) Fauna Japonica sive Descriptio Animalium, quae in Itinere per Japoniam, Jussu et Auspiciis Superiorum, qui Summum in India Batava Imperium Tenent, Suspecto, Annis 1823–1830 Collegit, Notis, Observationibus et Adumbrationibus Illustravit. Lugduni-Batavorum, 243 pp. [pls A–J, L–Q, 1–55]
- de Man JG (1888) Report on the podophthalmous Crustacea of the Mergui Archipelago, collected for the Trustees of the Indian Museum, Calcutta, by Dr. John Anderson F.R.S., Superintendent of the Museum. Zoological Journal of the Linnean Society 22: 1–305. [pls 1–19] <https://doi.org/10.1111/j.1096-3642.1888.tb00032.x>
- Fabricius JC (1798) Supplementum Entomologiae Systematicae. Proft et Storch, Hafniae, 572 pp.
- Forskål P (1775) Descriptiones Animalium Avium, Amphibiorum, Piscium, Insectorum, Vermium; quae in Itinere Orientali observavit. Mölleri, Haunia, 164 pp. <https://doi.org/10.5962/bhl.title.2154>
- Haswell WA (1879) On the Australian species of *Penaeus*, in the Macleay Museum, Sydney. Proceedings of the Linnean Society of New South Wales 4: 38–44. <https://doi.org/10.5962/bhl.part.22836>
- Hess W (1865) Beiträge zur Kenntnis der Decapoden-Krebse Ost-Australiens. Archiv für Naturgeschichte 31: 127–173. [pls 6–7] <https://doi.org/10.5962/bhl.part.15862>
- Holmes SJ (1900) Synopsis of California stalk-eyed Crustacea. Occasional papers of the California Academy of Sciences 7: 1–262. [pls 1–4] <https://doi.org/10.5962/bhl.title.31431>
- Holthuis LB (1980) FAO species catalogue. Vol. 1 - Shrimps and prawns of the world. An annotated catalogue of species of interest to fisheries. FAO Fisheries Synopsis 125(1): 1–271. [i–xvii]
- Ives JE (1891) Crustacea from the northern coast of Yucatan, the harbor of Vera Cruz, the west coast of Florida and the Bermuda Islands. Proceedings. Academy of Natural Sciences of Philadelphia 1891: 176–207. [pls 5–6]
- Kingsley JS (1878) Notes on the North American Caridea in the Museum of the Peabody Academy of Science at Salem, Mass. Proceedings. Academy of Natural Sciences of Philadelphia 1878: 89–98.
- Kishinouye K (1896) Note on a Japanese *Penaeus* and its classification. Zoological Magazine 8: 372–374. [in Japanese] [Dobutsugaku Zasshi]

- Kubo I (1943) Diagnosis of a new species of the genus *Penaeus*. Suisan Kenkyusi 38: 200–201.
- Kubo I (1949) Studies on penaeids of Japanese and its adjacent waters. Journal of the Tokyo College of Fisheries 36: 1–467.
- Latreille PA (1817) Pénée. *Penaeus*. Nouveau Dictionnaire d'Histoire Naturelle 25: 152–156.
- Linnaeus C (1767) Systema Naturæ per Regna tria Naturæ, Secundum Classes, Ordines, Genera, Species, cum Characteribus, Differentiis, Synonymis, Locis (13<sup>th</sup> Edn., Vol. 1). Vindobonae, 1327 pp. <https://doi.org/10.5962/bhl.title.156772>
- Ma KY, Chan TY, Chu KH (2011) Refuting the six-genus classification of *Penaeus* s.l. (Dendrobranchiata, Penaeidae): A combined analysis of mitochondrial and nuclear genes. Zoologica Scripta 40(5): 498–508. <https://doi.org/10.1111/j.1463-6409.2011.00483.x>
- Milne Edwards H (1834–1840) Histoire naturelle des Crustacés, comprenant l'anatomie, la physiologie et la classification de ces animaux. Librairie encyclopédique de Roret, Paris, 468 pp. [1–532, 1–638, 1–32.] [pls 1–42] <https://doi.org/10.5962/bhl.title.16170>
- Miquel JC (1984) Notes on Indo-West Pacific Penaeidae, 4. On the two subspecies of *Penaeus latisulcatus* Kishinouye. Crustaceana 46(1): 104–107. <https://doi.org/10.1163/156854084X00108>
- Muthu MS, Motoh H (1979) On a new species of *Penaeus* (Crustacea, Decapoda, Penaeidae) from North Borneo. Crustacean Research 9(0): 64–70. [https://doi.org/10.18353/rcrustacea.9.0\\_64](https://doi.org/10.18353/rcrustacea.9.0_64)
- Olivier AG (1811) Suite de l'Introduction à l'Histoire Naturelle des Insectes. Palèmon. In: Olivier AG (Ed.) Encyclopédie Méthodique. Histoire Naturelle. Insectes (Vol. 8). H. Agasse, Imprimeur-Libraire, Paris, 656–670.
- Osbeck P (1765) Reisenach Ostindien und China. Nebst O.Toreens Reise nach Suratte und C.G. Ekebergs Nachricht von der Landwirthschaft der Chineser. Aus dem Schwedischen übersetzt von J.G. Georgi. Rostock, 552 pp. <https://doi.org/10.5962/bhl.title.120128>
- Pérez Farfante I (1967) A new species and two new subspecies of shrimp of the genus *Penaeus* from the Western Atlantic. Proceedings of the Biological Society of Washington 80: 83–100.
- Pérez Farfante I (1969) Western Atlantic shrimps of the genus *Penaeus*. Fish Bulletin 67: 461–591.
- Pérez Farfante I, Kensley B (1997) Penaeoid and sergestoid shrimps and prawns of the world. Keys and diagnoses for the families and genera. Mémoires du Muséum National d'Histoire naturelle, Paris 175: 1–233.
- Rafinesque CS (1814) Précis des Découvertes et Travaux Somnologiques de Mr. C.S. Rafinesque-Schmaltz entre 1800 et 1814 ou Choix Raisonné de ses Principales Découvertes en Zoologie et en Botanique, pour Servir d'introduction à ses Ouvrages Futurs. Royale Typographie Militaire, Palerme, 56 pp. <https://doi.org/10.5962/bhl.title.6135>
- Randall JW (1840) Catalogue of the Crustacea brought by Thomas Nuttall and J.K. Townsend, from the West Coast of North America and the Sandwich Islands, with descriptions of such species as are apparently new, among which are included several species of different localities, previously existing in the collection of the Academy. Journal of the Academy of Natural Sciences of Philadelphia 8: 106–147. [pls 3–7] <https://doi.org/10.5962/bhl.title.119921>
- Stebbing TRR (1914) South African Crustacea. Part VII of S.A. Crustacea, for the Marine Investigations in South Africa. Annals of the South African Museum 15: 1–55. [pls 1–12] <https://doi.org/10.5962/bhl.part.22194>

- von Sternberg R (1997) Phylogenetic and systematic position of the *Penaeus* subgenus *Litopenaeus* (Decapoda: Penaeidae). *Revista de Biología Tropical* 44(3)–45(1): 441–451.
- von Sternberg R, Motoh H (1995) Notes on the phylogeny of the American *Penaeus* shrimps (Decapoda: Dendrobranchiata: Penaeidae). *Crustacean Research* 24(0): 146–156. [https://doi.org/10.18353/crustacea.24.0\\_146](https://doi.org/10.18353/crustacea.24.0_146)
- Stimpson W (1871) Notes on North American Crustacea, in the museum of the Smithsonian Institution. No. III. *Annals of the Lyceum of Natural History of New York* 10: 119–163. [preprint issued in 1871, paper in bound volume in 1874 with page numbers 92–136]
- Streets TH (1871) Catalogue of Crustacea from the Isthmus of Panama, collected by J.A. McNeil. *Proceedings. Academy of Natural Sciences of Philadelphia* 1871: 238–243.
- Tavares C, Gusmão J (2016) Description of a new Penaeidae (Decapoda: Dendrobranchiata) species, *Farfantepenaeus isabelae* sp. nov. *Zootaxa* 4171(3): 505–516. <https://doi.org/10.11646/zootaxa.4171.3.6>
- Timm L, Browder JA, Simon S, Jackson TL, Zink IC, Bracken-Grissom HD (2019) A tree money grows on: the first inclusive molecular phylogeny of the economically important pink shrimp (Decapoda: *Farfantepenaeus*) reveals cryptic diversity. *Invertebrate Systematics* 33: 488–500. <https://doi.org/10.1071/IS18044>
- Tirmizi NM (1971) *Marsupenaeus*, a new subgenus of *Penaeus* Fabricius, 1798 (Decapoda, Natantia). *Pakistan Journal of Zoology* 3: 193–194.
- Tsoi KH, Ma KY, Fennessy ST, Chu KH, Chan TY (2014) Verification of the cryptic species *Penaeus pulchricaudatus* in the commercially important kuruma shrimp *P. japonicus* (Decapoda: Penaeidae) using molecular taxonomy. *Invertebrate Systematics* 28(5): 476–490. <https://doi.org/10.1071/IS14001>
- Yang CH, Ma KY, Chu KH, Chan TY (2023) Making sense of the taxonomy of the most commercially important shrimps *Penaeus* Fabricius, 1798 s. l. (Crustacea: Decapoda: Penaeidae), a way forward. *Aquaculture (Amsterdam, Netherlands)* 563: 1–10. <https://doi.org/10.1016/j.aquaculture.2022.738955>
- Yu HP, Chan TY (1986) *The Illustrated Penaeoid Prawns of Taiwan*. Southern Materials Center, Taipei, 183 pp.

# Taxonomic study of the genus *Kuvera* Distant, 1906 (Hemiptera, Fulgoromorpha, Cixiidae) with descriptions of two new species from China

Yan Zhi<sup>1</sup>, Lin Yang<sup>2,3</sup>, Xiang-Sheng Chen<sup>2,3</sup>

**1** Key Laboratory of Medical Insects, Guizhou Medical University, Guiyang, Guizhou, 550025, China  
**2** Institute of Entomology, Guizhou University, Guiyang, Guizhou, 550025, China **3** The Provincial Special Key Laboratory for Development and Utilization of Insect Resources of Guizhou, Guizhou University, Guiyang, Guizhou, 550025, China

Corresponding author: Xiang-Sheng Chen ([chenxs3218@163.com](mailto:chenxs3218@163.com))

---

Academic editor: Pavel Stoev | Received 23 March 2022 | Accepted 13 December 2022 | Published 18 January 2023

---

<https://zoobank.org/917B8619-82C6-444D-A394-8D0E951DE940>

---

**Citation:** Zhi Y, Yang L, Chen X-S (2023) Taxonomic study of the genus *Kuvera* Distant, 1906 (Hemiptera, Fulgoromorpha, Cixiidae) with descriptions of two new species from China. ZooKeys 1141: 41–63. <https://doi.org/10.3897/zookeys.1141.84211>

---

## Abstract

Two new species of genus *Kuvera* Distant, 1906, *Kuvera campyloptropa* Zhi & Chen, **sp. nov.** and *K. elongata* Zhi & Chen, **sp. nov.**, and a new Chinese record, *K. basarukini* Emeljanov, 1998, are described and illustrated from China. The females of two other species of *Kuvera*, *K. laticeps* (Metcalf, 1936) and *K. ussuriensis* (Vilbaste, 1968), are described for the first time. An updated identification key to Chinese species of *Kuvera* is given.

## Keywords

Auchenorrhyncha, Eastern Palearctic region, Oriental region, planthopper, Sino-Japanese region, taxonomy

## Introduction

The planthopper genus *Kuvera* was established by Distant (1906), with *K. semihyalina* Distant, 1906 as the type species by original designation. This genus belongs to the tribe Semonini of subfamily Cixiinae (Hemiptera: Cixiidae). Diagnostic features of Semonini include that the postclypeus is swollen, its clypeofrontal suture is convex, and the median carina of frons is incomplete or obscure (Holzinger et al. 2002; Emeljanov

2002). Previously 25 species in this genus have been recorded successively from Eastern Palearctic, Sino-Japanese and Oriental regions (e.g., Distant 1906; Matsumura 1914; Muir 1922; Dlabola 1957; Vilbaste 1968; Anufriev 1987; Emeljanov 1998; Tsaour et al. 1991; Rahman et al. 2017; Luo et al. 2019; Bourgoïn 2022). The latest taxonomic works on *Kuvera* by Luo et al. (2019) included a description of two new species from China, a checklist of species and an identification key to 13 Chinese species, which were useful additions to the knowledge of the Chinese fauna.

The present study of Chinese specimens has found two new species and a new Chinese record. Females of two species, *K. laticeps* (Metcalf, 1936) and *K. ussuriensis* (Vilbaste, 1968), are also described for the first time.

## Materials and methods

Morphological terminology follows Bourgoïn (1987) for male genitalia, Bourgoïn et al. (2015) for wing venation and Bourgoïn (1993) for female genitalia. Body length was measured from apex of vertex to tip of forewing; vertex length represents the median length of the vertex (from the apical transverse carina to the tip of basal emargination). Fuchsin staining was used to highlight female genitalia structures studied. External morphology and drawings were done with the aid of a Leica MZ 12.5 stereomicroscope. Photographs were taken with KEYENCE VHX-6000 system. Illustrations were scanned with a CanoScan LiDE 200 and imported into Adobe Photoshop 7.0 for labeling and plate composition. The dissected male and female genitalia are preserved in glycerin in small plastic tubes pinned together with the specimens. Zoogeographic regionalization scheme follows Holt et al. (2013). The distribution map was prepared with SimpleMapp (Shorthouse 2010).

The type specimens are deposited in the Institute of Entomology, Guizhou University, Guiyang, Guizhou Province, China (**GUGC**).

## Taxonomy

### Genus *Kuvera* Distant, 1906

*Kuvera* Distant, 1906: 261; Tsaour et al. 1991: 50; Anufriev and Emeljanov 1988: 443; Emeljanov 1998: 133; Luo et al. 2019: 46.

*Latoliarus* Dlabola, 1957: 271; synonymized by Emeljanov 1998: 133.

**Type species.** *Kuvera semihyalina* Distant, 1906, original designation.

**Diagnosis.** For the diagnosis of *Kuvera* see Luo et al. (2019: 137).

**Remarks.** This genus is easily separated from other members in Semonini by the following character combinations: head including eyes narrower than pronotum; vertex short, wider than long, anterior margin of vertex obscure, with only residual

traces; vertex narrowest at subapical carina, widening towards anterior and posterior margins; anterior and posterior margins wide and parabolic, almost parallel; frons prominent, median carina only distinct on basal portion, not reaching the anterior margin of vertex; clypeus swollen, postclypeus with prominent median carina, anteclypeus carina sharp or arcuate; rostrum just reaching hind coxae; forewings with ScP+R usually forked distad of CuA, RP 3-branched, MP with 4 or 5 terminals, CuA 2 or 3-branched, and with 10–11 apical cells; metatibiotarsal formula: 6/7/(7–8); pygofer with a triangular medioventral process; aedeagus with 2 spinose processes arising near base of endosoma, and endosoma with 1–2 spinose processes; periandrium almost flat and widened at base; ovipositor elongate, orthopteroid and apically curved upwards; abdominal 9<sup>th</sup> tergite with a distinct and elliptic wax plate.

**Distribution.** China, Korea, Japan, (Eastern) Russia, India, Myanmar, Afghanistan.

**Key to the known species (males) of *Kuvera* from China (revised from Anufriev 1987 and Luo et al. 2019)**

- 1 Forewing crossed before middle by a curved, slightly broken macular fuscous fascia (Distant 1906: fig. 117)..... ***K. semihyalina* Distant, 1906**
- Forewing without fascia before middle..... **2**
- 2 Pronotum white..... ***K. longipennis* Matsumura, 1914**
- Pronotum yellow to dark brown ..... **3**
- 3 Spinose process of endosoma long, beyond the apex of the endosoma (Fig. 5H–J) ..... ***K. elongata* sp. nov.**
- Spinose process of endosoma not beyond the apex of the endosoma ..... **4**
- 4 One or both of the spinous processes on lateral sides of the periandrium curved to the opposite side over its dorsal surface..... **5**
- Neither of the spinous processes on lateral sides of the periandrium curved to the opposite side over its dorsal surface ..... **13**
- 5 Both spinose processes on lateral sides of the periandrium curved to the opposite side..... **6**
- Only one of the two spinose processes on lateral sides of the periandrium curved to the opposite side..... **7**
- 6 Spinose process on right side of periandrium strongly curved, apex directed left-ventrocaudally (Anufriev 1987: figs 69, 70) ..... ***K. toroensis* Matsumura, 1914**
- Spinose process on right side of periandrium slightly curved, apex directed left-dorsocephally (Tsaur et al. 1991: fig. 28) ..... ***K. transversa* Tsaur & Hsu, 1991**
- 7 Spinose process on right side of periandrium curved to left side (Fig. 6H–K) ..... ***K. laticeps* (Metcalf, 1936)**
- Spinose process on left side of periandrium curved to right side..... **8**
- 8 Left spinose process of periandrium S-shaped ..... **9**
- Left spinose process of periandrium not S-shaped ..... **11**

- 9 Anal segment with apical lobes symmetrical (Tsaur et al. 1991: fig. 30) .....  
 ..... ***K. hama* Tsaur & Hsu, 1991**
- Anal segment with apical lobes asymmetrical ..... **10**
- 10 Apex of left process reaching base of periandrium; endosoma process reaching  
 apex of sclerotized portion of endosoma (Luo et al. 2019: figs 10, 22) .....  
 ..... ***K. huoditangensis* Luo, Liu & Feng, 2019**
- Apex of left process not reaching base of periandrium; endosoma process  
 reaching middle of membranous portion of endosoma (Anufriev 1987:  
 figs 20–22)..... ***K. vilbastei* Anufriev, 1987**
- 11 Endosoma process long, longer than two-thirds of the left spinose process of  
 periandrium (Luo et al. 2019: figs 43, 44) .....  
 ..... ***K. longwangshanensis* Luo, Liu & Feng, 2019**
- Endosoma process short, shorter than half of the left spinose process of peri-  
 andrium..... **12**
- 12 Anal tube more or less parallel-sided in dorsal view; apex of left spinose pro-  
 cess of periandrium exceeding right lateral margin of periandrium (Fig. 3 F,  
 J, K)..... ***K. basarukini* Emeljanov, 1998**
- Anal tube widened in the middle in dorsal view; apex of left spinose process  
 of periandrium not reaching right lateral margin of periandrium (Anufriev  
 1987: figs 42–45)..... ***K. flaviceps* (Matsumura, 1900)**
- 13 Right process of periandrium originated ventral surface..... **14**
- Right process of periandrium originated right side..... **15**
- 14 Anal segment with apical lobes symmetrical (Anufriev 1987: fig. 67) .....  
 ..... ***K. ussuriensis* (Vilbaste, 1968)**
- Anal segment with apical lobes asymmetrical (Rahman et al. 2017;  
 Fig. 6F)..... ***K. yecheonensis* Rahman, Kwon & Suh, 2017**
- 15 The two spinous processes of periandrium nearly equal in length..... **16**
- The two spinous processes of periandrium not of equal length..... **18**
- 16 In lateral view, two spinose processes of periandrium arched (Tsaur et al.  
 1991: fig. 25)..... ***K. taiwana* Tsaur & Hsu, 1991**
- In lateral view, two spinose processes of periandrium almost straight ..... **17**
- 17 In dorsal view, two spinose processes of periandrium curved inwards (Anu-  
 friev 1987: fig. 50) ..... ***K. kurilensis* Anufriev, 1987**
- In dorsal view, two spinose processes of periandrium almost straight (Anu-  
 friev 1987: fig. 57) ..... ***K. tappanella* Matsumura, 1914**
- 18 Right process of periandrium longer than left one (Fig. 4H–K) .....  
 ..... ***K. campylotropa* sp. nov.**
- Left process of periandrium longer than right one..... **19**
- 19 Ventral base of periandrium triangular (Tsaur et al. 1991: fig. 29) .....  
 ..... ***K. communis* Tsaur & Hsu, 1991**
- Ventral base of periandrium roundly concaved (Tsaur et al. 1991: fig. 27) ....  
 ..... ***K. similis* Tsaur & Hsu, 1991**

***Kuvera basarukini* Emeljanov, 1998**

Figs 1A, B, 3

*Kuvera basarukini* Emeljanov, 1998: 133.

**Material examined.** CHINA: 1♂, Guizhou Province, Duyun City, Doupengshan (26°21'N, 107°23'E), 19 August 2017, leg. Liang-Jing Yang; 1♂, Guizhou Province, Rongjiang county, Xiaodanjiang (660–800 m) (26°20'N, 108°21'E), 13–14 September 2005, leg. Bin Zhang, Zi-Zhong Li.

**Redescription.** Body length: male: 5.5–5.9 mm ( $N = 2$ ).

**Coloration.** General color blackish brown (Figs 1A, B, 3A, B). Eyes brown, ocelli yellowish brown. Vertex brown, pronotum dark brown and mesonotum blackish brown. Frons generally yellowish brown, blackish brown above frontoclypeal suture. Clypeus blackish brown. Rostrum generally brown except darker tip. Forewing semi-translucent, with a small irregular blackish brown spot at branch of Y-vein, stigma blackish brown. Hind tibiae yellowish brown and abdominal sternites blackish brown.

**Head and thorax.** Vertex (Fig. 3A) broad, 2.2 times wider than long; anterior margin arched convex, posterior margin arched concave; median carina reaching transverse carinae, indistinct. Frons (Fig. 3B) 1.2 times as wide as long, median carina indistinct, extending from slightly above level of lateral ocelli to median ocellus. Clypeus with median carina distinct and elevated throughout. Pronotum (Fig. 3A) 2.2 times longer than vertex, posterior margin nearly at right angle. Mesonotum 1.6 times longer than pronotum and vertex combined. Forewing (Fig. 3C) 3.0 times longer than wide, with 10 apical and 6 subapical cells; fork Sc+RP distad of fork  $CuA_1+CuA_2$ ; first crossvein r-m basad of fork MP; RP 2 branches, MP with five terminals:  $MP_{11}$ ,  $MP_{12}$ ,  $MP_2$ ,  $MP_3$ , and  $MP_4$ , fork  $MP_1+MP_2$  basad of fork  $MP_3+MP_4$ . Hind tibia with 2–3 lateral spines, metatibiotarsal formula: 6/7/7–8, second segment of hind tarsus with 2–3 platellae.

**Male genitalia.** Pygofer (Fig. 3D, E) symmetrical, dorsal margin concave and U-shaped ventrally, widened towards apex; in lateral view, lateral lobes arched extended caudally. Medioventral process triangular in ventral view. Anal segment (Fig. 3D, F) long, tubular, symmetrical, apical lobes slightly enlarged, 2.2 times longer than wide in dorsal view; anal style finger-like, not extending beyond anal segment. Gonostyli (Fig. 3D, E, G) symmetrical in ventral view; in inner lateral view, apical part extended, apical margin round. Aedeagus (Fig. 3H–K) in total with three processes. Right apex of periandrium with a medium-sized spinose process, curved and apex directed left-ventrocephalad; spinose process on left side near apical 1/3 of periandrium being the longest, gently curved from left to right side over periandrium and apex directed to the right side; base of periandrium ventrally with one small tooth. Endosoma slender, structure simple, left side near the middle with a stout and short spinose process, apex directed dorsocephalad.

**Host plant.** Unknown.

**Distribution.** China (Guizhou), Russia (Sakhalin Island).

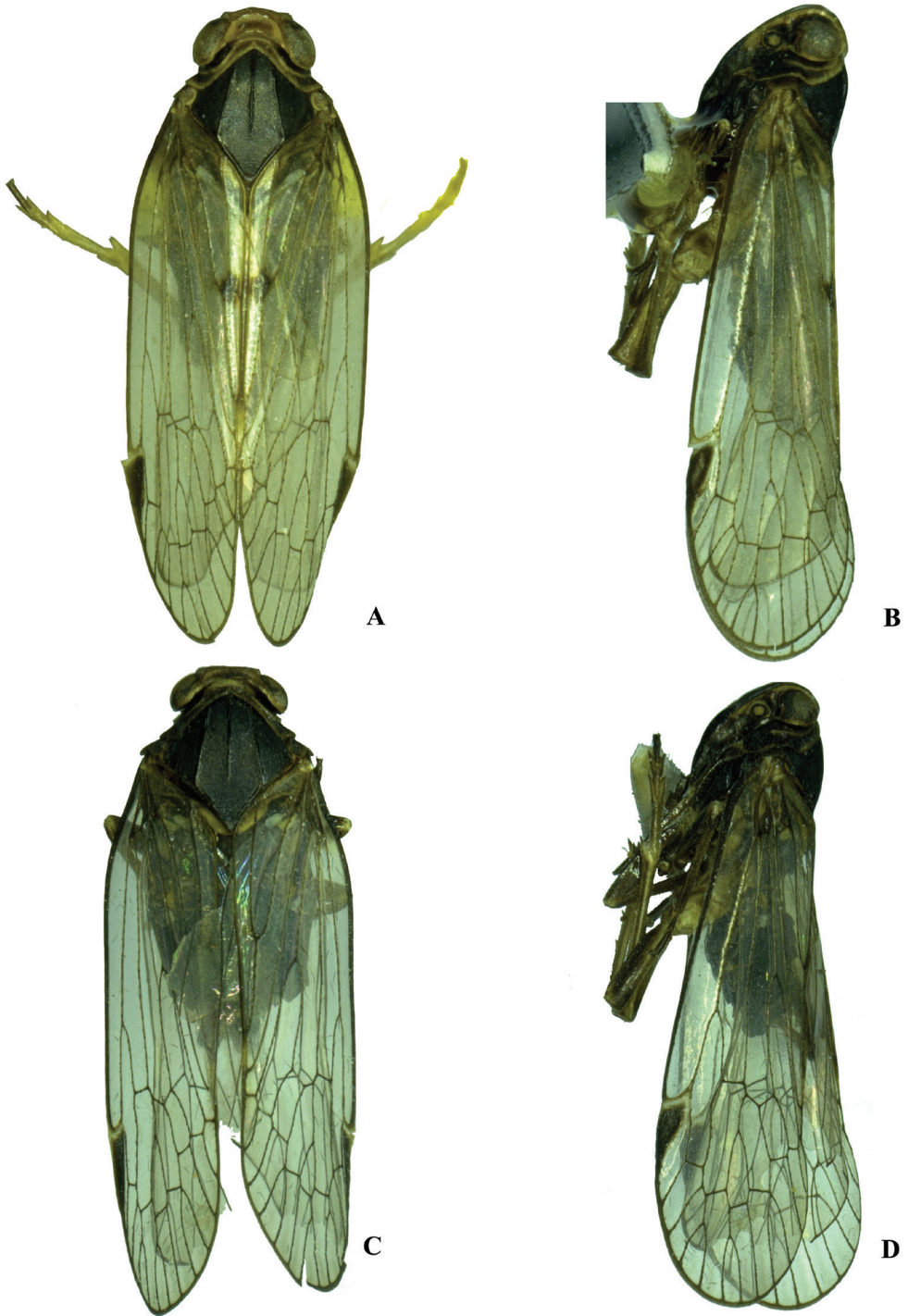


**Figure 1.** Habitus **A, B** *Kuvera basarukini* Emeljanov, 1998, male **A** dorsal view **B** lateral view **C, D** *Kuvera campylostropa* sp. nov., male **C** dorsal view **D** lateral view.

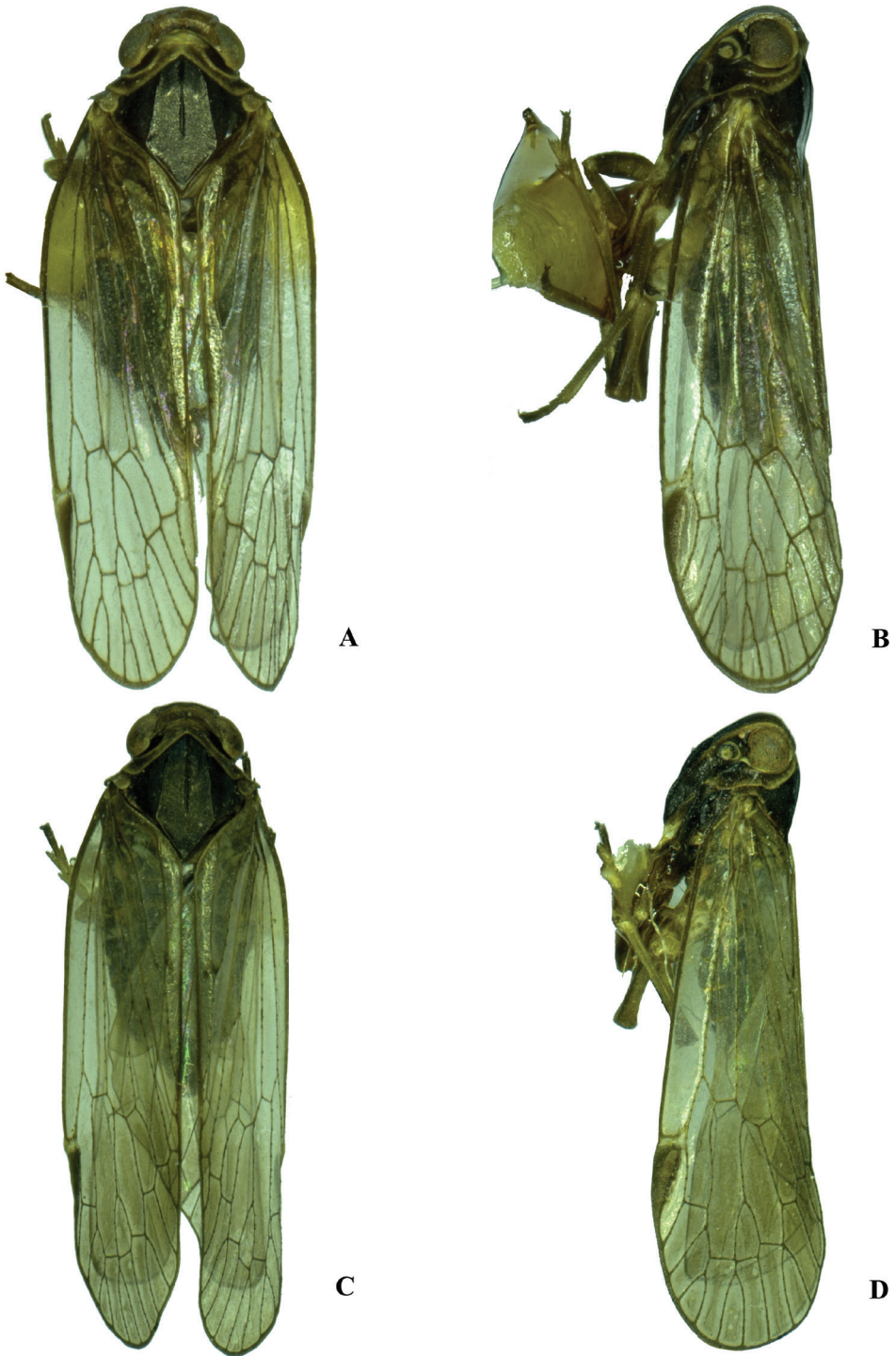


**Figure 2.** Habitus **A, B** *Kuvera elongata* sp. nov., male **A** dorsal view **B** lateral view **C, D** *Kuvera laticeps* (Metcalf, 1936), male **C** dorsal view **D** lateral view.

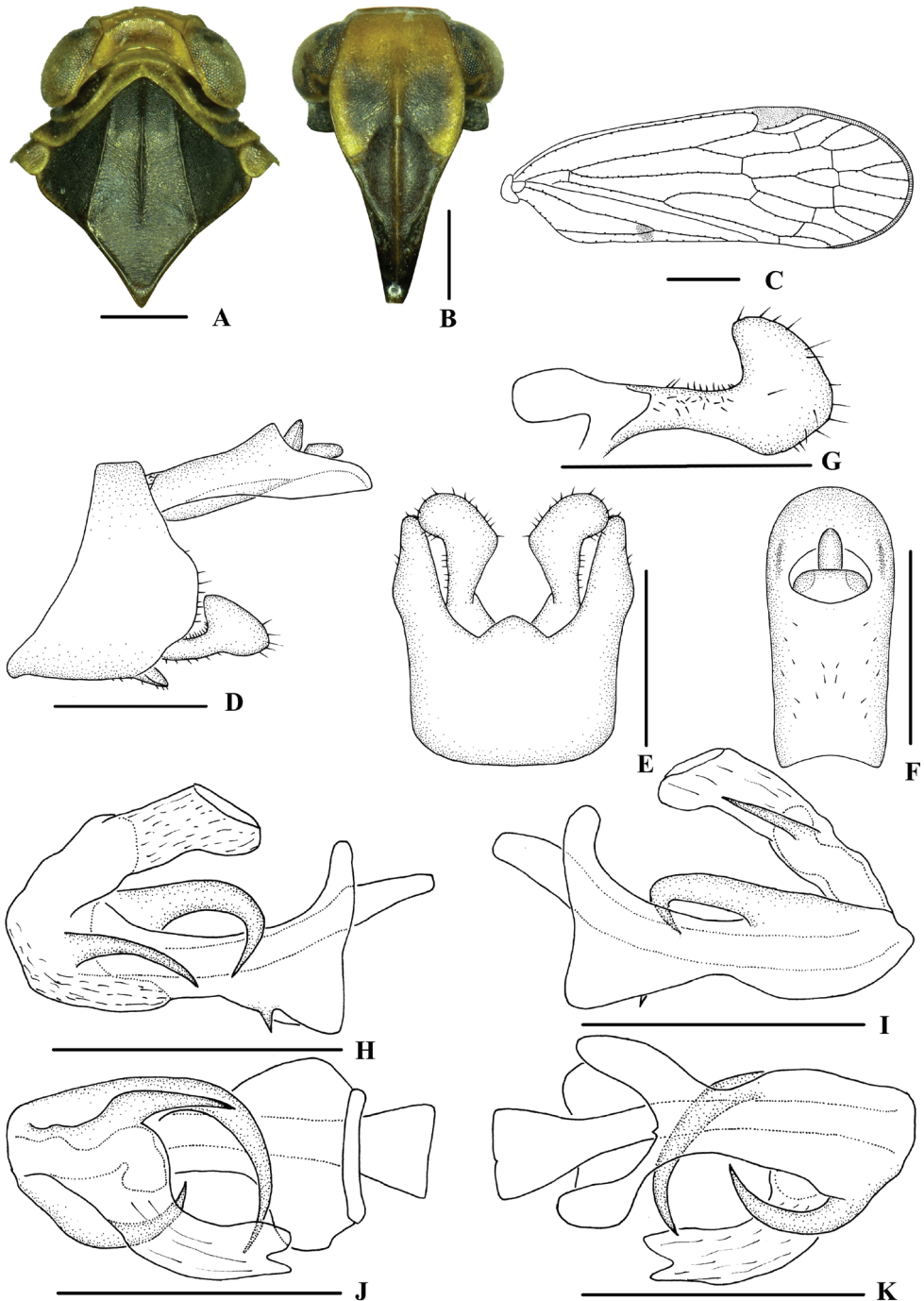


**Figure 3.** *Kuvera basarukini* Emeljanov, 1998, male **A** head and thorax, dorsal view **B** face, ventral view **C** forewing **D** genitalia, lateral view **E** pygofer and gonostyli, ventral view **F** anal segment, dorsal view **G** gonostyli, inner lateral view **H** aedeagus, right side **I** aedeagus, left side **J** aedeagus, dorsal view **K** aedeagus, ventral view. Scale bars: 0.5 mm (**A**, **B**, **D–K**); 1.0 mm (**C**).

**Remarks.** This species can be distinguished from other species of the genus by the following characters: anal segment symmetrical; aedeagus with three processes: right spinose process of periandrium curved and apex directed left-ventrocephalad; left spinose process of periandrium being the longest, curved over periandrium and apex exceeding right lateral margin of periandrium; spinose process of endosoma stout and short, apex directed dorsocephalad.

**Note.** This species is recorded from China for the first time.

***Kuvera campylotropa* Zhi & Chen, sp. nov.**

<https://zoobank.org/6F94F366-14A5-4582-ABDD-5CBA315DDAEF>

Figs 1C, D, 4

**Type material. Holotype:** ♂, CHINA: Yunnan Province, Lushui City, Pianma Town (26°1'N, 98°37'E), 17 June 2011, leg. Yu-Jian Li, Jian-Kun Long; paratypes: 1♂ 1♀, same data as holotype; 6♂♂ 1♀, Guizhou Province, Daozhen County, Xiannvdong Nature Reserve (29°3'N, 107°25'E), 26 August 2004, leg. Xiang-Sheng Chen.

**Description.** Body length: male 5.1–6.3 mm ( $N = 8$ ), female 6.1–6.5 mm ( $N = 2$ ).

**Coloration.** General color blackish brown (Figs 1C, D, 4A, B). Eyes dark brown, ocelli yellowish brown. Vertex dark brown, pronotum dark brown and mesonotum blackish brown. Face generally blackish brown. Rostrum generally dark brown except darker tip. Forewing semi-translucent, stigma blackish brown. Hind tibiae brown and abdominal sternites blackish brown.

**Head and thorax.** Vertex (Fig. 4A) broad, 4.2 times wider than long; anterior margin slightly arched convex, posterior margin slightly arched concave; median carina reaching transverse carinae. Frons (Fig. 4B) 1.2 times as wide as long, median carina indistinct, extending from slightly above level of lateral ocelli to median ocellus. Clypeus with median carina distinct and elevated throughout. Pronotum (Fig. 4A) 4.4 times longer than vertex, posterior margin nearly at right angle. Mesonotum 1.9 times longer than pronotum and vertex combined. Forewing (Fig. 4C) 3.1 times longer than wide, with 11 apical and 6 subapical cells; fork Sc+RP distad of fork  $CuA_1+CuA_2$ ; first crossvein r-m basad of fork MP; RP 3 branches, MP with five terminals:  $MP_{11}$ ,  $MP_{12}$ ,  $MP_2$ ,  $MP_3$ , and  $MP_4$ , fork  $MP_1+MP_2$  basad of fork  $MP_3+MP_4$ . Hind tibia with 3 lateral spines, metatibiotarsal formula: 6/7/8, second segment of hind tarsus with 3 platellae.

**Male genitalia.** Pygofer (Fig. 4D, E) symmetrical, dorsal margin concave and U-shaped ventrally, widened towards apex; in lateral view, lateral lobes arched extended caudally. Medioventral process triangular in ventral view. Anal segment (Fig. 4D, F) long, tubular, symmetrical, apical lobes slightly enlarged, 2.6 times longer than wide in dorsal view; anal style finger-like, not extending beyond anal segment. Gonostyli (Fig. 4D, E, G) symmetrical in ventral view; in inner lateral view, apical part extended, apical margin round. Aedeagus (Fig. 4H–K) in total with three processes. Spinose process on right side at apex of periandrium being the longest, slightly curved and apex directed left-dorsocephalad; left side in the middle with a strongly curved spinose

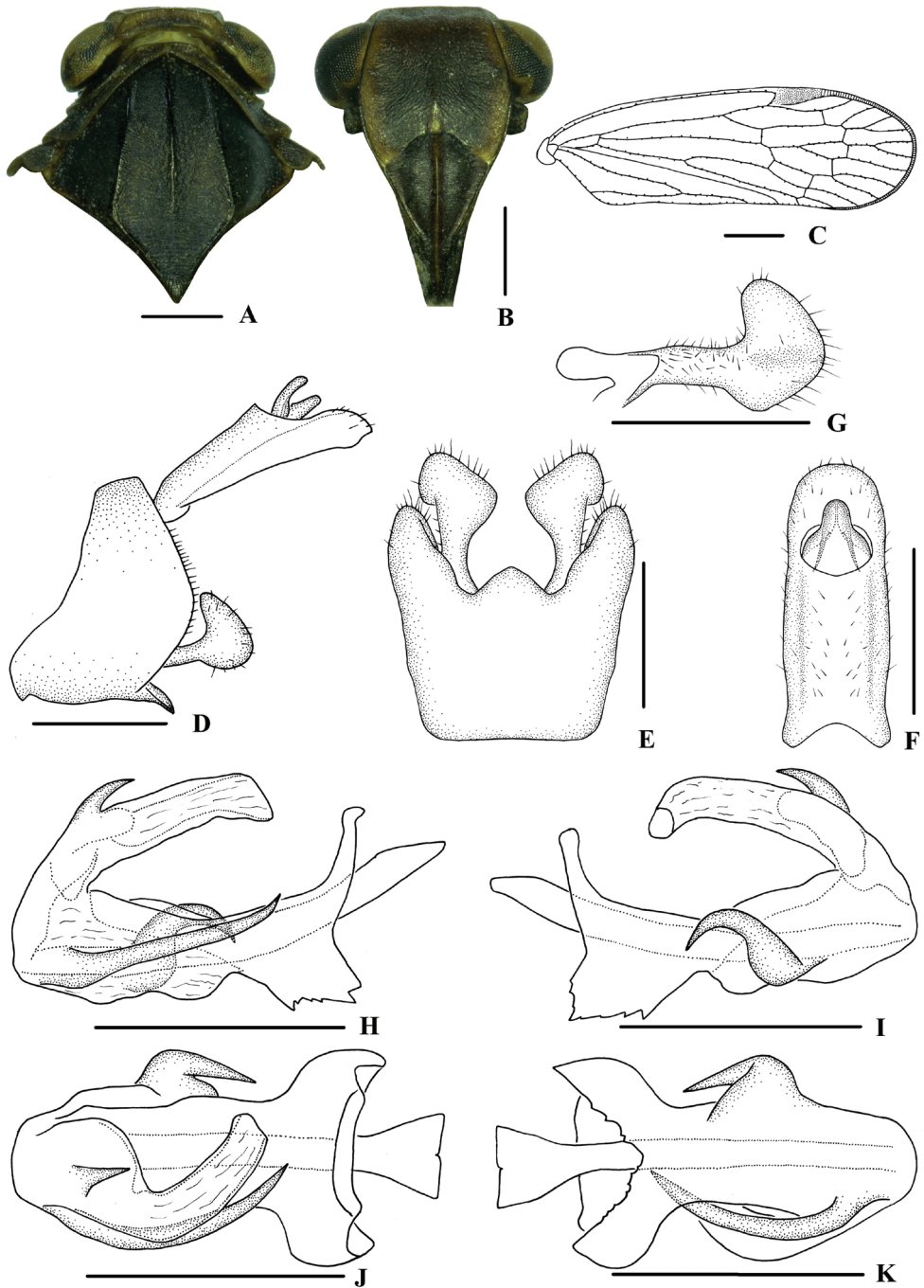


**Figure 4.** *Kuvera campylotropa* sp. nov., male **A** head and thorax, dorsal view **B** face, ventral view **C** forewing **D** genitalia, lateral view **E** pygofer and gonostyli, ventral view **F** anal segment, dorsal view **G** gonostyli, inner lateral view **H** aedeagus, right side **I** aedeagus, left side **J** aedeagus, dorsal view **K** aedeagus, ventral view. Scale bars: 0.5 mm (**A, B, D–K**); 1.0 mm (**C**).

process, apex directed ventrocephalad; base of periandrium ventrally with several small teeth. Endosoma slender, structure simple, dorsal margin near the middle with a stout and short spinose process, apex directed dorsocephalad.

**Host plant.** Unknown.

**Distribution.** China (Guizhou, Yunnan).

**Etymology.** The specific name is derived from the Latin *campylotropus*, meaning curved, referring to the strong curved spinose process on the left side of periandrium.

**Remarks.** This new species is similar to *K. ussuriensis* (Vilbaste, 1968), but differs in: (1) “right” spinose process of periandrium originating from right apex (in *K. ussuriensis*, “right” spinose process of periandrium originating from ventral apex); (2) left spinose process of periandrium shorter than right one in lateral view (the latter longer than right one); and (3) spinose process of endosoma not reaching apex of endosoma (in *K. ussuriensis*, spinose process of the endosoma nearly reaching apex of endosoma). It also closely resembles *Kuvera kurilensis* Anufriev, 1987, however, it differs in that: (1) right spinose process of periandrium longer than left one in lateral view (in *K. kurilensis*, both processes about equal in length); and (2) spinose process of endosoma not reaching apex of endosoma (in *K. kurilensis*, spinose process of endosoma nearly reaching apex of endosoma).

***Kuvera elongata* Zhi & Chen, sp. nov.**

<https://zoobank.org/0BB30DF7-8F44-4486-B262-8E069F7892E8>

Figs 2A, B, 5

**Type material. Holotype:** ♂, CHINA: Guizhou Province, Tongren City, Fanjingshan National Nature Reserve, Jinding (27°54'N, 108°42'E), 31 May 2002, leg. Xiang-Sheng Chen; **paratypes:** 8♂♂ 1♀, same data as holotype; 2♂♂, Guizhou Province, Tongren City, Fanjingshan National Nature Reserve, Yinjiang County, Yongyi Township, (27°54'N, 108°38'E), 29 May 2002, leg. Xiang-Sheng Chen.

**Description.** Body length: male 4.8–5.8 mm ( $N = 11$ ), female 6.0 mm ( $N = 1$ ).

**Coloration.** General color blackish brown (Figs 2A, B, 5A, B). Eyes dark brown, ocelli light yellowish. Vertex brown, pronotum dark brown and mesonotum blackish brown. Face generally blackish brown. Rostrum generally brown except darker tip. Forewing semi-translucent, stigma dark brown. Hind tibiae brown and abdominal sternites blackish brown.

**Head and thorax.** Vertex (Fig. 5A) broad, 2.7 times wider than long; anterior margin slightly arched convex, posterior margin arched concave; median carina reaching transverse carinae. Frons (Fig. 5B) 1.1 times as wide as long, median carina indistinct, extending from basal 1/4 to median ocellus. Clypeus with median carina distinct and elevated throughout. Pronotum (Fig. 5A) 2.3 times longer than vertex, posterior margin nearly at right angle. Mesonotum 1.6 times longer than pronotum and vertex combined. Forewing (Fig. 5C) 2.7 times longer than wide, with 11 apical and 6 sub-apical cells; fork Sc+RP distad of fork CuA<sub>1</sub>+CuA<sub>2</sub>; first crossvein r-m basad of fork

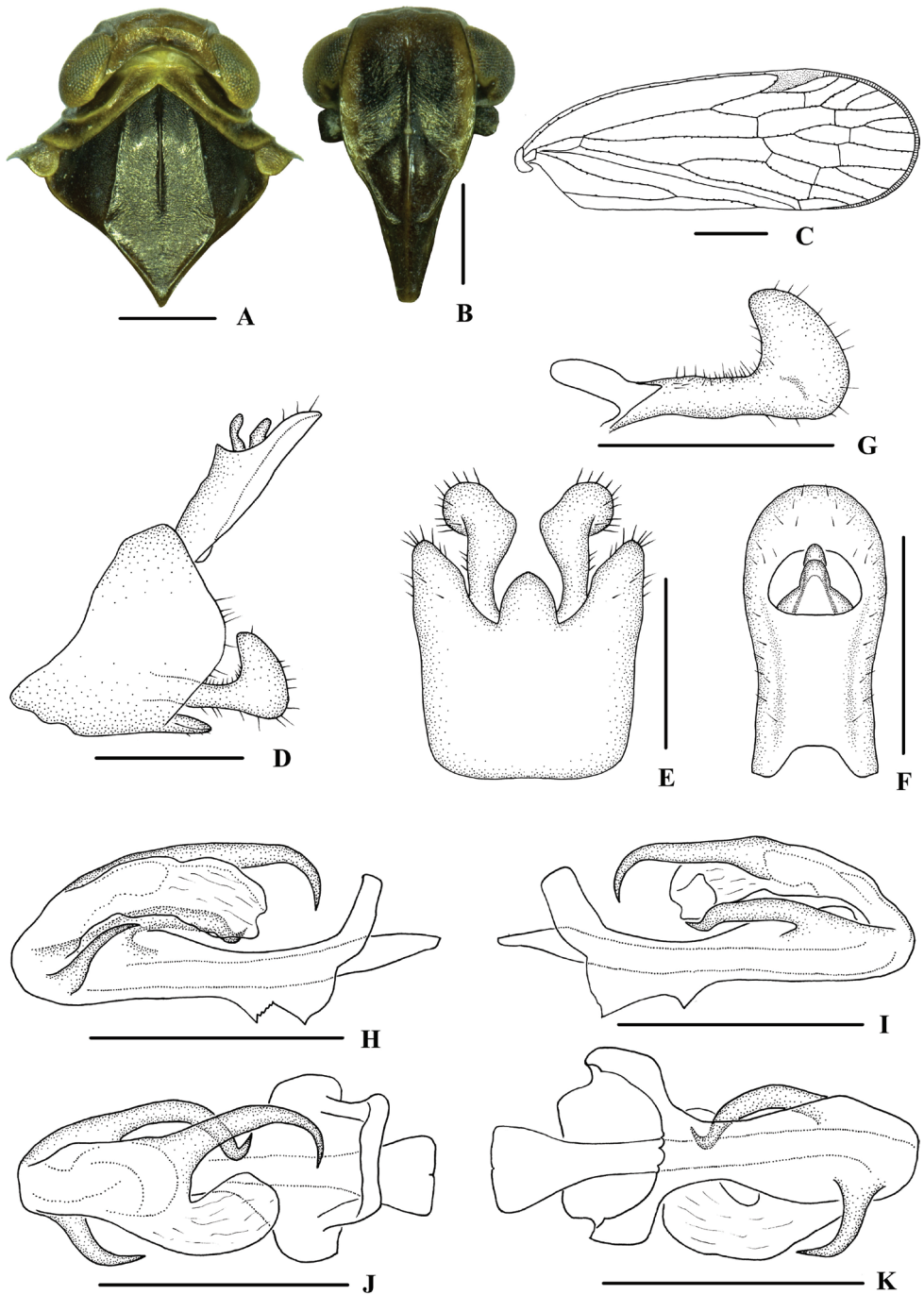


**Figure 5.** *Kuvera elongata* sp. nov., male **A** head and thorax, dorsal view **B** face, ventral view **C** forewing **D** genitalia, lateral view **E** pygofer and gonostyli, ventral view **F** anal segment, dorsal view **G** gonostyli, inner lateral view **H** aedeagus, right side **I** aedeagus, left side **J** aedeagus, dorsal view **K** aedeagus, ventral view. Scale bars: 0.5 mm (**A, B, D–K**); 1.0 mm (**C**).

MP; RP 3 branches, MP with five terminals:  $MP_{11}$ ,  $MP_{12}$ ,  $MP_2$ ,  $MP_3$ , and  $MP_4$ , fork  $MP_1+MP_2$  basad of fork  $MP_3+MP_4$ . Hind tibia with 3 lateral spines, metatibiotarsal formula: 6/7/8, second segment of hind tarsus with 2–3 platellae.

**Male genitalia.** Pygofer (Fig. 5D, E) symmetrical, dorsal margin concave and U-shaped ventrally, widened towards apex; in lateral view, lateral lobes arched extended caudally. Medioventral process campanulate in ventral view. Anal segment (Fig. 5D, F) long, tubular, symmetrical, apical lobes slightly enlarged, 2.0 times longer than wide in dorsal view; anal style finger-like, not extending beyond anal segment. Gonostyli (Fig. 5D, E, G) symmetrical in ventral view; in inner lateral view, apical part extended, apical margin round. Aedeagus (Fig. 5H–K) with three processes in total. Spinose process on right side at apex of periandrium being the shortest, slightly curved outward and apex directed dorsocephalad; left side near base with a slightly curved long spinose process, apex strongly recurved and directed to left side; base of periandrium ventrally with several small teeth. Endosoma slender, structure simple, left side near the middle with a stout and long spinose process, which extended beyond the apex of the endosoma, apex directed ventrad.

**Host plant.** Grass.

**Distribution.** China (Guizhou).

**Etymology.** The specific name is derived from the Latin *elongatus*, meaning elongated, referring to the elongated spinose process on the left side of endosoma.

**Remarks.** This new species is similar to *K. vilbastei* Anufriev, 1987 and *K. huoditangensis* Luo, Liu & Feng, 2019, but differs in: (1) left spinose process of periandrium not exceeding right lateral margin of periandrium (in *K. vilbastei* and *K. huoditangensis*, left spinose process of periandrium exceeding right lateral margin of periandrium); (2) spinose process of endosoma extending beyond the apex of the endosoma (spinose process of endosoma not extending beyond the apex of the endosoma in *K. vilbastei* and *K. huoditangensis*); and (3) anal segment symmetrical (asymmetrical in *K. vilbastei* and *K. huoditangensis*).

### *Kuvera laticeps* (Metcalf, 1936)

Figs 2C, D, 6, 7

*Cixius latifrons* Melichar, 1902: 85, preoccupied by *Cixius latifrons* Walker, 1851.

*Cixius laticeps* Metcalf, 1936: 180, nom. nov. for *Cixius latifrons* Melichar, 1902.

*Kuvera laticeps* (Metcalf, 1936): combination by Anufriev 1987: 6.

**Material examined.** CHINA: 16♂♂ 22♀♀, Guizhou Province, Weining County, Xue-shan Town (27°11'N, 104°6'E), 28–29 September 2016, leg. Jian-Kun Long, Hong-Xing Li, Ya-Lin Yao.

**Description.** Body length: male 5.4–6.2 mm ( $N=16$ ), female 6.1–6.8 mm ( $N=22$ ).

**Coloration.** General color blackish brown (Figs 2C, D, 6A, B). Eyes brown, ocelli yellow. Vertex brown, pronotum brown and mesonotum blackish brown.

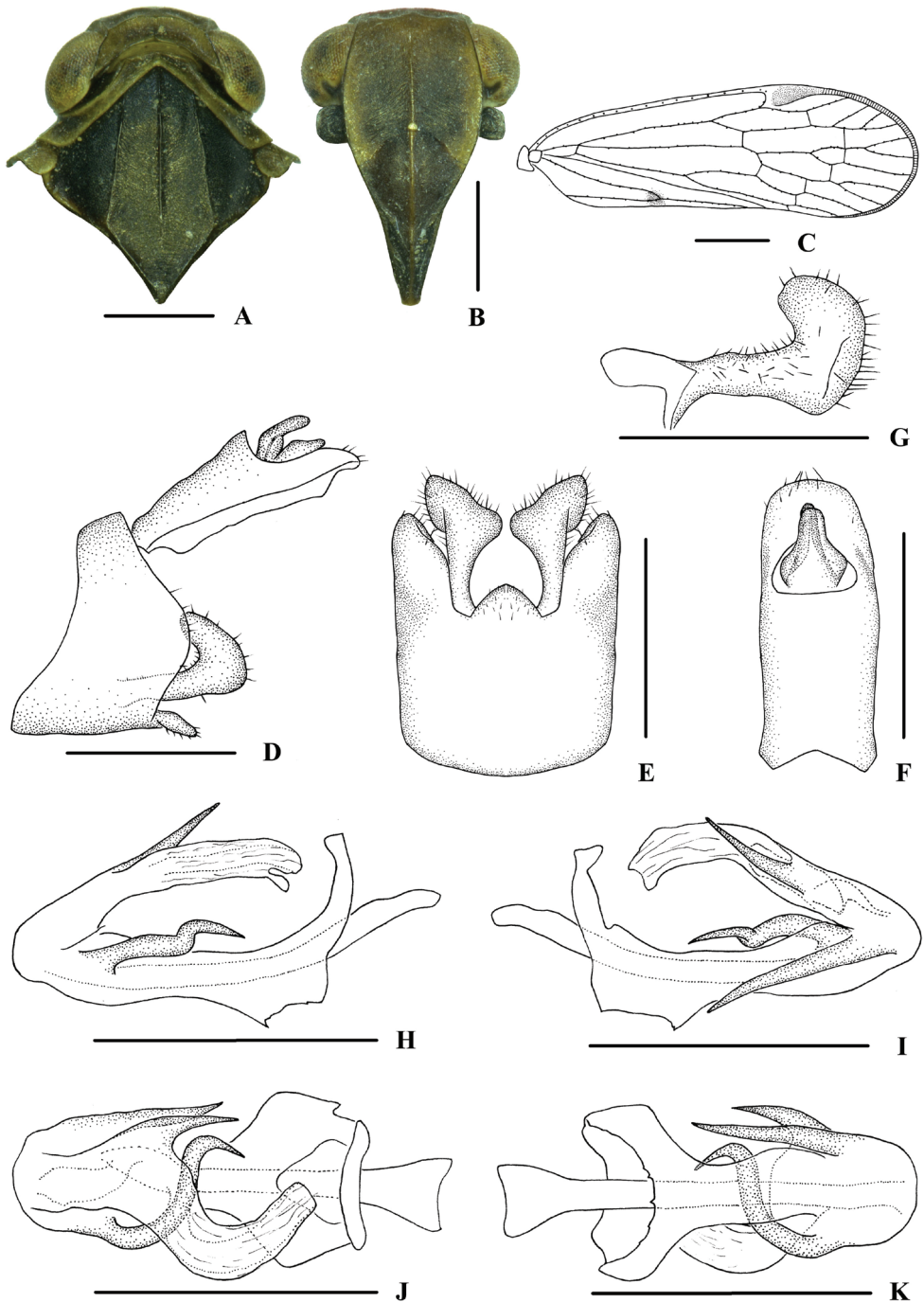


**Figure 6.** *Kuvera laticeps* (Metcalf, 1936), male **A** head and thorax, dorsal view **B** face, ventral view **C** forewing **D** genitalia, lateral view **E** pygofer and gonostyli, ventral view **F** anal segment, dorsal view **G** gonostyli, inner lateral view **H** aedeagus, right side **I** aedeagus, left side **J** aedeagus, dorsal view **K** aedeagus, ventral view. Scale bars: 0.5 mm (**A, B, D–K**); 1.0 mm (**C**).

Frons generally brown and clypeus blackish brown. Rostrum generally brown except darker tip. Forewing semi-translucent, with a very small irregular blackish brown spot at branch of Y-vein, stigma dark brown. Hind tibiae brown and abdominal sternites blackish brown.

**Head and thorax.** Vertex (Fig. 6A) broad, 3.0 times wider than long; anterior margin slightly arched convex, posterior margin arched concave; median carina reaching transverse carinae. Frons (Fig. 6B) 1.2 times as wide as long, median carina indistinct, extending from basal 1/4 to median ocellus. Clypeus with median carina distinct and elevated throughout. Pronotum (Fig. 6A) 2.8 times longer than vertex, posterior margin nearly at right angle. Mesonotum 1.6 times longer than pronotum and vertex combined. Forewing (Fig. 6C) 3.0 times longer than wide, with 11 apical and 6 sub-apical cells; fork Sc+RP distad of fork CuA<sub>1</sub>+CuA<sub>2</sub>; first crossvein r-m basad of fork MP; RP 3 branches, MP with five terminals: MP<sub>11</sub>, MP<sub>12</sub>, MP<sub>2</sub>, MP<sub>3</sub>, and MP<sub>4</sub>, fork MP<sub>1</sub>+MP<sub>2</sub> basad of fork MP<sub>3</sub>+MP<sub>4</sub>. Hind tibia with 3–4 lateral spines, metatibiotarsal formula: 6/7/8, second segment of hind tarsus with 2–4 platellae.

**Male genitalia.** Pygofer (Fig. 6D, E) symmetrical, dorsal margin concave and U-shaped ventrally, slightly widened towards apex; in lateral view, lateral lobes arched extended caudally. Medioventral process triangular in ventral view. Anal segment (Fig. 6D, F) long, tubular, nearly symmetrical, apical lobes slightly enlarged, 2.4 times longer than wide in dorsal view; anal style finger-like, not extending beyond anal segment. Gonostyli (Fig. 6D, E, G) symmetrical in ventral view; in inner lateral view, apical part extended, apical margin round. Aedeagus (Fig. 6H–K) in total with three processes. Spinose process on right side at apex of periandrium being the longest, gently curved from right to left side over periandrium, apex strongly recurved at 90° and directed apically; left side near base with a straight long spinose process, apex directed ventrocephalad; base of periandrium ventrally with several very small teeth. Endosoma slender, structure simple, left side near the middle with a stout and short spinose process, nearly straight, apex directed dorsocephalad.

**Female genitalia.** Tergite IX (Fig. 7A, B, D) moderately sclerotized, with a large wax plate, nearly oval, dorsal and ventral margins concave. Anal segment (Fig. 7C) rectangular, 2.1 times wider than long in dorsal view, anal style strap-like. Gonapophysis VIII (Fig. 7E) elongate, and slightly curved upwards. Gonapophysis IX (Fig. 7F) with two middle teeth, distance ratio between distal middle tooth to apex and length of denticulate portion is 2.6. Gonoplac (Fig. 7G) rod-like, 4.6 times longer than wide in lateral view. Posterior vagina pattern as shown in Figure 7H, I.

**Host plant.** Unknown.

**Distribution.** China (Guizhou, Sichuan).

**Note.** The female genitalia of this species are described and illustrated for the first time.

**Remarks.** This species can be distinguished from other species of the genus by the following characters: anal segment symmetrical; right spinose process of periandrium being the longest, S-shaped, curved over periandrium and apex exceeding left lateral margin of periandrium; left spinose process of periandrium straight, apex directed ventrocephalad; spinose process of endosoma stout and short straight, apex directed dorsocephalad.

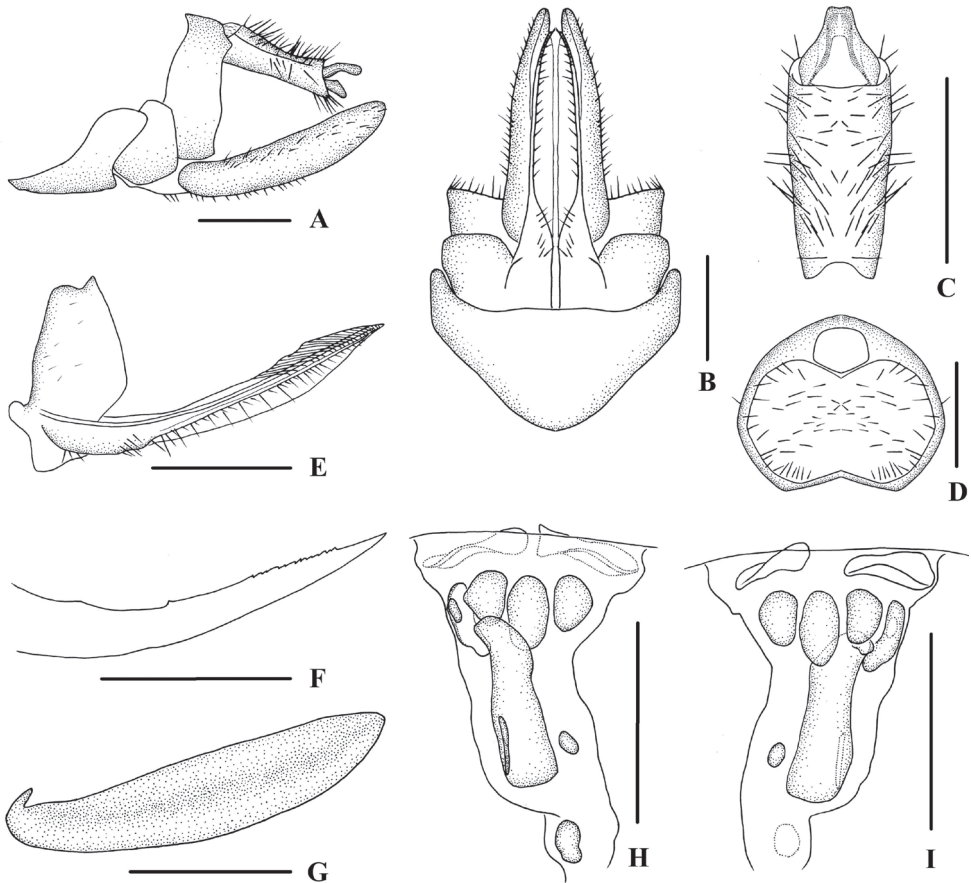


**Figure 7.** *Kuvera laticeps* (Metcalf, 1936), female **A** genitalia, lateral view **B** genitalia, ventral view **C** anal segment, dorsal view **D** tergite IX, caudal view **E** gonapophysis VIII and gonocoxa VIII, ventral view **F** gonapophysis IX, lateral view **G** gonoploc, inner lateral view **H** posterior vagina, ventral view **I** posterior vagina, dorsal view. Scale bars: 0.5 mm.

***Kuvera ussuriensis* (Vilbaste, 1968)**

Figs 8–10

*Betacixius ussuriensis* Vilbaste, 1968: 9.

*Kuvera ussuriensis* (Vilbaste, 1968): combination by Anufriev 1987: 17.

**Material examined.** CHINA: 4♂♂ 7♀♀, Hebei Province, Xinglong County, Wulingshan National Nature Reserve (40°36'N, 117°29'E), 14 August 2010, leg. Li-Xia Xie, Da-Xing Yang, Rong Huang; 50♂♂ 38♀♀, Shanxi Province, Yicheng County, Lishan National Nature Reserve, Dahe Forest Farm (35°27'N, 111°56'E), 23–25 July 2012, leg. Pei Zhang; 28♂♂ 23♀♀, Shanxi Province, Qinshui County, Zhongcun Town, Zhangma Village (35°35'N, 111°57'E), 22 July 2012, leg. Pei Zhang; 26♂♂ 28♀♀, Shanxi Province, Lishan National Nature Reserve (35°23'N, 111°59'E) (1300–

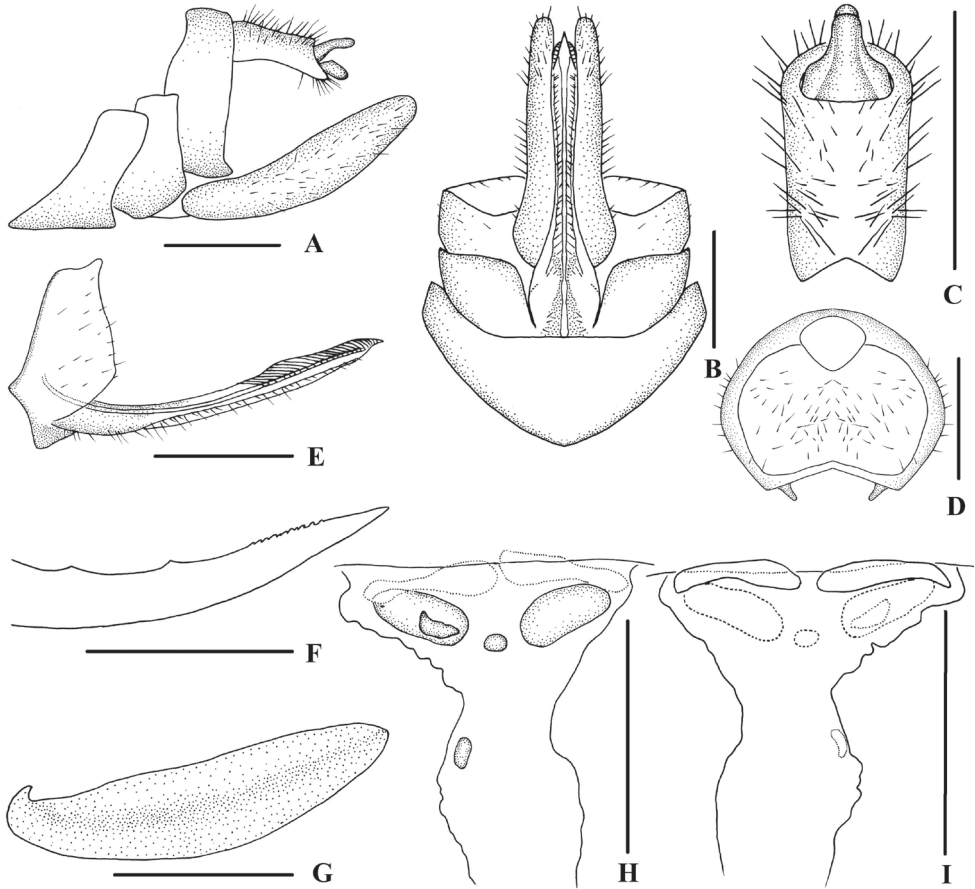


**Figure 8.** *Kuvera ussuriensis* (Vilbaste, 1968), female **A** genitalia, lateral view **B** genitalia, ventral view **C** anal segment, dorsal view **D** tergite IX, caudal view **E** gonapophysis VIII and gonocoxa VIII, ventral view **F** gonapophysis IX, lateral view **G** gonoplac, inner lateral view **H** posterior vagina, ventral view **I** posterior vagina, dorsal view. Scale bars: 0.5 mm.

2200 m), 31 July 2012, leg. Pei Zhang; 31♂♂ 23♀♀, Shanxi Province, Lishan National Nature Reserve (1300–2200 m), 12–18 July 2012, leg. Xiao-Hui Hou; 1♂ 4♀♀, Sichuan Province, Nanchong City, Dayou Township (30°48'N, 106°41'E), 10 May 2008, leg. Zai-Hua Yang; 5♂♂ 3♀♀, Sichuan Province, Luding County, Yanzigou Town (29°42'N, 102°1'E), 11 August 2015, leg. Hong-Ping Zhan, Wen-Song Li; 2♂♂ 2♀♀, Sichuan Province, Qingchuan County, Tangjiahe National Nature Reserve (32°35'N, 104°46'E), 24 August 2007, leg. Ze-Hong Meng; 6♂♂ 10♀♀, Mianyang City, Pingwu County, Baima Tibetan Township, Wanglang Nature Reserve (32°54'N, 104°9'E); leg. Zai-Hua Yang, Wen Zhang; 2♂♂ 4♀♀, Yunnan Province, Yingjiang County, Xima Town (24°45'N, 97°42'E), 29–30 May 2011, leg. Zai-Hua Yang, Jian-Kun Long; 4♂♂, Yunnan Province, Pingbian County, Daweishan National Nature Reserve (22°56'N, 103°42'E), 20 August 2017, leg. Nian Gong; 10♂♂ 13♀♀, Yunnan Province, Xichou County, Fadou (23°23'N, 104°47'E), 28 June 2013, leg. Yan Zhi, Qiang Luo, Yong-Jin



**Figure 9.** Adult of *Kuvera ussuriensis* (Vilbaste, 1968), dorsal view, female (Caohai National Natural Reserve, Weining County, Guizhou Province, 2 August 2017, photograph by Xiang-Sheng Chen).

Sui; 2♂♂ 2♀♀, Yunnan Province, Maguan County, Dulong Town, Jinzhuping Village (22°56'N, 104°30'E), 13–14 August 2017, leg. Yan Zhi, Qiang Luo, Nian Gong; 8♂♂ 8♀♀, Guangxi Province, Longsheng County, Huaping National Nature Reserve (25°36'N, 109°56'E), 26 April 2012, leg. Jian-Kun Long, Zai-Hua Yang; 7♂♂ 3♀♀, Guangxi Province, Longsheng County, Huaping National Nature Reserve, 18–19 May 2012, leg. Jian-Kun Long, Zhi-Hua Fan; 9♂♂ 10♀♀, Shaanxi Province, Zhouzhi County, Houzhenzi Town (33°51'N, 107°50'E), 4–7 August 2010, leg. Pei Zhang, Zhi-Min Chang, Yan-Li Zheng, Ke-Bin Li; 5♂♂ 5♀♀, Shaanxi Province Xi'an City, Cuihuashan (33°58'N, 109°1'E), 27–28 August 2008, leg. Yu-Jian Li; 2♂♂ 2♀♀, Shaanxi Province, Taibai County (34°4'N, 107°19'E), 22 August 2016, leg. Nian Gong; 2♂♂ 5♀♀, Hunan Province, Wugang City, Yunshan National Forest Park (26°40'N, 110°37'E), May 2016, leg. Xiang-Sheng Chen; 2♂♂, Hunan Province, Yongshun County, Xiaoxi Town (28°44'N, 110°15'E), 20–21 August 2016, leg. Yong-Shun Ding, Ying-Jian Wang; 6♂♂ 2♀♀, Anhui Province, Huangshan city, Tangkou town (30°4'N, 118°11'E) (500m), 20 May 2008, leg. Zheng-Guang Zhang; 22♂♂ 33♀♀, Guizhou Province, Weining County, Caohai National Nature Reserve (26°52'N, 104°14'E) (2171 m), 1–5 August 2017, leg. Caohai Collection Team; 1♂ 5♀♀, Guizhou Province, Weining County, Xueshan Town, Zhuopu Village (27°11'N, 104°6'E), 21 August 1986, leg. Zi-Zhong Li; 6♂♂ 17♀♀, Guizhou Province, Daozhen County, Xiannvdong (29°3'N, 107°25'E), 29–31 May 2004, leg. Bin Zhang, Pian Xu; 25♂♂ 44♀♀, Guizhou Province, Daozhen



**Figure 10.** The habitat of *Kuvera ussuriensis* (Vilbaste, 1968) (3 August 2017, Caohai National Natural Reserve, Weining County, Guizhou Province, photograph by Yan Zhi).

County, Sanqiao Town (29°3'N, 107°30'E), 22–24 May 2004, leg. Xiang-Sheng Chen, Bin Zhang, Pian Xu; 4♂♂ 17♀♀, Guizhou Province, Daozhen County, Dashahe Nature Reserve (29°9'N, 107°36'E), 29–31 May 2004, leg. Xiang-Sheng Chen; 2♂♂ 3♀♀, Guizhou Province, Daozhen County, Dashahe Nature Reserve, 20 August 2004, leg. Xiang-Sheng Chen; 3♂♂, Guizhou Province, Luodian County, Luosha Township, Zheren Village (25°41'N, 106°36'E), 9 May 2013, leg. Jian-Kun Long; 6♂♂ 14♀♀, Guizhou Province, Anlong County (25°5'N, 105°29'E), 27 August 2012, leg. Jian-Kun Long, Wei-Bin Zheng, Shi-Yan Xu; 8♂♂ 8♀♀, Guizhou Province, Suiyang County, Kuankuoshui National Nature Reserve (28°14'N, 107°12'E), 2–4 June 2010, leg. Yan-Li Zheng; 10♂♂ 6♀♀, Guizhou Province, Tongren City, Fanjingshan National Nature Reserve (27°55'N, 108°42'E), 20–24 September 2011, leg. Wei-Bin Zheng, Zhi-Min Chang, Xiao-Fei Yu, Zhi-Hua Fan; 17♂♂ 4♀♀, Guizhou Province, Tongren City, Fanjingshan National Nature Reserve, Yinjiang County, Yongyi Township, Dayuanzhi Village, (27°54'N, 108°38'E), 29 May 2002, leg. Xiang-Sheng Chen; 1♂, Guizhou Province, Tongren City, Fanjingshan National Nature Reserve, Heihewan (27°50'N, 108°46'E), 30 July 2014, leg. Meng-Shu Dong; 1♀, Guizhou Province, Tongren City, Fanjingshan National Nature Reserve, Jinding (27°54'N, 108°42'E), 1 September 1996, leg. Mao-Fa Yang; 3♀♀, Guizhou Province, Tongren City, Fanjingshan National Nature Reserve, Jinding, 30 July 2001, leg. Mao-Fa Yang, Guo-Dong Ren; 4♂♂ 6♀♀, Guizhou Province, Leishan County, Leigongshan National Forest Park (26°21'N,

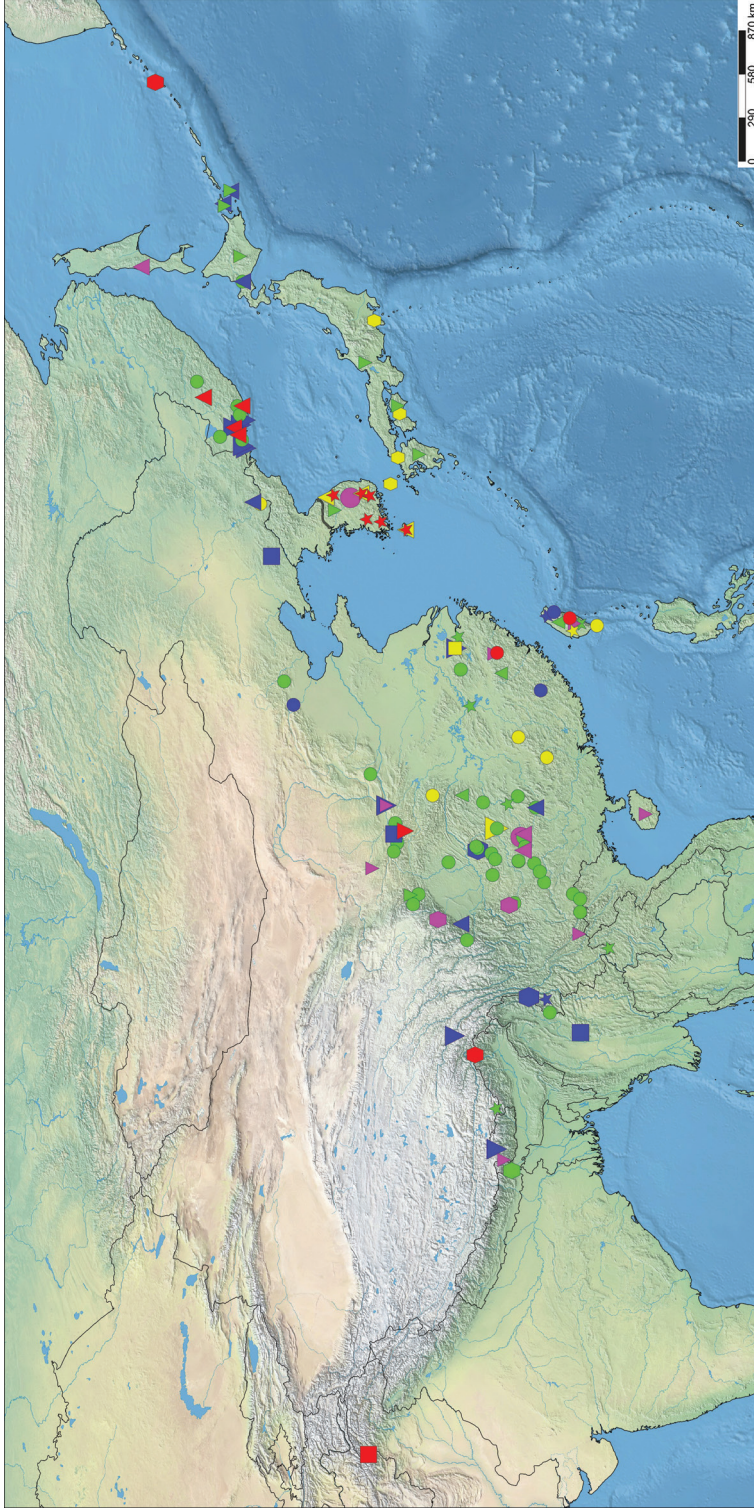


**Figure 11.** Distribution records of species from the genus *Kueneria*: *K. amurensis* (red triangle); *K. basarukini* (pink triangle); *K. brunnetii* (green hexagon); *K. brunnea* (red square); *K. campylotropa* sp. nov. (blue hexagon); *K. communis* (red circle); *K. elongata* sp. nov. (yellow inverse triangle); *K. flaviceps* (green inverse triangle); *K. hagibasanensis* (red star); *K. hallasanensis* (yellow triangle); *K. hama* (green triangle); *K. huoditangensis* (red inverse triangle); *K. kurlensis* (red hexagon); *K. latticeps* (pink hexagon); *K. ligustri* (yellow hexagon); *K. longipennis* (yellow star); *K. longwangshanensis* (yellow square); *K. pallidula* (blue triangle); *K. semihyalina* (blue square); *K. similis* (blue circle); *K. taiwana* (pink inverse triangle); *K. tappanella* (yellow circle); *K. toroensis* (green circle); *K. transversa* (blue star); *K. ussuriensis* (green circle); *K. vilbastei* (blue inverse triangle); and *K. yecheonensis* (pink circle).

108°9'E), 4–6 July 2011, leg. Wei-Bin Zheng, Jian-Kun Long; 3♂♂ 2♀♀, Guizhou Province, Leishan County, Leigongshan National Forest Park, Lianhuaping, 31 May–3 June 2005, leg. Zi-Zhong Li, Qiong-Zhang Song, Bin Zhang; 5♂♂ 4♀♀, Guizhou Province, Duyun City, Chachang (26°24'N, 107°36'E), 12 May 2014, leg. Ming Ning, Gai-Ping Yang, Ding-Guo Li; 2♂♂ 1♀, Guizhou Province, Duyun City, Chachang, 16 August 2014, leg. Gai-Ping Yang, Ding-Guo Li; 1♂ 4♀♀, Guizhou Province, Wangmo County, Dayi Town (25°10'N, 106°06'E), 22 August 2012, leg. Shi-Yan Xu, Wei-Bin Zheng; 1♂ 1♀, Guizhou Province, Guiyang City, Guizhou Botanical Garden (26°37'N, 106°44'E), 18 June 2008, leg. Jun-Qiang Ni; 3♂♂ 3♀♀, Guizhou Province, Guiyang City, Wudang District (26°38'N, 106°45'E), 5 June 2009, leg. Qiong-Zhang Song; 1♂ 2♀♀, Guizhou Province, Zunyi City, Loushuguan (28°1'N, 106°51'E), 21 September 2017, leg. Bin Yan; 15♂♂ 3♀♀, Guizhou Province, Xishui County, Linjiang (28°19'N, 106°12'E), 1 June 2006, leg. Xiang-Sheng Chen.

**Supplementary description. Female genitalia.** Tergite IX (Fig. 8A, B, D) moderately sclerotized, with a large wax plate, nearly oval, dorsal and ventral margins concave. Anal segment (Fig. 8C) rectangular, 1.8 times wider than long in dorsal view, anal style strap-like. Gonapophysis VIII (Fig. 8E) elongate, and slightly curved upwards. Gonapophysis IX (Fig. 8F) with two middle teeth, distance ratio between distal middle tooth to apex and length of denticulate portion is 2.9. Gonoplac (Fig. 8G) rod-like, 4.0 times longer than wide in lateral view. Posterior vagina pattern as shown in Figure 8H, I.

**Host plant.** *Artemisia mongolica* (Fisch. ex Bess.) Nakai (Asteraceae) (Fig. 10).

**Distribution.** China (Anhui, Guangxi, Guizhou, Hebei, Hunan, Shaanxi, Shanxi, Sichuan, Yunnan), Japan, Russia.

**Remarks.** This species can be distinguished from other species of the genus by the following characters: anal segment symmetrical; aedeagus with three processes: left spinose process of periandrium long, gently curved and apex directed left-ventrocephalad; ventral surface of periandrium with a spinose process, slightly curved and apex directed right-cephalad; spinose process of endosoma stout and long, nearly reaching apex of endosoma.

**Note.** The female genitalia of this species are described and illustrated for the first time.

## Discussion

The biology of few *Kuvera* species throughout the world are well-known. The plant associations of genus have been reported in several previous studies (Anufriev 1987; Emeljanov 2015; Luo et al. 2019). In this study, we found *Kuvera ussuriensis* (Vilbaste, 1968) on *Artemisia mongolica* (Fisch. ex Bess.) Nakai.

Based on data from published information and our field surveys, the distribution records of all twenty-seven known species of *Kuvera* was summarized in Figure 11. Up to now, the genus presents a distribution pattern in the Palearctic, Sino-Japanese, and Oriental regions. Compared with Luo et al. (2019), new distribution records of several species have been added recently (Luo et al. 2022 and this study). We believe that the

actual distribution range of most species is still unclear. *Kuvera brunettii* Muir, 1922, *K. brunnea* (Dlabola, 1957), *K. hagilsanensis* Rahman, Kwon & Suh, 2017, *K. hal-lasanensis* Rahman, Kwon & Suh, 2017, *K. ligustri* Matsumura, 1914, *K. longipennis* Matsumura, 1914 and *K. longwangshanensis* Luo, Liu & Feng, 2019 are known only from the type locality, and further collecting and investigation of this genus are still needed. The complex and variable geomorphological environment and rich biological resources of the distribution area create a variety of habitat types, which are likely reasons for the rich species diversity of the genus *Kuvera*.

## Acknowledgements

The authors are grateful to the specimen collectors for their hard work in the field collections. We wish to express our sincere thanks to Prof. A. Emeljanov (Zoological Institute, Russian Academy of Sciences, St. Petersburg, Russia) for providing related literature and Dr Wei Du (College of Life Sciences, Wuhan University) for identifying the host plant. This work was supported by the National Natural Science Foundation of China (No. 32060343, 31472033), the Science and Technology Support Program of Guizhou Province (grant no. 20201Y129), the Program of Excellent Innovation Talents, Guizhou Province (No. 20154021), the New Academic Talent Program of Guizhou Medical University (No. 19NSP066) and Doctoral Scientific Research Foundation of Guizhou Medical University (No. J[2020]019).

## References

- Anufriev GA (1987) Review of the cixiid genus *Kuvera* Distant (Homoptera, Auchenorrhyncha, Cixiidae). In: Kapustina OG (1987) [Taxonomy of the insects of Siberia and Soviet Far East], Taksonomii nasekomykh Sibiri i Dal'nego Vostoka SSR., Vladivostok Dalnauka, Russia, 4–21.
- Anufriev GA, Emeljanov AF (1988) Suborder Cicadinea (Auchenorrhyncha). In: Lehr PA (Ed.) Keys to the Insects of the Far East of the USSR (Vol. 2). Homoptera and Heteroptera. Nauka Publishing House, Leningrad, 496 pp.
- Bourgoin T (1987) A new interpretation of the homologies of the Hemiptera male genitalia, illustrated by the Tettigometridae (Hemiptera, Fulgoromorpha). Proceedings 6<sup>th</sup> Auchenorrhyncha Meeting, Turin, Italy, 7–11 September 1987, 113–120.
- Bourgoin T (1993) Female genitalia in Hemiptera Fulgoromorpha, morphological and phylogenetic data. *Annales de la Société Entomologique de France* 29(3): 225–244.
- Bourgoin T (2022) FLOW (Fulgoromorpha Lists On the Web): A knowledge and a taxonomy database dedicated to planthoppers (Insecta, Hemiptera, Fulgoromorpha, Fulgoroidea). Version 8, updated 03 February 2022. <https://flow.hemiptera-databases.org/flow/> [Accessed on: 16 March 2022]
- Bourgoin T, Wang RR, Asche M, Hoch H, Soulier-Perkins A, Stroiński A, Yap S, Szvedo J (2015) From micropterism to hyperpterism: recognition strategy and standardized homology-driv-

- en terminology of the forewing venation patterns in planthoppers (Hemiptera: Fulgoromorpha). *Zoomorphology* 134(1): 63–77. <https://doi.org/10.1007/s00435-014-0243-6>
- Distant WL (1906) Rhynchota. III. (Heteroptera Homoptera). In: Bingham CT (Ed.) The fauna of British India including Ceylon and Burma. Taylor & Francis, London, 503 pp. <https://doi.org/10.1080/00222930608562592>
- Dlabola J (1957) Die Zikaden Afghanistans (Homopt.-Auchenorrhyncha) nach den Ergebnissen der von Herrn J. Klapperich in den Jahren 1952–1953 nach Afghanistan unternommenen Expedition. *Mitteilungen der Münchner Entomologischen Gesellschaft*, E V. München 47(5): 265–303.
- Emeljanov AF (1998) Contribution to the knowledge of the genus *Kuvera* Distant (Homoptera: Cixiidae). *Zoosystematica Rossica* 7(1): 133–137.
- Emeljanov AF (2002) Contribution to classification and phylogeny of the family Cixiidae (Hemiptera, Fulgoromorpha). *Denisia* 04: 103–112.
- Emeljanov AF (2015) Planthoppers of the family Cixiidae of Russia and adjacent territories. *Key to the fauna of Russia* 177: 1–252.
- Holt BG, Lessard JP, Borregaard MK, Fritz SA, Araújo MB, Dimitrov D, Fabre PH, Graham CH, Graves GR, Jönsson KA, Nogués-Bravo D, Wang Z, Whittaker RJ, Fjeldså J, Rahbek C (2013) An update of Wallace's zoogeographic regions of the world. *Science* 339(6115): 74–78. <https://doi.org/10.1126/science.1228282>
- Holzinger WE, Emeljanov AF, Kammerlander I (2002) The family Cixiidae Spinola, 1839 (Hemiptera: Fulgoromorpha)-a Review. *Denisia* 4: 113–138.
- Luo Y, Liu J, Feng J (2019) Two new species in the genus *Kuvera* Distant, 1906 (Hemiptera, Cixiidae, Cixiinae) from China. *ZooKeys* 832: 135–152. <https://doi.org/10.3897/zookeys.832.30301>
- Luo Y, Bourgoïn T, Zhang JL, Feng JN (2022) Distribution patterns of Chinese Cixiidae (Hemiptera, Fulgoroidea), highlight their high endemic diversity. *Biodiversity Data Journal* 10: e75303. <https://doi.org/10.3897/BDJ.10.e75303>
- Matsumura S (1914) Die Cixiinen Japans. *Annotationes Zoologicae Japonenses* 8: 393–434.
- Melichar L (1902) Homopteren aus West-China, Persien und dem Süd-Ussuri-Gebiete. *Annuaire du Musée Zoologique de l'Académie Impériale des Sciences de St.-Petersbourg*. Saint Petersburg 7: 76–146.
- Metcalf ZP (1936) Part 2. Cixiidae. In: Metcalf ZP (Ed.) *General Catalogue of the Homoptera*. Fascicule IV, North Carolina State College, Raleigh, 267 pp.
- Muir FAG (1922) New Indian Homoptera. *Records of the Indian Museum* 24: 343–355. <https://doi.org/10.26515/rzsi/v24/i3/1922/162723>
- Rahman MA, Kwon YJ, Suh SJ (2017) Three new species of the genus *Kuvera* Distant (Hemiptera: Fulgoromorpha: Cixiidae) from Korea. *Oriental Insects* 52(1): 66–78. <https://doi.org/10.1080/00305316.2017.1344741>
- Shorthouse DP (2010) SimpleMappr, an online tool to produce publication-quality point maps. <https://www.simplemappr.net> [Accessed on: 12 March 2022]
- Tsaur SC, Hsu TC, Van Stalle J (1991) Cixiidae of Taiwan, Part V. Cixiini except Cixius. *Journal of Taiwan Museum* 44(1): 1–78.
- Vilbaste J (1968) On the Cicadine Fauna of the Primorsk Region. Valgus Publishing, Tallinn, 195 pp. [In Russian]



# A remarkable new genus of Thripinae (Thysanoptera, Thripidae) without anteocellar setae from India

Remani Rajan Rachana<sup>1</sup>, Bellapu Amarendra<sup>1</sup>,  
Ramasamy Gandhi Gracy<sup>1</sup>, Katasani Venkata Nagarjuna Reddy<sup>1</sup>

<sup>1</sup> National Bureau of Agricultural Insect Resources (ICAR-NBAIR), Bengaluru, Karnataka 560024, India

Corresponding author: Remani Rajan Rachana ([vavarachana@gmail.com](mailto:vavarachana@gmail.com))

---

Academic editor: Elison Fabricio B. Lima | Received 11 October 2022 | Accepted 6 January 2023 | Published 19 January 2023

---

<https://zoobank.org/99F3C8DD-208B-4A9F-9D0D-B23164D8E127>

---

**Citation:** Rachana RR, Amarendra B, Gracy RG, Nagarjuna Reddy KV (2023) A remarkable new genus of Thripinae (Thysanoptera, Thripidae) without anteocellar setae from India. ZooKeys 1141: 65–73. <https://doi.org/10.3897/zookeys.1141.96170>

---

## Abstract

*Nandithrips pouzolziae* **gen. et sp. nov.** (Thripidae, Thripinae) is described from the flowers of *Pouzolzia petandra* subsp. *wightii* (Urticaceae) found in Nandi hills, Karnataka, India. This new genus is characterised by an apomorphy, ocellar setae pairs I and II are both absent, and also has a unique discontinuous pore plate distribution, with a single circular or oval pore plate medially on abdominal sternites II and V–VII of males. Partial mitochondrial cytochrome c oxidase subunit 1 (mtCOI) gene sequence of *N. pouzolziae* was sequenced and the annotated sequence was submitted to NCBI GenBank.

## Keywords

Bengaluru, Karnataka, Nandi hills, *Nandithrips pouzolziae*, *Pouzolzia petandra* subsp. *wightii*, thrips

## Introduction

The Thripinae (Thysanoptera, Thripidae) is the largest of the four subfamilies of the family Thripidae (ThripsWiki 2022). Members of this subfamily are characterised by having the head and legs smooth and without reticulations, the first vein and costa on the fore wing not fused near their base, meso- and metathoracic furca with or without a spinula, and a body that is generally not robustly sclerotised. They exhibit a broad range of plant associations, with many species inhabiting flowers or leaves, some living

on both flowers and leaves, many specifically associated with Poaceae, and a few on mosses. A very few species of thrips are predators (Mirab-balou et al. 2013). *Cyrlithrips cecidis* Tree & Mound is reported to cause gall induction of plants in Southeast Asia and Australia (Tree and Mound 2009). This subfamily includes almost all thrips species that are considered pests as well as all but one of the vectors of orthotospovirus infections (Mound et al. 2022). Currently, 229 extant genera and 1762 species belonging to this subfamily are known worldwide (ThripsWiki 2022), with 81 genera and 232 species recorded from India (Rachana and Varatharajan 2017).

The objective of this paper is to diagnose a new genus and species from Nandi hills, Karnataka, India. The new species was collected in the flowers of *Pouzolzia petandra* subsp. *wightii* (Benn. & R. Br.) Friis & Wilmot-Dear (Urticaceae), and compare these to related genera.

## Materials and methods

The specimens were collected by beating leaves and flowers of *Pouzolzia petandra* subsp. *wightii* onto a plastic tray. Specimens were removed with a fine brush into a collecting vial containing 90% ethyl alcohol and mounted onto slides with Canada balsam. They were examined using an Olympus BX 51 microscope and measured using a micrometre eyepiece. Photographs were taken with a Nikon DS-Vi1 camera mounted on a Nikon Eclipse 80i microscope. Keys to genera of the subfamily Thripinae were consulted in diagnosing the new genus (Ananthakrishnan and Sen 1980; Mound and Ng 2009; Masumoto 2010; Mirab-balou et al. 2013). Holotype and paratypes were deposited in the National Insect Museum, National Bureau of Agricultural Insect Resources (ICAR-NBAIR), Bengaluru, India. Using DNeasy Blood and Tissue Kit from Qiagen India Pvt. Ltd. and adhering to the manufacturer's instructions, DNA was extracted from the thrips specimens. The mitochondrial COI gene's standard DNA barcoding region was sequenced for the molecular analysis, and the Universal COI primers (LCO1490/HCO2198) were used in the PCR. Following the manufacturer's recommendations, the amplified products were purified using a Qiagen PCR purification kit, and the purified samples were then sequenced using Sanger's method. Utilizing NCBI Blast tools, the sequence was annotated, and the NCBI GenBank Database was used to generate the accession number.

## Taxonomic account

### *Nandithrips* gen. nov.

<https://zoobank.org/224FCC78-BFE4-442A-8F15-C38143ED1608>

**Type species.** *Nandithrips pouzolziae* sp. nov.

**Description. Female macroptera.** Mouth-cone short and rounded at apex, with 3-segmented maxillary palpi. Ocellar setae pairs I and II absent. Antennae 8-segmented, segment I without median dorsal apical setae, III and IV with forked sensoria, III–VI

with a few microtrichial rows (Fig. 5). Pronotum with two pairs of long posteroangular setae, outer pair shorter than inner pair; four pairs of posteromarginal setae, inner pair longer and thicker than the remaining pairs (Fig. 4). Mesonotum with median pair of setae anterior to submedian setae pair. Metanotum with median setae pair at or close to anterior margin, darker and stouter than sub median pair (Fig. 7). Prosternal ferna undivided, narrow at middle; basantra membranous and without setae; prospinasternum broad and transverse. Mesosternal furca with a spinula. Metasternal endofurca without spinula. Fore wing first vein with long gap in setal row, seven basal (first seta transparent) and three distal setae; clavus with five veinal and one discal setae; second vein with 6–9 setae; setae length on both veins increases abruptly beyond distal third of the forewing; posterior fringe cilia wavy (Fig. 8). Tarsi 2-segmented. Hind tibiae and tarsi each with two stout spines at apex. Abdominal tergites without ctenidia but a few microtrichia present on VIII anterolateral to spiracles, tergites without craspedum; tergites VI–VIII with S4 setae minute; tergite VIII with posteromarginal comb, microtrichia absent at middle (Fig. 12); tergite IX with two pairs of campaniform sensilla; tergite X with median slit more than two-thirds (Fig. 9); abdominal sternites without craspedum; sternite II with two pairs of posteromarginal setae, III–VII with three pairs, III–VI with S1, S2, and S3 at posterior margin, VII with S1 and S2 setae placed well ahead of posterior margin, S3 submarginal (Fig. 13). Sternites without discal setae. Ovipositor well developed.

**Male macroptera.** Abdominal tergite IX without median short and stout setae (Fig. 10); sternites II and V–VII each with a circular or oval pore plate medially (Fig. 11).

**Etymology.** In reference to the type locality.

**Generic relationships.** The absence of ctenidia on the abdominal tergites indicates that *Nandithrips* is not related to either the *Thrips* or *Frankliniella* genus groups (Mound and Palmer 1981). However, *Nandithrips* shares the apomorphic character, the lack of ocellar setae pair II, only with the African genus, *Bournierothrips* Bhatti, which is a member of the *Thrips* genus group. This character state appears to be a convergence, as this genus does not belong to the same genus group. *Bournierothrips* has ctenidia and other character states of the *Thrips* genus group and the lack of the ocellar setae pair II seems to be an additional loss in that lineage which already lacks ocellar setae pair I. Even though both the genera share a unique apomorphic character within the subfamily Thripinae, they may not be closely related. The host plant association of the two genera appears to be different: this genus was collected in the flowers of *Pouzolzia petandra* subsp. *wightii*, but all described *Bournierothrips* species are associated with mosses, and the genus is endemic to Africa.

The lack of microtrichial fields laterally on the abdominal tergites indicates that this genus is not related to *Scirtothrips* genus-group (Masumoto and Okajima 2007), and presence of long setae on the pronotum suggests that it is not related to *Anaphothrips* genus group (Mound and Masumoto 2009). The general appearance of *Nandithrips* suggests that it is not related to *Taeniothrips* genus group even though it shares some character states like the absence of ocellar setae I and ctenidia (Mound and Palmer 1981; Wang et al. 2020). The absence of a pair of dorsoapical setae on the first antennal segment indicates that it is not related to the two major genus-groups centred on *Trichromothrips* and *Mycterothrips* (Masumoto and Okajima 2005, 2006), even though

*Nandithrips* shares several characters with *Trichromothrips* genus group like the absence of ocellar setae pair I, ctenidia, craspeda, and discal setae on sternites and the position of S1 and S2 setae on sternite VII.

It is similar to the Old World flower-inhabiting genus, *Lefroyothrips* Priesner in colour, appearance, the absence of paired dorso-apical setae on antennal segment I, sculpture and chaetotaxy of the meso- and metanota, the absence of ctenidia and craspeda, and the presence of a group of microtrichia anterior to spiracle on abdominal segment VIII; however, *Nandithrips* is distinguished from *Lefroyothrips* in lacking ocellar setae pair I, the tergite VIII with the posteromarginal comb interrupted medially, the position of S2 setae on abdominal sternite VII, the pore gland shape and distribution on the sternites of males, and the stout thorn-like setae on tergite IX of males absent. Many of the characters of *Nandithrips*, particularly the absence of a pair of dorso apical setae on the first antennal segment, are shared with species of the flower-inhabiting genera *Ceratothrips* Reuter and *Projectothrips* Moulton. However, *Nandithrips* differs from *Ceratothrips* by lacking ocellar setae pair I, tergite VIII with the posteromarginal comb interrupted medially, the position of S1 and S2 setae on abdominal sternite VII, and the pore gland shape and distribution on the sternites of males. *Projectothrips* is a highly distinctive genus because of the elongate, slender, eighth antennal segment that is about nine times as long as wide. This genus shares several character states with the members of *Megalurothrips* genus group (*Craspedothrips* zur Strassen, *Megalurothrips* Bagnall, *Odontothripiella* Bagnall, and *Odontothrips* Amyot & Serville) and *Ceratothripoides* Bagnall, *Retanathrips* Mound & Nickle, and *Pezothrips* Karny. However, the absence of a pair of dorsoapical setae on the first antennal segment indicates that it is not related to these genera. Even though Mound and Palmer (1981) included *Ceratothripoides*, *Ceratothrips*, *Craspedothrips*, *Lefroyothrips*, *Megalurothrips*, *Odontothripiella*, *Odontothrips*, and *Projectothrips* in the *Megalurothrips* genus group, *Ceratothrips*, *Lefroyothrips*, and *Projectothrips* may not belong in this group because of the absence of dorso-apical setae on antennal segment I (Masumoto and Okajima 2020). Moreover, Zhang et al. (2019) showed in their phylogenetic analysis based on morphological data that *Craspedothrips*, *Megalurothrips*, and *Odontothrips*, genera with dorsoapical setae on antennal segment I, are included in the same clade and this clade was the sister-group to *Mycterothrips* Trybom, not *Ceratothripoides*. According to their analysis, *Ceratothripoides* seems to be the sister group of *Pezothrips*, but the systematic positions of these two genera are unresolved.

Mound and Palmer (1981) indicated that the absence of ocellar setae I is an apomorphic condition and presence/absence of this setae pair appears to be remarkably constant within genera and genus groups within the subfamily Thripinae. They also mentioned that ocellar setae pair II is remarkably constant in size and position. Hence, after examining multiple specimens (59 females, 22 males) of this genus, we assume that this apomorphic character, the absence of ocellar setae II, is constant within *Nandithrips*. Minaei and Mound (2021) stated that character-state reversals have often been interpreted as apomorphies, such that an unusual looking species is given separate taxonomic status on the basis of the absence of a single character state and, moreover,

loss of a character occurs quite commonly. They also stressed the importance of evaluating a new taxon in relation to the structure of closely related taxa under circumstances of apparent absence or loss of a character state. Understanding well the depth of their observations, and after examining multiple specimens of both sexes, we ascertain that the absence of ocellar setae II is stable across all the examined specimens and looked for the other characters which justify its diagnosis as a new genus. One more character state which is unique to *Nandithrips* is the pore plate distribution in males, and this character is very important in discussing the novelty of taxa if males are known. In the subfamily Thripinae, wherever males are known, eight groups of pore plate distribution has been suggested: medially on sternites III + IV + V ( $\pm$  VI, VII, and VIII); medially only on sternites indicated (III, III–IV, and VII); C-shaped pore plate on sternites III + IV + V ( $\pm$  VI and VII); two or three pore plates on several sternites; multiple small pore plates on at least III–VI; on antecostal ridge of at least IV–VI (rarely only II); gland aperture on antecostal ridge of III (no pore plate), and pore plates or glandular structures absent (Mound 2009). However, *Nandithrips* has a unique discontinuous pore plate distribution with a single circular or oval pore plate medially on sternites II and V–VII, and this condition is not shared with any of the genera in the subfamily Thripinae, wherever males are known. In the new genus, an abrupt increase in setae length on both the veins beyond the distal third of the fore wing is noticeable, which is also not shared with any other genera in the subfamily Thripinae.

To conclude, although *Nandithrips* is a member of the subfamily Thripinae, more precise relationships are not clear.

***Nandithrips pouzolziae* sp. nov.**

<https://zoobank.org/D2708492-9BDC-479A-885E-A39BE4F1E9F6>

**Type material.** *Holotype* female, Nandi hills (13.37°N, 77.68°E), Bengaluru, Karnataka, India, in the flowers of *Pouzolzia petandra* subsp. *wightii* (Fig. 1), 16 September 2022, Amarendra B. (ICAR/NBAIR/THYS/16092022). *Paratypes* 58 females, 22 males with same data as holotype.

**Description. Female macroptera (Fig. 2).** With the character states given in the generic diagnosis above. Body golden-yellow except head, metanotum and clavus brown; antennal segments I–IV pale yellow, V yellow basally and shaded brown apically, VI brown with base slightly pale, VII and VIII brown (Fig. 5); fore wing slightly dusky except pale base and apex (Fig. 8); all legs yellow; prominent body setae pale to brown. Head wider than long; ocellar setae pair III situated at the tangent between the fore and hind ocelli. Postocular setae six pairs, pairs I and III subequal and the longest, pair V situated far from pair IV (Fig. 6). Antennal segment II without microtrichial rows, III–VI with microtrichial rows, III–IV with apical neck, III–V with pedicel (Fig. 5). Pronotum weakly sculptured with transverse striae (Fig. 4). Mesonotum sculptured with transverse anastomosing striae; campaniform sensilla present anteromedially. Metanotum with irregular transverse lines anteriorly, irregu-



**Figure 1.** *Pouzolzia petandra* subsp. *wightii*.

lar reticulate sculpture medially, longitudinal striations laterally; campaniform sensilla present (Fig. 7). Abdominal tergite I transversely striate; II–VIII with a few striations laterally. Abdominal sternites without discal setae.

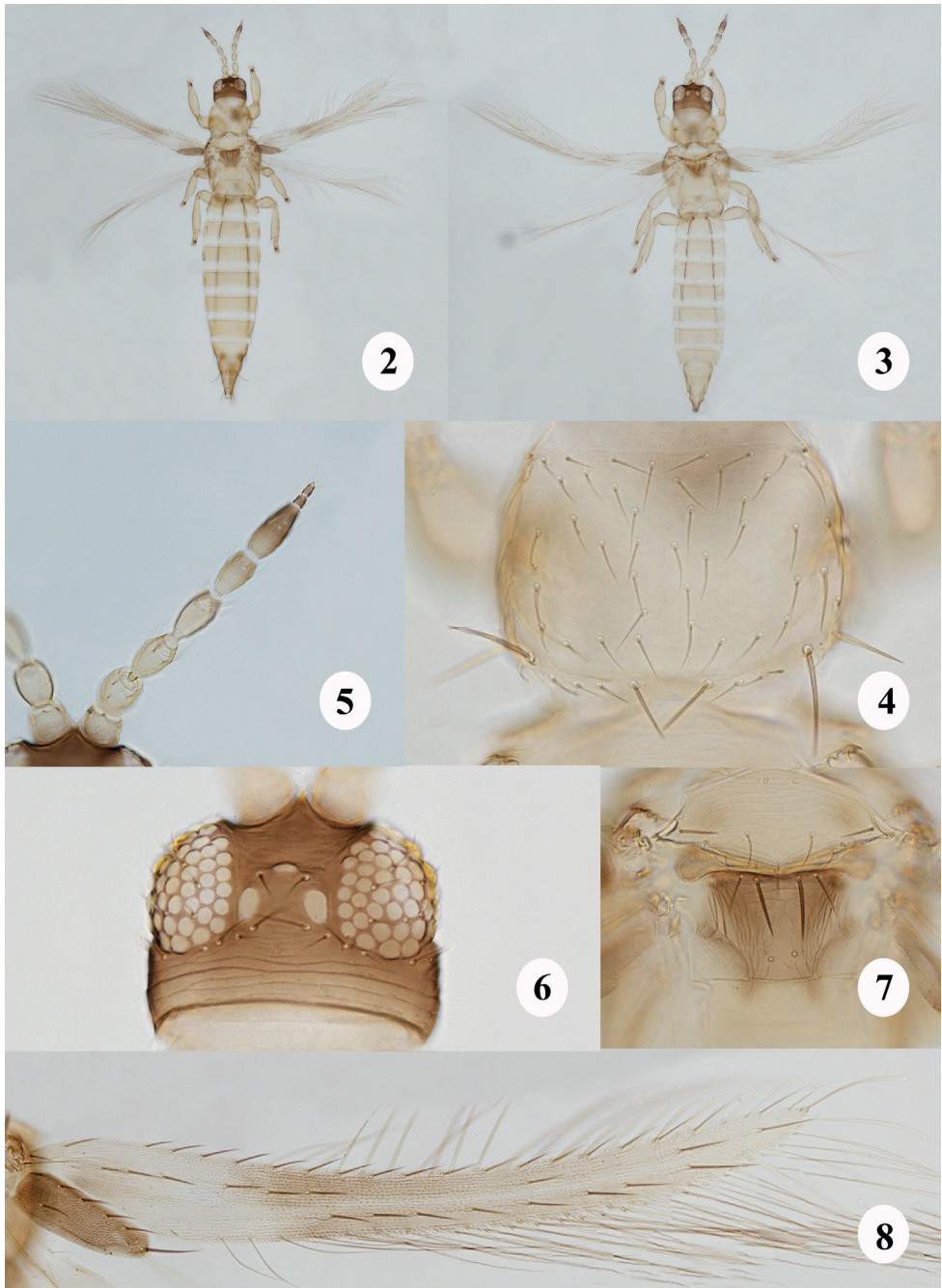
Measurements (holotype female in microns). Body length 1200. Head, length 90; width across eyes 115; ocellar setae III 18; postocular setae I 23. Pronotum length 100; width 143; outer posteroangular setae 38; inner posteroangular setae 58. Fore wing length 520. Antennal segments III–VIII length 40, 35, 33, 38, 5, 8.

**Male macroptera (Fig. 3).** General structure as in female but smaller. Abdominal tergite IX with S1 and S2 setae subequal in length, S2 setae positioned anterior to S1 setae (Fig. 10); sternites II and V–VII each with a circular or oval pore plate medially (Fig. 11).

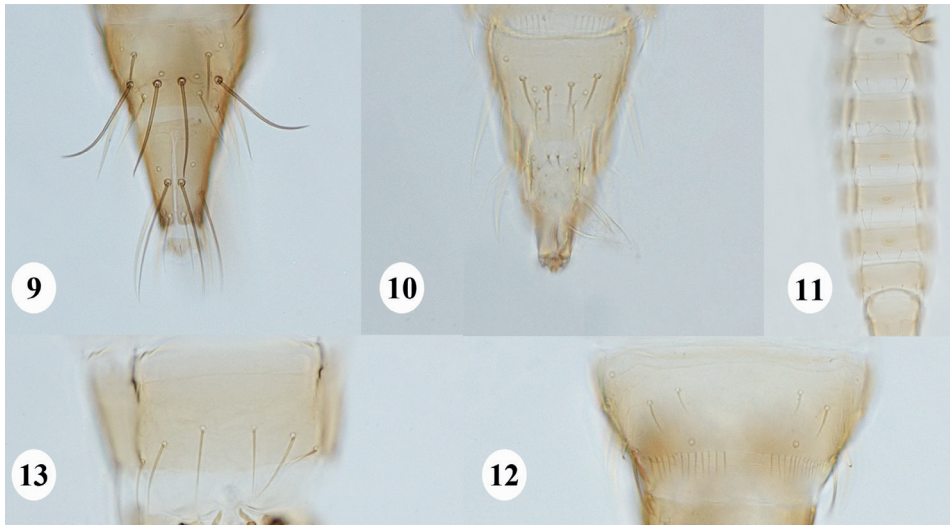
Measurements (paratype male in microns). Body length 850. Head, length 70; width across eyes 100; ocellar setae III 13. Pronotum, length 88; width 125; outer posteroangular setae 33; inner posteroangular setae 40. Fore wing length 450. Antennal segments III–VIII length 38, 35, 28, 35, 5, 8.

**Etymology.** In reference to the host plant of this species.

**Molecular characterization.** A partial mtCOI gene of *N. pouzolziae* was sequenced and the annotated gene sequence was deposited in the National Centre for Biotechnology Information (NCBI) database, accession number OP714094.



**Figures 2–8.** *Nandithrips pouzolziae* sp. nov. **2** female **3** male **4** prothorax **5** antenna **6** head **7** pterothorax **8** fore wing.



**Figures 9–13.** *Nandithrips pouzolziae* sp. nov. **9** female abdominal tergites IX–X **10** male abdominal tergites IX–X **11** pore plate on abdominal sternites II and V–VII **12** abdominal tergite VIII **13** abdominal sternite VII.

## Acknowledgements

We are grateful to A.N. Sringeswara, University of Agricultural Sciences, Bengaluru for identifying the host plant. We wish to express our cordial thanks to Masami Masumoto of the Yokohama Plant Protection Station for his informative discussions during the study. We extend special thanks to the editor Elison Fabricio B. Lima and three reviewers for their comments and valuable suggestions for improving the quality of this article. Thanks are also due to R. Varatharajan, Manipur University, and V.S. Chinnu, University of Agricultural Sciences, Bengaluru, for providing useful references. This study was financially supported by the SERB, Department of Science and Technology, New Delhi, through a Core Research Grant Project entitled “Taxonomy and diversity of terebrantian thrips (Thysanoptera: Terebrantia) from south India with special reference to Western Ghats” (CRG/2021/006228) to the first author. We thank Dr S.N. Sushil, Director, ICAR-NBAIR for his support and providing necessary facilities.

## References

- Ananthkrishnan TN, Sen S (1980) Taxonomy of Indian Thysanoptera. Handbook Series No. 1. Zoological Survey of India, Calcutta, 234 pp.
- Masumoto M (2010) Key to genera of the subfamily Thripinae (Thysanoptera: Thripidae) associated with Japanese plant quarantine. Research Bulletin of Plant Protection Japan 46: 25–5.
- Masumoto M, Okajima S (2005) *Trichromothrips* Priesner (Thysanoptera, Thripidae) of Japan and Taiwan, with descriptions of four new species and a review of the *Trichromothrips* group of genera. Zootaxa 1082(1): 1–27. <https://doi.org/10.11646/zootaxa.1082.1.1>

- Masumoto M, Okajima S (2006) A revision of and key to the world species of *Mycterothrips* Trybom (Thysanoptera, Thripidae). *Zootaxa* 1261(1): 1–90. <https://doi.org/10.11646/zootaxa.1261.1.1>
- Masumoto M, Okajima S (2007) The genus *Scirtothrips* Shull (Insecta, Thysanoptera, Thripidae) and three related genera in Japan. *Zootaxa* 1552(1): 1–33. <https://doi.org/10.11646/zootaxa.1552.1.1>
- Masumoto M, Okajima S (2020) Two new species of *Pezothrips* (Thysanoptera, Thripidae) in Japan and Europe, with designation of lectotype of type species. *Zootaxa* 4743: 075–091. <https://doi.org/10.11646/zootaxa.4743.1.6>
- Minaei K, Mound LA (2021) Character-state evaluation when discriminating Thysanoptera taxa (Insecta). *Zootaxa* 5061(2): 377–382. <https://doi.org/10.11646/zootaxa.5061.2.10>
- Mirab-balou M, Minaei K, Chen XX (2013) An illustrated key to the genera of Thripinae (Thysanoptera, Thripidae) from Iran. *ZooKeys* 317: 27–52. <https://doi.org/10.3897/zookeys.317.5447>
- Mound LA (2009) Sternal pore plates (glandular areas) of male Thripidae (Thysanoptera). *Zootaxa* 2129(1): 29–46. <https://doi.org/10.11646/zootaxa.2129.1.2>
- Mound LA, Masumoto M (2009) Australian Thripinae of the *Anaphothrips* genus-group (Thysanoptera), with three new genera and thirty-three new species. *Zootaxa* 2042(1): 1–76. <https://doi.org/10.11646/zootaxa.2042.1.1>
- Mound LA, Ng YF (2009) An illustrated key to the genera of Thripinae (Thysanoptera) from South East Asia. *Zootaxa* 2265(1): 27–47. <https://doi.org/10.11646/zootaxa.2265.1.2>
- Mound LA, Palmer JM (1981) Phylogenetic relationships between some genera of Thripidae (Thysanoptera). *Entomologica Scandinavica* 15: 153–17.
- Mound LA, Wang Z, Lima EFB, Marullo R (2022) Problems with the concept of “Pest” among the diversity of pestiferous thrips. *Insects* 13(1): e61. <https://doi.org/10.3390/insects13010061>
- Rachana RR, Varatharajan R (2017) Checklist of terebrantian thrips (Insecta: Thysanoptera) recorded from India. *Journal of Threatened Taxa* 9(1): 9748–9755. <https://doi.org/10.11609/jott.2705.9.1.9748-9755>
- ThripsWiki (2022) ThripsWiki—providing information on the world thrips. <http://thrips.info/> [Accessed on 14.12.2022].
- Tree DJ, Mound LA (2009) Gall-induction by an Australian insect of the family Thripidae (Thysanoptera: Terebrantia). *Journal of Natural History* 43(19–20): 1147–1158. <https://doi.org/10.1080/00222930902807767>
- Wang Z, Yajin L, Xiaoli T, Mound LA (2020) Phylogenetic analysis of the *Taeniothrips* genus-group, with revision of the species of *Ctenothrips* and *Vulgateothrips* (Thysanoptera, Thripinae). *Zootaxa* 4750(3): 301–327. <https://doi.org/10.11646/zootaxa.4750.3.1>
- Zhang S, Mound LA, Feng J (2019) Morphological phylogeny of Thripidae (Thysanoptera: Terebrantia). *Invertebrate Systematics* 33(4): 671–696. <https://doi.org/10.1071/IS19001>



# A new stream treefrog of the genus *Hyloscirtus* (Amphibia, Hylidae) from the Río Negro-Sopladora National Park, Ecuador

Juan C. Sánchez-Nivicela<sup>1,2,3</sup>, José M. Falcón-Reibán<sup>4</sup>, Diego F. Cisneros-Heredia<sup>1,3</sup>

**1** Universidad San Francisco de Quito USFQ, Colegio de Ciencias Biológicas y Ambientales COCIBA, Instituto de Biodiversidad Tropical IBIOTROP, Laboratorio de Zoología Terrestre, Museo de Zoología, Quito 170901, Ecuador **2** Universidad Nacional de Colombia, Facultad de Ciencias, Grupo de Investigación Evolución y Ecología de Fauna Neotropical, Bogotá D.C., Colombia **3** Instituto Nacional de Biodiversidad, División de Herpetología, Quito, Ecuador **4** Universidad Complutense de Madrid, Facultad de Ciencias Biológicas, Madrid, España

Corresponding author: Diego F. Cisneros-Heredia ([diego.cisnerosheredia@gmail.com](mailto:diego.cisnerosheredia@gmail.com))

---

Academic editor: Anthony Herrel | Received 13 July 2022 | Accepted 19 December 2022 | Published 19 January 2023

---

<https://zoobank.org/1E409C8A-5371-4330-ACCD-C1F02E06037C>

---

**Citation:** Sánchez-Nivicela JC, Falcón-Reibán JM, Cisneros-Heredia DF (2023) A new stream treefrog of the genus *Hyloscirtus* (Amphibia, Hylidae) from the Río Negro-Sopladora National Park, Ecuador. ZooKeys 1141: 75–92. <https://doi.org/10.3897/zookeys.1141.90290>

---

## Abstract

Recent surveys in the Río Negro-Sopladora National Park revealed a striking new species of *Hyloscirtus*. The new species is easily diagnosed from all other congeners by its large body size (64.9 mm SVL in adult female); broad dermal fringes in fingers and toes; prepollex not projected into a prepollical spine and hidden under thenar tubercle; dorsum greyish-green, with paler-hued reticulum, yellow spots and black speckles; throat, venter, flanks and hidden surfaces of limbs golden-yellow with large black blotches and spots; fingers, toes and webbing yellow with black bars and spots; iris pale pink with black periphery. It is currently known only from its type locality, in the high montane forest on the southern slopes of the Cordillera Oriental of the Andes, southeastern Ecuador. The new species might be related to the *H. larinopygion* species group based on its morphology.

## Keywords

Hylid frogs, *Hyloscirtus larinopygion* species group, Morona-Santiago, mountain forest, new species, taxonomy

*“In a stream in the forest there lived a Hyloscirtus.  
Not a nasty, dirty stream, with spoor of contamination and a muddy smell,  
nor yet a dry, bare, sandy stream with nothing in it to perch on or to eat:  
it was a Hyloscirtus-stream, and that means environmental quality.”*  
(adapted from the opening of “The Hobbit” by J. R. R. Tolkien)

## Introduction

The genus *Hyloscirtus* Peters, 1882 currently includes 39 species of stream-breeding treefrogs, representing a distinct group of riverine amphibians distributed from Costa Rica to Bolivia (Faivovich et al. 2005; Frost 2022). Broad dermal fringes on fingers and toes are synapomorphic for *Hyloscirtus*, and molecular evidence supports their monophyly (Faivovich et al. 2005; Almendáriz et al. 2014; Rivera-Correa et al. 2016; Ron et al. 2018; Reyes-Puig et al. 2022). Three monophyletic species groups have been recognised inside *Hyloscirtus*: *Hyloscirtus armatus* group, *Hyloscirtus bogotensis* group, and *Hyloscirtus larinopygion* group (Faivovich et al. 2005).

The *Hyloscirtus larinopygion* species group has been diagnosed by having a large body size (SVL > 60 mm) and dark brown or grey dorsum with pale marks (Duellman et al. 2016; Ron et al. 2018). Two strongly supported clades are identified within this species group, showing latitudinal replacement among each other and sympatry in central and southern Ecuador (Almendáriz et al. 2014; Rivera-Correa et al. 2016; Rojas-Runjaic et al. 2018; Ron et al. 2018; Reyes-Puig et al. 2022). Fourteen species distributed across the Andes of southern Colombia and southern Ecuador are part of the northern clade of the *H. larinopygion* species group. The southern clade currently includes four species inhabiting the Andes of southern Ecuador and northern Peru (Ron et al. 2018; Reyes-Puig et al. 2022).

Seven species of the northern clade and three species of the southern clade (marked with asterisks) of the *H. larinopygion* group occur in restricted ranges across mountain forests on the eastern Andean slopes of Colombia and Ecuador, above 2000 m elevation: \**Hyloscirtus condor* Almendáriz, Brito-M., Batallas-R. & Ron, 2014; \**H. hillisi* Ron, Caminer, Varela-Jaramillo & Almeida-Reinoso, 2018; *H. lindae* (Duellman & Altig, 1978); *H. pacha* (Duellman & Hillis, 1990); *H. pantostictus* (Duellman & Berger, 1982); *H. psarolaimus* (Duellman & Hillis, 1990); *H. sethmacfarlanei* Reyes-Puig, D. Recalde, F. Recalde, Koch, Guayasamin, Cisneros-Heredia, Jost & Yáñez-Muñoz, 2022; *H. staufferorum* (Duellman & Coloma, 1993); \**H. tapichalaca* (Kizirian, Coloma & Paredes-Recalde, 2003); and *H. tigrinus* Mueses-Cisneros & Anganoy-Criollo, 2008.

Recent expeditions to the Río Negro-Sopladora National Park, on the eastern slopes of the Andes of southeastern Ecuador, resulted in the discovery of a magnificent new species of *Hyloscirtus*. Herein, we describe this new species based on its distinctive morphology and colouration.

## Materials and methods

Fieldwork was carried out between February and March 2020 at the Río Negro-Sopladora National Park, on the border between the provinces of Morona-Santiago and Azuay, southeastern Andes of Ecuador. Surveyed ecosystems included paramo grasslands and montane and foothill evergreen forests, between 1000 and 3400 m elevation on the River Paute basin. We used the complete species inventory field methodology (Angulo et al. 2006), with nocturnal surveys carried out between 19:00 and 23:00. Field coordinates were obtained using a Garmin Handheld Navigator GPS and are referenced to datum WGS84.

The specimen was euthanised with a 5% lidocaine solution, fixed in 10% formalin, and preserved in 70% ethanol, following recommendations by McDiarmid (1994) and Simmons and Muñoz Saba (2005). All procedures in this study comply with the guidelines for managing live amphibians and reptiles in field investigations (Beaupre et al. 2004). The study was carried out under scientific research authorisation N° 019-2018-IC-FAU-DNB/MAE and framework contract for access to genetic resources N° MAE-DNB-CM-2018-0106.

We reviewed diagnostic characters used for the taxonomy of the *Hyloscirtus larinopygion* species group based on data obtained from the direct study of specimens, photographs of preserved and live frogs with verified identification from Anfíbios del Ecuador BioWeb database (Ron et al. 2019), CalPhotos (Berkeley Natural History Museums 2012) and MCZbase (Museum of Comparative Zoology 2022); and from the literature, including original descriptions (Duellman 1973; Duellman and Altig 1978; Duellman and Berger 1982; Ruiz-Carranza and Lynch 1982; Duellman and Hillis 1990; Ardila-Robayo et al. 1993; Duellman and Coloma 1993; Faivovich et al. 2005; Faivovich and De la Riva 2006; Mueses-Cisneros and Anganoy-Criollo 2008; Coloma et al. 2012; Rivera-Correa and Faivovich 2013; Almendáriz et al. 2014; Duellman et al. 2016; Rivera-Correa et al. 2016; Rojas-Runjaic et al. 2018; Ron et al. 2018; Yáñez-Muñoz et al. 2021; Reyes-Puig et al. 2022). The following specimens were examined for comparisons and are deposited in the following scientific collections: Museo de Zoología, Universidad San Francisco de Quito, Quito (**ZSFQ**); División de Herpetología, Instituto Nacional de Biodiversidad, Quito (**DHMECN**); Museo de Zoología, Pontificia Universidad Católica del Ecuador, Quito (**QCAZ**): *Hyloscirtus condor*: Cerro Plateado, Zamora-Chinchipec, Ecuador (QCAZ-65235–7). *Hyloscirtus criptico*: Cuellaje, Imbabura, Ecuador (QCAZ 42149). *Hyloscirtus hillisi*: El Quimi, Morona-Santiago, Ecuador (QCAZ68655–56). *Hyloscirtus larinopygion*: Moran, Carchi, Ecuador (DHMECN 3799). *Hyloscirtus lindae*: Parque Nacional Sumaco, Napo, Ecuador (ZSFQ 812); Sendero Oyacachi–El Chaco, Napo, Ecuador (2633–35); Guango Lodge, Napo, Ecuador (DHMECN 12483). *Hyloscirtus pacha*: Vía Gualaceo-Limón, Morona-Santiago (QCAZ 10489). *Hyloscirtus pantostictus*: Santa Barbara, Sucumbíos, Ecuador (ZSFQ 2147, 2188), La Bonita, Sucumbíos, Ecuador (ZSFQ 2187). *Hyloscirtus psarolaimus*: Parque Nacional Sumaco, Napo, Ecuador (ZSFQ 844).

*Hyloscirtus ptychodactylus*: Pilaló, Cotopaxi, Ecuador (KU 209781). *Hyloscirtus staufferorum*: Parque Nacional Sumaco, Napo, Ecuador (ZSFQ 854, 55). *Hyloscirtus tapichalaca*: Tapichalaca, Zamora-Chinchipe, Ecuador (QCAZ 17776).

Format, definitions, and terminology used for the species description follow standards proposed by Duellman (1970) and Duellman and Hillis (1990). Webbing formulae follow the notation system proposed by Savage and Heyer (1967) and Myers and Duellman (1982). We use the definitions and terminology for the colouration patterns of body and limbs proposed by Savage (2002) and for eye colouration descriptions by Glaw and Vences (1997). Sex and maturity were determined by inspection of gonads through a dorsolateral incision. The following measurements were taken with digital calipers (0.01 mm accuracy, rounded to the nearest 0.1 mm) under a stereomicroscope by a single person: Snout-vent length (SVL), head length (HL), head width (HW), inter-narial distance (IND), interorbital distance (IOD), eye width (EW), eye-nostril distance (EN), eye diameter (ED), tympanum diameter (TD), tibial length (TL), foot length (FL), disc of Finger III width (Fin3DW). Colouration patterns in life and other relevant characteristics were obtained from field notes and photographs taken in the field.

## Results

The specimen collected at Río Negro-Sopladora National Park has broad dermal fringes in fingers and toes, a large body size (64.9 mm in SVL) and lacks mental glands. Broad dermal fringes are a putative morphological synapomorphy of the genus *Hyloscirtus* (Faivovich et al. 2005; Rivera-Correa and Faivovich 2013), and the other two characteristics suggest that this specimen might be related to species included in the *Hyloscirtus larinopygion* species group (Faivovich et al. 2005; Rivera-Correa and Faivovich 2013; Duellman et al. 2016)—although some species of the group have mental glands, e.g., *H. caucanus* (Brunetti et al. 2015). The specimen from Río Negro-Sopladora National Park shows some phenetic characteristics like those present in species of the northern clade of the *H. larinopygion* group. Species of the northern clade are morphological distinct from species of the southern clade as follows (condition for species of the southern clade in parentheses): HW/HL < 1.1 (HW/HL ≥ 1.1); longer snouts, usually EN/ED > 0.75 (EN/ED < 0.65); dentigerous processes of vomer in contact or slightly separated and having numerous vomerine teeth (widely separated, with few vomerine teeth); forearms robust and slightly thicker than upper arm (forearms and arms hypertrophied, similar to species of the *Hyloscirtus armatus* species group); enlarged, broad, elliptical prepollex, hidden under thenar tubercle (protruding, curved prepollex spine); colouration on dorsum different from colouration on flanks, hidden surfaces of thighs and venter (coloration similar on dorsal, flanks and venter) (Fig. 1). The distinction between both clades of the *H. larinopygion* species group has been consistently identified in several studies (Almendáriz et al. 2014; Rivera-Correa et al. 2016; Rojas-Runjaic et al. 2018; Ron et al. 2018).

The specimen from Río Negro-Sopladora National Park shows a unique colouration pattern with pale coloured background and dark marks on dorsal, lateral, and

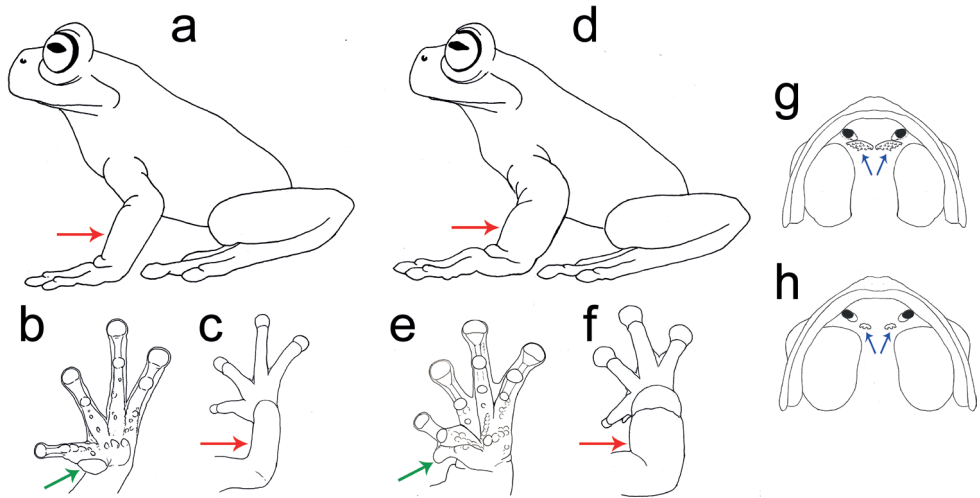


**Figure 1.** General morphology of species of the northern (**a–c, g**) and southern (**d–f, h**) clades of the *Hyloscirtus larinopygion* species group. Red arrows in **a** and **c** show non-hypertrophied forearms, while **d** and **f** show hypertrophied forearms. Green arrow in **b** shows prepollex hidden under thenar tubercle, while **e** shows prepollex protruding in a prepollical spine. Blue arrows in **g** show dentigerous processes of vomer slightly separated with numerous vomerine teeth, while **h** show dentigerous processes of vomer notoriously separated with few vomerine teeth. Illustrations by José M. Falcón-Reibán and Juan C. Sánchez-Nivicela.

ventral surfaces, while most species currently under the *H. larinopygion* group have dark-coloured backgrounds with dark or pale marks (except for *H. sarampiona* and some specimens of *H. larinopygion* and *H. psarolaimus*). While it is known from a single individual, we propose that the population of *Hyloscirtus* from the Río Negro-Sopladora National Park corresponds to an undescribed taxon, and we described it below.

## Systematics

### *Hyloscirtus tolkieni* sp. nov.

<https://zoobank.org/0DA4A78A-D514-43FA-B5DA-8F5074F9E353>

Figs 2–4, 5o, 6o, 7o

English common name: Río Negro Stream Treefrog

Spanish common name: Rana de Torrente de Río Negro

**Holotype** (Figs 2–4) ZSFQ-4142 (field number JCS-1613), adult female collected at Puente de Piedra (2°47'13"S, 78°36'16"W; 3190 m), Parque Nacional Río Negro-Sopladora, provincia de Morona Santiago, República del Ecuador, by José M. Falcón-Reibán, Juan C. Sánchez-Nivicela, and Tarquino Valverde, on 5 February 2020.

**Diagnosis.** *Hyloscirtus tolkieni* differs from other congeneric species by the following combination of characters: large body size (64.9 mm SVL in a single adult female); broad dermal fringes in fingers and toes; discs slightly expanded; head 7% wider than long; snout truncate in dorsal and lateral view; tympanic membrane and annulus

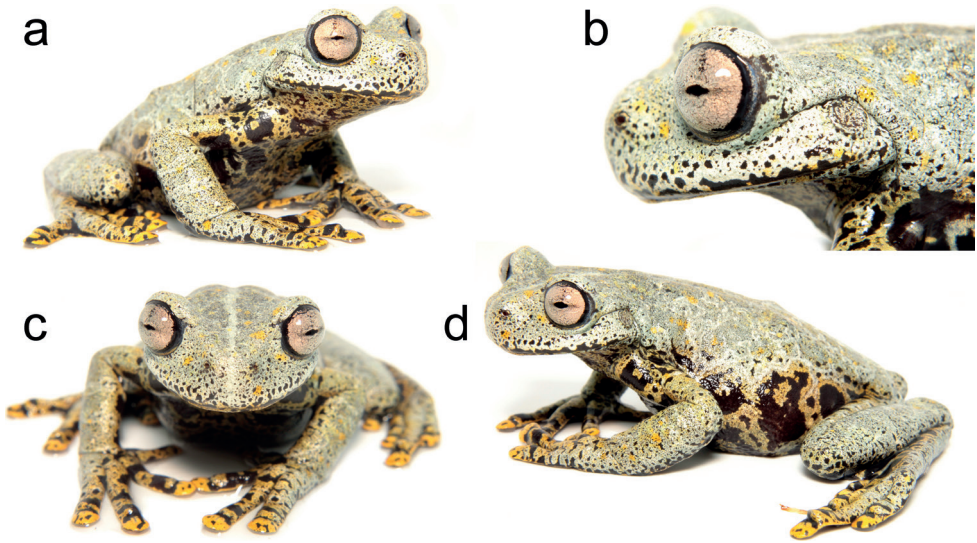


**Figure 2.** Holotype of *Hyloscirtus tolkieni* sp. nov. (SVL = 64.9 mm) in life: **a** fronto-lateral view **b** lateral view of head **c** frontal view **d** dorso-lateral view. Photographs by Juan C. Sánchez-Nivicela.

evident, partially covered by supratympanic fold; dentigerous process of vomers slightly separated, with 9–13 vomerine teeth; forearm robust and slightly thicker than arm; discs slightly expanded; broad dermal fringes in fingers and toes; prepollex enlarged, hidden under thenar tubercle and not projected into a prepollical spine; subarticular tubercles on hands and feet rounded and poorly projected; calcar tubercle present; dorsum greyish-green, with paler-hued reticulum, yellow spots and black speckles; throat, venter, flanks and hidden surfaces of limbs yellow with large black blotches and spots; fingers, toes and webbing yellow with black bars and spots; iris pale pink with black periphery, sclera greyish-blue, and nictitating membrane yellow (Figs 2–4).

*Hyloscirtus tolkieni* is readily distinguishable from all other species of *Hyloscirtus* by its greyish-green dorsum with paler reticulations, yellow spots, and black speckles. Based on its colouration pattern, *Hyloscirtus tolkieni* (characteristics in parentheses) is easily differentiated from all other species of the northern clade of the *Hyloscirtus larinopygion* species group (Figs 5–7) as follows: Dorsal surfaces of *H. antioquia*, *H. caucanus*, *H. criptico*, *H. larinopygion*, *H. lindae*, *H. pacha*, *H. pantostictus*, *H. princecharlesi*, *H. psarolaimus*, *H. ptychodactylus*, *H. sethmacfarlanei* and *H. staufferorum* are dark or light brown or black with or without paler or darker marks, *H. sarampiona* is pale olive green with orange spots, and *H. tigrinus* is green or yellow with thick black reticulum or stripes (greyish-green dorsum with paler reticulum, yellow spots and black speckles). Flanks of *H. antioquia*, *H. caucanus*, *H. criptico*, *H. lindae*, *H. pacha*, *H. pantostictus*, *H. princecharlesi*, *H. ptychodactylus*, *H. sarampiona*, *H. sethmacfarlanei* and *H. staufferorum* are dark brown or black with or without paler or darker marks; bluish grey or cream with dark bars, blotches, or spots in *H. larinopygion* and *H. psarolaimus*; and yellow or green with thick black stripes or reticulum in *H. tigrinus* (yellow flanks with large black blotches and spots). Fingers, toes and

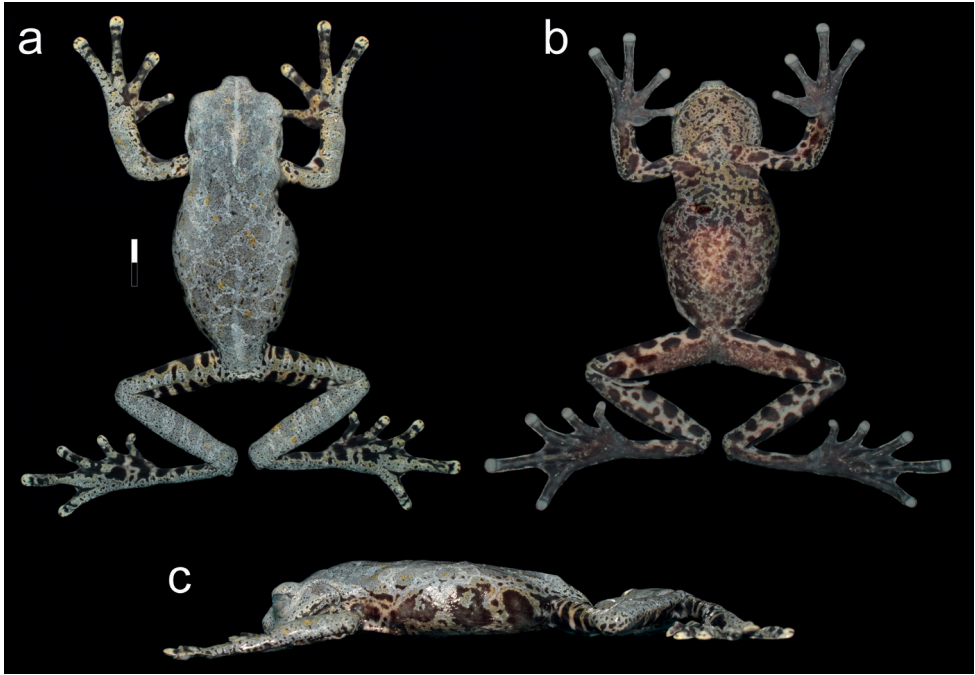


**Figure 3.** Holotype of *Hyloscirtus tolkieni* sp. nov. in preservative **a** dorsal view **b** ventral view **c** lateral view. Scale bar: 1 cm.

discs are dark brown in *H. criptico* and *H. staufferorum*; dark brown with orange discs in *H. lindae*; bluish grey with dark bars in *H. larinopygion*; dark brown with pale bars in *H. pacha*; black with pale discs in *H. caucanus* and *H. pantostictus*; black with orange or red spots in *H. princecharlesi* and *H. sethmacfarlanei*; cream with dark marks in *H. psarolaimus*; black with reddish-brown marks in *H. ptychodactylus*; dark olive green with orange dots in *H. sarampiona*; and yellow or green with black marks in *H. tigrinus* (yellow with black marks). Irises of *H. criptico*, *H. pacha*, *H. pantostictus*, *H. princecharlesi*, and *H. staufferorum* are dark grey or brown without reticulations; grey with dark grey reticulations in *H. sethmacfarlanei*; grey with burgundy reticulations in *H. antioquia*; pale yellow with brown reticulations in *H. caucanus*; golden with black reticulations in *H. larinopygion*; dark brown with minute grey flecks in *H. lindae*; dull bronze with black reticulations in *H. psarolaimus*; pale blue in *H. ptychodactylus*; gold with black reticulations in *H. sarampiona*; and light grey or yellow with black reticulations in *H. tigrinus* (pale pink with very thin, almost imperceptible, reticulations). Snout rounded in dorsal view in *H. antioquia*, *H. caucanus*, *H. larinopygion*, *H. lindae*, *H. pacha*, *H. pantostictus*, *H. psarolaimus*, *H. sarampiona*, *H. staufferorum*, and *H. tigrinus* (truncated). Vomerine teeth 12–20 in *H. antioquia* and 21–25 in *H. staufferorum* (9–13). Calcar tubercles absent in *H. princecharlesi* (present).

*Hyloscirtus tolkieni* has non-protruding prepollex and narrower head ( $HW/HL = 1.07$ ), more vomerine teeth (9–13), and thinner forearms than species of the southern clade of the *H. larinopygion* species group (including *H. condor*, *H. diabolus*,

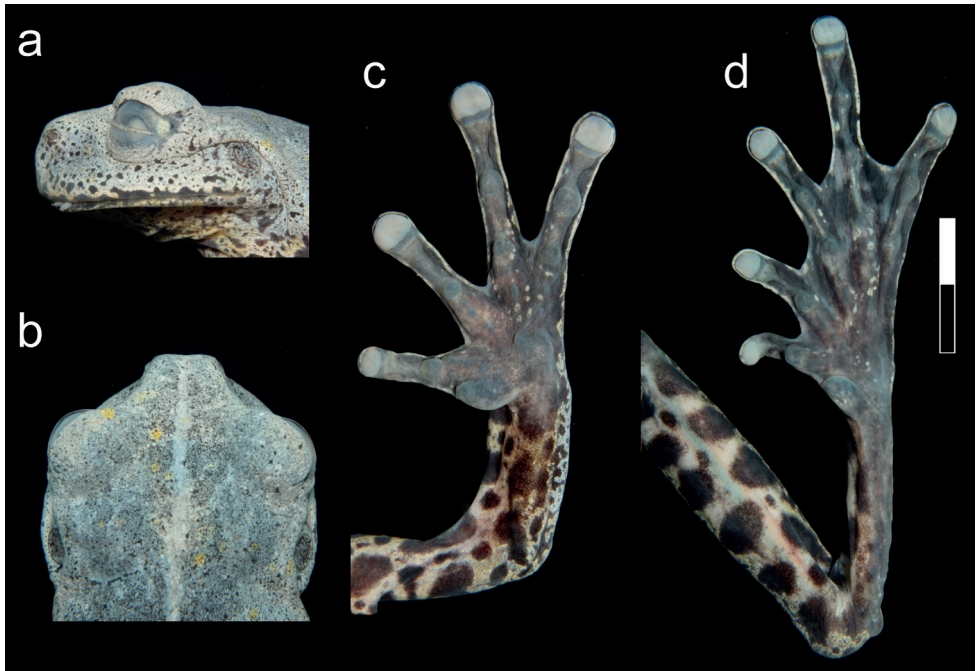


**Figure 4.** Details of *Hyloscirtus tolkienii* sp. nov. in preservative **a** lateral view of head **b** dorsal view of head **c** ventral view of hand **d** ventral view of foot. Scale bar: 1 cm.

*H. hillisi* and *H. tapichalaca*), which have protruding prepollical spines, wider heads ( $HW/HL \geq 1.10$ ), less vomerine teeth (2–6), and hypertrophied forearms. Also, all species of the southern clade of the *H. larinopygion* species group are dark-coloured dorsally and ventrally.

*Hyloscirtus tolkienii* differs from species of the *H. armatus* species group by the absence of clusters of keratinised spines on the prepollex and the proximal ventral surface of the humerus (present in *H. armatus* and *H. charazani*), non-expanded prepollex (expanded in *H. armatus* and *H. charazani*), robust but not hypertrophied forearms (hypertrophied in *H. armatus* and *H. charazani*), and absence of a skin fold in the proximoventral portion of upper arm (present in *H. armatus*, *H. charazani*, and *H. chlorostea*).

*Hyloscirtus tolkienii* differs from species of the *H. bogotensis* species group, including *H. albopunctulatus* and *H. phyllognathus* that inhabit the eastern Andes of Ecuador, and from *H. jahni*, single member of its homonym group, by its larger body size with 64.9 mm in SVL (smaller in the *H. bogotensis* and *H. jahni* species groups with  $SVL < 36$  mm), greyish-green dorsum with paler reticulum, yellow spots and black speckles (green or brown dorsum with or without pale or dark spots and speckles and pale lines in the *H. bogotensis* and *H. jahni* species groups), ventral surfaces yellow with large black blotches and spots (venter cream or yellowish without dark marks in the *H. bogotensis* and *H. jahni* species groups).

**Description of the holotype.** Adult female (Figs 2–4), 64.9 mm SVL, body robust. Head wider than long ( $HW/HL = 1.07$ ,  $HW/SVL = 0.31$ ,  $HL/SVL = 0.29$ );

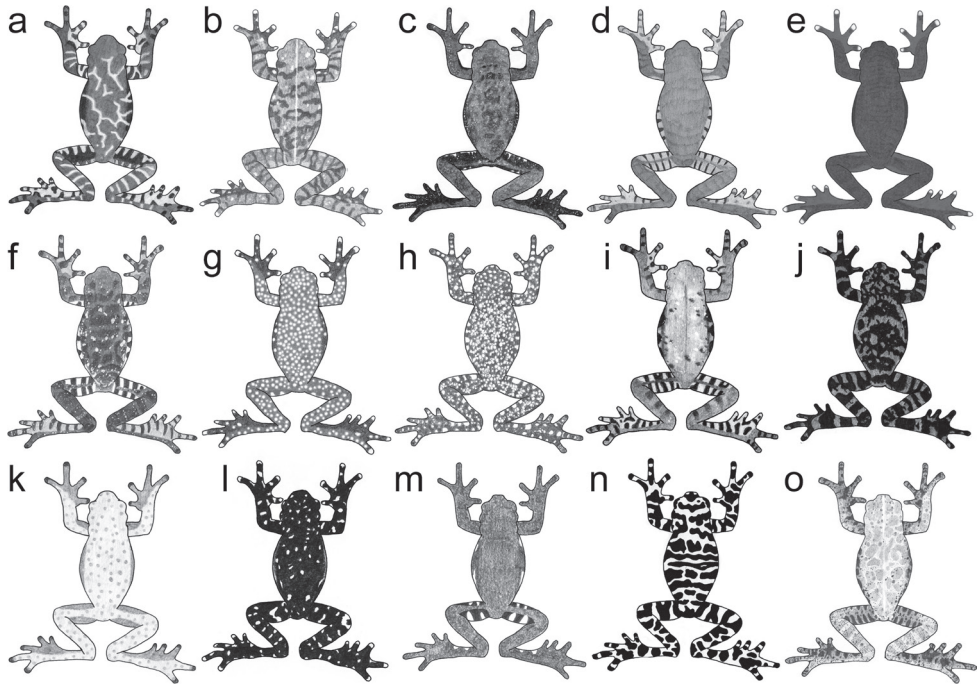


**Figure 5.** Dorsal colouration patterns in species of the northern clade of the *Hyloscirtus larinyopygion* species group **a** *H. antioquia* **b** *H. caucanus* **c** *H. criptico* **d** *H. larinyopygion* **e** *H. lindae* **f** *H. pacha* **g** *H. pantostictus* **h** *H. princecharlesi* **i** *H. psarolaimus* **j** *H. ptychodactylus* **k** *H. sarampiona* **l** *H. sethmacfarlanei* **m** *H. staufferorum* **n** *H. tigrinus* **o** *H. tolkien* sp. nov. Illustrations by José M. Falcón-Reibán.

snout truncate in dorsal and lateral view; canthus rostralis rounded, distinct; loreal region slightly concave, nearly vertical; lips rounded, slightly flared; nostrils slightly protuberant, openings directed anterolaterally, located at level of anterior margin of lower jaw, area between nostril slightly concave; dorsal surface of internarial region concave; interorbital distance shorter than eye (IOD/ED = 0.91); eye prominent (ED/HL = 0.37, ED/EN = 1.33); tympanic membrane and annulus evident (TD/ED = 0.41); supratympanic fold prominent, extending from below eye across upper and posterior margins of tympanum towards posterior end of mouth and down to arm insertion; region between head and suprascapula slightly depressed; dentigerous processes of vomer prominent, oval, in transverse position, between choanae, narrowly separated, left process with 9 vomerine teeth and right one with 13; choanae small, rounded, separated about 4× their maximum diameter; tongue cordiform, broad, attached to 80% of mouth floor; mental gland absent (Figs 2–4).

Skin on dorsum shagreen, throat slightly granular, flanks and venter granular, posterior surfaces of limbs strongly granular; pectoral fold absent; cloacal opening directed posteroventrally at upper level of thighs; supraclacal flap present; two pairs of swollen, thick, vertical, pericloacal folds.

Forearms robust, slightly thicker than arms, not hypertrophied; axillary membrane absent; ulnar fold present, covering dorsal surface of forearms; fingers long,

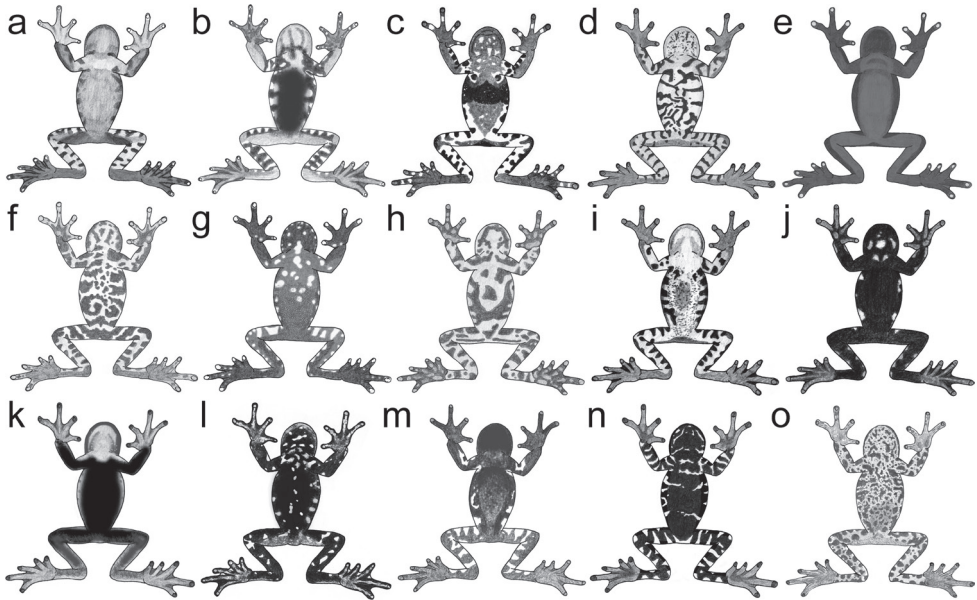


**Figure 6.** Ventral colouration patterns in species of the northern clade of the *Hyloscirtus larinyopygion* species group: **a** *H. antioquia* **b** *H. caucanus* **c** *H. criptico* **d** *H. larinyopygion* **e** *H. lindae* **f** *H. pacha* **g** *H. pantostictus* **h** *H. princecharlesi* **i** *H. psarolaimus* **j** *H. ptychodactylus* **k** *H. sarampiona* **l** *H. sethmacfarlanei* **m** *H. staufferorum* **n** *H. tigrinus* **o** *H. tolkienei* sp. nov. Illustrations by José M. Falcón-Reibán.

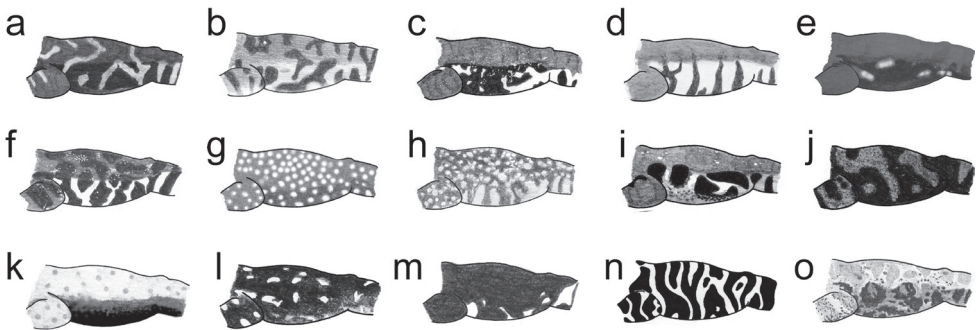


**Figure 7.** Flank colouration patterns in species of the northern clade of the *Hyloscirtus larinyopygion* species group: **a** *H. antioquia* **b** *H. caucanus* **c** *H. criptico* **d** *H. larinyopygion* **e** *H. lindae* **f** *H. pacha* **g** *H. pantostictus* **h** *H. princecharlesi* **i** *H. psarolaimus* **j** *H. ptychodactylus* **k** *H. sarampiona* **l** *H. sethmacfarlanei* **m** *H. staufferorum* **n** *H. tigrinus* **o** *H. tolkienei* sp. nov. Illustrations by José M. Falcón-Reibán.

with thick lateral fringes; discs round, slightly expanded; all discs with rounded pads, circumferential groove of each disc clearly defined; disc on Finger III wider than tympanum ( $Fin3DW/TD = 1.11$ ); relative lengths on fingers  $I < II < IV < V$ ; webbing formula:  $III3-3IV$ ; palmar surface with deep grooves; subarticular tubercles round and poorly projected, distal tubercles larger; supernumerary tuber-

cles small, rounded; thenar tubercle large, elliptical; palmar tubercle flat, bifid, same length as thenar; broad elliptical prepollex hidden under thenar tubercle (Figs 2–4).

Hindlimbs robust ( $TL/SVL = 0.48$ ,  $FL/SVL = 0.48$ ); small calcar tubercle present; short and thin inner tarsal fold; without outer tarsal fold or tubercles; inner metatarsal tubercle large, ovoid; outer metatarsal tubercle indistinct; toes long, with thick lateral fringes, bearing discs slightly smaller than those on fingers; relative lengths of toes:  $I < II < III = V < IV$ ; Toe I with last phalange twisted inside on both feet; webbing formula:  $I2-2III1\frac{2}{3}-2\frac{1}{2}III2-3IV3-2V$ . Subarticular tubercles large, round; supernumerary tubercles low, round, and sparse (Figs 2–4).

**Colouration in life.** Dorsal surfaces of head, body and limbs greyish-green, with thick paler-hued reticulum, yellow spots, and black speckles; head with a light greyish-green medial line; throat, venter and flanks yellow (more intense on the throat and turning greyish towards posterior end of venter) with large black blotches and spots; hidden surfaces of limbs yellow with transversely distributed black oval dots; fingers, toes and webbing yellow with black bars and spots; iris pale pink with black periphery, sclera greyish-blue, and nictitating membrane yellow (Fig. 2)

**Colouration in preservative.** Same colouration patterns as described for the colouration in life, but greyish-green dorsal areas turned darker grey, yellow on venter and flanks turned golden-grey to grey (Figs 3–4).

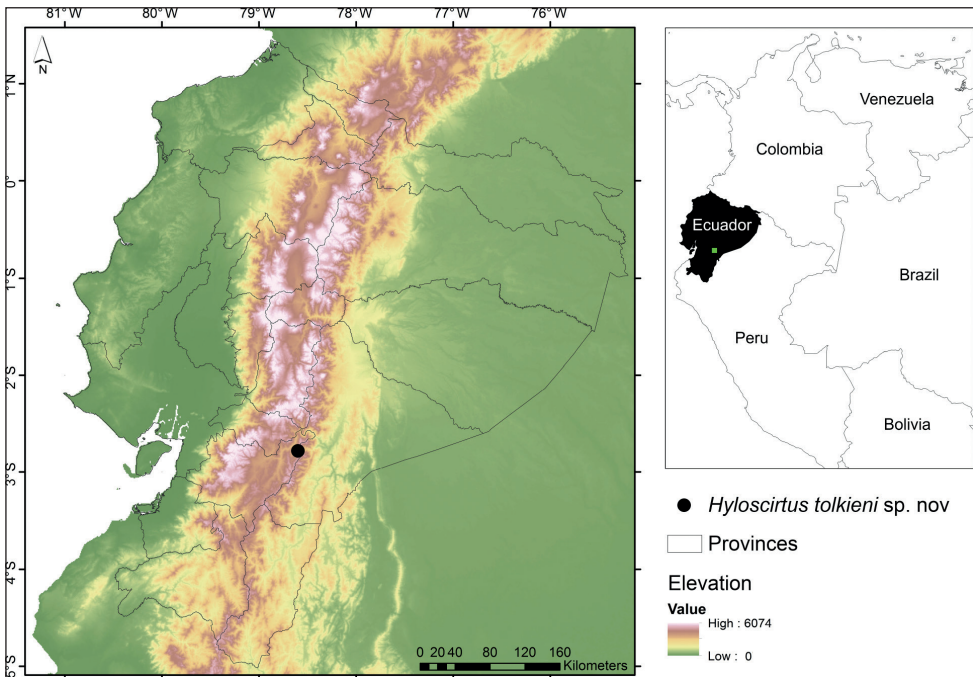


**Figure 8.** Map showing the type locality of *Hyloscirtus tolkienii* sp. nov. at the Río Negro-Sopladora National Park, province of Morona Santiago, Republic of Ecuador.



**Figure 9.** Habitat of *Hyloscirtus tolkieni* sp. nov. General landscape (above, red arrow pointing to collection site); and at the collection site inside the forest (below). Photographs by Juan C. Sánchez-Nivicela.

**Measurements of the holotype (in mm).** SVL=64.9, HL=18.8, HW=20.2, IND=4.6, IOD=6.3, EW=4.9, EN=5.2, ED=6.9; TD=2.8, TL=31.2, FL=30.9, Fin3DW=3.1.

**Etymology.** The specific epithet *tolkieni* is in honour of the writer, poet, philologist, and academic John Ronald Reuel Tolkien (J.R.R. Tolkien, 1892–1973), creator of Middle-earth and author of fantasy works like “The Hobbit” and “The Lord of the Rings”. The amazing colours of the new species evoke the magnificent creatures that seem to only exist in fantasy worlds.

**Distribution, natural history, and conservation status.** *Hyloscirtus tolkieni* is only known from its type locality on the southeastern slopes of the Cordillera Oriental of the Andes of Ecuador, at 3190 m elevation, in the Río Negro-Sopladora National Park, province of Morona Santiago (Fig. 8). The ecosystem in the area is High Montane Forest of the Eastern Cordillera of the Southern Andes of Ecuador (MAE et al. 2013). The holotype was active at night at 20:30 amidst tree branches, c. 5 m above ground and 8 m from the nearest stream (Fig. 9). It was found in sympatry with an undescribed species of *Pristimantis*.

Very few herpetological surveys have been conducted in the region, with James A. Peters being one of the few herpetologists that visited the area (Peters 1973). Our surveys were carried out over 13 effective days, and we could not detect additional individuals of *H. tolkieni*, despite focalised searches. The type locality of *H. tolkieni* is officially protected as part of the Río Negro-Sopladora National Park, a protected area created in 2018 where little habitat loss has occurred. Large, forested areas remain unstudied in the national park, and the species may have a wider distribution beyond the immediate surrounding of its type locality. In the absence of sufficient information to evaluate the conservation status and extinction risk of *H. tolkieni*, we propose that it be classified under the Data Deficiency category until more data is obtained (IUCN 2012, 2017; Ortega-Andrade et al. 2021). Urgent research and monitoring actions should be established to study its life history and ecology, population size and trends, survey new sites where additional populations may exist and evaluate if threats are impacting its long-term conservation, such as invasive species, emerging diseases, or climate changes.

### Key to the species of the northern clade of the *Hyloscirtus larinyopygion* species group

This key helps to identify adult female and male stream treefrogs of the northern clade of the *H. larinyopygion* species group, using characters that can easily be observed in the field and lab (no dissections required). This key is probably not useful to identify juveniles and ontogenetic variation in many species of the group remains unknown. This key was expanded and corrected from the keys presented by Duellman and Hillis (1990) and Duellman and Coloma (1993). Colours in preservative are shown in parentheses.

- 1a Background dorsal colouration in shades of green or yellow (turning paler green or greyish cream) (Fig. 5k, n, o) ..... **2**
- 1b Background dorsal colouration in shades of brown (Fig. 5a–j, l–m) ..... **4**
- 2a Dorsum green or yellow (greyish cream) with thick black reticulum or stripes (Fig. 5n)..... ***H. tigrinus***
- 2b Dorsum green (grey) without thick dark reticulum or stripes ..... **3**
- 3a Dorsum pale olive green with orange dots (grey with cream spots) (Fig. 5k); venter black (Fig. 6k).....***H. sarampiona***
- 3b Dorsum greyish-green with paler reticulum, yellow spots, and black speckles (green turns to grey) (Fig. 5o); venter, flanks, and hidden surfaces of limbs yellow (golden-grey) with large black blotches and spots (Fig. 6o) ..... ***H. tolkieni***

- 4a Venter (excluding throat) uniformly or predominantly black or dark brown (Fig. 5b, e, j, m) ..... **5**
- 4b Venter mostly pale or dark with distinctive darker or paler markings..... **8**
- 5a Discs on fingers orange or yellow (pale) ..... **6**
- 5b Discs on fingers dark..... **7**
- 6a Dorsum and venter dark brown (Figs 5e, 6e), discs on fingers orange in life.....  
..... ***H. lindae***
- 6b Dorsum brown with dark brown transversal bars (Fig. 5b), venter black with pale marks (Fig. 6b), discs on fingers cream in life..... ***H. caucanus***
- 7a Throat uniformly dark (Fig. 6m); hidden surfaces of limbs black with broad cream bars (Fig. 7m); iris dark brown..... ***H. staufferorum***
- 7b Throat with irregular, large, pale spots (Fig. 6j); hidden surfaces of limbs black, sometimes with reddish-brown (Fig. 7j); iris pale blue in life.... ***H. ptychodactylus***
- 8a Dorsum with orange or red (pale) circular dots on a dark background ..... **9**
- 8b Dorsum without orange or red (pale) circular dots. If orange (pale) markings are present, they are in the form of flecks or blotches but not circular dots ..... **10**
- 9a Discs on fingers yellow (white); venter black with white mottling on belly and orange dots (white) on the throat (Fig. 6g)..... ***H. pantostictus***
- 9b Discs on fingers grey, venter black with pale yellow (cream) marbling or reticulation (Fig. 6h) ..... ***H. princecharlesi***
- 9c Disc on fingers with red spots (yellowish white); venter black with red (yellowish white) dots (Fig. 6l)..... ***H. sethmacfarlanei***
- 10a Venter cream to brownish or dirty grey ..... **11**
- 10b Venter dark brown with pale markings..... **12**
- 11a Venter dirty grey (Fig. 6a); dorsum brown with orange (grey) reticulation (Fig. 5a); flanks grey or black with yellow (cream) markings delimited with blue or pale-grey outline (Fig. 7a); iris grey with burgundy reticulations in life .....  
..... ***H. antioquia***
- 11b Venter cream to brownish grey with diffuse dark spots and pale flecks (Fig. 6i); dorsum brown with small dark brown and cream flecks (Fig. 5i); flanks cream with vertical dark bars (Fig. 7i); iris dull bronze with black reticulations in life ...  
..... ***H. psarolaimus***
- 12a Flank black with orange (cream) speckles and some white and brown blotches (Fig. 7c); venter mottled dark brown with orange (cream) speckles and pale marks (Fig. 6c) ..... ***H. criptico***
- 12b Flanks dark with pale reticulum or pale with black vertical bars ..... **13**
- 13a Dorsum brown with small orange (cream) flecks (Fig. 5f); venter dark brown with bold cream reticulum (Fig. 6f); hidden surfaces of limbs black with narrow, vertical, cream bars (Fig. 7f)..... ***H. pacha***
- 13b Dorsum brown with or without dark-brown reticulation (Fig. 5d); flanks, venter, and hidden surfaces of limbs white or light bluish grey (cream) with black bars or reticulation (Figs 6d, 7d)..... ***H. larinopygion***

## Acknowledgements

We express our gratitude to Fabián Rodas and Naturaleza y Cultura Internacional for providing support and funding for field and lab work; and to Eduardo Toral, with whom we conducted the first expedition and whose work was essential for this project. The work of Naturaleza y Cultura Internacional, Fabián Rodas and Eduardo Toral was vital for the declaration of the Río Negro-Sopladora National Park. We are grateful to FONAPA and the Cutín team for providing equipment and facilities; to our friends from El Copal and Sevilla de Oro, especially to the Rojas Villavicencio and Villavicencio Valverde families for their hospitality and help during fieldwork; to Tarquino Valverde, our field companion; and to Diego Armijos-Ojeda and two anonymous reviewers for their comments. The following people provided working space and support during our work at their respective institutions: Mario H. Yáñez-Muñoz (DHMECN); John D. Lynch (ICN); William E. Duellman, Linda Trueb, Juan M. Guayasamin and Elisa Bonaccorso (KU); and Carolina Reyes-Puig and Emilia Peñaherrera (ZSFQ). Naturaleza y Cultura Internacional funded this research as part of the research project “Evaluación de Especies Detonadoras de Herpetofauna en el Parque Nacional Río Negro-Sopladora”. Work by DFCH was funded by Universidad San Francisco de Quito USFQ.

## References

- Almendáriz A, Brito J, Batallas D, Ron S (2014) Una especie nueva de rana arbórea del género *Hyaloscirtus* (Amphibia: Anura: Hylidae) de la Cordillera del Cóndor. *Papéis Avulsos de Zoología* 54(4): 33–49. <https://doi.org/10.1590/0031-1049.2014.54.04>
- Angulo A, Rueda Almonacid JV, Rodríguez Mahecha JV, La Marca E (2006) Técnicas de inventario y monitoreo para los anfibios de la región tropical andina. *Conservación Internacional Colombia*, Bogotá, 299 pp.
- Ardila-Robayo MC, Ruiz-Carranza PM, Roa-Trujillo SH (1993) Una nueva especie de *Hyla* del grupo *larinopygion* (Amphibia: Anura: Hylidae) del sur de la Cordillera Central de Colombia. *Revista de la Academia Colombiana de Ciencias Exactas, Físicas y Naturales* 18: 559–566.
- Beaupre SJ, Jacobson ER, Lillywhite HB, Zamudio KR (2004) Guidelines for Use of Live Amphibians and Reptiles in Field and Laboratory Research. *American Society of Ichthyologists and Herpetologists*, 24 pp.
- Berkeley Natural History Museums (2012) CalPhotos. <https://calphotos.berkeley.edu/> [April 17, 2022]
- Brunetti AE, Hermida GN, Luna MC, Barsotti AMG, Jared C, Antoniazzi MM, Rivera-Correa M, Berneck BVM, Faivovich J (2015) Diversity and evolution of sexually dimorphic mental and lateral glands in Cophomantini treefrogs (Anura: Hylidae: Hylinae): Mental and Lateral Glands in Cophomantini. *Biological Journal of the Linnean Society* 114(1): 12–34. <https://doi.org/10.1111/bj.12406>

- Coloma LA, Carvajal-Endara S, Dueñas JF, Paredes-Recalde A, Morales-Mite M, Almeida-Reinoso D, Tapia EE, Hutter CR, Toral E, Guayasamin JM (2012) Molecular phylogenetics of stream treefrogs of the *Hyloscirtus larinopygion* group (Anura: Hylidae), and description of two new species from Ecuador. *Zootaxa* 3364(1): 1–78. <https://doi.org/10.11646/zootaxa.3364.1.1>
- Duellman WE (1970) 1 The Hylid Frogs of Middle America. Monograph of the Museum of Natural History, The University of Kansas, Lawrence, 448 pp. <https://doi.org/10.5962/bhl.title.2835>
- Duellman WE (1973) Descriptions of New Hylid Frogs from Colombia and Ecuador. *Herpetologica* 29: 219–227.
- Duellman WE, Altig R (1978) New Species of Tree Frogs (Family Hylidae) from the Andes of Colombia and Ecuador. *Herpetologica* 34: 177–185.
- Duellman WE, Berger TJ (1982) A New Species of Andean Treefrog (Hylidae). *Herpetologica* 38: 456–460.
- Duellman WE, Coloma LA (1993) *Hyla staufferorum*, a New Species of Treefrog in the *Hyla larinopygion* Group from the Cloud Forests of Ecuador. Occasional Papers of the Museum of Natural History, The University of Kansas, 11 pp. <https://doi.org/10.5962/bhl.part.15140>
- Duellman WE, Hillis DM (1990) Systematics of Frogs of the *Hyla larinopygion* Group. Occasional Papers of the Museum of Natural History, The University of Kansas 23 pp.
- Duellman WE, Marion AB, Hedges SB (2016) Phylogenetics, classification, and biogeography of the treefrogs (Amphibia: Anura: Arboranae). *Zootaxa* 4104(1): 1–1. <https://doi.org/10.11646/zootaxa.4104.1.1>
- Faivovich J, De la Riva I (2006) On “*Hyla*” *chlorostea* Reynolds and Foster, 1992, a Hylid of Uncertain Relationships, with Some Comments on *Hyloscirtus* (Anura: Hylidae). *Copeia* 2006(4):785–791. [https://doi.org/10.1643/0045-8511\(2006\)6\[785:OHCRAF\]2.0.CO;2](https://doi.org/10.1643/0045-8511(2006)6[785:OHCRAF]2.0.CO;2)
- Faivovich J, Haddad CFB, Garcia PCA, Frost DR, Campbell JA, Wheeler WC (2005) Systematic review of the frog family Hylidae, with special reference to Hylinae: Phylogenetic analysis and taxonomic revision. *Bulletin of the American Museum of Natural History* 294(1): 1–1. [https://doi.org/10.1206/0003-0090\(2005\)294\[0001:SROTFF\]2.0.CO;2](https://doi.org/10.1206/0003-0090(2005)294[0001:SROTFF]2.0.CO;2)
- Frost DR (2022) *Hyloscirtus* Peters, 1882 | Amphibian Species of the World. Amphibian Species of the World: an Online Reference. <https://doi.org/10.5531/db.vz.0001>
- Glaw F, Vences M (1997) A Review of Anuran Eye Colouration: Definitions, Taxonomic Implications and Possible Functions. *Herpetologica Bonnensis. Societas Herpetologica Europaea*, Bonn, 125–138.
- IUCN (2012) IUCN Red List Categories and Criteria: Version 3.1.( 2<sup>nd</sup> edn.). International Union for Conservation of Nature and Natural Resources IUCN, Gland, Switzerland and Cambridge, 32 pp.
- IUCN (2017) Guidelines for using the IUCN Red List Categories and Criteria. Version 13. Standards and Petitions Subcommittee, IUCN Species Survival Commission, 108 pp.
- MAE Galeas R, Guevara JE, Medina-Torres B, Chinchero MÁ, Herrera X [Eds] (2013) Sistema de Clasificación de los Ecosistemas del Ecuador Continental. Ministerio del Ambiente del Ecuador (MAE), Subsecretaría de Patrimonio Natural, Quito, 232 pp.

- McDiarmid RW (1994) Preparing amphibians as scientific specimens. In: Heyer R, Donnelly MA, McDiarmid RW, Hayek L-AC, Foster MS (Eds) *Measuring and Monitoring Biological Diversity: Standard Methods for Amphibians*. Smithsonian Institution, 275–276.
- Mueses-Cisneros JJ, Anganoy-Criollo MA (2008) Una Nueva Especie del Grupo *Hyloscirtus larinopygion* (Amphibia: Anura: Hylidae) del Suroccidente de Colombia. *Papéis Avulsos de Zoologia*, São Paulo, 48 pp. <https://doi.org/10.1590/S0031-10492008001500001>
- Museum of Comparative Zoology (2022) MCZbase: The database of the Zoological Collections, Museum of Comparative Zoology, Harvard University. MCZbase: The database of the Zoological Collections. [https://mczbase.mcz.harvard.edu/SpecimenSearch.cfm?collection\\_id=1#](https://mczbase.mcz.harvard.edu/SpecimenSearch.cfm?collection_id=1#) [April 17, 2022]
- Myers CW, Duellman WE (1982) A New Species of *Hyla* from Cerro Colorado, and Other Tree Frog Records and Geographical Notes from Western Panama. *American Museum Novitates*, 32 pp.
- Ortega-Andrade HM, Rodes Blanco M, Cisneros-Heredia DF, Guerra Arévalo N, López de Vargas-Machuca KG, Sánchez-Nivicela JC, Armijos-Ojeda D, Cáceres Andrade JF, Reyes-Puig C, Quezada Riera AB, Székely P, Rojas Soto OR, Székely D, Guayasamin JM, Sivichay Pesántez FR, Amador L, Betancourt R, Ramírez-Jaramillo SM, Timbe-Borja B, Gómez Laporta M, Webster Bernal JF, Oyagata Cachimuel LA, Chávez Jácome D, Posse V, Valle-Piñuela C, Padilla Jiménez D, Reyes-Puig JP, Terán-Valdez A, Coloma LA Pérez Lara MaB, Carvajal-Endara S, Urgilés M, Yáñez Muñoz MH (2021) Red List assessment of amphibian species of Ecuador: A multidimensional approach for their conservation. *PLoS ONE* 16(5): e0251027. <https://doi.org/10.1371/journal.pone.0251027>
- Peters JA (1973) The frog genus *Atelopus* in Ecuador (Anura: Bufonidae). *Smithsonian Contributions to Zoology* 145: 1–49. <https://doi.org/10.5479/si.00810282.145>
- Reyes-Puig JP, Recalde D, Recalde F, Koch C, Guayasamin JM, Cisneros-Heredia DF, Jost L, Yáñez-Muñoz MH (2022) A spectacular new species of *Hyloscirtus* (Anura: Hylidae) from the Cordillera de Los Llanganates in the eastern Andes of Ecuador. *PeerJ* 10: e14066. <https://doi.org/10.7717/peerj.14066>
- Rivera-Correa M, Faivovich J (2013) A New Species of *Hyloscirtus* (Anura: Hylidae) from Colombia, with a Rediagnosis of *Hyloscirtus larinopygion* (Duellman, 1973). *Herpetologica* 69(3): 298–313. <https://doi.org/10.1655/HERPETOLOGICA-D-12-00059>
- Rivera-Correa M, García-Burneo K, Grant T (2016) A new red-eyed of stream treefrog of *Hyloscirtus* (Anura: Hylidae) from Peru, with comments on the taxonomy of the genus. *Zootaxa* 4061(1): 29–40. <https://doi.org/10.11646/zootaxa.4061.1.3>
- Rojas-Runjaic FJM, Infante-Rivero EE, Salerno PE, Meza-Joya FL (2018) A new species of *Hyloscirtus* (Anura, Hylidae) from the Colombian and Venezuelan slopes of Sierra de Perijá, and the phylogenetic position of *Hyloscirtus jahni* (Rivero, 1961). *Zootaxa* 4382(1): e121. <https://doi.org/10.11646/zootaxa.4382.1.4>
- Ron SR, Caminer MA, Varela-Jaramillo A, Almeida-Reinoso D (2018) A new treefrog from Cordillera del Cóndor with comments on the biogeographic affinity between Cordillera del Cóndor and the Guianan Tepuis (Anura, Hylidae, *Hyloscirtus*). *ZooKeys* 809: 97–124. <https://doi.org/10.3897/zookeys.809.25207>

- Ron SR, Merino-Viteri A, Ortiz DA (2019) Anfibios del Ecuador. Version 2019.0. <https://bioweb.bio/faunaweb/amphibiaweb/> [March 24, 2019]
- Ruiz-Carranza PM, Lynch JD (1982) Dos nuevas especies de *Hyla* (Amphibia: Anura) de Colombia, con aportes al conocimiento de *Hyla bogotensis*. *Caldasia* XIII: 647–671.
- Savage JM (2002) The Amphibians and Reptiles of Costa Rica: a Herpetofauna Between Two Continents, Between Two Seas. University of Chicago Press, Chicago, 934 pp.
- Savage JM, Heyer WR (1967) Variation and distribution in the tree-frog genus *Phyllomedusa* in Costa Rica, central America: With 6 figures. *Beiträge zur Neotropischen Fauna* 5(2): 111–131. <https://doi.org/10.1080/01650526709360400>
- Simmons JE, Muñoz Saba Y (2005) Cuidado, Manejo y Conservación de las Colecciones Biológicas. Conservación Internacional, Bogotá.
- Yáñez-Muñoz MH, Reyes-Puig JP, Batallas-Revelo D, Broaddus C, Urgilés-Merchán M, Cisneros-Heredia DE, Guayasamin JM (2021) A new Andean treefrog (Amphibia: *Hyloscirtus bogotensis* group) from Ecuador: an example of community involvement for conservation. *PeerJ* 9: e11914. <https://doi.org/10.7717/peerj.11914>

# A new species of the *Cyrtodactylus brevipalmatus* group (Squamata, Gekkonidae) from the uplands of western Thailand

L. Lee Grismer<sup>1,2</sup>, Attapol Rujirawan<sup>3</sup>, Siriwadee Chomdej<sup>4</sup>,  
Chatmongkon Suwannapoom<sup>5</sup>, Siriporn Yodthong<sup>6</sup>,  
Akrachai Aksornneam<sup>3</sup>, Anchalee Aowphol<sup>3</sup>

**1** Herpetology Laboratory, Department of Biology, La Sierra University, 4500 Riverwalk Parkway, Riverside, California 92505, USA **2** Department of Herpetology, San Diego Natural History Museum, PO Box 121390, San Diego, California 92112, USA **3** Animal Systematics and Ecology Speciality Research Unit, Department of Zoology, Faculty of Science, Kasetsart University, Bangkok 10900, Thailand **4** Department of Biology, Faculty of Science, Chiang Mai University, Chiang Mai 50200, Thailand **5** Division of Fishery, School of Agriculture and Natural Resources, University of Phayao, Phayao 56000, Thailand **6** Department of Biology, Faculty of Science, Thaksin University, Pa Phayom, Phattalung 93210, Thailand

Corresponding author: Anchalee Aowphol ([fsciocl@ku.ac.th](mailto:fsciocl@ku.ac.th))

Academic editor: T. Ziegler | Received 16 November 2022 | Accepted 26 December 2022 | Published 19 January 2023

<https://zoobank.org/34377D39-2C3B-4626-8C50-8335C128E462>

**Citation:** Grismer LL, Rujirawan A, Chomdej S, Suwannapoom C, Yodthong S, Aksornneam A, Aowphol A (2023) A new species of the *Cyrtodactylus brevipalmatus* group (Squamata, Gekkonidae) from the uplands of western Thailand. ZooKeys 1141: 93–118. <https://doi.org/10.3897/zookeys.1141.97624>

## Abstract

An integrative systematic analysis recovered a new species of the *Cyrtodactylus brevipalmatus* group from the uplands of Thong Pha Phum National Park, Kanchanaburi Province in western Thailand. *Cyrtodactylus thongphaphumensis* **sp. nov.** is deeply embedded within the *brevipalmatus* group, bearing an uncorrected pairwise sequence divergence of 7.6–22.3% from all other species based on a 1,386 base pair segment of the mitochondrial NADH dehydrogenase subunit 2 gene (ND2) and adjacent tRNAs. It is diagnosable from all other species in the *brevipalmatus* group by statistically significant mean differences in meristic and normalized morphometric characters as well as differences in categorical morphology. A multiple factor analysis recovered its unique and non-overlapping placement in morphospace as statistically significantly different from that of all other species in the *brevipalmatus* group. The description of this new species contributes to a growing body of literature underscoring the high degree of herpetological diversity and endemism across the sky-island archipelagos of upland montane tropical forest habitats in Thailand, which like all other upland tropical landscapes, are becoming some of the most imperiled ecosystems on the planet.

**Keywords**

Bent-toed gecko, genetics, Indochina, integrative taxonomy, montane forests, morphology

**Introduction**

The gekkonid genus *Cyrtodactylus* Gray, 1827 contains well over 350 named and unnamed species and constitutes the third largest vertebrate genus on the planet (Grismer et al. 2021a, b; Uetz et al. 2022). To date, its extensive distribution extends across at least eight biogeographic regions and crosses a number of well-established biogeographic barriers from South Asia to western Melanesia (Grismer et al. 2022a). The ecological plasticity, phylogenetic relationships, and geographic distribution among, and within its 32 geographically circumscribed monophyletic species groups, are indicative of its ability to disperse across ephemeral seaways, major river systems, basins, mountain ranges, and land bridges, followed by extensive in situ diversification within specific geographic areas (Grismer et al. 2020, 2021a, b, 2022a).

Within Indochina and northern Sundaland, the *Cyrtodactylus brevipalmatus* group is one of the most ecologically and morphologically specialized groups within *Cyrtodactylus* (sec. Grismer et al. 2020, 2021a, b). All members bear a similar morphology, behavior, and color pattern adapted to an arboreal life style (Grismer et al. 2022b). The latest phylogenetic taxonomic treatment of the group (Grismer et al. 2022c) described four new species from Thailand, resulting in ten described and potentially as many undescribed populations needing further study. One of these undescribed populations, *C.* sp. 9 from Thong Pha Phum National Park, Kanchanaburi Province in western Thailand (Fig. 1), was first recognized on the basis of molecular phylogenetic evidence from a single specimen (Chomdej et al. 2021). We collected and sequenced eight additional specimens which corroborate the results of Chomdej et al. (2021) in that all eight specimens plus the specimen of Chomdej et al. (2021) form a monophyletic lineage deeply nested within the *brevipalmatus* group (Grismer et al. 2022c). Univariate and multivariate analyses of the eight new specimens recovered statistically significant morphological and morphospacial differences from all other members of the group which unequivocally indicate that it requires species-level recognition (Grismer et al. 2022c). As such, it is described herein.

**Materials and methods****Genetic data**

Methods for DNA extraction, sequencing, and editing followed Grismer et al. (2021c) and resulted in a 1,386 base pair segment of the mitochondrial NADH dehydrogenase subunit 2 gene (ND2) and adjacent tRNAs. All material examined is listed in Grismer et al. (2022c: table 1) along with GenBank accession numbers.

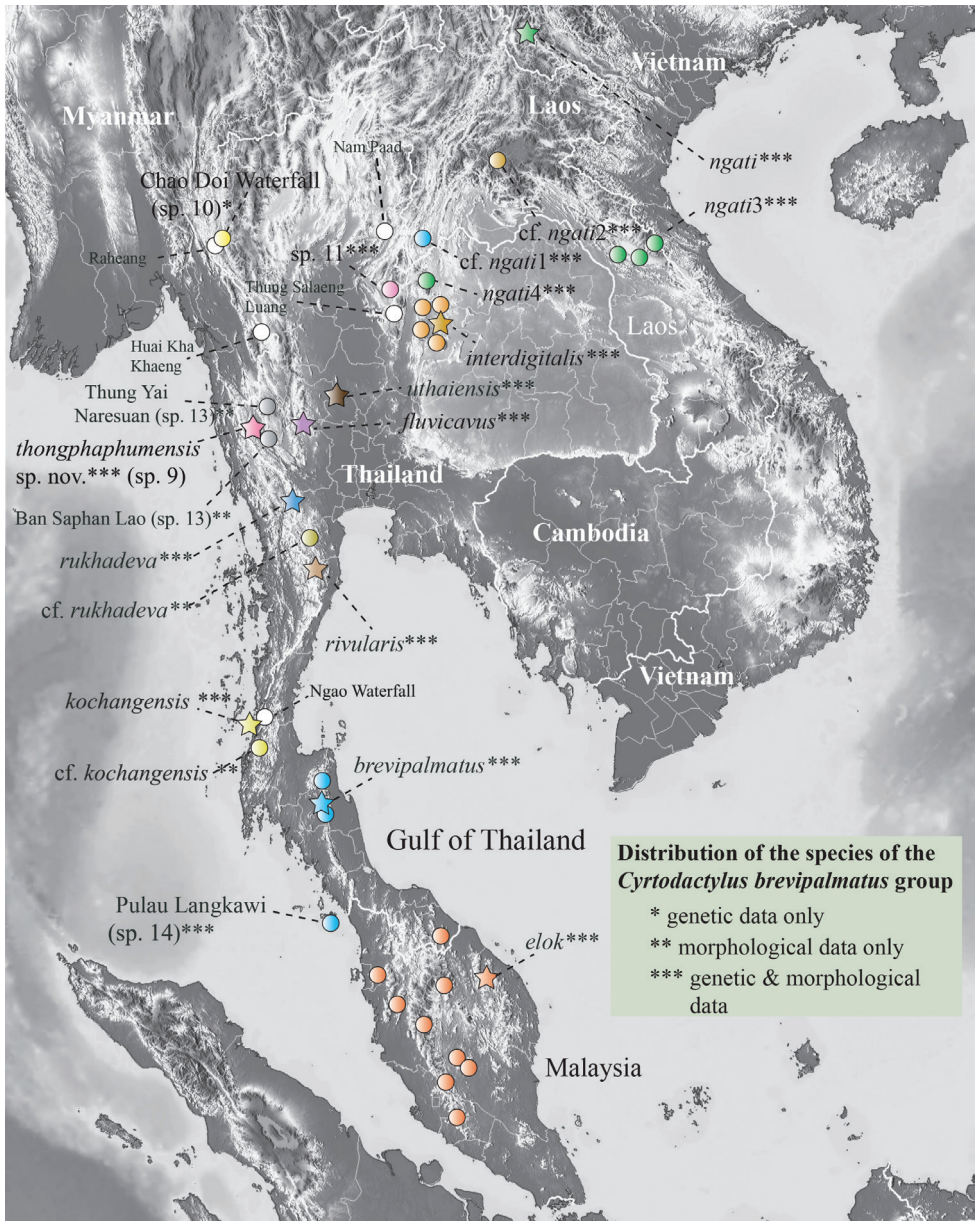


**Figure 1.** Distribution of nominal species and unnamed populations of the *Cyrtodactylus brevipalmatus* group. Stars denote type localities. White circles are literature localities from which specimens were not examined and remain unidentified. Locality data for all material examined is in Grismer et al. (2022c: table 1).

## Morphological data

The morphological data taken included 17 meristic, 18 normalized morphometric, and eight categorical characters (Grismer et al. 2022c) (Table 1). Normalization of the morphometric characters followed the method of Chan and Grismer (2022).

**Table 1.** Descriptions of morphometric, meristic, and categorical characters.

Abbreviations	Characters
<b>Morphometric characters</b>	
SVL	snout-vent length, taken from the tip of the snout to the vent
TL	tail length, taken from the vent to the tip of the tail—original or partially regenerated
TW	tail width, taken at the base of the tail immediately posterior to the postcloacal swelling
HumL	humeral length, taken from the proximal end of the humerus at its insertion point in the glenoid fossa to the distal margin of the elbow while flexed 90°
ForL	forearm length, taken on the ventral surface from the posterior margin of the elbow while flexed 90° to the inflection of the flexed wrist
FemL	femur length, taken from the proximal end of the femur at its insertion point in the acetabulum to the distal margin of the knee while flexed 90°
TibL	tibia length, taken on the ventral surface from the posterior margin of the knee while flexed 90° to the base of the heel
AG	axilla to groin length, taken from the posterior margin of the forelimb at its insertion point on the body to the anterior margin of the hind limb at its insertion point on the body
HL	head length, the distance from the posterior margin of the retroarticular process of the lower jaw to the tip of the snout
HW	head width, measured at the angle of the jaws
HD	head depth, the maximum height of head measured from the occiput to base of the lower jaw posterior to the eyes
ED	eye diameter, the greatest horizontal diameter of the eye-ball
EE	eye to ear distance, measured from the anterior edge of the ear opening to the posterior edge of the bony orbit
ES	eye to snout distance or snout length, measured from anteriormost margin of the bony orbit to the tip of snout
EN	eye to nostril distance, measured from the anterior margin of the bony orbit to the posterior margin of the external nares
IO	interorbital distance, measured between the dorsomedial-most edges of the bony orbits
IN	internarial distance, measured between the external nares across the rostrum
EL	ear length, greatest oblique length across the auditory meatus.
<b>Meristic characters</b>	
SL	supralabial scales, counted from the largest scale at the corner of the mouth or posterior to the eye, to the rostral scale
IL	infralabial scales, counted from termination of enlarged scales at the corner of the mouth to the mental scale
PVT	paravertebral tubercles between the limb insertions, counted in a straight line immediately left of the vertebral column
LRT	longitudinal rows of body tubercles, counted transversely across the body midway between the limb insertions from one ventrolateral body fold to the other
VS	longitudinal rows of ventral scales, counted transversely across the abdomen midway between limb insertions from one ventrolateral fold to the other
VSM	transverse rows of ventral scales, counted along the midline of the body from the postmentals to just anterior to the cloacal opening, stopping where the scales become granular
TL4E	expanded subdigital lamellae on the fourth toe proximal to the digital inflection, counted from the base of the first phalanx where it contacts the body of the foot to the largest scale on the digital inflection—the large contiguous scales on the palmar and plantar surfaces were not counted
TL4U	small, generally unmodified subdigital lamellae distal to the digital inflection on the fourth toe, counted from the digital inflection to the claw including the claw sheath
TL4T	total number of subdigital lamellae beneath the fourth toe, TL4E + TL4U = TL4T
FL4E	number of expanded subdigital lamellae on the fourth finger proximal to the digital inflection, counted the same way as with TL4E
FL4U	small generally unmodified subdigital lamellae distal to the digital inflection on the fourth finger, counted the same way as with TL4U
FL4T	total number of subdigital lamellae beneath the fourth toe, FL4E + FL4U = FL4T
FS	enlarged femoral scales, counted from each thigh and combined as a single metric
PCS	enlarged precloacal scales, counted as a single metric
PP	number of precloacal pores in males, counted as a single metric
FP	femoral pores in males, counted from each thigh and combined as a single metric
BB	number of dark body bands, counted from between the dark band on the nape and the hind limb insertions on the body
<b>Categorical characters</b>	
FKT	tubercles on the flanks (present or absent)
SC1	slightly enlarged medial subcaudals (present or absent)
SC2	single distinctly enlarged, unmodified, row of medial subcaudal scales (present or absent)
SC3	enlarged medial subcaudals intermittent, medially furrowed, posteriorly emarginated (yes or no)
DCT	dorsolateral caudal tubercles (small or large)
VLF1	DCT forming a ventrolateral caudal fringe (narrow or wide)
VLF2	ventrolateral caudal fringe scales generally homogenous or not (yes or no)
TLcross	cross-section of the tail (round or square)

## Phylogenetic analyses

Following Grismer et al. (2022c), an input file implemented in BEAUti (Bayesian Evolutionary Analysis Utility) v. 2.4.6 was run in BEAST (Bayesian Evolutionary Analysis Sampling Trees) v. 2.4.6 (Drummond et al. 2012) on CIPRES (Cyberinfrastructure for Phylogenetic Research; Miller et al. 2010) in order to generate a BEAST phylogeny, employing a lognormal relaxed clock with unlinked site models and linked trees and clock models. bModelTest (Bouckaert and Drummond 2017), implemented in BEAST, was used to numerically integrate over the uncertainty of substitution models while simultaneously estimating phylogeny using Markov chain Monte Carlo (MCMC). MCMC chains were run using a Yule prior for 40,000,000 million generations and logged every 4,000 generations. The BEAST log file was visualized in Tracer v. 1.7.0 (Rambaut et al. 2018) to ensure effective sample sizes (ESS) were well-above 200 for all parameters. A maximum clade credibility tree using mean heights at the nodes was generated using TreeAnnotator v. 1.8.0 (Rambaut and Drummond 2013) with a burn-in of 1,000 trees (10%). Nodes with Bayesian posterior probabilities (BPP) of 0.95 and above were considered strongly supported (Huelsenbeck et al. 2001; Wilcox et al. 2002). Uncorrected pairwise sequence divergences were calculated in MEGA 11 (Tamura et al. 2021) using the complete deletion option to remove gaps and missing data from the alignment prior to analysis.

## Statistical analyses

All statistical analyses were conducted using R Core Team (2018). A Levene's test for the normalized morphometric and meristic characters was conducted to test for equal variances across all groups. Characters with equal variances ( $F \geq 0.05$ ) were analyzed by an analysis of variance (ANOVA) and TukeyHSD post hoc test. Those with unequal variances ( $F < 0.05$ ) were subjected to Welch's F-test and Games-Howell *post hoc* test.

Morphospacial clustering and positioning among the species was analyzed using multiple factor analysis (MFA) on a concatenated data set comprised of 38 characters including non-metric categorical characters which cannot be used in a principal component analysis (Suppl. material 1). The MFA was implemented using the *mfa()* command in the R package FactorMineR (Husson et al. 2017) and visualized using the Factoextra package (Kassambara and Mundt 2017). A non-parametric permutation multivariate analysis of variance (PERMANOVA) from the *vegan* package 2.5–3 in R (Oksanen et al. 2020) was used to determine the statistical significance of centroid locations and group clustering. The analysis used a Euclidean (dis)similarity matrix with 50,000 permutations based on the loadings of the first four dimensions recovered from the MFA. The highly morphologically derived *Cyrtodactylus elok* was not included so as to prevent biasing the morphospacial relationships among the other species (see Grismer et al. 2022b).

## Results

### Phylogenetic analysis

The BEAST analysis recovered the Thong Pha Phum population as being deeply embedded within the *brevipalmatus* group and the strongly supported (1.00) sister lineage to two sister groups composed of (1) *C. interdigitalis*, *C. uthaiensis*, and *C. sp. 11* and (2) *C. cf. ngati1*, *C. cf. ngati2*, *C. ngati3*, *C. ngati4*, and *C. ngati* (Fig. 2). The uncorrected pairwise sequence divergence between the Thong Pha Phum population and all other species of the *brevipalmatus* group ranges from 7.6–22.3%. (Table 2).

### Statistical analyses

The ANOVA and TukeyHSD *post hoc* and Welch’s F-test and Games-Howell *post hoc* tests of the adjusted morphometric and meristic characters were consistent with the phylogenetic and pairwise distance data in recovering a number of sta-

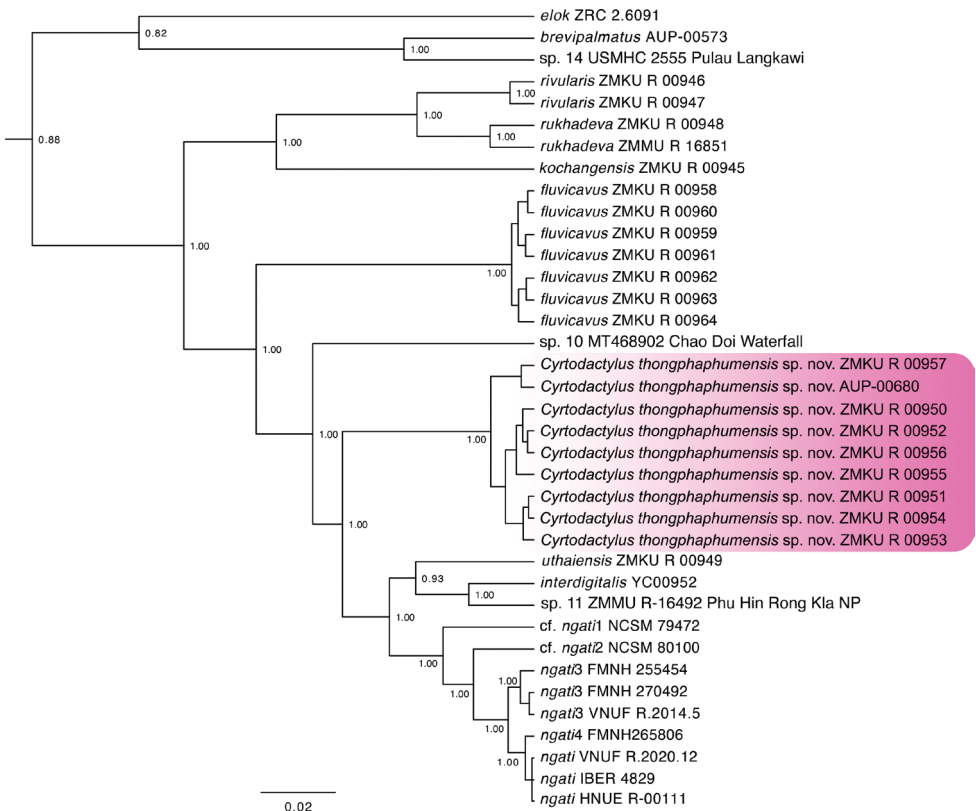


**Figure 2.** Maximum clade credibility BEAST phylogeny of the *Cyrtodactylus brevipalmatus* group highlighting the new species described herein. Bayesian posterior probabilities (BPP) are listed at the nodes.

**Table 2.** Mean (minimum–maximum) percentages of uncorrected pairwise sequence divergence (*p*-distances) among the putative species of the *Cyrtodactylus brevipalmatus* group based on 1,386 base pairs of mitochondrial NADH dehydrogenase subunit 2 gene (ND2) and adjacent tRNAs. Intraspecific *p*-distances are in bold font. n/a = data not applicable.

Species	1. <i>C. brevipalmatus</i>	2. <i>C. cf. ngant1</i>	3. <i>C. cf. ngant2</i>	4. <i>C. elok</i>	5. <i>C. fluminis</i>	6. <i>C. interdigitalis</i>	7. <i>C. kochanogensis</i>	8. <i>C. ngat1, C. ngat2 and C. ngat3</i>	9. <i>C. rimularis</i>	10. <i>C. rubbudaeva</i>	11. <i>C. thongphaphumensis</i> sp. nov.	12. <i>C. sp.10</i>	13. <i>C. sp.11</i>	14. <i>C. sp.14</i>	15. <i>C. utaiensis</i>
N	1	1	1	1	7	1	1	7	2	2	9	1	1	1	1
1.	n/a														
2.	21.03	n/a													
3.	21.68	4.39	n/a												
4.	20.77	22.58	21.42	n/a											
5.	18.86 (18.84–18.97)	10.64 (10.58–10.84)	11.02 (10.97–11.23)	20.15 (20.13–20.26)	<b>0.10</b> (0.00–0.26)										
6.	20.77	6.97	9.16	22.84	12.02 (12.00–12.13)	n/a									
7.	19.35	14.58	14.71	20.90	12.31 (12.26–12.31)	15.23	n/a								
8.	20.70 (20.65–20.90)	3.30 (2.84–4.00)	3.71 (3.35–4.26)	21.11 (20.90–21.42)	11.34 (11.10–11.87)	8.13 (7.74–8.65)	14.58 (14.45–14.84)	<b>0.84</b> (0.00–1.55)							
9.	20.00	15.87	15.03	21.61	12.57	15.48	12.26	15.03	<b>0.52</b>						
10.	20.65 (20.13–21.16)	15.42 (15.61–16.13)	15.48 (14.84–15.23)	21.61 (21.42–21.81)	12.25 (12.26–13.03)	16.00 (15.23–15.74)	13.10 (12.00–12.52)	15.23 (14.71–15.48)	4.65	<b>1.55</b>					
11.	20.34 (20.13–20.65)	7.93 (7.74–8.00)	9.51 (9.42–9.55)	22.02 (21.16–22.06)	9.75 (9.55–9.94)	8.96 (8.77–9.03)	13.22 (13.03–13.29)	8.81 (8.13–9.68)	13.12 (12.77–13.42)	13.25 (12.52–13.94)	<b>0.22</b> (0.00–0.52)				
12.	19.87	9.29	10.84	21.94	10.12 (10.06–10.32)	10.19	13.68	10.21 (10.06–10.45)	13.94 (13.68–14.19)	14.32 (13.68–14.97)	8.06 (7.87–8.13)	n/a			
13.	20.39	7.23	8.90	22.19	11.12 (11.10–11.23)	3.87	14.58	8.28 (8.00–8.65)	15.35 (15.10–15.61)	15.61 (14.97–16.26)	8.96 (8.77–9.03)	10.45	n/a		
14.	6.45	20.90	20.65	20.00	18.34 (18.32–18.45)	20.13	19.10	20.52 (20.26–20.65)	19.74 (19.48–20.00)	20.00 (19.48–20.52)	19.60 (19.48–19.87)	18.84	19.61	n/a	
15.	19.74	5.81	8.13	21.16	10.12 (10.06–10.32)	7.1	13.94	6.97 (6.58–7.61)	13.94 (13.68–14.19)	13.94 (13.29–14.58)	7.80 (7.61–7.87)	8.39	6.58	19.48	n/a

**Table 3.** Significant *p*-values from the results of the ANOVA and Welch’s *F* (\*) analyses comparing the normalized morphometric and meristic characters of *Cyrtodactylus thongphaphumensis* sp. nov. to other species of the *Cyrtodactylus brevipalmatus* group. Only species with and *N* > 2 are included. No significant differences were recovered for SVL. Abbreviations are in the Materials and methods.

Morphometric characters	AG*	HumL*	ForL	FemL	TibL	HL	HW	HD*	ED*	EE*	ES	EN*	IO	EL	IN
<i>C. brevipalmatus</i>						0.01	< 0.001				< 0.001	0.03			
<i>C. fluvicavus</i>			0.0					0.007			0.013	0.023		0.007	
<i>C. interdigitalis</i>					0.00		0.007								
<i>C. ngati</i>	< 0.001						< 0.001	0.042			0.007	< 0.001		< 0.001	0.000
<i>C. ngati</i> 3	0.001				0.01	0.03	0.003	0.043		0.001	0.019	0.019			0.003
<i>C. rukhadeva</i>	0.02	0.004			0.02			0.033							
Meristic characters	SL	IL*	PVT*	LRT	VS	VSM	TL4E	TL4T	FL4E	FL4U*	FL4T*	FS	PCS*	BB*	
<i>C. brevipalmatus</i>			< 0.001	0.003						0.022			< 0.001	0.05	
<i>C. fluvicavus</i>			< 0.001	< 0.001						0.001	0.004	0.020			
<i>C. interdigitalis</i>			0.003		< 0.001	0.005			0.043		0.01			< 0.001	
<i>C. ngati</i>	0.003		0.016	0.011				0.000	< 0.001	< 0.001			< 0.001	< 0.001	
<i>C. ngati</i> 3			0.001	0.042						< 0.001	0.001				
<i>C. rukhadeva</i>	0.029		< 0.001		0.002									0.001	

**Table 4.** Summary statistics from the PERMANOVA analysis from the loadings of dimension 1–4 of the MFA comparing *Cyrtodactylus thongphaphumensis* sp. nov. to all other species the *Cyrtodactylus brevipalmatus* group with sample sizes > 1. Bold fonts denote significant differences.

OTU pairs	F model	R <sup>2</sup>	<i>p</i> -value	<i>p</i> -adjusted
<i>C. rukhadeva</i>	88.504	0.847	<b>0.000</b>	<b>0.001</b>
<i>C. cf. ngati</i> 2	56.471	0.876	<b>0.020</b>	1.000
<i>C. ngati</i> 3	59.321	0.868	<b>0.006</b>	0.324
<i>C. interdigitalis</i>	85.773	0.896	<b>0.002</b>	0.112
<i>C. ngati</i>	134.367	0.937	<b>0.006</b>	0.332
<i>C. brevipalmatus</i>	80.229	0.879	<b>0.001</b>	<b>0.025</b>
<i>C. fluvicavus</i>	55.127	0.809	<b>0.000</b>	<b>0.008</b>
<i>C. rivularis</i>	9.485	0.542	<b>0.022</b>	1.000
<i>C. sp. 13</i>	30.716	0.793	<b>0.022</b>	1.000

tistically significant differences between the Thong Pha Phum population and all other species (Table 3). Thong Pha Phum population plotted separately in the MFA with meristic data contributing 16.5% of the inertia in dimension 1, categorical morphology contributing 15.3% of the inertia in dimension 2, and normalized morphometric data contributing 13.6% of the inertia in dimension 3 (Fig. 3). The PERMANOVA analysis recovered the morphospacial position of the Thong Pha Phum population as being statistically different from *C. brevipalmatus*, *C. cf. ngati*2, *C. ngati*3, *C. ngati*, *C. fluvicavus*, *C. interdigitalis*, *C. rivularis*, *C. rukhadeva*, and *Cyrtodactylus* sp. 13 (Table 4).

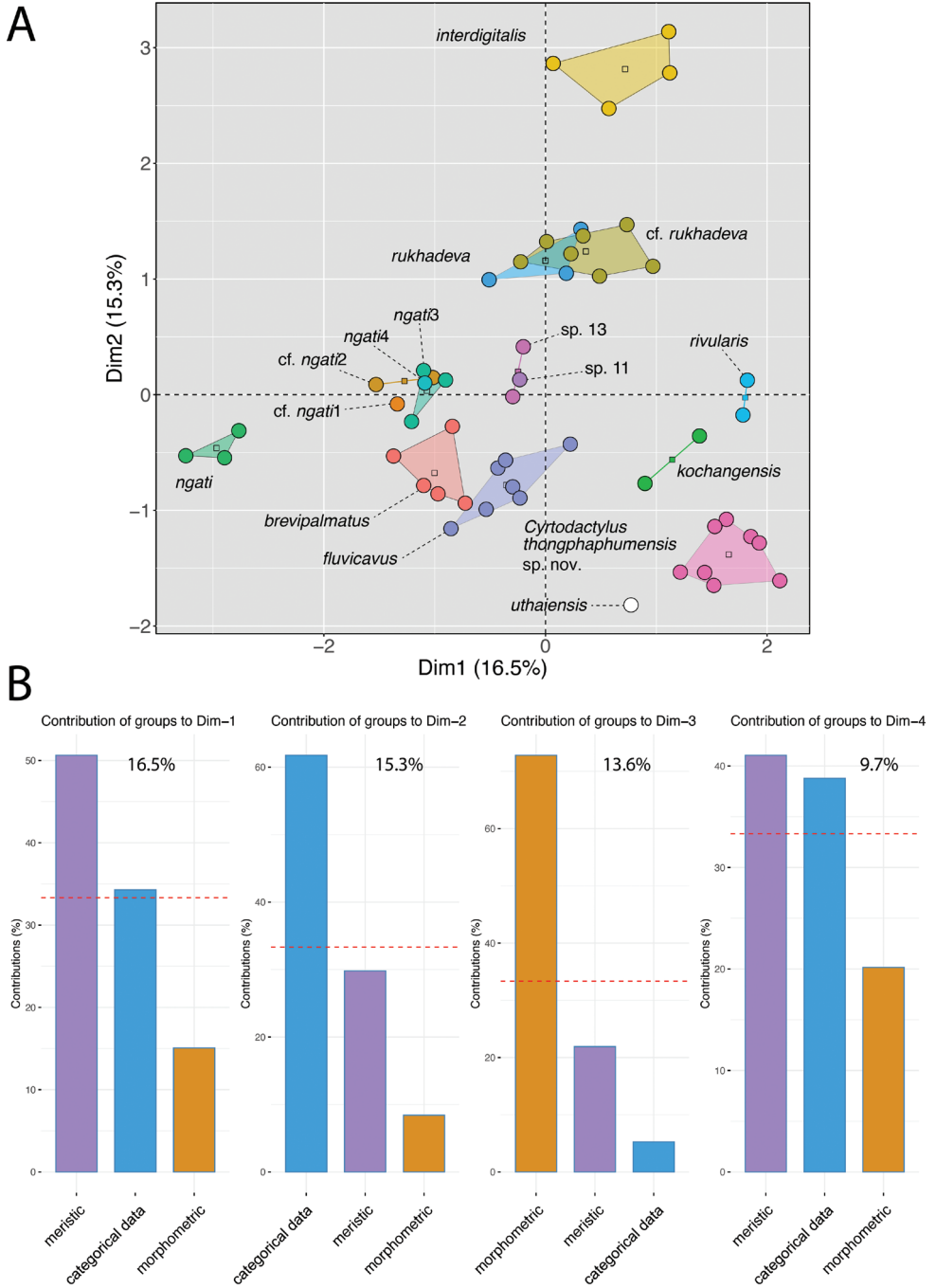


**Figure 3. A** MFA of the species-level lineages based on the BEAST phylogeny (Fig. 2) **B** Percent contributions of each data type to the inertia of dimensions 1–4 of the MFA. Percentage values on the bar graphs are the amounts of inertia for the respective dimensions.

## Taxonomy

Given the phylogenetic delimitation of the Thong Pha Phum population (Fig. 2), its statistically significant diagnostic morphological differences (Table 3), its statistically significant diagnostic placement in morphospace (Fig. 3, Table 4), and its notable difference in pairwise sequence divergence from all other species (Table 2), we describe it below as new species.

### *Cyrtodactylus thongphaphumensis* sp. nov.

<https://zoobank.org/4BB0E9B3-1BFF-49BC-BF77-79BF8CC95D27>

Suggested Common Name: Thong Pha Phum Bent-toed Gecko

Figs 4, 5

*Cyrtodactylus* sp. 9 Chomdej et al. 2021: 2; Grismer et al. 2022b: 248; Grismer et al. 2022c: 115.

**Type material. Holotype.** Adult male ZMKU R 00953 from Thong Pha Phum National Park, Pilok Subdistrict, Thong Pha Phum District, Kanchanaburi Province, Thailand (14.69339°N, 98.40534°E, 914 m a.s.l.), collected by Korkhwan Termprayoon, Akrachai Aksornneam, Natee Ampai, and Siriporn Yodthong on 8 April 2019.

**Paratypes.** Adult males ZMKU R 00951, ZMKU R 00954 and ZMKU R 00956 and adult females ZMKU R 00950, ZMKU R 00952, ZMKU R 00955, and ZMKU R 00957 bear the same collection data as the holotype.

**Diagnosis.** *Cyrtodactylus thongphaphumensis* sp. nov. can be separated from all other species of the *brevipalmatus* group by the combination of having 12–14 supralabials, 8–10 infralabials, 30–36 paravertebral tubercles, 19–21 rows of longitudinally arranged tubercles, 30–34 longitudinal rows of ventrals, 150–173 transverse rows of ventrals, 8–10 expanded subdigital lamellae on the fourth toe, 11–14 unexpanded subdigital lamellae on the fourth toe, 20–24 total subdigital lamellae on the fourth toe; seven or eight expanded subdigital lamellae on the fourth finger, 10–12 unexpanded subdigital lamellae on the fourth finger, 18–20 total subdigital lamellae on the fourth finger; 12–16 total number of enlarged femoral scales, 12–16 total number of femoral pores in males; 15 preloacal pores in males; 15–17 enlarged preloacals; enlarged femorals and enlarged preloacals not continuous; proximal femorals smaller than distal femorals; small tubercles on forelimbs and flanks; large dorsolateral caudal tubercles and wide ventrolateral caudal fringe; ventrolateral caudal fringe composed scales of different size; tail square in cross-section; maximum SVL 76.6 mm; 3–5 dark transverse body bands (Table 5).

**Description of holotype (Fig. 4).** Adult male SVL 73.2 mm; head moderate in length (HL/SVL 0.27), width (HW/HL 0.70), depth (HD/HL 0.39), distinct from neck, triangular in dorsal profile; lores concave slightly anteriorly, weakly inflated posteriorly; prefrontal region concave; canthus rostralis rounded; snout elongate (ES/HL 0.40), rounded in dorsal profile; eye large (ED/HL 0.25); ear opening horizontally

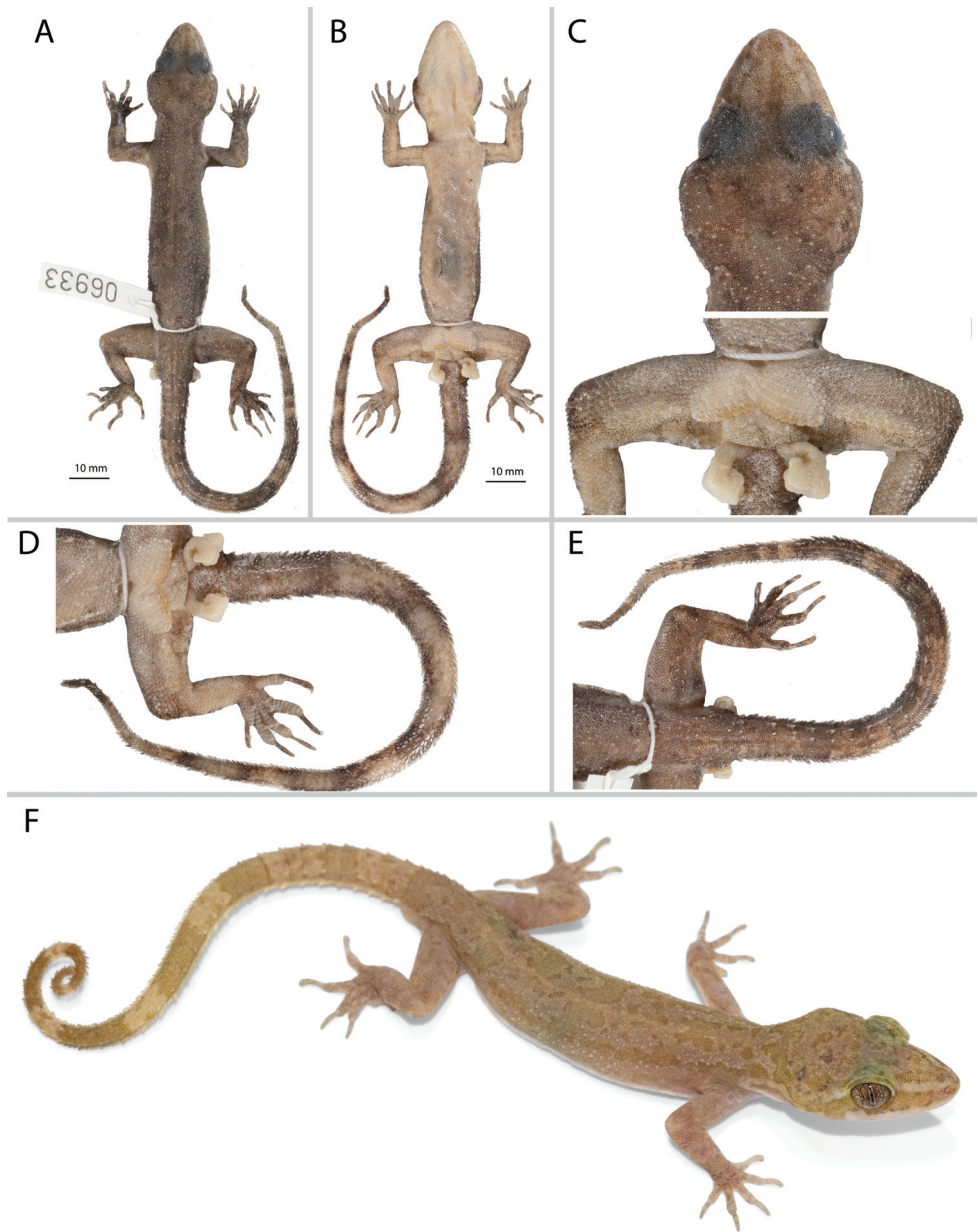


**Figure 4.** Adult male holotype of *Cyrtodactylus thongphaphumensis* sp. nov. ZMKU R 00953 (field no. AA 06933) from Thong Pha Phum National Park, Pilok Subdistrict, Thong Pha Phum District, Kan-  
chanaburi Province, Thailand. **A** dorsal view **B** ventral view **C** dorsal view of head and ventral view of pelvic region **D** dorsal view of tail and **E** ventral view of tail in preservative **F** holotype in life.

elliptical, small; eye to ear distance greater than diameter of eye; rostral rectangular, divided by a dorsal furrow, bordered posteriorly by large left and right supranasals and one small azygous internasal, bordered laterally by first supralabials; external nares bor-

dered anteriorly by rostral, dorsally by large supranasal, posteriorly by two unequally sized smaller postnasals, bordered ventrally by first supralabial; 14R/14L rectangular supralabials, second through eighth supralabials nearly same size as first, then tapering below eye; 10R/10L infralabials tapering smoothly to just below and slightly past posterior margin of eye; scales of rostrum and lores flat to slightly domed, larger than granular scales on top of head and occiput; scales of occiput intermixed with distinct, small tubercles; superciliaries subrectangular, largest anterodorsally; mental triangular, bordered laterally by first infralabials and posteriorly by large left and right trapezoidal postmentals contacting medially for 45% of their length posterior to mental; one row of enlarged, square to rectangular sublabials extending posteriorly to sixth(L) and fifth(R) infralabial; gular and throat scales small, granular, grading posteriorly into slightly larger, flatter, smooth, imbricate, pectoral and ventral scales.

Body relatively short (AG/SVL 0.46) with well-defined ventrolateral folds; dorsal scales small, granular interspersed with larger, conical, semi-regularly arranged, weakly keeled tubercles; tubercles extend from occipital region onto base of tail and slightly beyond as paravertebral rows; smaller tubercles extend anteriorly onto nape and occiput, diminishing in size anteriorly; approximately 20 longitudinal rows of tubercles at midbody; approximately 34 paravertebral tubercles; tubercles on flanks; 34 longitudinal rows of flat, imbricate, ventral scales much larger than dorsal scales; 166 transverse rows of ventral scales; 15 large, pore-bearing, precloacal scales; no deep precloacal groove or depression; and two rows of enlarged post-precloacal scales on midline.

Forelimbs moderate in stature, relatively short (ForL/SVL 0.13); granular scales of forearm larger than those on body, interspersed with large flat tubercles; palmar scales rounded, slightly raised; digits well-developed, relatively short, inflected at basal interphalangeal joints; digits narrower distal to inflections; subdigital lamellae wide, transversely expanded proximal to joint inflections, narrower transverse lamellae distal to joint inflections; claws well-developed, claw base sheathed by a dorsal and ventral scale; 8R/8L expanded and 11R/11L unexpanded lamellae beneath the fourth finger; hind limbs larger and thicker than forelimbs, moderate in length (TibL/SVL 0.14), covered dorsally by granular scales interspersed with moderately sized, conical tubercles dorsally and posteriorly and anteriorly by flat, slightly larger, subimbricate scales; ventral scales of thigh flat, imbricate, larger than dorsals; subtibial scales flat, imbricate; one row of 6R/8L enlarged pore-bearing femoral scales not continuous with enlarged pore-bearing precloacal scales, terminating distally at knee; 7R/8L enlarged femoral scales; proximal femoral scales smaller than distal femorals, the former forming an abrupt union with much smaller, rounded, ventral scales of posteroventral margin of thigh; plantar scales flat, subimbricate; digits relatively long, well-developed, inflected at basal interphalangeal joints; 8R/8L wide, transversely expanded subdigital lamellae on fourth toe proximal to joint inflection extending onto sole, and 12R/12L unexpanded lamellae beneath the fourth toe distal to joint inflection; and claws well-developed, claw base sheathed by a dorsal and ventral scale.

Tail original, 94.6 mm long (TL/SVL 1.29), 5.0 mm in width at base, tapering to a point; nearly square in cross-section; dorsal scales flat, intermixed with tubercles



Paratypes of *Cyrtodactylus thongphaphumensis* sp. nov.

**Figure 5.** Paratypes of *Cyrtodactylus thongphaphumensis* sp. nov. in preservative from Thong Pha Phum National Park, Pilok Subdistrict, Thong Pha Phum District, Kanchanaburi Province, Thailand.

forming paravertebral rows anteriorly and larger tubercles forming dorsolateral longitudinal rows; large, posteriorly directed, semi-spinose tubercles forming wide ventrolateral caudal fringe; larger scales of ventrolateral fringe occur at regular intervals; medial subcaudals enlarged but not paired, an enlarged single medial subcaudal longitudinal row absent; subcaudals, larger than dorsal caudals; base of tail bearing hemipenial swellings; 3R/3L conical postcloacal tubercles at base of hemipenial swellings; and postcloacal scales flat, imbricate.

**Coloration in life (Fig. 4).** Ground color of the head body, limbs, and tail dull yellow; diffuse darker mottling on the top of the head; wider, pale-brown pre- and postorbital stripe extends from external nares to angle of jaw; whitish canthal and postorbital stripe dorsal to pale-brown pre- and postorbital stripe; faint, pale brown, nuchal band bearing two posteriorly directed projections; paired dark-brown paravertebral blotches on nape; four wide, irregularly shaped and broken transverse body bands edged in slightly

pale brown between limb insertions; band interspaces bearing irregularly shaped scattered pale-brown markings; very faint pale-brown speckling on limbs and digits; seven wide pale-brown caudal bands separated by seven paler colored bands; posterior five pale-brown caudal bands encircle tail; ventral surfaces of body and limbs beige, generally immaculate, subcaudal region generally darker; iris orange-gold in color bearing black vermiculations.

**Variation (Fig. 5, Table 5).** Individuals of the type series are very similar in overall coloration and pattern. TL and TW of complete original tails (ZMKU R 00951–00952, ZMKU R 00954, ZMKU R 00957) are 80.1–94.7 mm (mean  $89.1 \pm 6.5$  mm;  $N = 4$ ) and 4.2–4.9 mm (mean  $4.7 \pm 0.3$ ;  $N = 4$ ), respectively. ZMKU R 00956 has a short, partially regenerated tail which lacks banding (TL 27.7 mm, TW 5.1 mm). Similarly, the posterior sections of the tails in ZMKU R 00950 (TL 75.5 mm, TW 5.0 mm) and ZMKU R 00955 (TL 73.3 mm, TW 4.7 mm) are regenerated. Specimens ZMKU R 00950, ZMKU R 00952, and ZMKU R 00954 have three as opposed to four body bands in the holotype and ZMKU R 00955 has five body bands. Raw morphometric and meristic differences within and among all species of the *brevipalmatus* group are listed in Table 5.

**Distribution.** *Cyrtodactylus thongphaphumensis* sp. nov. is currently known only from the type locality at Thong Pha Phum National Park, Pilok Subdistrict, Thong Pha Phum District, Kanchanaburi Province, Thailand (Fig. 1).

**Etymology.** The specific epithet *thongphaphumensis* is in reference to the type locality of Thong Pha Phum National Park.

**Comparisons.** *Cyrtodactylus thongphaphumensis* sp. nov. is the sister species to a clade composed of eight lineages in the phylogenetic sequence of *C. utthaiensis*, sp. 11, *C. interdigitalis*, *C. cf. ngati1*, *C. cf. ngati2*, *C. ngati3*, and the sister lineages *C. ngati4* and *C. ngati* (Fig. 2). *Cyrtodactylus thongphaphumensis* sp. nov. differs from those lineages by an uncorrected pairwise sequence divergence of 7.6–9.7% and from all members of the *brevipalmatus* group by 7.6–22.3% (Table 2). It differs discretely from *C. elok* by having as opposed to lacking paravertebral tubercles, femoral and precloacal pores, and by having 19–21 as opposed to 4–7 longitudinal rows of tubercles. It differs from *C. brevipalmatus*, *C. fluvicavus*, *C. interdigitalis*, *C. ngati*, *C. ngati3*, and *C. rukhadeva* in having statistically significant different mean values of combinations of the morphometric characters of AG, HumL, ForL, TibL, HL, HW, HD, EE, ES, EN, EL, and IN (Table 3). It differs further from those same species in having statistically significant different mean values of combinations of the meristic characters SL, PVT, LRT, VS, VSM, TL4T, FL4E, FL4U, FL4T, FS, PCS, and BB (Table 3). Discrete differences between *Cyrtodactylus thongphaphumensis* sp. nov. and other putative species and populations are presented in Table 5.

**Natural history.** All individuals were found in hill evergreen forest at 914 m elevation (Fig. 6). Specimens ( $N = 8$ ) were collected at night (1900–2100 h) during the dry season (April) on tree trunks (62.5%;  $N = 5$ ), on a building (12.5%;  $N = 1$ ), and the ground (25.0%;  $N = 2$ ) with a temperature of 27.0 °C and relative humidity of 71.1%. The holotype (ZMKU R 00953) and four paratypes (ZMKU R 00950, ZMKU R 00954, ZMKU R 00956–00957) were found on tree trunks  $\leq 160$  cm above ground level. One specimen (ZMKU R 00951) was found on a building. Two

**Table 5.** Sex and raw meristic, categorical, and morphometric data used in the analyses from specimens in the *Cyrtodactylus brevipalmatus* group. Abbreviations: R/L = right/left; / = data unavailable.

Species	<i>Cyrtodactylus thongphaphimmensis</i> sp. nov.						<i>C. brevipalmatus</i> ( <i>C. sp. 14</i> )		<i>C. brevipalmatus</i>			
	ZMKU R 00950 paratype ♀	ZMKU R 00951 paratype ♂	ZMKU R 00952 paratype ♀	ZMKU R 00953 holotype ♂	ZMKU R 00954 paratype ♂	ZMKU R 00955 paratype ♀	ZMKU R 00956 paratype ♂	ZMKU R 00957 paratype ♀	LSUHC 15076 ♀	LSUHC 11788 ♀	THNHM 10670 ♀	THNHM 14112 ♀
Suprabials (SL)	12	13	13	14	13	13	13	13	12	10	14	12
Infralabials (IL)	8	8	10	10	9	10	10	9	8	10	11	11
Paravertebral tubercles (PVT)	32	33	34	34	36	36	30	30	39	37	38	37
Longitudinal rows of tubercles (LRT)	21	19	20	20	21	21	19	19	15	16	17	14
Ventral scales (VS)	34	33	33	34	30	33	32	33	38	38	36	39
Ventral scales along middle of the body (VSM)	173	158	156	166	159	159	150	169	176	170	154	160
Expanded subdigital lamellae on 4 <sup>th</sup> toe (TL4E)	9	10	9	8	10	8	9	9	7	8	9	8
Unmodified subdigital lamellae on 4 <sup>th</sup> toe (TL4U)	12	14	13	12	13	12	11	13	13	11	11	12
Total subdigital lamellae 4 <sup>th</sup> toe (TL4T)	21	24	22	20	23	20	20	22	20	19	20	20
Expanded subdigital lamellae on 4 <sup>th</sup> finger (FL4E)	8	7	7	8	8	8	8	8	8	8	8	8
Unmodified subdigital lamellae on 4 <sup>th</sup> finger (FL4U)	10	12	12	11	12	12	11	12	9	11	10	10
Total subdigital lamellae 4 <sup>th</sup> finger (FL4T)	18	19	19	19	20	20	19	20	17	19	17	18
Enlarged femoral scales (RL)	5R/7L	8R/8L	8R/8L	7R/8L	8R/8L	7R/8L	7R/6L	8R/8L	0	0	8R/8L	7R/7L
Total enlarged femoral scales (FS)	12	16	16	15	16	15	13	16	16	10	11	14
Total femoral pores in males (FP)	/	16	/	14	15	/	12	/	7	/	/	/
Enlarged predoctal scales (PCS)	17	15	15	15	15	15	15	15	7	7	8	7
Predoccal pores in males (PP)	/	15	/	15	15	/	15	/	7	/	/	/
Postdoctal tubercles (PCT)	2	2R/3L	3	3	2R/3L	2R/3L	3	2	3	3	2	3
Body bands (BB)	3	4	3	4	3	5	4	4	4	6	3	5

Meristic data

Species	<i>Cyrtodactylus thongphaphimmensis</i> sp. nov.										<i>C. brevipalmatus</i> (C. sp. 14)		<i>C. brevipalmatus</i> (C. sp. 14)	
	ZMKU R 00950 paratype ♀	ZMKU R 00951 paratype ♂	ZMKU R 00952 paratype ♀	ZMKU R 00953 holotype ♂	ZMKU R 00954 paratype ♂	ZMKU R 00955 paratype ♀	ZMKU R 00956 paratype ♂	ZMKU R 00957 paratype ♀	LSUHC 1899	LSUHC 15076	LSUHC 11788	THNHM 10670	THNHM 14112	
<b>Institutional catalog number</b>														
<b>Sex</b>	♀	♂	♀	♂	♂	♀	♂	♀	♂	♀	♀	♀	♀	
<b>Categorical data</b>														
Small tubercles on flank (FKT)	present	present	present	present	present	present	present	present	present	present	present	present	present	
Dorsolateral caudal tubercles (DCT)	large	large	large	large	large	large	large	small	small	small	/	small	present	
Ventrolateral caudal fringe narrow or wide (VLF1)	wide	wide	wide	wide	wide	wide	wide	narrow	narrow	narrow	/	narrow	narrow	
Ventrolateral caudal fringe scales generally homogeneous (VLF2)	no	no	no	no	no	no	no	no	no	no	/	/	no	
Tail cross-section (TLcross)	square	square	square	square	square	square	square	circular	circular	circular	/	circular	circular	
Slightly enlarged medial subcaudals (SC1)	present	present	present	present	present	present	present	present	present	present	/	/	absent	
Single enlarged medial subcaudal (SC2)	absent	absent	absent	absent	absent	absent	absent	absent	absent	absent	/	/	absent	
Enlarged medial subcaudals intermittent, medially furrowed, posteriorly emarginate (SC3)	no	no	no	no	yes	no	/	no	no	no	/	/	no	
<b>Morphometric data</b>														
SVL	73.1	73.5	73.7	73.2	64.4	76.6	76.6	74.2	68.8	70.8	64.1	66.0	63.8	
AG	34.8	33.9	35.4	33.6	28.5	37.1	33.2	35.1	35.7	33.4	30.1	30.0	26.5	
Huml	8.4	7.2	9.0	9.0	7.2	8.0	8.1	8.6	9.7	9.3	8.0	9.6	9.5	
ForL	9.5	9.1	9.2	9.8	9.2	10.0	8.6	9.8	9.9	9.8	9.3	8.2	8.7	
FemL	12.8	11.6	12.3	12.5	10.9	13.7	10.8	12.5	12.0	12.6	11.5	11.7	9.8	
TibL	10.5	10.1	10.6	10.6	9.9	11.1	10.0	11.4	11.6	12.2	10.5	9.7	8.2	
HL	19.9	20.9	20.1	20.0	17.6	20.4	19.3	20.0	19.3	19.3	19.0	17.9	18.2	
HW	14.5	14.3	15.7	13.9	12.8	14.7	14.4	14.1	13.2	13.8	12.3	12.3	12.0	
HD	7.8	7.7	7.9	7.7	7.0	8.2	7.8	7.6	8.0	7.6	7.6	7.3	7.0	
ED	5.0	5.1	5.0	5.0	4.8	5.6	5.3	4.9	5.2	4.5	4.3	5.3	4.4	
EE	5.9	5.9	6.0	5.9	5.3	6.1	6.0	6.0	5.7	5.9	4.9	5.7	5.7	
ES	7.9	8.5	7.9	7.9	7.3	8.2	7.9	7.9	7.4	7.6	7.0	7.0	7.2	
EN	6.0	6.1	6.0	5.8	5.4	6.1	6.0	5.9	5.7	5.4	4.9	5.3	5.4	
IO	5.4	5.5	5.8	5.5	4.9	5.7	5.6	5.3	5.4	4.7	4.7	4.2	5.2	
EL	1.1	1.5	1.5	1.2	1.2	1.0	1.2	1.3	1.0	1.4	1.1	1.3	1.0	
IN	2.3	2.4	2.2	2.0	2.0	2.3	2.2	2.2	1.7	2.1	2.3	2.1	2.2	

Institutional catalog number	<i>C. elok</i>			<i>C. flavicannus</i>						<i>C. interdigitalis</i>				
	LSUHC 8238	LSUHC 12180	LSUHC 12181	ZMMU R-16144	ZMKUR 00959	ZMKUR 00958	ZMKUR 00960	ZMKUR 00961	ZMKUR 00962	ZMKUR 00963	ZMKUR 00964	TINHM paratype	TINHM 20226 paratype	TINHM 20228 paratype
Sex	♀	♂	♂	♀	♂	♂	♂	♀	♀	♀	♀	♀	♀	♀
Suprabials (SL)	11	8	13	9	12R/12L	13R/12L	13R/12L	11R/12L	12R/12L	13R/12L	12R/11L	14	14	12
Infrabials (IL)	11	8	11	9	10R/10L	10R/10L	9R/10L	10R/10L	10R/10L	10R/10L	10R/10L	9	9	8
Paravertebral tubercles (PVT)	0	0	0	0	30	28	27	27	28	26	28	32	32	33
Longitudinal rows of tubercles (LRT)	6	7	4	4	17	17	14	16	17	18	16	19	19	20
Ventral scales (VS)	45	45	47	36	34	37	33	30	36	37	39	42	42	40
Ventral scales along middle of the body (VSM)	190	225	234	192	155	154	155	172	164	175	170	187	187	170
Expanded subdigital lamellae on 4 <sup>th</sup> toe (TL4E)	10	9	9	9	9R/9L	10R/10L	9R/9L	9R/9L	10R/11L	9R/10L	9R/9L	12	10	
Unmodified subdigital lamellae on 4 <sup>th</sup> toe (TL4U)	11	10	11	9	11R/11L	12R/11L	10R/10L	12R/12L	11R/11L	10R/10L	12R/13L	14	13	
Total subdigital lamellae 4 <sup>th</sup> toe (TL4T)	21	19	20	18	20R/20L	22R/21L	19R/19L	21R/21L	21R/22L	19R/20L	22R/22L	26	23	
Expanded subdigital lamellae on 4 <sup>th</sup> finger (FL4E)	8	9	9	9	8R/8L	8R/8L	8R/8L	8R/8L	7R/7L	8R/9L	7R/7L	9	8	
Unmodified subdigital lamellae on 4 <sup>th</sup> finger (FL4U)	12	13	9	8	10R/10L	10R/10L	10R/9L	11R/11L	10R/10L	9R/9L	10R/10L	12	11	
Total subdigital lamellae 4 <sup>th</sup> finger (FL4T)	20	22	18	17	18R/18L	18R/18L	18R/17L	19R/19L	17R/17L	17R/18L	17R/17L	21	21	
Enlarged femoral scales (R/L)	0	0	0	0	5R/6L	4R/5L	5R/6L	6R/6L	5R/6L	5R/6L	6R/6L	11R/8L	10R/9L	
Total enlarged femoral scales (FS)	0	0	0	0	11	9	11	12	11	11	12	14	19	
Total femoral pores in males (FP)	/	0	0	/	11	8	10	/	/	/	/	/	/	
Enlarged pretoeal scales (PCS)	8	8	8	7	15	14	14	15	14	15	15	14	15	
Predoeal pores in males (PP)	/	8	8	/	15	14	14	/	/	/	/	/	/	
Postoeal tubercles (PCT)	3	2	3	3	3R/2L	3R/2L	3R/3L	1R/1L	3R/2L	3R/3L	2R/2L	3	2	
Body bands (BB)	5	5	3	3	3	3	3	3	3	3	3	5	5	

Morphological character	Categorical data		
	present	absent	present
Small tubercles on flank (FKT)	present	absent	present
Dorsolateral caudal tubercles (DCT)	small	large	small
Ventrolateral caudal fringe narrow or wide (VLFN)	narrow	wide	narrow
Ventrolateral caudal fringe scales generally homogenous (VLF2)	no	no	no
Tail cross-section (TLCross)	circular	square	circular
Slightly enlarged medial subcaudals (SC1)	present	absent	present

Institutional catalog number	<i>C. elok</i>				<i>C. flavicans</i>				<i>C. interdigitalis</i>								
	LSUHC 8238	LSUHC 12180	LSUHC 12181	ZMMU R-16144	ZMKUR 00959	ZMKUR 00958	ZMKUR 00960	ZMKUR 00961	ZMKUR 00962	ZMKUR 00963	ZMKUR 00964	THNHM 20226	THNHM 20228	paratype			
Sex	♀	♂	♂	♀	♂	♂	♂	♀	♀	♀	♀	♀	♀	♀			
Single enlarged medial subcaudal (SC2)	absent	absent	absent	absent	absent	absent	absent	absent	absent	absent	absent	absent	absent	/			
Enlarged medial subcaudals	no	no	no	no	no	no	no	no	no	no	no	yes	yes	/			
intermittent, medially furrowed, posteriorly emarginate (SC3)																	
<b>Morphometric data</b>																	
SVL	80.2	78.2	84.8	78.6	72.5	72.0	69.6	68.4	76.8	65.7	78.2	81.2	74.8				
AG	39.7	37.8	41.5	36.2	33.4	33.6	32.0	30.4	35.6	30.6	38.1	34.5	33.7				
Huml	10.2	9.1	10.1	1.7	9.1	8.8	9.0	8.0	10.0	7.5	10.1	9.8	10.2				
ForL	11.5	11.7	11.8	10.2	10.5	10.3	10.5	10.1	11.1	8.8	10.8	10.6	10.5				
FemL	12.9	14.2	14.6	13.1	13.1	12.5	12.5	13.5	14.1	11.5	13.9	14.7	13.2				
TibL	13.5	14.0	13.8	12.3	11.3	10.6	10.2	9.9	11.2	9.4	12.3	13.1	11.9				
HL	21.8	21.6	21.9	21.7	20.1	20.5	19.7	20.1	21.2	18.6	21.3	20.8	19.9				
HW	15.6	16.1	15.9	15.1	14.0	13.4	12.9	13.0	14.9	13.0	15.4	14.0	13.4				
HID	9.6	9.8	10.4	9.8	8.5	8.1	8.3	7.9	8.1	7.8	8.3	3.4	8.6				
ED	4.8	5.0	5.7	5.0	5.0	5.0	4.9	4.7	5.1	4.5	5.3	5.3	5.5				
EE	6.4	7.1	7.0	6.8	6.5	5.9	5.7	5.8	6.1	5.4	6.5	5.8	6.2				
ES	8.6	8.7	9.5	8.6	8.5	8.3	8.2	8.1	9.2	7.3	9.3	8.3	7.8				
EN	6.0	6.2	6.5	6.2	6.5	6.2	5.9	6.1	6.6	5.6	6.5	6.0	5.5				
IO	5.7	5.4	5.4	3.9	5.5	5.4	5.3	5.1	5.6	5.0	5.6	4.8	4.7				
EL	1.9	1.4	1.5	1.4	1.4	1.5	1.7	1.4	1.8	1.6	1.8	1.3	1.3				
IN	2.7	2.6	2.5	3.1	2.3	2.4	2.5	2.3	2.3	2.3	2.6	2.1	2.2				
<b>Meristic data</b>																	
Species	<i>C. elok</i>				<i>C. ngati</i>				<i>C. ngati3</i>				<i>C. cf. ngati4</i>				
	<i>C. koehangensis</i>	<i>C. cf. koehangensis</i>	<i>C. cf. koehangensis</i>	<i>C. cf. koehangensis</i>	HNUE-R00111	IEBR 4829	VNUF R-2020.12	HNUE-R00112	FMNH 255454	FMNH 270493	FMNH 270492	FMNH 265806	NCSM 79472	ZMMU R-14917	NCSM 80100	ZMKUR 00947	ZMKUR R 00946
Institutional catalog number	ZMKUR 00945	THNHM 01667	THNHM 01667	THNHM 01667	THNHM 01667	THNHM 01667	THNHM 01667	THNHM 01667	THNHM 01667	THNHM 01667	THNHM 01667	THNHM 01667	THNHM 01667	THNHM 01667	THNHM 01667	THNHM 01667	THNHM 01667
Sex	♀	♂	♂	♂	♀	♀	♀	♀	♀	♂	♂	♂	♀	♀	♀	♀	♀
Supralabials (SL)	12R/13L	12	10	10	10	10	10	10	13	13	13	10	14	9	12	13R/12L	13R/12L
Infralabials (IL)	9R/9L	10	9	9	9	9	9	9	10	9	11	8	11	10	12	11R/10L	10R/9L
Paravertebral tubercles (PVT)	34	29	39	40	38	40	28	27	26	27	28	32	29	34	29	34	33
Longitudinal rows of tubercles (LRT)	14	19	18	17	22	19	18	17	18	17	19	18	24	19	20	18	17
Ventral scales (VS)	35	34	38	36	35	32	37	36	36	33	33	36	35	34	35	34	37
Ventral scales along middle of the body (VSM)	172	159	168	164	178	158	159	166	156	156	158	166	164	166	165	160	166

Species	<i>C. kochangensis</i>		<i>C. cf. kochangensis</i>		<i>C. ngati</i>				<i>C. ngati3</i>			<i>C. cf. ngati1</i>		<i>C. cf. ngati2</i>		<i>C. rivularis</i>		
	ZMKU R 00945	♀	THNHM 01667	♂	HNUE- R00111	IEBR 4829	VNUF R-2020.12	HNUE- R00112	FMINH 255454	FMINH 270493	FMINH 270492	FMNH 265806	NCSM 79472	ZMMU R-14917	NCSM 80100	ZMKU R 00947	ZMKU R 00946	
Expanded subdigital lamellae on 4 <sup>th</sup> toe (TL4E)	9R/8L	8	8	9	9	10	10	10	10	10	8	10	9	8	10	9R/9L	9R/9L	♀
Unmodified subdigital lamellae on 4 <sup>th</sup> toe (TL4U)	12R/11L	13	11	10	11	11	10	11	11	11	11	11	12	10	10	13R/13L	12R/13L	♀
Total subdigital lamellae 4 <sup>th</sup> toe (TL4T)	21R/19L	21	13	16	17	16	16	21	21	21	19	21	21	18	20	22R/22L	21R/22L	♀
Expanded subdigital lamellae on 4 <sup>th</sup> finger (FL4E)	8R/8L	8	6	6	7	6	6	8	8	8	8	8	9	7	9	8R/8L	8R/8L	♀
Unmodified subdigital lamellae on 4 <sup>th</sup> finger (FL4U)	10R/10L	12	9	9	9	9	9	10	10	10	10	10	8	9	10	11R/10L	12R/12L	♀
Total subdigital lamellae 4 <sup>th</sup> finger (FL4T)	18R/18L	20	15	15	18	18	15	18	18	18	18	18	17	16	19	19R/18L	20R/20L	♀
Enlarged femoral scales (RL)	6R/6L	7R/7L	10R/10L	9R/8L	10R/9L	9R/7L	8R/9L	9R/9L	8R/9L	9R/9L	9R/9L	8R/8L	9R/8L	7R/8L	7R/8L	8R/8L	8R/8L	♀
Total enlarged femoral scales (FS)	12	14	20	17	19	16	17	16	17	18	16	16	17	15	15	16	16	♀
Total femoral pores in males (FP)	/	14	14	/	/	/	/	/	14	15	13	13	/	/	/	/	/	♀
Enlarged prebasal scales (PCS)	12	16	13	13	13	13	13	15	13	13	13	13	12	13	13	15	15	♀
Prebasal pores in males (PP)	/	16	/	/	/	/	/	/	13	13	13	13	/	/	/	/	/	♀
Postbasal tubercles (PCT)	1R/1L	3	3	2	1	2	2	0	0	0	0	0	2	3	4	2R/2L	3R/3L	♀
Body bands (BB)	5	5	6	6	6	6	6	3	4	3	3	3	3	3	3	3	3	♀

	Categorical data															
	present	present	present	present	present	present	present	present	present	present	present	present	present	present	present	present
Small tubercles on flank (FKT)	present	present	present	present	present	present	present	present	present	present	present	present	present	present	present	present
Dorsolateral caudal tubercles (DCT)	large	small														
Ventrolateral caudal fringe narrow or wide (VLF1)	wide	narrow														
Ventrolateral caudal fringe scales generally homogeneous (VLF2)	no	no	no	no	no	no	no	no	no	no	no	no	no	no	no	no
Tail cross-section (TLcross)	square	/	/	/	/	/	/	/	/	/	/	/	/	/	/	/
Slightly enlarged medial subcaudals (SC1)	present	present	present	present	present	present	present	present	present	present	present	present	present	present	present	present
Single enlarged medial subcaudal (SC2)	absent	absent	absent	absent	absent	absent	absent	absent	absent	absent	absent	absent	absent	absent	absent	absent
Enlarged medial subcaudals intermittent, medially furrowed, posteriorly emarginate (SC3)	no	no	no	no	no	no	no	no	no	no	no	no	no	no	no	no

SVL	Morphometric data															
	60.1	70.2	66.5	68.1	69.3	46.6	83.6	70.2	74.1	73.8	78.0	87.1	77.7	73.9	68.1	
	60.1	70.2	66.5	68.1	69.3	46.6	83.6	70.2	74.1	73.8	78.0	87.1	77.7	73.9	68.1	

Species	<i>C. kochangensis</i>		<i>C. cf. kochangensis</i>		<i>C. ngati</i>				<i>C. ngati3</i>		<i>C. ngati4</i>		<i>C. cf. ngati1</i>		<i>C. cf. ngati2</i>		<i>C. rivularis</i>	
	ZMMU R-16851	ZMKU R-00945	THNHM 01667	HINU- R00111	IEBR 4829	VNUF R-2020.12	HINU- R00112	FMNH 255454	FMNH 270493	FMNH 270492	FMNH 265806	NCSM 79472	ZMMU R-14917	NCSM 80100	ZMKU R-00946	ZMKU R-00947	ZMKU R-00948	ZMKU R-00949
Sex	♂	♀	♂	♂	♀	♀	♀	♀	♂	♂	♂	♀	♀	♀	♀	♀	♀	♀
AG	29.0	29.0	31.5	28.8	29.8	30.2	19.7	41.3	35.4	37.0	31.3	38.2	41.9	36.8	34.8	33.2	33.2	33.2
Huml	6.5	6.5	10.2	7.9	8.1	8.5	5.6	8.6	8.7	8.6	6.9	8.7	11.5	9.2	8.1	7.6	7.6	7.6
ForL	7.6	10.4	8.6	9.2	10.0	10.1	6.5	10.2	9.3	10.4	10.0	10.3	10.4	10.7	9.7	9.1	9.1	9.1
FemL	10.4	10.4	12.1	11.5	11.5	11.5	7.6	13.7	12.7	13.0	13.1	13.1	15.2	14.2	11.4	10.4	10.4	10.4
TibL	8.4	11.8	11.8	10.8	11.1	11.8	7.8	12.5	11.8	11.2	11.1	12.8	12.6	12.7	11.2	10.3	10.3	10.3
HL	17.3	18.3	18.3	20.1	20.4	20.7	16.1	21.7	20.6	20.3	20.7	21.2	22.1	21.4	20.3	19.3	19.3	19.3
HW	11.6	12.1	12.1	12.6	12.0	11.8	8.8	13.8	12.5	13.0	12.3	12.7	14.8	13.5	14.9	13.7	13.7	13.7
HD	6.5	7.8	7.8	7.4	7.2	6.6	5.1	9.2	8.4	9.1	7.6	8.3	8.7	9.2	8.2	8.2	8.2	8.2
ED	4.2	5.2	5.2	3.8	4.1	3.4	2.6	4.9	4.9	4.9	4.8	6.5	4.6	6.0	5.8	5.6	5.6	5.6
EE	5.0	4.9	4.9	5.8	5.5	5.9	4.4	6.9	6.1	6.2	5.7	5.3	6.5	6.2	6.5	6.2	6.2	6.2
ES	6.9	7.5	7.5	7.5	7.6	6.9	5.0	9.0	8.3	8.3	8.2	8.7	8.8	8.4	8.3	7.9	7.9	7.9
EN	5.2	5.5	5.5	6.7	6.3	6.2	4.5	6.5	6.2	6.1	6.2	6.2	6.6	6.0	6.1	5.8	5.8	5.8
IO	4.2	4.0	4.0	5.6	5.4	5.6	4.2	6.6	5.6	5.4	5.1	4.9	3.5	5.7	5.8	5.5	5.5	5.5
EL	1.0	1.3	1.3	0.8	0.8	0.7	0.3	1.3	1.1	1.2	1.0	1.5	1.2	0.9	1.1	1.1	1.1	1.1
IN	1.9	2.2	2.2	2.8	2.6	2.6	2.0	2.8	2.5	2.5	2.3	2.7	2.2	2.5	2.3	2.0	2.0	2.0

Species	<i>C. rubradava</i>		<i>C. cf. rubradava</i>		<i>C. cf. rubradava</i>		<i>C. sp. 11</i>		<i>C. sp. 13</i>		<i>C. sp. 13</i>		<i>C. rubradava</i>	
	ZMMU R-16851	ZMMU R-16852	ZMKU R-00948	THNHM 24622	THNHM 24838	THNHM 03251	THNHM 03252	THNHM 03253	THNHM 03254	THNHM 01807	ZMMU R-16492	THNHM 00104	THNHM 27821	ZMKU R-00949
Sex	♂	♀	♀	♂	♀	♂	♂	♀	♂	♂	♂	♀	♀	♂
Supralabials (SL)	11	9	14	11	13	13	11	12	13	12	11	12	15	13R/15L
Infralabials (IL)	10	11	9	10	10	10	10	10	11	10	9	10	11	10R/11L
Paravertebral tubercles (PVT)	27	30	30	26	28	27	27	30	30	26	30	33	29	33
Longitudinal rows of tubercles (LRT)	19	20	19	18	19	18	18	19	19	19	18	18	20	17
Ventral scales (VS)	34	43	38	38	36	37	37	39	34	35	34	37	36	36
Ventral scales along middle of the body (VSM)	154	152	165	162	158	157	159	168	160	161	160	159	165	159
Expanded subdigital lamellae on 4 <sup>th</sup> toe (TL4E)	9	9	9	8	9	9	10	9	10	10	9	9	7	8R/ (broken)L
Unmodified subdigital lamellae on 4 <sup>th</sup> toe (TL4U)	11	11	12	11	13	12	12	15	13	13	10	12	12	12R/ (broken)L
Total subdigital lamellae 4 <sup>th</sup> toe (TL4T)	20	18	21	19	22	21	22	14	23	23	19	21	19	20
Expanded subdigital lamellae on 4 <sup>th</sup> finger (FL4E)	9	8	8	7	8	8	8	8	8	8	10	8	8	7R/7L

Meristic data

Species	<i>C. rubradena</i>				<i>C. cf. rubradena</i>				<i>C. sp. 11</i>		<i>C. sp. 13</i>		<i>C. ubaitensis</i>	
	ZMMU R-16851	ZMMU R-16852	ZMKUR 00948	ZMKUR 00949	THNHM 24838	THNHM 03251	THNHM 03252	THNHM 03253	THNHM 03254	THNHM 01807	ZMMU R-16492	THNHM 00104	THNHM 27821	ZMKUR 00949
<b>Sex</b>	♂	♀	♀	♀	♀	♂	♂	♀	♂	♂	♂	♀	♀	♂
Unmodified subdigital lamellae on 4 <sup>th</sup> finger (FL4U)	10	9	11	10	11	10	10	12	12	12	9	11	10	11R/11L
Total subdigital lamellae 4 <sup>th</sup> finger (FL4T)	19	17	19	17	17	18	18	20	20	20	19	19	18	18R/18L
Enlarged femoral scales (RL)	9R/8L	8R/8L	9R/8L	9R/L	9R/9L	9R/7L	7R/7L	6R/7L	5R/8L	7R/7L	9R/8L	9R/9L	7R/10L	8R/8L
Total enlarged femoral scales (FS)	17	16	17	18	18	16	14	13	13	14	17	18	17	16
Total femoral pores in males (FP)	17	/	/	14	/	12	13	/	11	13	17	/	/	12
Enlarged precoxal scales (PCS)	17	13	15	15	15	14	13	15	15	14	13	14	16	14
Predcoxal pores in males (PP)	17	/	/	15	/	14	13	/	15	14	13	/	/	14
Postcoxal tubercles (PCT)	3	2	2R/3L	3	2	3	2	2	3	2	3	3	3	3R/3L
Body bands (BB)	3	3	3	3	3	4	4	/	/	5	3	3	/	6
<b>Categorical data</b>														
Small tubercles on flank (FKT)	present	present	present	present	present	present	present	present	present	present	present	present	present	present
Dorsolateral caudal tubercles (DCT)	small	small	small	small	small	small	small	small	small	/	large	small	small	large
Ventrolateral caudal fringe narrow or wide (VLF1)	narrow	narrow	narrow	narrow	narrow	narrow	narrow	narrow	narrow	/	wide	narrow	narrow	wide
Ventrolateral caudal fringe scales generally homogenous (VLF2)	yes	yes	yes	yes	yes	yes	yes	yes	yes	/	yes	yes	yes	no
Tail cross-section (TLcross)	square	square	square	square	square	square	square	square	square	/	square	circular	circular	circular
Slightly enlarged medial subcaudals (SC1)	absent	absent	absent	absent	absent	absent	absent	absent	absent	/	present	present	present	present
Single enlarged medial subcaudal (SC2)	present	present	present	present	present	present	present	present	present	/	absent	absent	absent	absent
Enlarged medial subcaudals intermittent, medially furrowed, posteriorly emarginate (SC3)	no	no	no	no	no	no	no	no	no	no	no	no	no	yes
<b>Morphometric data</b>														
SVL	74.9	71.7	71.6	68.3	71.8	73.6	75.3	74.7	73.2	61.5	68.1	63.7	72.9	58.1
AG	34.6	32.6	33.9	27.3	29.9	30.9	31.3	32.2	30.3	26.2	34.6	25.8	30.6	26.6
HumL	10.7	10.4	7.9	9.8	8.3	12.2	11.3	11.8	11.0	10.1	10.3	7.6	10.1	7.0
FemL	8.6	7.9	9.6	8.7	8.5	9.0	10.6	9.6	9.2	7.9	8.5	8.1	9.6	8.3
FemL	12.6	11.8	10.5	10.8	10.9	11.5	10.2	11.9	12.1	9.5	12.6	10.7	12.8	10.0
TibL	10.1	9.3	11.2	9.7	10.7	10.9	11.7	11.3	11.1	9.1	11.4	10.1	10.2	8.4
HL	20.2	19.2	19.7	19.7	19.9	20.8	21.3	20.8	21.5	17.9	18.4	17.6	19.9	16.1
HW	14.6	13.4	14.0	13.1	13.9	14.9	15.0	13.1	14.1	11.8	13.1	11.9	13.8	10.9

Species	<i>C. rubbadeva</i>				<i>C. cf. rubbadeva</i>				<i>C. sp. 11</i>		<i>C. sp. 13</i>		<i>C. utahensis</i>		
	ZMMU R-16851	ZMMU R-16852	ZMKUR 00948	THNHM 24622	THNHM 24838	THNHM 03251	THNHM 03252	THNHM 03253	THNHM 03254	THNHM 01807	ZMMU R-16492	THNHM 00104	THNHM 27821	ZMKUR 00949	
<b>Sex</b>	♂	♀	♀	♂	♀	♂	♂	♀	♂	♂	♂	♀	♀	♂	♂
HID	9.2	8.5	8.3	7.3	8.9	8.2	8.2	8.1	8.9	7.5	8.3	7.7	8.4	6.3	
ED	4.6	4.3	5.5	4.9	5.1	5.8	5.4	5.0	5.5	4.7	4.4	4.1	5.3	4.6	
EE	6.2	6.2	5.8	5.1	6.2	5.6	5.7	5.4	6.2	4.3	6.2	4.9	6.3	4.7	
ES	8.3	7.7	7.9	7.4	8.1	8.4	8.8	8.1	8.6	7.3	7.7	7.2	8.0	6.4	
EN	6.3	5.7	5.8	5.4	6.0	6.2	6.4	5.8	6.2	5.3	5.5	5.6	5.9	4.9	
IO	3.3	3.1	5.6	4.5	4.7	5.6	5.7	5.7	5.6	4.2	2.9	4.8	6.1	4.3	
EL	1.2	1.0	1.4	1.6	1.5	1.2	1.3	1.2	1.2	0.9	0.9	1.4	1.4	1.5	
IN	2.2	2.1	2.1	2.0	2.2	2.4	2.5	2.4	2.3	2.0	2.3	2.1	2.3	1.8	



**Figure 6.** Habitat of the type locality at Thong Pha Phum National Park, Pilok Subdistrict, Thong Pha Phum District, Kanchanaburi Province, Thailand.

specimens (ZMKU R 00952, ZMKU R 00955) were found on ground. At night, the new species was found to co-occur with other gekkonid lizards, *Cyrtodactylus oldhami* (Theobald, 1876), *Gekko kaengkrachanense* (Sumontha, Pauwels, Kunya, Limlikhitak-sorn, Ruksue, Taokratok, Ansermet & Chanhome, 2012), and *Hemidactylus garnotii* Duméril & Bibron, 1836.

## Discussion

The discovery of new populations of the *Cyrtodactylus brevipalmatus* group across the archipelago of the upland sky-island habitats in Thailand will likely be commonplace with increased field work. Many such undescribed populations have already been reported and photographed on social networking platforms and these populations will be sampled and analyzed in order to ascertain their species status. Grismer et al. (2022c) pointed out that for several years many such populations went unanalyzed and were simply placed in the synonymy of either *C. brevipalmatus* or *C. interdigitalis*, only to be elevated later to species status following data-rich phylogenetic delimitation and morphological diagnostic analyses (Grismer et al. 2021c, 2022c). This current

work not only contributes to an increased understanding of the unrealized diversity within the *brevipalmatus* group, but to a growing body of literature underscoring the high degree of herpetological diversity and endemism across a sky-island archipelago of upland montane tropical forests in Thailand (see Suwannapoom et al. 2022) which like many other upland tropical landscapes, are becoming some of the most imperiled ecosystems on the planet.

## Acknowledgements

This work was financially supported by Office of the Permanent Secretary, Ministry of Higher Education, Science, Research and Innovation (Grant No. RGNS 64-038), Thailand Research Fund (DBG6080010) and Unit of Excellence 2023 on Biodiversity and Natural Resources Management, University of Phayao (FF66-UoE003). This research was reviewed and approved by the Institutional Animal Care and Use Committee of Faculty of Science, Kasetsart University (ACKU61-SCI-008) and the Department of National Parks, Wildlife and Plant Conservation, Thailand provided the research permission. We would like to thank Charoen Jaichon (Thong Pha Phum National Park) for facilitating the fieldwork. Wachara Sanguansombat and Sunchai Makchai (Thailand Natural History Museum) made specimens in their care available for study. Natee Ampai and Korkhwan Termprayoon assisted with fieldwork. Evan Quah, Vinh Luu, Olivier Pauwels, and an anonymous reviewer improved the manuscript.

## References

- Bouckaert RR, Drummond AJ (2017) bModelTest: Bayesian phylogenetic site model averaging and model comparison. *BMC Evolutionary Biology* 17(1): 42–42. <https://doi.org/10.1186/s12862-017-0890-6>
- Chan KO, Grismer LL (2022) GroupStruct: An R package for allometric size correction. *Zootaxa* 5124(4): 471–482. <https://doi.org/10.11646/zootaxa.5124.4.4>
- Chomdej S, Pradit W, Suwannapoom C, Pawangkhanant P, Nganvongpanit K, Poyarkov NA, Che J, Gao Y, Gong S (2021) Phylogenetic analyses of distantly related clades of bent-toed geckos (genus *Cyrtodactylus*) reveal an unprecedented amount of cryptic diversity in northern and western Thailand. *Scientific Reports* 11(1): e2328. <https://doi.org/10.1038/s41598-020-70640-8>
- Drummond AJ, Suchard MA, Xie D, Rambaut A (2012) Bayesian phylogenetics with BEAUti and BEAST 1.7. *Molecular Biology and Evolution* 29(8): 1969–1973. <https://doi.org/10.1093/molbev/mss075>
- Grismer LL, Wood Jr PL, Le MD, Quah ESH, Grismer JL (2020) Evolution of habitat preference in 243 species of Bent-toed geckos (Genus *Cyrtodactylus* Gray, 1827) with a discussion of karst habitat conservation. *Ecology and Evolution* 10(24): 13717–13730. <https://doi.org/10.1002/ece3.6961>

- Grismer LL, Wood Jr PL, Poyarkov NA, Le MD, Kraus F, Agarwal I, Oliver PM, Nguyen SN, Nguyen TQ, Karunarathna S, Welton LJ, Stuart BL, Luu VQ, Bauer AM, O'Connell KA, Quah ESH, Chan KO, Ziegler T, Ngo H, Nazarov RA, Aowphol A, Chomdej S, Suwannapoom C, Siler CD, Anuar S, Tri NV, Grismer JL (2021a) Phylogenetic partitioning of the third-largest vertebrate genus in the world, *Cyrtodactylus* Gray, 1827 (Reptilia; Squamata; Gekkonidae) and its relevance to taxonomy and conservation. *Vertebrate Zoology* 71: 101–154. <https://doi.org/10.3897/vertebrate-zoology.71.e59307>
- Grismer LL, Wood Jr PL, Poyarkov NA, Le MD, Karunarathna S, Chomdej S, Suwannapoom C, Qi S, Liu S, Che J, Quah ESH, Kraus F, Oliver PM, Riyanto A, Pauwels OSG, Grismer JL (2021b) Karstic landscapes are foci of species diversity in the World's Third-Largest Vertebrate genus *Cyrtodactylus* Gray, 1827 (Reptilia: Squamata; Gekkonidae). *Diversity (Basel)* 13(5): 183–183. <https://doi.org/10.3390/d13050183>
- Grismer LL, Suwannapoom C, Pawangkhanant P, Nazarov RA, Yushchenko PV, Naiduangchan M, Le MD, Luu VQ, Poyarkov NA (2021c) A new cryptic arboreal species of the *Cyrtodactylus brevipalmatus* group (Squamata: Gekkonidae) from the uplands of western Thailand. *Vertebrate Zoology* 71: 723–746. <https://doi.org/10.3897/vz.71.e76069>
- Grismer LL, Poyarkov NA, Quah ESH, Grismer JL, Wood Jr PL (2022a) The biogeography of bent-toed geckos, *Cyrtodactylus* (Squamata: Gekkonidae). *PeerJ* 10: e13153. <https://doi.org/10.7717/peerj.13153>
- Grismer LL, Rujirawan A, Yodthong S, Stuart BL, Le MD, Le DT, Chuaynkern Y, Wood Jr PL, Aowphol A (2022b) The taxonomy and phylogeny of the *Cyrtodactylus brevipalmatus* group (Squamata: Gekkonidae) with emphasis on *C. interdigitalis* and *C. ngati*. *Vertebrate Zoology* 72: 245–269. <https://doi.org/10.3897/vz.72.e80615>
- Grismer LL, Aowphol A, Yodthong S, Ampai N, Termprayoon K, Aksornneam A, Rujirawan A (2022c) Integrative taxonomy delimits and diagnoses cryptic arboreal species of the *Cyrtodactylus brevipalmatus* group (Squamata, Gekkonidae) with descriptions of four new species from Thailand. *ZooKeys* 1129: 109–162. <https://doi.org/10.3897/zookeys.1129.90535>
- Huelsenbeck JP, Ronquist F, Nielsen R, Bollback JP (2001) Bayesian inference of phylogeny and its impact on evolutionary biology. *Science* 294(5550): 2310–2314. <https://doi.org/10.1126/science.1065889>
- Husson F, Josse J, Le S, Mazet J (2017) FactoMine R: exploratory data analysis and data mining. R package, version 1.36.
- Kassambara A, Mundt F (2017) Factoextra: extract and visualize the result of multivariate data analyses. R package, version 1.0.5.999.
- Miller MA, Pfeiffer W, Schwartz T (2010) Creating the CIPRES Science Gateway for inference of large phylogenetic trees. In: Gateway Computing Environments Workshop (GCE), New Orleans (USA), November 2010, IEEE, 1–8. <https://doi.org/10.1109/GCE.2010.5676129>
- Oksanen J, Blanchet FG, Friendly M, Kindt R, Legendre P, McGlenn D, Minchin PR, O'Hara RB, Simpson GL, Solymos P, Stevens MHH, Szoecs E, Wagner H (2020) Package 'vegan'. Version 2.5-7. <https://cran.r-project.org/web/packages/vegan/>
- R Core Team (2018) R: A language and environment for statistical computing. R Foundation for Statistical Computing. Vienna. <http://www.R-project.org> [accessed 1 June 2022]

- Rambaut A, Drummond AJ (2013) TreeAnnotator v1.8.0 MCMC Output Analysis. <https://beast.community/treeannotator>
- Rambaut A, Drummond AJ, Xie D, Baele G, Suchard MA (2018) Posterior summarization in Bayesian phylogenetics using Tracer 1.7. *Systematic Biology* 67(5): 901–904. <https://doi.org/10.1093/sysbio/syy032>
- Suwannapoom S, Grismer LL, Pawangkhanant P, Poyarkov NA (2022) A new species of stream toad of the genus *Ansonia* Stolickzka, 1870 (Anura: Bufonidae) from Nakhon Si Thammarat Range in southern Thailand. *Zootaxa* 5168(2): 119–136. <https://doi.org/10.11646/zootaxa.5168.2.2>
- Tamura K, Stecher G, Kumar S (2021) MEGA11: Molecular evolutionary genetics analysis version 11. *Molecular Biology and Evolution* 38(7): 3022–3027. <https://doi.org/10.1093/molbev/msab120>
- Uetz P, Freed P, Hošek J (2022) The Reptile Database. <http://www.reptile-database.org> [Accessed 13 July 2022]
- Wilcox TP, Zwickl DJ, Heath TA, Hillis DM (2002) Phylogenetic relationships of the Dwarf Boas and a comparison of Bayesian and bootstrap measures of phylogenetic support. *Molecular Phylogenetics and Evolution* 25(2): 361–371. [https://doi.org/10.1016/S1055-7903\(02\)00244-0](https://doi.org/10.1016/S1055-7903(02)00244-0)

## Supplementary material I

### Data frame for the multiple factor analysis of the putative species of the *Cyrtodactylus brevipalmatus* group

Authors: L. Lee Grismer, Attapol Rujirawan, Siriwadee Chomdej, Chatmongkon Suwannapoom, Siriporn Yodthong, Akrachai Aksornneam, Anchalee Aowphol

Data type: morphological data

Copyright notice: This dataset is made available under the Open Database License (<http://opendatacommons.org/licenses/odbl/1.0/>). The Open Database License (ODbL) is a license agreement intended to allow users to freely share, modify, and use this Dataset while maintaining this same freedom for others, provided that the original source and author(s) are credited.

Link: <https://doi.org/10.3897/zookeys.1141.97624.suppl1>

# Species richness under a vertebral stripe: integrative taxonomy uncovers three additional species of *Pholidobolus* lizards (Sauria, Squamata, Gymnophthalmidae) from the north-western Colombian Andes

Adolfo Amézquita<sup>1\*</sup>, Luis A. Mazariegos-H<sup>1</sup>, Santiago Cañaverl<sup>1</sup>,  
Catalina Orejuela<sup>2</sup>, Leidy Alejandra Barragán-Contreras<sup>2</sup>, Juan M. Daza<sup>3\*</sup>

**1** Laboratory of Biodiversity and Cloud Forests Conservation, Bioconservancy.org, Jardín, Colombia  
**2** Department of Biological Sciences, Universidad de los Andes, Bogotá, Colombia **3** Grupo Herpetológico de Antioquia, Universidad de Antioquia, Medellín, Colombia

Corresponding authors: Adolfo Amézquita ([aamezquita@bioconservancy.org](mailto:aamezquita@bioconservancy.org)); Juan M. Daza ([jumadaza@gmail.com](mailto:jumadaza@gmail.com))

Academic editor: A. Herrel | Received 12 September 2022 | Accepted 19 December 2022 | Published 19 January 2023

<https://zoobank.org/55DA3862-51E6-49CA-A4CF-F4534D96A267>

**Citation:** Amézquita A, Mazariegos-H LA, Cañaverl S, Orejuela C, Barragán-Contreras LA, Daza JM (2023) Species richness under a vertebral stripe: integrative taxonomy uncovers three additional species of *Pholidobolus* lizards (Sauria, Squamata, Gymnophthalmidae) from the north-western Colombian Andes. *ZooKeys* 1141: 119–148. <https://doi.org/10.3897/zookeys.1141.94774>

## Abstract

The systematic study of biodiversity underlies appropriate inference in most other fields of biological research, yet it remains hampered by disagreements on both theoretical and empirical issues such as the species concept and the operational diagnosis of a species. Both become particularly challenging in those lineages where morphological traits are evolutionarily constrained by their adaptive value. For instance, cryptic organisms often conserve or converge in their external appearance, which hinders the recognition of species boundaries. An integrative approach has been adopted to study microgeographic variation in the leaf-litter lizard *Pholidobolus vertebralis* and test three predictions derived from the evolutionary species concept. Molecular data provided unambiguous evidence of divergence among the three recovered new clades and a common evolutionary history for each of them. The broadly sympatric clades were indeed diagnosable from externally visible traits, such as head scales, adult size, and sexually dimorphic ventral colouration. Also, they barely overlapped on the phenotypic space that summarised 39 morphometric and meristic traits. These clades are

\* These authors contributed equally to this work.

described as three species and an available name is suggested for a recovered fourth clade. The geographic distribution of the new and proximate species suggests a role for elevation on evolutionary divergence; it also raises interesting questions on the speciation pattern of an otherwise underestimated cryptic lineage.

### Keywords

Cryptic species, elevation, leaf-litter lizards, phenotypic space, tropical Andes

## Introduction

The external appearance of many animal species is known to reduce the probability of being detected against natural backgrounds, which arguably impedes eventual predation at its earliest stage: detection (Krebs and Davies 1993). Therefore, natural selection has promoted the evolution of roughly similar appearance in some species that share microhabitats, no matter the phylogenetic distance that separates them. Because microhabitats vary at very small spatial scales, natural selection has also driven the persistence of multiple colouration patterns within a single species, which presumably reduces the learning rate and the formation of a prey search image by potential predators (Ruxton et al. 2008). Both across-species resemblance and within-species variation may play against the interest of systematics and taxonomy. Many lineages are often hidden under a similar appearance and a single name, until alternative sources of evidence and thorough analyses reveal deep evolutionary divisions among them (Sites-Jr. and Marshall 2004). The combination of molecular, morphological, and distributional data has been instrumental to decipher the limits and the relationships within species complexes, once believed to represent a single evolutionary lineage (Padial et al. 2010).

Lizards in many species bear a mid-dorsal vertebral stripe or line. It presumably contributes to conceal them against the leaf litter or vegetation, by mimicking the petiole and midrib of dead leaves, and thereby breaking their body silhouettes to the eyes of potential predators (Ruxton et al. 2004). The occurrence of vertebral stripes across phylogenetically distant species of lizards (e.g., in the neotropical families Gymnophthalmidae, Dactyloidae, Sphaerodactylidae, Teiidae, and Tropiduridae; Avila-Pires 1995) arguably reflects evolutionary convergence. Their existence across closely related species may instead reflect evolutionary conservatism of a valuable survival trait. To the untrained eye, it may also conceal the existence of well differentiated lineages and complex evolutionary histories. Both convergence and conservatism explain the low value of cryptic colouration in taxonomic studies, which claim instead for multiple sources of evidence to avoid overlooking diversity hidden under a single taxonomic entity.

The neotropical lizards in the genus *Pholidobolus* (Gymnophthalmidae) are distributed throughout the mid to high elevation Andes, from northern Peru and throughout Ecuador up to Colombia (Hurtado-Gómez et al. 2018; Parra et al. 2020). Most intrageneric diversity has been acknowledged in the southern part of its distribution with the recent description of a new species in Peru (Venegas et al. 2016) and four in Ecuador (Parra et al. 2020). Instead, Colombian populations of *Pholidobolus* have been frequently and deliberately assigned to *P. vertebralis* (Hurtado-Gómez et al. 2018), a

species bearing a hallmark mid-dorsal vertebral stripe, which indeed inspired its epithet (O'Shaughnessy 1879). The species was known to present both within- and among-localities morphometric variation, which caused some taxonomic instability (Hernández-Ruz and Bernal-González 2011; Doan and Cusi 2014; Venegas et al. 2016). The availability of new specimens and molecular data led to the description of a new species of *Pholidobolus* in high-elevation Paramos of Colombia, *P. paramuno* (Hurtado-Gómez et al. 2018). We became aware of additional geographic variation in body size and ventral colouration in the north-western Colombian Andes, which led us to operationally recognise three morphs occurring as close as 1.5–3.2 km (pairwise map distances) from each other. We aimed at testing whether the available and newly collected evidence were compatible with the existence of multiple lineages, where each (1) had accumulated enough molecular differences as to infer a common evolutionary history, (2) could be diagnosed based on morphometric traits, and (3) exhibited a geographic distribution that convincingly allowed reproductive exchange among individuals of the same morph, but not from different morphs. Those lineages fulfilling at least the first two conditions (Sites-Jr. and Marshall 2004; de Queiroz 2005; de Queiroz 2007), are herein recognised and described as new species.

## Materials and methods

### Study area

To conduct phylogenetic and morphometric analyses, we collected specimens along the northern half of the Colombian Western Andes (Cordillera Occidental), and in the northern extreme of the Colombian Central Andes (Cordillera Central), at elevations between 1400–3100 m (Suppl. material 1). The area encloses hills with remnants of cloud forest and small patches of elfin forests; the foothills are mainly covered by a matrix of regenerating forests, cattle pastures, and crops. Around half of the individuals were collected within a small range where three out of the four studied forms occur: the 3500-ha Mesenia-Paramillo Nature Reserve (**MPNR**), ~ 14 km south-west of the municipality of Jardín (Antioquia). According to a weather station at the visitor's centre, at 2170-m elevation, precipitation is typically bimodal with peaks in April and October, and total annual values exceeding 5000 mm; the average temperature is 15 °C, with maximum daily fluctuations of 10–23 °C.

### Phylogenetic analyses

To build a phylogenetic hypothesis including the studied lizards, we extracted DNA from liver and muscle samples. Lizards were previously euthanised with an overdose of lidocaine and most of them were photographed, in dorsal and ventral views, against a standard white background. They were afterwards fixed in 10% formalin, and finally stored in 70% ethanol. We extracted DNA using either the Qiagen DNeasy or the GeneJET genomic DNA purification kits and following the standard manufacturer's

protocols for tissue samples. We assembled a molecular matrix including four genomic regions: three mitochondrial and one nuclear region. A fragment of the 12S ribosomal gene was amplified using the primers 12Sa and 12Sb (Kocher et al. 1989), the 16S ribosomal gene using the primers 16SCL and 16SDH (Santos et al. 2003), the protein-coding gene NADH dehydrogenase subunit 4 using the primers ND4 and Leu (Arévalo et al. 1994), and the nuclear protein-coding genes oocyte maturation factor MOS using the primers G73 and G74 (Saint et al. 1998).

We aligned each region using MAFFT under default parameters (Katoh and Standley 2013), and simultaneously estimated the best partition scheme and the model evolution using ModelFinder (Kalyaanamoorthy et al. 2017). We inferred a maximum likelihood tree and nodal support using the ultrafast bootstrap method on 5000 pseudoreplicates as implemented in IQTREE (Hoang et al. 2018; Minh et al. 2020). Lastly, to graphically represent the genetic differentiation among the focal lineages of this study, i.e., those with adjacent, parapatric or overlapping distributions in the north-western Colombian Andes, we estimated uncorrected genetic distances between individuals using MEGA (Kumar et al. 2016). We added *P. vertebralis* to this group, because it is the species to which many of the addressed specimens had been formerly assigned (Hurtado-Gómez et al. 2018).

## Meristic and morphometric data

We examined and measured 101 individuals. To record meristic traits, we followed definitions for *Pholidobolus* lizards originally proposed by Montanucci (1973), adopted for other gymnophthalmids by Harris (1994) and Kizirian (1996), and later implemented for new species of *Pholidobolus* (Venegas et al. 2016; Hurtado-Gómez et al. 2018): number of pre-frontal scales (**PF**), supraoculars (**SPO**), superciliaries (**SC**), lower palpebrals (**LP**), suboculars (**SO**), postoculars (**PO**), temporal (**TE**), supralabials (**SL**), infralabials (**IL**), pregonals (**PG**), gulars (**GU**), and collar scales (**CL**); we also counted the number of dorsal transverse rows of scales (**DT**), dorsal longitudinal rows (**DL**), transversal ventral rows (**TV**), and the number of scale rows around mid-body (**SAM**). In addition, we took the following morphometric measurements on 94 adult individuals using a digital calliper and to the nearest 0.01 mm: adult snout-vent length (SVL), head length (**HL**), head width (**HW**), head height (**HH**), jaw length (**JL**), snout length (**SL**), length of the longest finger (**LLF**), length of the longest toe (**LLT**), pelvis width (**PW**), and tail width (**TW**). Tail length was measured but excluded from multivariate analyses, because many individuals showed signs of a regenerated tail.

To test whether the recovered lineages could be differentiated from the combined set of meristic and morphometric traits, we conducted discriminant analysis coupled to principal component analysis, DAPC (Jombart et al. 2010). In brief, DAPC aims at discriminating groups of individuals and predicting group membership by using a linear combination of intercorrelated descriptors previously summarised by principal components analysis (PCA). Although PCA alone is often used to graphically depict among-groups variation in multiple traits, this technique is unsupervised, i.e., it is focused on trait covariation yet ignores the group identity of individuals, which increases

the risk of overlooking differences among the compared groups (Jombart 2008; Jombart et al. 2010). To conduct DAPC, we used as output variable the identity of the four clades recovered in the phylogenetic analysis; as input variables, we used all meristic and morphometric traits. To account for among-traits differences in variance, the variables were centred to the mean = 0 and scaled, i.e., divided by their estimated standard deviation. To estimate the minimum number of principal components that best summarised morphology and predicted clade membership, we used cross-validation with 90% of the data as training set and the remaining 10% as validation set. At each level of PCA retention, we used 10000 replicates to estimate the mean successful assignment of lizards to the correct clade, and the concomitant value of root mean square error (RMSE). We then selected the number of PCs that maximised the former and minimised the latter, or a lower number when the contribution of additional PCs was considered negligible, i.e., < 1% of successful assignments. We finally ran the definitive DAPC with the selected number of principal components and picked the lowest number of discriminant functions that eventually led to a classification success > 90%. All analyses in this section were conducted on the R package ADEGENET (Jombart and Ahmed 2011).

Male ventral colouration differed at first sight among the clades. To visualise and validate photographic comparisons of the colour hues, we took ventral pictures of both males and females, and adjusted them for white balance using the plugin Auto White Balance Correction Master on the software FIJI (Schindelin et al. 2015); the original macro was written by Vytas Bindokas (Univ. of Chicago). To quantitatively illustrate colour differences among the three males selected as new species' holotypes, we additionally conducted image segmentation analyses on the R package RECOLORIZE (Weller et al. 2021), grouping slightly varying hues into a lower number of categories with the method kmeans, and depicting the corresponding result on the sRGB colour space.

The hemipenes of two of the three defined holotypes were extracted following Savage (1997), filled with petroleum jelly, and stained with Alizarin 75%. For description of external morphology, we used the terminology in Dowling and Savage (1960), modified for lizards by Savage (1997). The hemipenes were later preserved in 70% alcohol and deposited together with the holotypes at the MHUA: Museo de Herpetología Universidad de Antioquia, Medellín, Colombia. The hemipenis of the third holotype specimen was revised in situ. To facilitate comparisons with all the closely related species of *Pholidobolus*, we gathered similar data from previously published material (LaMarca and García-Pérez 1990; Hernández-Ruz 2005; Hernández-Ruz and Bernal-González 2011; Doan and Cusi 2014; Hurtado-Gómez et al. 2018; Parra et al. 2020).

## Results

### Phylogenetic relationships

The reconstructed phylogenetic hypothesis (Fig. 1) grouped the lizards we sampled into four clades, each with nodal support above 95%. None of them was nested within

the specimens currently assigned to *P. vertebralis* in Ecuador (Parra et al. 2020), where the type locality has been situated (Uzzell 1973). Two of them (clades C and D in Fig. 1) were sister clades with a nodal support of 93%, yet indeed distributed in different mountain chains: the Western and Central Colombian Andes. Another one (clade B in Fig. 1) was sister to the clade including the former two and the Ecuadorian specimens currently assigned to *P. vertebralis*, and the fourth (clade A in Fig. 1) was sister to a clade including all the previously mentioned plus one Colombian (*P. paramuno*) and nine Ecuadorian species of *Pholidobolus*, including the polyphyletic *P. macbrydei* (Parra et al. 2020).

The distribution of pairwise genetic distances was clearly discontinuous among the lineages with adjacent, parapatric or overlapping distribution in the north-western Colombian Andes: much shorter among individuals of the same recovered clade than among individuals of different clades (Fig. 2). Indeed, the within-clade distribution did not overlap with the among-clades distribution of distances. The sole exception were the Ecuadorian individuals currently assigned to *P. vertebralis*, to which many of the addressed specimens had been formerly assigned. They exhibited the largest within-clade variation. Among the three sympatric lineages of the Colombian Western Andes, which we erect as new species hereafter, genetic distances ranged 2.5–6.3% (Table 1, Fig. 2).

## Uniqueness and variation

The three clades of the Colombian Western Andes (Clades A / B / D in Fig. 1) were unique and diagnosable regarding the combination of four externally visible traits (Fig. 3): the existence of a prefrontal scale (absent / present / present), the number of supraocular scales (2 / 3 / 3–4), the dominant hue of male ventral colouration (pink to orange / orange / grey to black), and the range of variation in male body (snout to vent) length; 42.6–57.9 ( $n = 15$  males), 60.0–68.2 ( $n = 9$ ), and 35.4–54.7 mm ( $n = 22$ ).

Regarding the whole set of morphometric and meristic traits, the first cross-validation analysis indicated that seven principal components summarised enough variation as to attempt phenotypic discrimination and classification of individuals. The existence of near discrete clades was further supported by the scatter of individuals

**Table 1.** Genetic distances. Average uncorrected genetic distances among the species of *Pholidobolus* with adjacent, parapatric or overlapping distributions in the north-western Colombian Andes. The species to which some of these individuals had been formerly added, *P. vertebralis* is added for comparison.

Species	<i>Pa</i>	<i>Pc</i>	<i>Pm</i>	<i>Po</i>	<i>Pp</i>	<i>Pv</i>
<i>P. argosi</i> sp. nov.		0.066	0.066	0.065	0.060	0.047
<i>P. celsiae</i> sp. nov.	0.066		0.029	0.027	0.060	0.014
<i>P. marianus</i>	0.066	0.029		0.028	0.061	0.021
<i>P. odinsae</i> sp. nov.	0.065	0.027	0.028		0.058	0.017
<i>P. paramuno</i>	0.060	0.060	0.061	0.058		0.040
<i>P. vertebralis</i>	0.047	0.014	0.021	0.017	0.040	

throughout the phenotypic space created by the two first discriminant axes (Fig. 4A). We recovered four consistent clusters with bare overlap among them, three corresponding to the Western Andean clades and one from the Central Andean clade; only four out of 81 individuals were plotted in the wrong cluster. Indeed, the resulting DAPC correctly assigned 91% of the revised specimens to the corresponding phylogenetic clade (Fig. 4B). According to the dimensionless loading coefficients of DAPC, which vary between 0–1, the largest contributions of standardised traits to the discriminating task were from the number of dorsal longitudinal scale rows (0.30), the number of ventral transverse scale rows (0.18), and the number of lower palpebrals (0.18).

Regarding sexual dimorphism, males had wider heads than expected from their body size, though the pattern could not be corroborated in one clade due to the capture of a single female (Fig. 5). There was also sexual dichromatism, with females being generally pink to pale orange, or cream in the two clades (A and D) we could check (Fig. 6). In contrast, males of the Clade A (Fig. 1) were pink to pale orange, with more black marks than females; in the Clade D (Fig. 1) they were black to medium grey; and in the Clade B (Fig. 1), they were bright orange with black blotches on the scale edges (Fig. 6). The smallest, and presumably youngest, individuals of all clades were usually grey to cream, and lacked the black patterning (Fig. 6).

### Geographic distribution

During this and parallel studies, all but one individual were captured at altitudes above 1500 m and up to 3100 m. They were thus absent in the lower elevation valley of the Cauca River, which separates the Western and Central Andean chains of Colombia. Among-clades differences in distribution were thus best described in terms of Andean chain and elevation. One clade (clade C in Fig. 1) was found exclusively on the Central Andes (Fig. 7A), where they exhibit some degree of altitudinal segregation with the recently described *P. paramuno* (Hurtado-Gómez et al. 2018): between 1900–2800 for the former and between 2600–3100 m elevation for the latter (Fig. 7B). Among the Western Andean clades (Fig. 7A), there was some degree of altitudinal segregation as well (Fig. 7B). One (clade D in Fig. 1) occurred in the north-eastern slopes, between 1700–2500 m; the second (clade A) in the hilltops, 2400–3000 m a.s.l.; and the third one (clade B) was found at 1900 m elevation in the south-western slopes. Remarkably, the two clades occurring at elevations below 2500 m were found on opposite slopes and thereby basins of the Western Andes (Fig. 7A). The slope-elevation segregation was more evident in the MPNR, where they occur within a radius of 3.5 km without evidence of syntopy, despite our intensive search in the area.

### Systematics

Based on the collected samples and evidence, we recognise the existence of four phylogenetically independent lineages. A name is available for the specimens from the

northern Central Andes (Cordillera Central) in Colombia (Clade C in Fig. 1). The species *Prionodactylus* [*Pholidobolus*] *marianus* (Ruthven 1921) was described from San Pedro (Antioquia, Colombia) based on specimens collected by the late Brother Nicéforo María on March 25, 1921. The religious community Hermanos de La Salle owns a retreat house at the municipality of San Pedro de Los Milagros (Antioquia, Colombia, 75°33.60'W, 6°27.60'N), a small town less than 20 km north to the city of Medellín. San Pedro (its short name) is a well-known collection locality particularly associated to the work by Brother N. María and Brother M.A. Serna (Donegan et al. 2009), both pivotal contributors and curators of the Natural History Museum at the Universidad de La Salle. The reported altitude where the *P. marianus* holotype was collected (2560 m elevation [Uzzell 1973]) can be found less than 200 m away from the retreat house. Because the specimens we collected at San Pedro (MHUA-R12643, MHUA-R12645, MHUA-R12646, MHUA-R12648) are nested in our analyses within the green clade (Figs 1, 2, 4, 5, 7), we propose to resurrect the name *Pholidobolus marianus* for all specimens in this clade (Figs 1, 4, 7).

The specimens of the Colombian Western Andes (Cordillera Occidental) were grouped into three diagnosable (Fig. 3), morphologically distinctive (Fig. 4), genetically discontinuous (Fig. 2), and phylogenetically independent (Fig. 1) clades. None of them was nested in our analyses within the Ecuadorian specimens assigned to *P. vertebralis*; moreover, they were found near 650 km north of its type locality (Uzzell 1973). Therefore, we erect three new species for these lineages and provide below formal descriptions of them. To facilitate actual and future comparisons with other *Pholidobolus* of the northern Colombian Andes, we followed Hurtado-Gómez et al. (2018) regarding terminology and descriptions.

***Pholidobolus argosi* sp. nov.**

<https://zoobank.org/63913FC3-DE51-4941-8D35-08A8BF38FE67>

Figs 1, 3, 6

**Type material. Holotype.** (Figs 1, 3; Table 2). Adult male. Field original label: “AA\_7058.” Museum ID: MHUA-R13905. Type locality in Colombia, Antioquia: municipality of Andes, 5°29.92'N, 75°54.27'W, 2500 m elevation, Mesenia-Paramillo Nature Reserve, in secondary forest, amidst the leaf litter, 7 October 2020. Collected by Ubiel Rendón and Luis A. Mazariegos-H.

**Paratypes.** Fourteen males, six females, and one juvenile. Table 2 shows field codes, localities, elevation, and geographic coordinates. Eighteen specimens were collected in Colombia, Antioquia: municipality of Andes, Mesenia-Paramillo Nature Reserve (MPNR), and one in Colombia, Caldas: municipality of Riosucio, MPNR, years 2018, 2019, and 2020. Collected by Ubiel Rendón, Luis A. Mazariegos, Jorge Jaramillo, and Osman López. The two other specimens from Colombia, Antioquia: Andes, Santa Rita, year 2009. Collected by Cornelio Bota.

**Table 2.** Type series. Identity, sex and geographic location of type specimens of the three new species of *Pholidobolus* lizards described here.

Species	Voucher	Type	Field code	Sex	Locality	Elev (m)	GPS coordinates
<i>P. argosi</i>	MHUAR13905	holotype	AA7058	male	MPNR	2500	5°29.92'N, 75°54.27'W
<i>P. argosi</i>	MHUAR12011	paratype		juvenile	Santa Rita	2730	5°34.75'N, 75°57.68'W
<i>P. argosi</i>	MHUAR12012	paratype		male	Santa Rita	2730	5°34.75'N, 75°57.68'W
<i>P. argosi</i>	MHUAR13851	paratype	AA7010	male	MPNR	2500	5°29.92'N, 75°54.27'W
<i>P. argosi</i>	MHUAR13852	paratype	AA7014	male	MPNR	2740	5°29.54'N, 75°54.31'W
<i>P. argosi</i>	MHUAR13853	paratype	AA7017	female	MPNR	2740	5°29.54'N, 75°54.31'W
<i>P. argosi</i>	MHUAR13854	paratype	AA7039	male	MPNR	2500	5°29.92'N, 75°54.27'W
<i>P. argosi</i>	MHUAR13855	paratype	AA7048	male	MPNR	2740	5°29.54'N, 75°54.31'W
<i>P. argosi</i>	MHUAR13856	paratype	AA7049	male	MPNR	2740	5°29.54'N, 75°54.31'W
<i>P. argosi</i>	MHUAR13857	paratype	AA7050	male	MPNR	2740	5°29.54'N, 75°54.31'W
<i>P. argosi</i>	MHUAR13858	paratype	AA7051	female	MPNR	2740	5°29.54'N, 75°54.31'W
<i>P. argosi</i>	MHUAR13859	paratype	AA7052	female	MPNR	2740	5°29.54'N, 75°54.31'W
<i>P. argosi</i>	MHUAR13860	paratype	AA7053	male	MPNR	2740	5°29.54'N, 75°54.31'W
<i>P. argosi</i>	MHUAR13861	paratype	AA7054	female	MPNR	2740	5°29.54'N, 75°54.31'W
<i>P. argosi</i>	MHUAR13862	paratype	AA7055	female	MPNR	2740	5°29.54'N, 75°54.31'W
<i>P. argosi</i>	MHUAR13863	paratype	AA7059	male	MPNR	2500	5°29.92'N, 75°54.27'W
<i>P. argosi</i>	MHUAR13864	paratype	AA7066	male	MPNR	2840	5°28.76'N, 75°54.37'W
<i>P. argosi</i>	MHUAR13865	paratype	AA7067	male	MPNR	2840	5°28.76'N, 75°54.37'W
<i>P. argosi</i>	MHUAR13866	paratype	AA7068	male	MPNR	2840	5°28.76'N, 75°54.37'W
<i>P. argosi</i>	MHUAR13867	paratype	AA7179	female	MPNR	2500	5°29.92'N, 75°54.27'W
<i>P. argosi</i>	MHUAR13868	paratype	AA7180	male	MPNR	2490	5°29.39'N, 75°51.35'W
<i>P. argosi</i>	MHUAR13869	paratype	AA7181	male	MPNR	2840	5°28.76'N, 75°54.37'W
<i>P. celsiae</i>	MHUAR13906	holotype	AA7061	male	MPNR	1900	5°28.01'N, 75°53.44'W
<i>P. celsiae</i>	MHUAR13148	paratype		juvenile	Mampay	1720	5°21.51'N, 75°52.91'W
<i>P. celsiae</i>	MHUAR13520	paratype		male	La Suiza	1830	4°43.93'N, 75°35.09'W
<i>P. celsiae</i>	MHUAR13870	paratype	AA7002	male	MPNR	1900	5°28.01'N, 75°53.44'W
<i>P. celsiae</i>	MHUAR13871	paratype	AA7056	male	MPNR	1900	5°28.01'N, 75°53.44'W
<i>P. celsiae</i>	MHUAR13872	paratype	AA7057	female	MPNR	1900	5°28.01'N, 75°53.44'W
<i>P. celsiae</i>	MHUAR13873	paratype	AA7069	male	MPNR	1900	5°28.01'N, 75°53.44'W
<i>P. celsiae</i>	MHUAR13874	paratype	AA7070	male	MPNR	1900	5°28.01'N, 75°53.44'W
<i>P. celsiae</i>	MHUAR13875	paratype	AA7071	male	MPNR	1900	5°28.01'N, 75°53.44'W
<i>P. celsiae</i>	MHUAR13876	paratype	AA7072	male	MPNR	1900	5°28.01'N, 75°53.44'W
<i>P. celsiae</i>	MHUAR13877	paratype	AA7073	male	MPNR	1900	5°28.01'N, 75°53.44'W
<i>P. celsiae</i>	MHUAR13878	paratype	AA7074	female	MPNR	1900	5°28.01'N, 75°53.44'W
<i>P. celsiae</i>	MHUAR13879	paratype	AA7161	male	MPNR	1900	5°28.01'N, 75°53.44'W
<i>P. celsiae</i>	MHUAR13880	paratype	AA7172	male	MPNR	1900	5°28.01'N, 75°53.44'W
<i>P. odinsae</i>	MHUAR13907	holotype	AA7090	male	MPNR	2180	5°29.76'N, 75°53.35'W
<i>P. odinsae</i>	MHUAR12574	paratype		male	Santa Rita	2150	5°35.52'N, 75°57.15'W
<i>P. odinsae</i>	MHUAR12584	paratype		juvenile	Quebradona	2240	5°45.38'N, 75°43.37'W
<i>P. odinsae</i>	MHUAR12986	paratype		juvenile	La Isla	1730	5°51.50'N, 76°9.73'W
<i>P. odinsae</i>	MHUAR13883	paratype	AA7009	male	MPNR	1920	5°31.62'N, 75°51.75'W
<i>P. odinsae</i>	MHUAR13884	paratype	AA7011	female	MPNR	1920	5°31.62'N, 75°51.75'W
<i>P. odinsae</i>	MHUAR13885	paratype	AA7012	female	MPNR	1920	5°31.62'N, 75°51.75'W
<i>P. odinsae</i>	MHUAR13886	paratype	AA7013	male	MPNR	2300	5°31.13'N, 75°51.74'W
<i>P. odinsae</i>	MHUAR13887	paratype	AA7015	male	MPNR	1920	5°31.62'N, 75°51.75'W
<i>P. odinsae</i>	MHUAR13888	paratype	AA7016	female	MPNR	2210	5°29.62'N, 75°53.40'W
<i>P. odinsae</i>	MHUAR13889	paratype	AA7019	juvenile	MPNR	2300	5°31.13'N, 75°51.74'W
<i>P. odinsae</i>	MHUAR13898	paratype	AA7182	female	MPNR	2310	5°29.46'N, 75°53.33'W
<i>P. odinsae</i>	MHUAR13899	paratype	AA7183	female	MPNR	2310	5°29.46'N, 75°53.33'W
<i>P. odinsae</i>	MHUAR13904	paratype	AA7188	male	MPNR	2230	5°30.96'N, 75°50.63'W

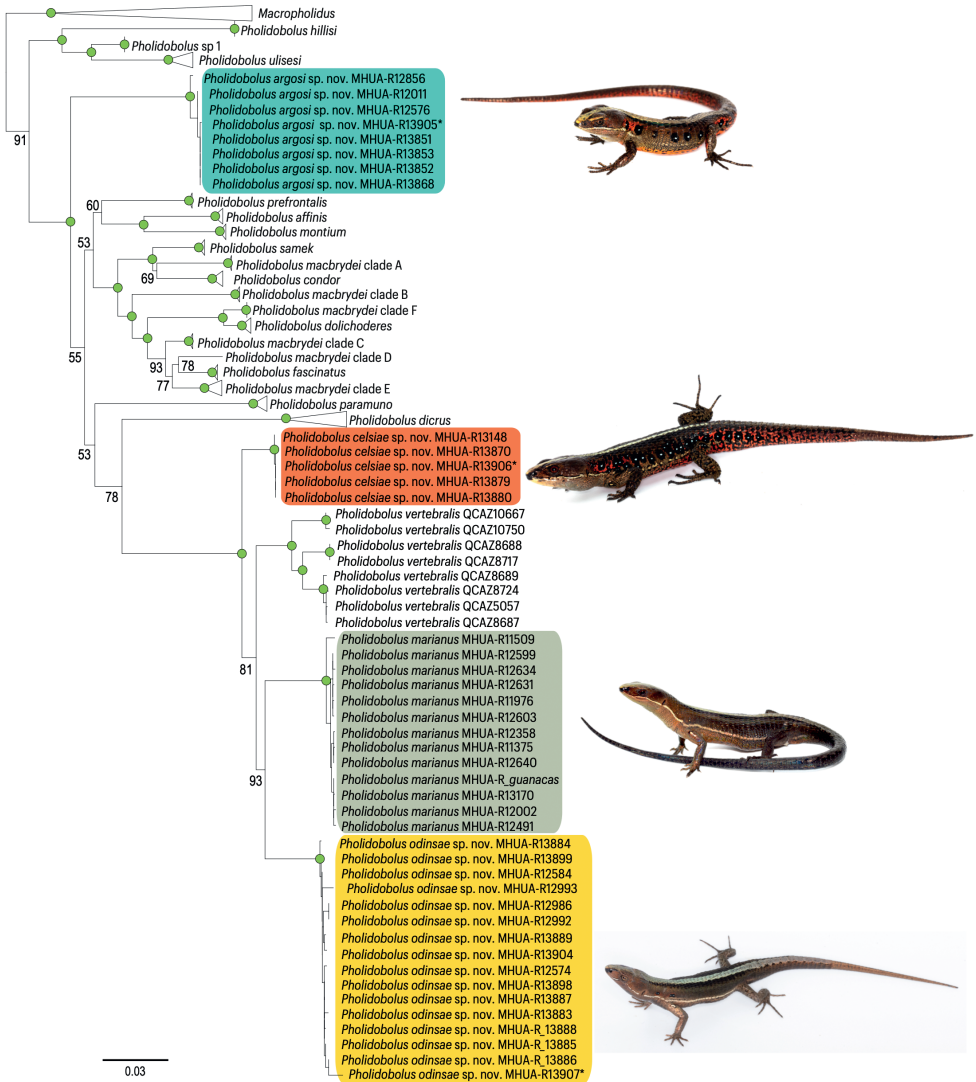


**Figure 1.** Molecular phylogenetic hypothesis. Recovered relationship between species of the leaf-litter lizards in the genus *Pholidobolus*, including *P. vertebralis* near its type locality in Ecuador. The three recovered clades from the Colombian Western Andes are outlined in blue (clade A), orange (clade B) and yellow (clade D). A fourth clade of the Colombian Central Andes is outlined in green (clade C). Green dots indicate nodal support of at least 95%. See Methods for further details on the phylogenetic analysis and Suppl. material 2 for the detailed tree with individuals as terminal nodes.

**Diagnosis.** The species can be diagnosed combining the following characters: (1) two supraocular scales; (2) prefrontal scales absent; (3) 9–17 temporal scales; (4) dorsal scales keeled; (5) 28–32 transverse rows of dorsal scales; (6) 20–22 transverse rows of ventral scales; (7) 26–35 scales around mid-body; (8) 1–2 (usually 1) rows of lateral scales; (9) lateral and medial ventral scales equal in size; (10) 0–5 femoral pores;

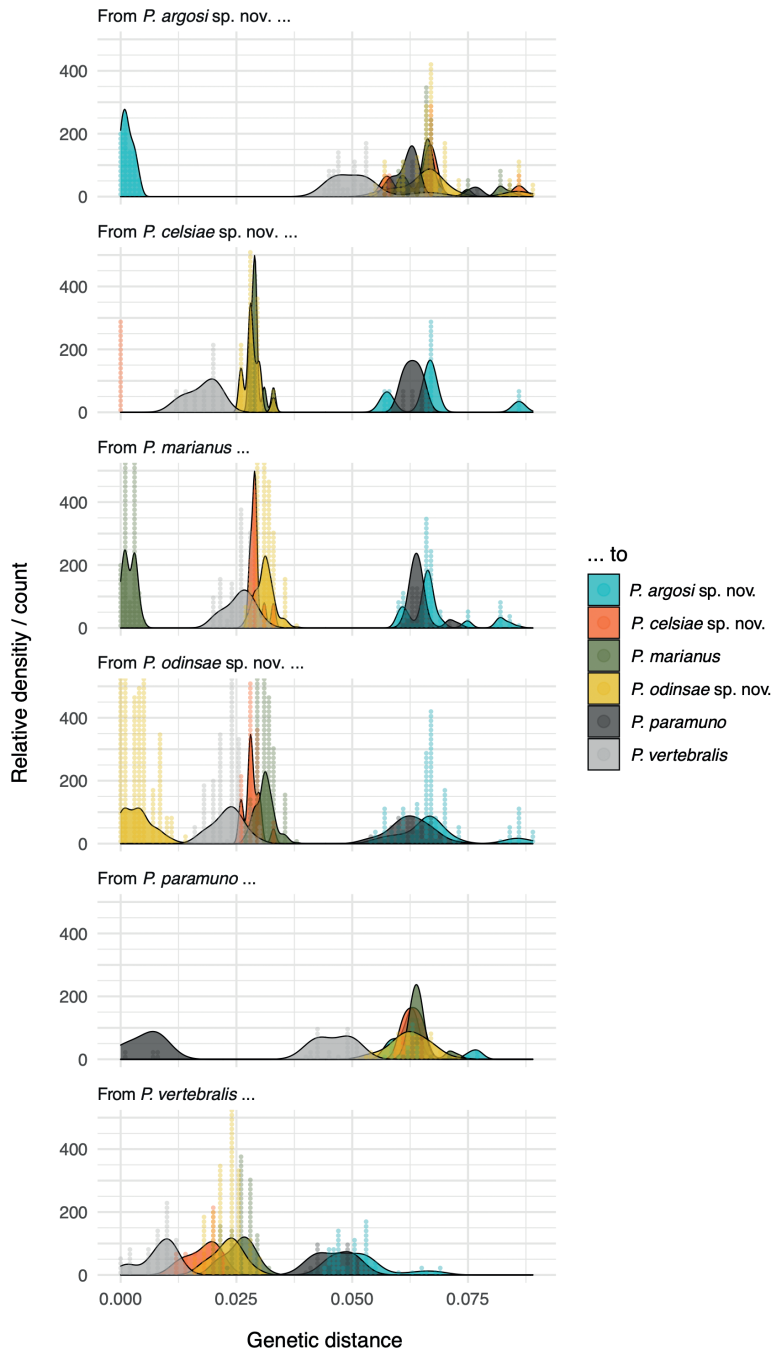


**Figure 2.** Within and among clades genetic distances. Distribution of uncorrected 16S genetic distances among individuals of leaf-litter lizards in the genus *Pholidobolus*. We include four species of the northern Colombian Andes, and *P. vertebralis* near its type locality in Ecuador. Pairwise distances among individuals of the same clade are indicated with the same colour; pairwise distances among individuals from different clades are represented by different colours. Dots denote each of the calculated distances, whose distribution is summarised by Kernel density smooths.

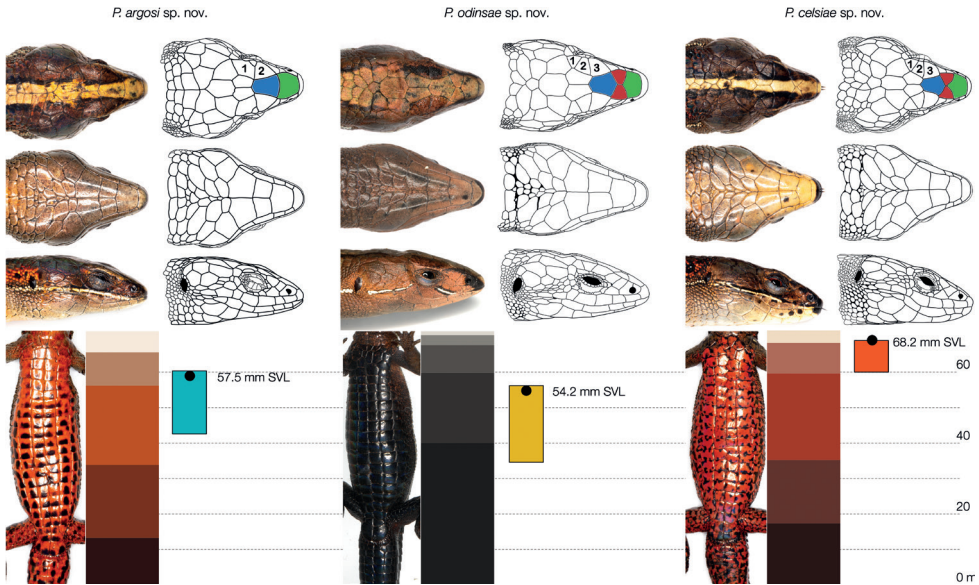


**Figure 3.** Key morphological features of the three new species on the holotypes. External morphological traits allowing unambiguous diagnosis of the three north-western Colombian clades of *Pholidobolus* lizards recovered in our phylogenetic analysis. *Pholidobolus argosi* sp. nov. lacks one supraocular (numbered) and the prefrontal (filled in red) scales, both of which are present in the other two species. Males of *P. odinsae* sp. nov. exhibit predominantly black and dark grey ventral colouration, which is red with black markings in males of the two other species, as further shown by the image segmentation analyses: the stacked areas denote the proportion of pixels with each summarised hue. Lastly, *P. celsiae* sp. nov. reaches larger adult body size than the other two species, as evidenced by blue (clade A in Fig. 1), orange (B), and yellow (D) bars, which denote range of variation, and the black points, that represent the actual body size of the shown holotypes.

(11) no sexual dimorphism in number of femoral pores; (12) labial scales pale, often crossed dorsally by a longitudinal white stripe bordered with black; (13) ventral head colouration paler towards the anterior end; (14) cream or white vertebral stripe bordered by two black stripes, originating on the rostral scale, completely covering the dorsal region of the head and the vertebral region of the body, reaching only the anterior portion of the tail, with maximum width of four scales on the body; (15) lateral colour brown, orange towards the shoulders and anterior part of the tail, with some ocelli, usually less than seven between limbs insertions, each white in centre and surrounded by black scales, with a longitudinal white line in the head, pale and discontinuous towards the body; (16) venter pink to pale orange, with few black markings in females; vivid orange with much more and much larger black markings in adult males; (17) subcylindrical and bilobed hemipenial body with 6–8 and 7–9 rows of spinulated flounces in the lateral columns of the sulcate and asulcate sides, respectively; (18) lateral columns of spinulated flounces connecting in the proximal region of the asulcate side.

**Comparisons.** *Pholidobolus vertebralis* differs from *P. argosi* sp. nov. (character states in parenthesis) in having the lateral ventral scales smaller than the medial ventrals (lateral and medial ventral scales equal in size). The other species from the north-western and central Colombian Andes (Fig. 7) differ from *P. argosi* sp. nov. in having prefrontal scales (absent), and 3–4 supraocular scales (2). In addition, males in *P. paramuno* are ventrally reddish brown and in *P. odinsae* sp. nov. are black to grey (pink to pale orange). Lastly, males of *P. celsiae* sp. nov. are larger in size (Table 3), between 60.7–68.6 mm of snout–vent length (42.6–57.9 mm).

**Description of the holotype.** Adult male; snout-vent length 57.5 mm; tail length 111.0 mm; other body measurements can be found in Table 4. Head scales smooth, juxtaposed, glossy, with small pits organised mainly around their margins. Rostral single, hexagonal, wider than high, dorsally in broad contact with the internasal and laterally in contact with the first supralabial and the nasal. Frontonasal single, wider than long, hexagonal, in contact with the nasal, loreal and the frontal one. Prefrontal scales absent. Frontal single, pentagonal, longer than wide, wider anteriorly, in contact with the frontonasal. Frontoparietals two, pentagonal, longer than wide, narrower anteriorly, contacting the first two supraoculars laterally, and the parietal and interparietals posteriorly. Supraoculars two, wider than longer and increasing in size antero-posteriorly, contacting the superciliaries laterally and the parietal and postocular posteriorly. Interparietal single, hexagonal, longer than wide, narrower than the parietals and contacting laterally the parietals and posteriorly the postparietals. Parietals two, pentagonal, wider than long, slightly shorter and wider than the interparietal, contacting the temporals laterally and the postparietals posteriorly. Postparietals in two rows, two in the anterior row and four in the posterior row. Nasal single, rhomboidal, wider than high, contacting the first and second supralabials, the loreal and frenocular. Loreal single, quadrangular, over the frenocular, in contact with first superciliary dorsally. Frenocular single, triangular, in contact with the first infraocular and the second and third supralabials. Superciliaries three, the anteriormost noticeable larger than the others, contacting the uppermost preocular. Suboculars four contacting supralabials three to five. Postoculars two, the dorsal one larger than the ventral one. Temporals 13, contacting supralabials five to seven. Supralabials seven and infralabials six. Mental single, pentagonal, wider than long, contacting the first infralabial and postmental. Postmental single, pentagonal, contacting the first three infralabials and the anterior genials. Genials in three pairs, the anterior one quadrangular, the posteriors pairs pentagonals and larger than the anterior one, contacting infralabials three, three and four, and five respectively. Pregulars two. Gular scales seven, wider than long, in two longitudinal rows; collar scales ten, decreasing in size laterally. Dorsal scales longer than wide, hexagonal, keeled, imbricate, arranged in 31 transverse rows. Longitudinal rows of dorsal scales 17, the first two rows in each side weakly keeled and rounded. Lateral row scales at mid-body one, smooth, at least half the size of adjacent scales. Scales around mid-body 31. Longitudinal rows of ventrals eight, quadrangular. Transverse rows of ventrals 18. Cloacal plates in two rows of two scales each, the anterior one quadrangular, the posterior row rounded, larger than the anterior one. Tail scales arranged in 80 rings, hexagonal and keeled dorsally, quadrangular and smooth ventrally.

**Table 3.** Meristic and morphometric traits. Summary of meristic and morphometric (in mm) traits in adult lizards of the four clades of *Pholidobolus* studied here. Mean  $\pm$  sd (min – max).

Trait	<i>P. argosi</i> sp. nov. (n = 21)	<i>P. celsiae</i> sp. nov. (n = 11)	<i>P. marianus</i> comb. nov. (n = 24)	<i>P. odinsae</i> sp. nov. (n = 35)
Prefrontals	0 $\pm$ 0 (0–0)	2.0 $\pm$ 0.0 (2–2)	2.0 $\pm$ 0.0 (2–2)	2.0 $\pm$ 0.0 (2–2)
Supraoculars	2.0 $\pm$ 0.0 (2–2)	3.0 $\pm$ 0.0 (3–3)	3.4 $\pm$ 0.5 (3–4)	3.0 $\pm$ 0.2 (3–4)
Superciliaries	3.9 $\pm$ 0.4 (3–5)	3.9 $\pm$ 0.3 (3–4)	3.7 $\pm$ 0.6 (3–5)	4.0 $\pm$ 0.2 (3–5)
Lower palpebrals	3.9 $\pm$ 0.7 (2–5)	4.4 $\pm$ 0.7 (3–5)	5.4 $\pm$ 1.1 (4–7)	3.9 $\pm$ 0.8 (2–5)
Suboculars	4.1 $\pm$ 0.6 (3–5)	4.9 $\pm$ 0.9 (4–6)	3.9 $\pm$ 0.8 (3–6)	5.2 $\pm$ 1.1 (3–7)
Postoculars	2.0 $\pm$ 0.0 (2–2)	2.1 $\pm$ 0.3 (2–3)	2.9 $\pm$ 0.6 (2–4)	2.2 $\pm$ 0.5 (2–4)
Temporal	12.5 $\pm$ 1.8 (9–17)	21.8 $\pm$ 4.8 (14–28)	13.8 $\pm$ 2.7 (10–19)	19.9 $\pm$ 3.3 (11–26)
Supralabials	6.9 $\pm$ 0.4 (6–8)	7.2 $\pm$ 0.4 (7–8)	6.9 $\pm$ 0.5 (6–8)	7.1 $\pm$ 0.4 (7–8)
Infralabials	5.6 $\pm$ 0.6 (5–7)	4.6 $\pm$ 0.7 (4–6)	4.9 $\pm$ 0.7 (3–6)	4.8 $\pm$ 0.7 (4–6)
Pregulars	2.1 $\pm$ 0.2 (2–3)	2.4 $\pm$ 0.5 (2–3)	3.8 $\pm$ 0.9 (2–6)	2.3 $\pm$ 0.6 (2–4)
Gulars	7.1 $\pm$ 0.4 (6–8)	7.6 $\pm$ 0.5 (7–8)	7.9 $\pm$ 1.3 (4–10)	8.1 $\pm$ 0.6 (7–9)
Collar scales	10.3 $\pm$ 1.5 (7–13)	11.2 $\pm$ 1.6 (9–14)	10.3 $\pm$ 1.7 (6–13)	10.9 $\pm$ 2.0 (6–17)
Dorsal transverse	30.1 $\pm$ 1.0 (28–32)	29.5 $\pm$ 0.9 (28–31)	30.3 $\pm$ 1.2 (28–32)	29.9 $\pm$ 1.0 (28–32)
Dorsal longitudinal	18.8 $\pm$ 1.2 (17–21)	24.9 $\pm$ 1.0 (23–26)	22.3 $\pm$ 1.9 (19–26)	22.5 $\pm$ 2.0 (20–26)
Around mid-body	31.3 $\pm$ 2.3 (26–35)	39.6 $\pm$ 1.5 (37–43)	35.9 $\pm$ 2.6 (30–42)	38.4 $\pm$ 3.4 (31–45)
Transversal ventral	21.1 $\pm$ 0.7 (20–22)	19.6 $\pm$ 1.0 (18–21)	21.2 $\pm$ 1.2 (19–24)	19.8 $\pm$ 1.2 (17–23)
Head width	8.70 $\pm$ 1.20 (6.6–11.3)	11.89 $\pm$ 1.20 (7.4–14.6)	7.53 $\pm$ 0.98 (5.9–9.7)	8.02 $\pm$ 1.02 (6.0–10.0)
Head length	11.77 $\pm$ 1.79 (9.1–15.0)	15.05 $\pm$ 2.46 (10.4–17.9)	10.66 $\pm$ 1.56 (7.6–14.5)	11.24 $\pm$ 1.39 (8.6–15.0)
Head height	6.13 $\pm$ 0.87 (5.0–7.7)	8.44 $\pm$ 1.51 (5.2–9.7)	5.32 $\pm$ 0.71 (3.9–7.1)	5.41 $\pm$ 0.63 (4.2–6.7)
Jaw length	9.51 $\pm$ 1.42 (7.2–13.2)	12.77 $\pm$ 1.56 (9.4–14.5)	10.15 $\pm$ 1.88 (7.1–14.1)	9.67 $\pm$ 1.50 (7.4–13.2)
Longest finger	5.25 $\pm$ 0.58 (4.1–6.4)	5.80 $\pm$ 0.79 (4.7–6.8)	4.75 $\pm$ 0.47 (4.0–5.6)	4.72 $\pm$ 0.63 (3.9–6.3)
Pelvis width	6.57 $\pm$ 0.70 (4.8–7.6)	8.60 $\pm$ 1.01 (6.2–9.6)	6.57 $\pm$ 0.91 (4.2–7.9)	6.67 $\pm$ 0.97 (4.9–8.9)
Longest toe	8.13 $\pm$ 0.77 (6.8–10.2)	9.42 $\pm$ 0.90 (7.4–10.2)	7.19 $\pm$ 0.65 (5.7–8.2)	7.19 $\pm$ 1.06 (5.3–10.8)
Tail width	5.50 $\pm$ 0.59 (4.3–6.6)	7.61 $\pm$ 1.42 (5.1–9.5)	4.97 $\pm$ 0.60 (4.1–6.1)	5.69 $\pm$ 0.97 (3.9–8.1)
Snout-vent length	50.85 $\pm$ 4.23 (42.6–57.9)	62.38 $\pm$ 7.19 (45.0–68.6)	46.97 $\pm$ 4.81 (35.6–55.8)	48.36 $\pm$ 5.71 (35.4–60.3)

Limbs pentadactyl with clawed fingers. Dorsal brachial and antebrachial scales lanceolate to polygonal, longer than wide, imbricate and smooth. Ventral brachial and antebrachial scales lanceolate to polygonal, almost as long as wide, juxtaposed, much smaller than the dorsal ones. Dorsal hand scales hexagonal, wider but shorter than the dorsal antebrachial scales. Finger length formula IV > III > II > V > I. Supradigital scales quadrangular, imbricate and wider than long. Palmar scales polygonal, juxtaposed, and small. Subdigital lamellae domelike with a quadrangular base, and often divided longitudinally, with six on finger I, 10 on II, 12 on III, 15 on IV, and 10 on V. Thigh scales on the dorsal, anterior and ventral surfaces lanceolate to rhomboidal, longer than wide, those in the dorsal surface smooth and the others smooth and imbricate. Thigh scales on the posterior surface of the legs rounded, smooth, juxtaposed and much smaller than those of the anterior and dorsal surfaces. Five femoral pores per leg; preanal pores absent. Anterior and ventral crus scales polygonal and smooth. Lateral and posterior crus scales rounded, small and subimbricate. Toe length formula IV > III > V > II > I. Supradigital scales quadrangular, imbricate and longer than wide. Plantar scales polygonal, juxtaposed and small. Subdigital lamellae domelike with a quadrangular base, and often divided longitudinally, with six on Toe I, 10 on II, 16 on III, 20 on IV, and 11 on V.

**Table 4.** Holotypes. Sex, body measurements (in mm), and voucher identity of the holotypes of the new lizard species describe herein.

Trait	<i>P. argosi</i> sp. nov.	<i>P. celsiae</i> sp. nov.	<i>P. odinsae</i> sp. nov.
Sex	male	male	male
Snout-vent length	57.5	68.2	54.2
Head length	14.9	16.6	11.2
Head width	11.3	14.6	8.8
Head height	7.6	9.7	6.3
Jaw length	10.5	12.8	10.9
Length of the longest finger	6.4	6.1	4.9
Length of the longest toe	8.8	10.0	7.4
Pelvis width	7.6	9.6	6.3
Tail length	111.0	79.0	50.0
Tail width	6.4	9.5	5.0

**Colouration.** In life, dorsally brown, bisected by a mid-dorsal (i.e. vertebral) cream, pale brown, or white stripe, extending from the head to the base of the tail; vertebral stripe bordered with darker, usually black, stripes; on the head, the pale stripe extends from the first supralabial to the shoulder dorsally reaching the rostral scale, and laterally bordering the supraocular and parietal scales; sides of neck, flanks, and limbs predominantly brown, usually with less than ten white ocelli, bordered by a black stripe; white or cream lateral line from the supralabials to the shoulder; cream and interrupted lateral stripe, running between the insertions of fore and hind limbs, not extending towards the tail; scattered red scales, more common and grouped above the shoulder and along the lateral surface of the tail; throat pink to cream; chest, belly and base of the tail pink to pale orange, often with black blotches, apparently more common in adult males (Figs 1, 3, 6). In preservative, brown surfaces become paler, the dorsal and lateral stripes become white, and the red surfaces on the flanks, chest, belly and tail fade to white or very pale pink.

**Etymology.** The species epithet is dedicated to the Grupo Argos Foundation, for their commitment to sustainable development, and their voluntary actions directed to education and environmental restoration. Through its program “Sembrando Futuro”, they promote the conservation and recovery of water resources, depleted gallery forests, mangroves, and the habitat of the spectacled bear, an umbrella species for the conservation of entire Andean ecosystems.

**Distribution, ecology, and conservation.** The species is currently known from the hilltops of the western Andes, near the municipalities of Andes and Caramanta, within the department of Antioquia. Most specimens were seen amongst the leaf litter of elfin forests; some were collected on secondary forests at the edge of cloud forests. The observed specimens appeared clearly heliothermic: within minutes after the sun appeared, they came out of the leaf litter, remained exposed, and extended their ribs increasing the dorsal surface available for sunlight capture. Under sunny conditions, several individuals could be seen at once in at least two of the spots from where the

species is known. Its distribution seems thus to be very patchy, known presently from fewer than five locations and in any case less than 500 km<sup>2</sup> (Fig. 7). The cloud and elfin forests are severely fragmented in the area, and remain mainly as small patches on hilltops, which are preserved to protect water sources for crops downhill. Therefore, until new information is collected, we suggest listing the new species as Endangered EN B1ab(iii), B2ac(iii), under the IUCN criteria (IUCN 2012). Many individuals showed signs of a regenerated tail.

***Pholidobolus celsiae* sp. nov.**

<https://zoobank.org/A75418D8-7BB3-4764-848B-4ADBD2E12D47>

**Type material. *Holotype*.** Adult male, with genitalia in a separate microvial. Original label: AA\_7061. Museum ID: MHUA-R13906. Type locality in Colombia, Risaralda: Municipality of Mistrató, 5°28.01'N, 75°53.44'W, secondary forest, under rocks, 7 October 2020. Collected by Ubiel Rendón and Luis A. Mazariegos-H.

***Paratypes*.** Eleven males, two females, and one juvenile. Table 2 shows field codes, localities, elevation, and geographic coordinates. Twelve specimens were collected in Colombia, Risaralda: Mistrató, Mesenia-Paramillo Nature Reserve (MPNR), May 2018, June 2019, and October 2020. Collected by Ubiel Rendón, Luis A. Mazariegos-H., Jorge Jaramillo, and Osman López. One from Colombia: Risaralda, Municipality of Mistrató, Mampay village. Collected by Juan P. Hurtado. The other from Colombia, Risaralda: Municipality of Pereira, vereda La Suiza, Santuario de Fauna y Flora Otún Quimbaya. Collected by Melisa Galeano.

**Diagnosis.** The species can be diagnosed combining the following characters: (1) three supraocular scales; (2) prefrontal scales present; (3) 14–28 temporal scales; (4) dorsal scales keeled; (5) 28–32 transverse rows of dorsal scales; (6) 18–21 transverse rows of ventral scales; (7) 36–44 scales around mid-body; (8) 1–3 rows of lateral scales; (9) lateral and medial ventral scales equal in size; (10) 5–6 femoral pores; (11) no sexual dimorphism in number of femoral pores; (12) labial scales pale, often with black markings; (13) ventral head colouration homogeneous in females; with irregular orange or black markings, and paler towards the anterior half in males; (14) white to cream vertebral stripe bordered by two black stripes, originating on the rostral scale, completely covering the dorsal region of the head and the vertebral region of the body, reaching only the anterior portion of the tail, with maximum width of two scales on the body; (15) lateral colour pattern brown and dark orange to red, with numerous ocelli, usually more than seven between the limbs insertions, white in centre and surrounded by black scales, with a longitudinal pale line laterally, continuous and white in the head, pale and discontinuous towards the body; (16) venter pink to pale orange, or brown, with darker marking towards the edge of scales in females; vivid orange to red, with scattered black markings towards the edge of scales in males; (17) subcylindrical and bilobed hemipenial body with 4–5 and 7–9 rows of spinulated flounces in the lateral columns of the sulcate and asulcate sides, respectively; (18) lateral columns of spinulated flounces connecting in the distal region of the asulcate side.

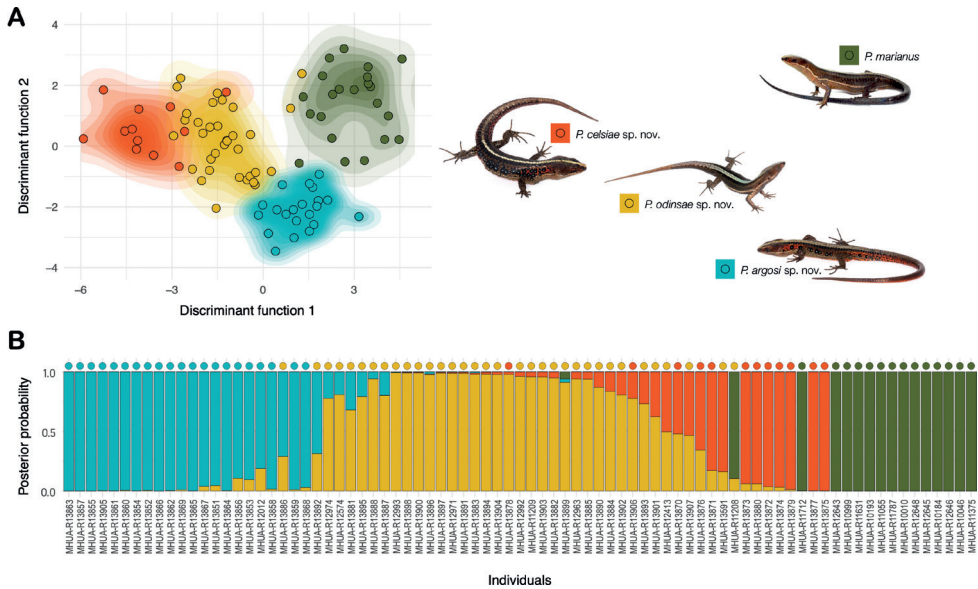


**Figure 4.** Discriminant and classification analysis based on lizard morphology. Classification analysis of lizards in four species of *Pholidobolus* based on the whole set of meristic and morphometric traits **A** distribution of individuals (dots) of the recovered phylogenetic clades (colours) in the two-dimensional phenotypic space created by the discriminant analysis of principal components (DAPC) summarising all traits **B** actual (dot colour) and predicted (bar colour) membership of each lizard (museum identity) to the recovered clades; predicted membership is estimated from the DAPC and represents the probability of assignment of each lizard to one or more lineages (colours). See Methods for further detail on the underlying statistical analyses.

**Comparisons.** *Pholidobolus vertebralis* differs from *P. celsiae* sp. nov. (character states in parenthesis) in having the lateral ventral scales smaller than the medial ventrals (lateral and medial ventral scales equal in size). The other species from the northwestern and central Colombian Andes (Fig. 7) differ from *P. celsiae* sp. nov. in exhibiting smaller adult body size in males (Table 2), between 35.4–54.7 mm in *P. odinsae* sp. nov., and 42.6–57.9 mm in *P. argosi* sp. nov. (60.7–68.6 mm). In addition, males of *P. argosi* sp. nov. lack prefrontal scales (present) and have two supraocular scales (3–4). Lastly, males of *P. odinsae* sp. nov. exhibit black to grey and males of *P. paramuno* reddish brown ventral coloration (orange).

**Description of the holotype.** Adult male; snout-vent length 68.2 mm; tail length 79.0 mm; other body measurements in Table 4. Head scales smooth, juxtaposed, glossy, with small pits organised mainly around their margins. Rostral single, hexagonal, wider than high, dorsally in broad contact with the internasal and laterally in contact with the first supralabial and the nasal. Frontonasal single, wider than long, pentagonal, in contact with the nasal, loreal and prefrontals. Prefrontals two, wider laterally and narrower medially, in wide contact with the first superciliary, the frontal and the anterior supraocular. Frontal single, hexagonal, longer than wide, wider anteriorly, in contact with the prefrontals, the first supraocular and the frontoparietals. Frontoparietals two, pentagonal, longer than wide, narrower anteriorly, contacting the first two supraoculars

laterally, and the parietal and interparietals posteriorly. Supraoculars three, the anterior-most nearly as wide as long and the other two wider than long, decreasing in size antero-posteriorly, contacting the superciliaries laterally and the parietal and postocular posteriorly. Interparietal single, heptagonal, longer than wide, narrower than the parietals and contacting laterally the parietals and posteriorly the postparietals. Parietals two, hexagonal, wider than long, slightly shorter and wider than the interparietal, contacting the temporals laterally and the postparietals posteriorly. Postparietals in two rows, three in the anterior row and four in the posterior row. Nasal single, wider than high, contacting the first and second supralabials, the loreal and frenocular. Loreal single, quadrangular, over the frenocular, in contact with first superciliary dorsally. Frenocular single, triangular, in contact with the first infraocular and the second and third supralabials. Superciliaries four, the anteriormost noticeable larger than the others, contacting the uppermost preocular. Suboculars five contacting supralabials three to five. Postoculars two, ventral larger than dorsal. Temporals 17 contacting supralabials five to seven. Supralabials seven and infralabials five. Mental single, pentagonal, wider than long, contacting the first infralabial and postmental. Postmental single, pentagonal, contacting the first two infralabials and the anterior genials. Genials in three pairs, the anterior one quadrangular and the posterior two pentagonal. The anterior two in contact medially and the posterior one separated by postgenials; contacting infralabials two, three, and four. Pregulars two. Gular scales seven, wider than long, in two longitudinal rows; collar scales 13 decreasing in size laterally. Dorsal scales longer than wide, hexagonal, keeled, imbricate, arranged in 29 transverse rows. Longitudinal rows of dorsal scales 23, the first two rows in each side weakly keeled and rounded. Lateral row scales at mid-body one, smooth, at least half the size of adjacent scales. Scales around mid-body 39. Longitudinal rows of ventrals six, quadrangular. Transverse rows of ventrals 20. Cloacal plates in two rows of two quadrangular scales each, the posterior row larger than the anterior one, in contact with two small scales laterally. Tail scales arranged in 54 rings, hexagonal and keeled dorsally, quadrangular and smooth ventrally.

Limbs pentadactyl with clawed fingers. Dorsal brachial and antebrachial scales lanceolate to polygonal, almost as long as wide, imbricate and smooth. Ventral brachial and antebrachial scales lanceolate to polygonal, almost as long as wide, juxtaposed, much smaller than the dorsal ones. Dorsal hand scales hexagonal, wider but shorter than the dorsal antebrachial scales. Finger length formula  $IV = III > II > V > I$ . Supradigital scales quadrangular and imbricate. Palmar scales polygonal, juxtaposed and small. Subdigital lamellae domelike with a quadrangular base, and often divided longitudinally, with four on finger I, 8 on II, 12 on III, 13 on IV, and 7 on V. Thigh scales on the dorsal, anterior and ventral surfaces lanceolate to rhomboidal, longer than wide, those in the dorsal surface keeled and the others smooth and imbricate. Thigh scales on the posterior surface of the legs rounded, smooth, juxtaposed and much smaller than those of the anterior and dorsal surfaces. Five femoral pores per leg; preanal pores absent. Anterior and ventral crus scales polygonal and keeled. Lateral and posterior crus scales rounded, small and subimbricate. Toe length formula  $IV > III > II > IV > I$ . Supradigital scales quadrangular, imbricate and longer than wide. Plantar scales polygonal, juxtaposed and small. Subdigital lamellae domelike with a quadrangular base, and often divided

longitudinally, with four on Toe I, 8 on II, 13 on III, 15 on IV, and 9 on V. Thigh scales on the dorsal, anterior and ventral surfaces lanceolate to rhomboidal, longer than wide, those in the dorsal surface keeled and the others smooth and imbricate. Thigh scales on the posterior surface of the legs rounded, smooth, juxtaposed and much smaller than those of the anterior and dorsal surfaces. Five femoral pores per leg; preanal pores absent. Anterior and ventral crus scales polygonal and keeled. Lateral and posterior crus scales rounded, small and subimbricate. Toe length formula  $IV > III > V > II > I$ . Supradigital scales quadrangular, imbricate and longer than wide. Plantar scales polygonal, juxtaposed and small. Subdigital lamellae domelike with a quadrangular base, and often divided longitudinally, with seven on I, nine on II, 13 on III, 18 on IV, and 10 on V.

**Colouration.** In life, dorsally dark brown, bisected by a mid-dorsal (i.e. vertebral) cream, or white stripe, extending from the head to the base of the tail; vertebral stripe bordered with darker, usually black, stripes; on the head, the pale stripe extends from the first supralabial to the shoulder dorsally reaching the rostral scale, and laterally not in contact with the supraocular and parietal scales; sides of neck, flanks, and limbs predominantly brown; neck, flanks and tail base usually with more than 10 white ocelli, bordered by a black stripe; white or cream lateral line from the supralabials to the shoulder; cream and interrupted lateral stripe, running between the insertions of fore and hind limbs, not extending towards the tail; many red scales, more common in males and grouped above the shoulder and along the lateral surface of the tail; throat cream to pale brown in males, paler towards the anterior extreme; throat pink in females; chest, belly and base of the tail cream to pink in females, but orange in males, often with black blotches, apparently more common in adult males (Figs 1, 3, 6). In preservative, brown surfaces become paler, the dorsal and lateral stripes become white, and the red surfaces on the flanks, chest, belly and tail fade to white or very pale pink.

**Etymology.** The species epithet is dedicated to the Celsia Foundation, for their voluntary contribution to the restoration of cloud and dry forests in the tropical Andes, through their reforestation program Reverde-C, which already planted more than one million trees. In addition, their program for children education in rural areas, already benefited more than 16000 students in terms of school infrastructure, teacher training, and further logistic support during the Covid pandemic. We believe their commitment contributes to the well-being and education of direct neighbours and thereby stakeholders of Colombian protected nature.

**Distribution, ecology, and conservation.** The specimens were mostly collected in open areas with secondary vegetation, at the edge of a cloud forest. Groups of up to nine eggs were found together with adult individuals under a rock, suggesting communal nesting. Also, the observed specimens appeared clearly heliothermic: within minutes after the sun appeared, they came out of their refuges, remained exposed, and extended their ribs increasing the dorsal surface available for sun basking. The species is currently known from three localities, two of them within protected areas: the Mesenia-Paramillo Nature Reserve, and the Santuario de Flora y Fauna (SFF) Otún-Quimbaya. Further explorations are needed to ascertain the species distribution. In the meantime, we suggest listing the new species as Endangered EN B1ab(iii), B2ac(iii), under the IUCN criteria (IUCN 2012). Many individuals showed signs of a regenerated tail.

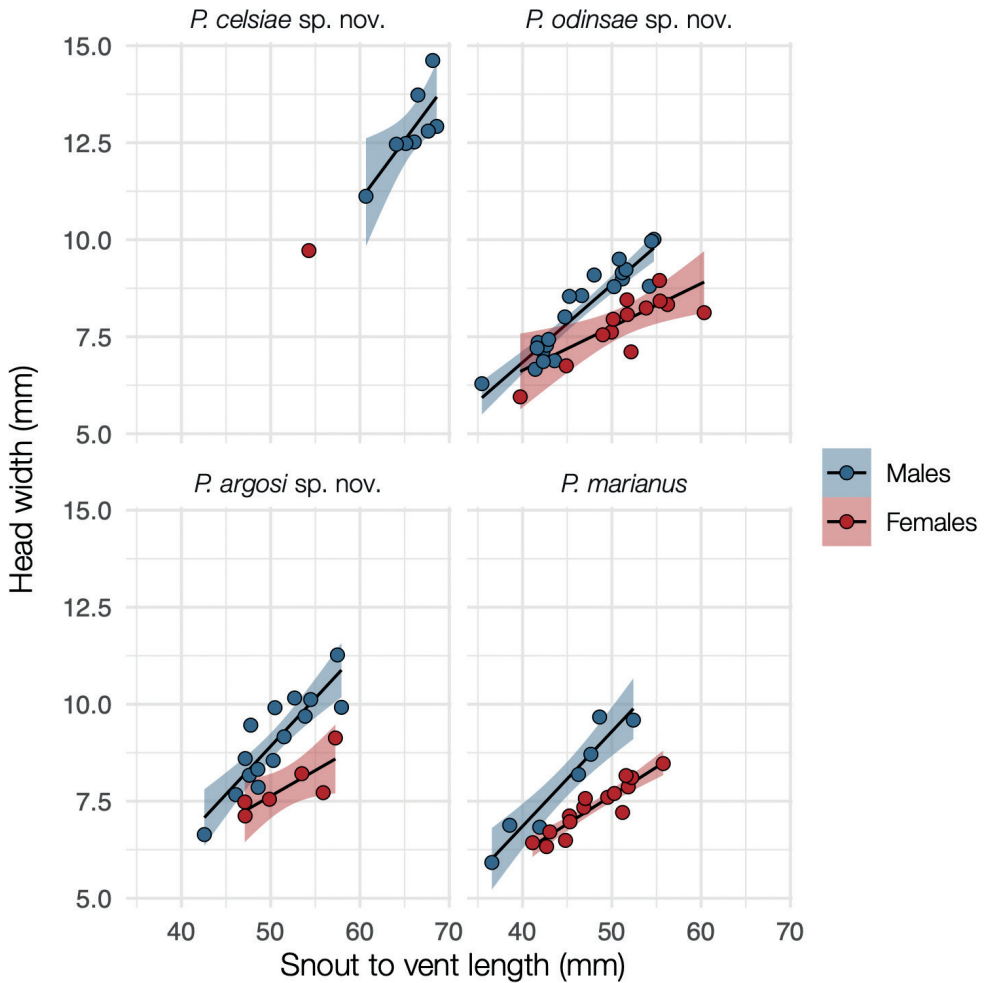


**Figure 5.** Sexual dimorphism in the lizard head width. Relationship between head width and body size across four species of *Pholidobolus* lizards. Males exhibit disproportionately wider heads compared to females. Only one female was available for *P. celsiae* sp. nov. Lines denote linear regression, and the coloured shadows indicate the 95% confidence interval of the line slope. Non-overlapping blue and red shadows represent significant differences in the slope of the head width to body size relationship, between males and females.

***Pholidobolus odinsae* sp. nov.**

<https://zoobank.org/9C94C382-240C-4E33-9C91-24C1363959FF>

**Type material. Holotype.** (Figs 1, 3) Adult male, with genitalia in a separate microvial. Original field label: AA\_7090. Museum ID: MHUA-R13907. Type locality in Colombia, Antioquia: Municipality of Jardín, Mesenia-Paramillo Nature Reserve, 5°29.76'N, 75°53.35'W, visitor centre, among pastures, 14 November 2020. Collected by Ubiel Rendón and Luis A. Mazariegos-H.

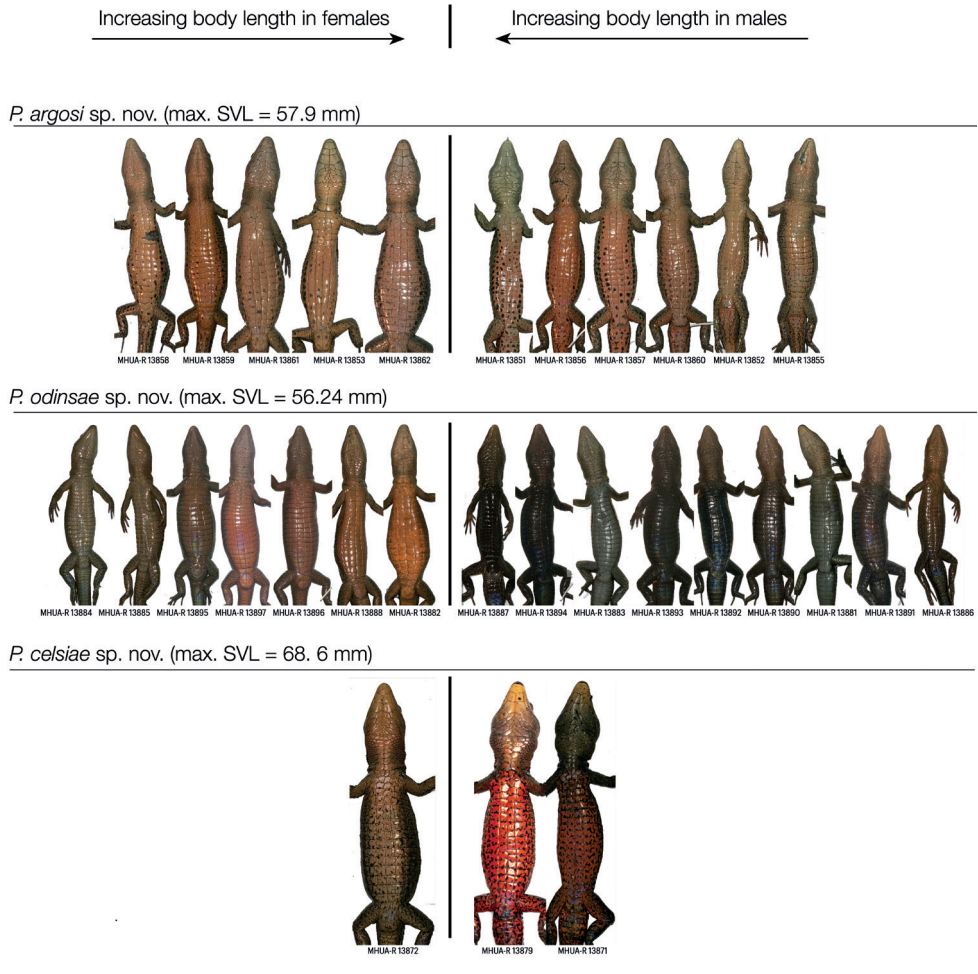


**Figure 6.** Variation in lizard ventral colouration. Among-species, among-sexes, and among-individuals variation in ventral colouration of three lizard species in the genus *Pholidobolus*. Pictures were taken immediately after euthanasia to reflect colour in life. To depict eventual covariation with body size, individuals are sorted from the smallest (extremes) to the largest (middle) one.

**Paratypes.** Six males, five females, and three juveniles. Table 2 shows field codes, localities, elevation, and geographic coordinates. Eleven specimens were collected in Colombia, Antioquia: Municipality of Jardín, Mesenia-Paramillo Nature Reserve (MPNR), between June 2018 and June 2020. Collected by Osman López, Ubiel Rendón, Jorge Jaramillo, and Luis A. Mazariegos. One from Colombia, Antioquia: Municipality of Andes, vereda Santa Rita, El Chaquiro. One from Colombia, Antioquia: Municipality of Jericó, vereda Quebradona, Finca La Aurora. The other from Colombia, Chocó: Municipality of Carmen de Atrato, vereda La Isla, Finca Gualandai.

**Diagnosis.** The species can be diagnosed combining the following characters: (1) 3–4 (usually 3) supraocular scales; (2) prefrontal scales present; (3) 11–28 temporal scales; (4) dorsal scales keeled; (5) 28–32 transverse rows of dorsal scales; (6) 17–23 transverse rows of ventral scales; (7) 31–45 scales around mid-body; (8) 3–5 rows of lateral scales; (9) lateral and medial ventral scales equal in size; (10) 0–2 femoral pores; (11) no sexual dimorphism in number of femoral pores; (12) labial scales similar in colour to other head scales, crossed by a curved pale lip line, best described as two oblique white lines converging in the eye; (13) ventral head colouration homogeneous; (14) cream or white vertebral stripe bordered by two black stripes, originating on the rostral scale, completely covering the dorsal region of the head and the vertebral region of the body, reaching only the anterior portion of the tail, with maximum width of four scales on the body; (15) lateral colour pattern brown, with a complete longitudinal line laterally, white and continuous from the posteroventral edge of the ear until the insertion of the hind limbs; with very few ocelli usually above the insertion of the forelimbs and absent between the limbs insertions, small; ocelli white in centre and surrounded by black scales and, beyond that, sometimes a few reddish scales; (16) venter strongly dimorphic in colouration between the sexes, uniformly pink to pale orange in females, sometimes with very few black speckles but no markings; usually glossy black and sometimes medium grey in males; (17) hemipenial body with 7–8 and 11–12 rows of spinulated flounces in the lateral columns of the sulcate and asulcate sides, respectively; (18) lateral columns of spinulated flounces connecting in the medial region of the asulcate side.

**Comparisons.** *Pholidobolus vertebralis* differs from *P. odinsae* sp. nov. (character states in parenthesis) in having the lateral ventral scales smaller than the medial ventrals (lateral and medial ventral scales equal in size). The other species from the north-western and central Colombian Andes (Fig. 7) differ from *P. odinsae* sp. nov. in ventral colouration of males: reddish brown in *P. paramuno*, and pink to orange in *P. argosi* sp. nov. and *P. celsiae* sp. nov. (black to grey). In addition, males of *P. argosi* sp. nov. lack prefrontal scales (present) and have two supraocular scales (3–4). Lastly, males of *P. celsiae* sp. nov. are larger in size (Table 3), between 60.7–68.6 mm (35.4–54.7 mm).

**Description of the holotype.** Adult male; snout-vent length 54.2 mm; tail length 50.0 mm; other body measurements in Table 4. Head scales smooth, juxtaposed, glossy, with small pits organized mainly around their margins. Rostral single, hexagonal, wider than high, dorsally in broad contact with the internasal and laterally in contact with the first supralabial and the nasal. Frontonasal single, wider than long, pentagonal, in contact with the nasal, loreal and prefrontals. Prefrontals two, wider laterally and narrower medially, in contact, touching the frontonasal, the frontal, the anterior supraocular, and the loreal. Frontal single, hexagonal, longer than wide, wider anteriorly, in contact with the prefrontals, the first supraocular and the frontoparietals. Frontoparietals pentagonal, longer than wide, narrower anteriorly, contacting one to three supraoculars laterally, and the parietal and interparietals posteriorly. Supraoculars four, the anterior most nearly as wide as long and the other two wider than long, decreasing in size antero-posteriorly, contacting the superciliaries laterally and the

parietal and uppermost postocular posteriorly. Interparietal single, heptagonal, longer than wide, narrower than the parietals and contacting laterally the parietals and posteriorly the postparietals. Parietals two, hexagonal, wider than long, slightly shorter and wider than the interparietal, contacting the temporals laterally and the postparietals posteriorly. Postparietals in two rows, three in the anterior row and two in the posterior row. Nasal single, rhomboidal, wider than high, contacting the first and second supralabials, the loreal and frenocular. Loreal single, quadrangular, over the frenocular, in contact with first superciliary dorsally. Frenocular single, quadrangular in contact with the first infraocular and the second and third supralabials. Superciliaries three, the anteriormost noticeable larger than the others, contacting the uppermost preocular. Suboculars five, contacting supralabials three to five. Postoculars two, increasing in size antero-posteriorly. Temporals 26, contacting supralabials five to eight. Supralabials eight and infralabials six. Mental single, pentagonal, wider than long, contacting the first infralabial and post-mental. Postmental single, pentagonal, contacting the first two infralabials and the anterior genials. Genials in three pairs, the anterior one quadrangular and the posterior two pentagonal. The anterior two in contact medially and the posterior one separated by postgenials; contacting infralabials two, three, and four. Pregulars two. Gular scales eight, wider than long, in two longitudinal rows; collar scales 17, decreasing in size laterally. Dorsal scales longer than wide, hexagonal, keeled, imbricate, arranged in 30 transverse rows. Longitudinal rows of dorsal scales 24, the first two rows in each side weakly keeled and rounded. Lateral row scales at mid-body one, smooth, at least half the size of adjacent scales. Scales around mid-body 45. Longitudinal rows of ventrals six, quadrangular. Transverse rows of ventrals 20. Cloacal plates in two rows of two quadrangular scales each, the posterior row larger than the anterior one, in contact with two small scales laterally. Tail scales arranged in 62 rings, hexagonal and keeled dorsally, quadrangular and smooth ventrally.

Limbs pentadactyl with clawed fingers. Dorsal brachial and antebrachial scales lanceolate to polygonal, longer than wide, imbricate and smooth. Ventral brachial and antebrachial scales lanceolate to polygonal, almost as long as wide, juxtaposed, much smaller than the dorsal ones. Dorsal hand scales hexagonal, wider but shorter than the dorsal antebrachial scales. Finger length formula  $IV = III > II > V > I$ . Supradigital scales quadrangular, imbricate and longer than wide. Palmar scales polygonal, juxtaposed and small. Subdigital lamellae domelike with a quadrangular base, and often divided longitudinally, with six on finger I, 8 on II, 13 on III, 15 on IV, and 7 on V. Thigh scales on the dorsal, anterior and ventral surfaces lanceolate to rhomboidal, longer than wide, those in the dorsal surface smooth and the others smooth and imbricate. Thigh scales on the posterior surface of the legs rounded, smooth, juxtaposed and much smaller than those of the anterior and dorsal surfaces. Two femoral pores per leg; preanal pores absent. Anterior and ventral crus scales polygonal and smooth. Lateral and posterior crus scales rounded, small and subimbricate. Toe length formula  $IV > III > V > II > I$ . Supradigital scales quadrangular, imbricate and longer than wide. Plantar scales polygonal, juxtaposed and small. Subdigital lamellae domelike with a quadrangular base, and often divided longitudinally, with five on Toe I, 9 on II, 13 on III, 15 on IV, and 7 on V.

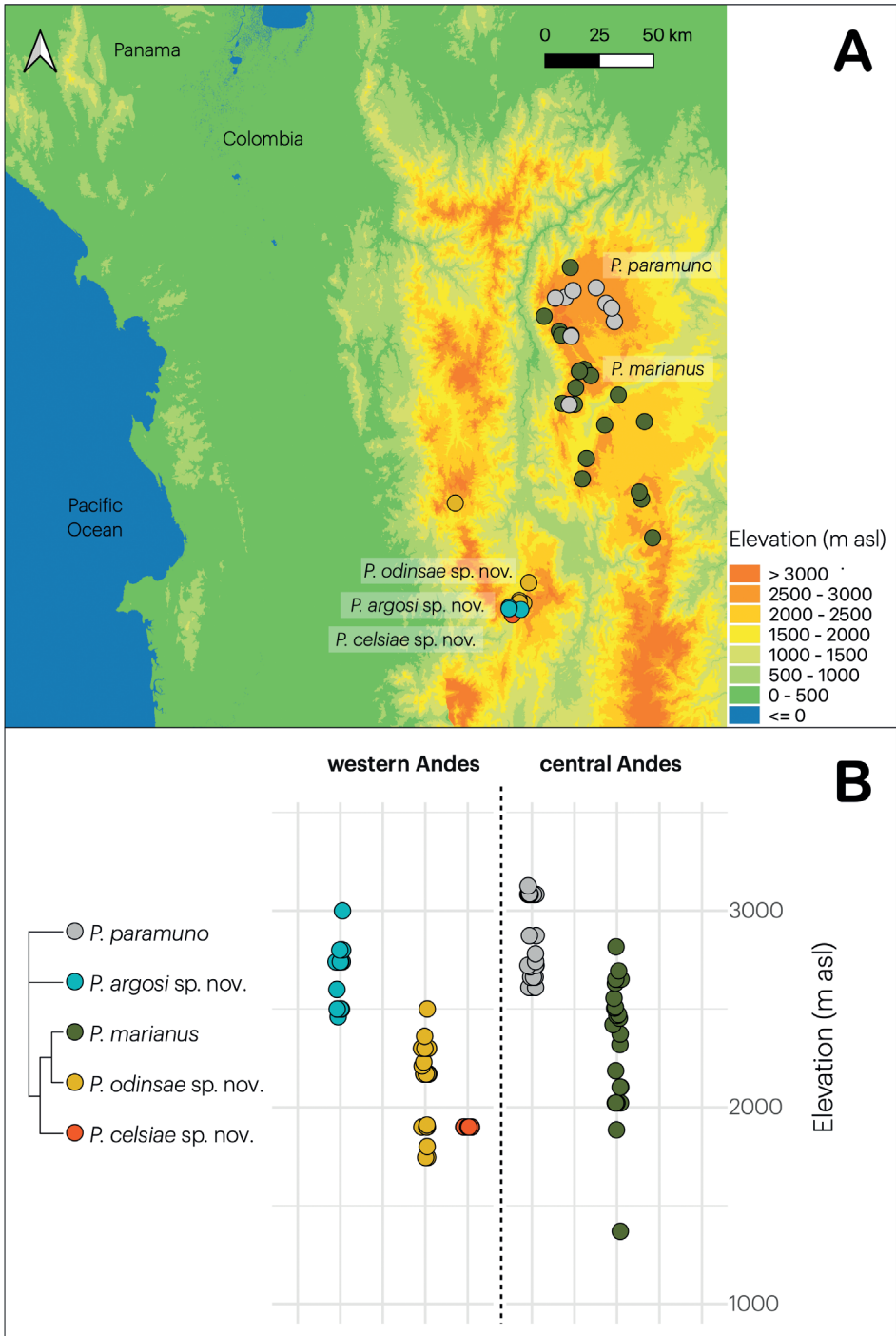


**Figure 7.** Geographic and altitudinal distribution. Geographic (A) and altitudinal (B) distribution of five species of *Pholidobolus* lizards across the north of the Western and Central Colombian Andes. The cladogram summarises the recovered phylogenetic relationship among them (Fig. 1). Each dot represents an individual deposited in the MHUA-R collection at the Universidad de Antioquia.

**Colouration.** In life, dorsally brown or pale brown, bisected by a mid-dorsal (i.e. vertebral) white stripe, extending from the head to the mid tail; vertebral stripe bordered with darker, usually dark brown or black, stripes; on the head, the pale stripe extends from the first supralabial to the shoulder dorsally reaching the rostral scale, and laterally including the frontonasal, prefrontal, frontal, frontoparietal, interparietal, and postparietal scales; sides of neck, flanks, and limbs predominantly brown, usually with less than five, small and white ocelli, bordered by a black stripe, and predominantly on the shoulders; white or cream lateral line from the supralabials, passing through the shoulder and extending continuously up to the insertion of the limbs, but not towards the tail; very few scattered red scales, more common around the shoulder ocelli; throat cream to pink in females, but grey to black in males; chest, belly and base of the tail pink to orange in adult females, but grey to black in males, with bare or no patterning in all cases (Figs 1, 3, 6). In preservative, brown surfaces become paler, the dorsal and lateral stripes become white, the orange chest, belly and tail of females fade to white or very pale pink, and the black chest, belly and tail of males fade into dark grey.

**Etymology.** The species epithet is dedicated to the company Odinsa, for their decisive involvement in the Cartama Conservation Project, in southwestern Antioquia, aimed at restoring ecosystem services by regenerating the Andean forest along the Quebrada San Antonio basin. Together with other stakeholders, the initiative planted more than 320000 native trees during 2019–2020 alone.

**Distribution, ecology, and conservation.** The species is currently known from forest edges, and open areas including pastures, crops, and around human buildings. Most specimens were seen and found amongst grass or leaf litter even hundreds of metres away from the nearest forests. They appeared clearly heliothermic: within minutes after the sun appeared, they came out of their refuges, remain exposed, and extended their ribs increasing the dorsal surface available for sun basking. Under sunny conditions, the species seems to be abundant at the known localities. Its distribution seems not to be patchy, and it is known from more than five locations. Although they encompass less than 500 km<sup>2</sup> (Fig. 7), the actual distribution could arguably exceed this threshold area, given the species adaptability to disturbed habitats. Therefore, we suggest listing the new species as Data Deficient, DD (IUCN 2012), until proper information is collected to evaluate the species conservation status. Many individuals showed signs of a regenerated tail.

## Discussion

This study provides unambiguous phylogenetic, genetic, morphological, and geographic evidence of independent evolutionary history in four lineages of *Pholidobolus* lizards, formerly assigned to *P. vertebralis*. Based on the available evidence, their evolution would have occurred at mid and high elevation Andes, and led to the origin of several geographically proximate species yet occupying a small area each. The only exception would be *P. vertebralis*, whose status as a single species is thus challenged by at least two lines of evidence.

First, most *Pholidobolus* species occupy small areas. The genus currently comprises 13 species, 11 of which are considered endemic: five are known from a single locality

and four others from areas below 7000 km<sup>2</sup>, mostly in Ecuador. To the best of our knowledge, the three new species described herein, and the single species resurrected, exhibit small distribution ranges. In contrast, *P. vertebralis* is the only taxon believed to occur throughout 110000 km<sup>2</sup> and three countries: Ecuador, Colombia and Venezuela (Doan and Cusi 2014). In Ecuador, a single study including molecular data added four additional species to the genus with small distribution each (Parra et al. 2020); the same is true for the four species addressed in this study, and for a single species in a previous one (Hurtado-Gómez et al. 2018). Altogether, the evidence suggests that the geographic distribution of the putative *P. vertebralis* is extremely atypical, if not an artifact created by the lack of genetic sampling and associated research on the entire distribution range.

Second, the genus distribution appears to exclude low elevation areas. The available evidence supports that most *Pholidobolus* species occur above 1000 m elevation, sometimes on hilltops, but mostly confined to one side of the Andes or the other (Uzzell 1973; Parra et al. 2020). Throughout our study area, two species were indeed found on the hilltops, and two out of three were confined to one of the slopes of the Colombian Central and Western Andes, but no specimens were found from low elevation areas. In contrast, *P. vertebralis* is reported in Colombia throughout the three Andean chains, which are indeed separated by two low elevation areas: the Magdalena and the Cauca river valleys. The species distribution is thus highly atypical, because it includes the opposite sides of likely geographic barriers, the low elevation valleys, and because its area is much larger than for any other species in the genus. Such atypical distribution may instead reflect the existence of several valid species currently assigned to *P. vertebralis*.

If our argument holds, we anticipate that new species will be recognised once enough molecular and morphological data are collected throughout the distribution of *P. vertebralis sensu lato*. We also suggest revising published decisions on the validity of species previously regarded as synonyms of *P. vertebralis*. For instance, the main argument to synonymise *Prionodactylus* [*Pholidobolus*] *palmeri* and *P. marianus* was that the holotype “falls within my concept of *P. vertebralis*” (Uzzell 1973). Although the author reported quantitative morphological data, they were not explicitly invoked to support this decision. Likewise, the species *Euspondylus* [*Pholidobolus*] *ampuedae* [*ampuedai*] was synonymised with *P. vertebralis* yet recognising that “I was unable to examine any specimens of *Euspondylus* [*Pholidobolus*] *ampuedae* [*ampuedai*]” (Uzzell 1973), and rooting this decision on the shape of a pale lip line. The species status was later revalidated as *Prionodactylus* [*Pholidobolus*] *ampuedai* by LaMarca and García-Pérez (1990), but again synonymised with *Cercosaura* [*Pholidobolus*] *vertebralis* by Doan and Cusi (2014). This formerly acknowledged species was described from Villa Páez, State of Táchira, Venezuela, near the border with Colombia; it was later thought to be distributed along the Colombian Eastern Andes (Cordillera Oriental), which would render its distribution disjunct with the other Colombian species we address here (Fig. 7A). Behind those decisions was the acknowledgement of large morphological variation within the specimens assigned by then to *P. vertebralis*. Such variation is compatible with a polyphyletic nature of the taxon. To test this hypothesis, a modern analysis of morphological variation and the collection of molecular data are both strictly required.

The findings and arguments exposed here have relevant implications not only for the systematics of the group, but also for the recognition of appropriate conservation

units. One of the foremost tasks in conservation is the delineation of biologically meaningful units, which implies the recognition of ecologically discrete and evolutionarily significant lineages. Particularly in the tropics, the task is hampered by the paucity of information on the genotype, phenotype, and geographic distribution of most taxa, which is further aggravated by the contrast between the extremely high level of species richness and the meagre resources devoted to analysing it. During centuries, species recognition was mainly based on detailed written accounts of species external morphology. Now, much more consideration is needed to examine the extent of variation in external morphology that is merely attributable to phylogenetic signal. Morphology is often evolutionarily conserved, due to the adaptive value of the phenotype. Dorsal colouration is cryptic and arguably conserved in *Pholidobolus* species; ventral colouration instead probably plays a crucial role as mate recognition signal and could therefore bear important and overlooked information for species delimitation. The adoption of integrative approaches involving systematics and other branches of biology will probably contribute to untangling true diversity levels, by ascertaining the number and distribution of evolutionarily independent lineages. This information is badly needed to delimit biologically meaningful conservation units, which could allow sound, scientifically based, decisions on conservation actions and priorities.

## Acknowledgements

We are deeply grateful to Osman López, Ubiel Rendón, and Jorge Jaramillo for invaluable help in collecting the lizards. Field work was supported by Bioconservancy.org, and molecular sequencing and analyses by the Colombian Institute for Science and Technology (Colciencias) as well as the Instituto de Biología, Universidad de Antioquia, Colombia.

## References

- Arévalo E, Davis SK, Sites Jr JW (1994) Mitochondrial DNA sequence divergence and phylogenetic relationships among eight chromosome races of the *Sceloporus grammicus* complex (Phrynosomatidae) in Central Mexico. *Systematic Biology* 43(3): 387–418. <https://doi.org/10.1093/sysbio/43.3.387>
- Avila-Pires TCS (1995) Lizards of the Brazilian Amazon. *Zoologische Verhandelingen*. Leiden, 706 pp. <https://repository.naturalis.nl/pub/317788>
- de Queiroz K (2005) Ernst Mayr and the modern concept of species. *Proceedings of the National Academy of Sciences of the United States of America* 102(suppl\_1): 6600–6607. <https://doi.org/10.1073/pnas.0502030102>
- de Queiroz K (2007) Species concepts and species delimitation. *Systematic Biology* 56(6): 879–886. <https://doi.org/10.1080/10635150701701083>
- Doan TM, Cusi JC (2014) Geographic distribution of *Cercosaura vertebralis* O'Shaughnessy, 1879 (Reptilia: Squamata: Gymnophthalmidae) and the status of *Cercosaura ampuedai* (Lancini, 1968). *Check List* 10(5): 1195–1200. <https://doi.org/10.15560/10.5.1195>

- Donegan T, Avendaño-C JE, Huertas B, Flórez P (2009) Avifauna de San Pedro de los Milagros, Antioquia: Una comparación entre colecciones antiguas y evaluaciones rápidas. *Boletín Científico Museo de Historia Natural Universidad de Caldas* 13: 63–72.
- Dowling HG, Savage JM (1960) A guide to the snake hemipenis: A survey of basic structure and systematic characteristics. *Zoologica [Scientific Contributions of the New York Zoological Society]* 45(2): 17–28. <https://doi.org/10.5962/p.203350>
- Harris DM (1994) Review of the teiid lizard genus *Ptychoglossus*. *Herpetological Monograph* 8: 226–275. <https://doi.org/10.2307/1467082>
- Hernández-Ruz EJ (2005) Notas taxonómicas y biológicas de *Cercosaura ampuedai* (Lancini, 1968) en la vertiente oriental de la Cordillera Oriental de Colombia. *Publicações Avulsas do Instituto Pau Brasil de Historia Natural [São Paulo]* 8–9: 1–14.
- Hernández-Ruz EJ, Bernal-González CA (2011) Variación morfológica en *Cercosaura vertebralis* (Sauria: Gymnophthalmidae) en Colombia. *Ingenierías & Amazonia* 4: 48–57.
- Hoang DT, Chernomor O, von Haeseler A, Minh BQ, Vinh LS (2018) UFBoot2: Improving the ultrafast bootstrap approximation. *Molecular Biology and Evolution* 35(2): 518–522. <https://doi.org/10.1093/molbev/msx281>
- Hurtado-Gómez JP, Arredondo JC, Nunes PMS, Daza JM (2018) A new species of *Pholidobolus* (Squamata: Gymnophthalmidae) from the Paramo ecosystem in the northern Andes of Colombia. *South American Journal of Herpetology* 13(3): 271–18. <https://doi.org/10.2994/SAJH-D-15-00014.1>
- IUCN (2012) IUCN Red List Categories and Criteria: Version 3.1. (2<sup>nd</sup> edn.). IUCN, Gland/ Cambridge.
- Jombart T (2008) adegenet: A R package for the multivariate analysis of genetic markers. *Bioinformatics* 24(11): 1403–1405. <https://doi.org/10.1093/bioinformatics/btn129>
- Jombart T, Ahmed I (2011) adegenet 1.3-1: New tools for the analysis of genome-wide SNP data. *Bioinformatics* 27(21): 3070–3071. <https://doi.org/10.1093/bioinformatics/btr521>
- Jombart T, Devillard S, Balloux F (2010) Discriminant analysis of principal components: A new method for the analysis of genetically structured populations. *BMC Genetics* 11(1): 94–94. <https://doi.org/10.1186/1471-2156-11-94>
- Kalyaanamoorthy S, Minh BQ, Wong TK, von Haeseler A, Jermin LS (2017) ModelFinder: Fast model selection for accurate phylogenetic estimates. *Nature Methods* 14(6): 587–589. <https://doi.org/10.1038/nmeth.4285>
- Katoh K, Standley DM (2013) MAFFT Multiple Sequence Alignment Software Version 7: Improvements in performance and usability. *Molecular Biology and Evolution* 30(4): 772–780. <https://doi.org/10.1093/molbev/mst010>
- Kizirian DA (1996) A review of Ecuadorian *Proctoporus* (Squamata: Gymnophthalmidae) with descriptions of nine new species. *Herpetological Monograph* 10: 85–155. <https://doi.org/10.2307/1466981>
- Kocher TD, Thomas WK, Meyer A, Edwards SV, Pábo S, Villablanca FX, Wilson AC (1989) Dynamics of mitochondrial DNA evolution in animals: Amplification and sequencing with conserved primers. *Proceedings of the National Academy of Sciences of the United States of America* 86(16): 6196–6200. <https://doi.org/10.1073/pnas.86.16.6196>
- Krebs JR, Davies NB (1993) *An Introduction to Behavioural Ecology*. Blackwell Science Ltd, Victoria.

- Kumar S, Stecher G, Tamura K (2016) MEGA7: Molecular evolutionary genetics analysis version 7.0 for bigger datasets. *Molecular Biology and Evolution* 33(7): 1870–1874. <https://doi.org/10.1093/molbev/msw054>
- LaMarca E, García-Pérez JE (1990) *Prionodactylus ampuedai* (Sauria: Teiidae): a new lizard record for Colombia, with taxonomic comments on the species. *Bulletin of the Maryland Herpetological Society* 26: 111–115.
- Minh BQ, Schmidt HA, Chernomor O, Schrempf D, Woodhams MD, von Haeseler A, Lanfear R (2020) IQ-TREE 2: New models and efficient methods for phylogenetic inference in the genomic era. *Molecular Biology and Evolution* 37(5): 1530–1534. <https://doi.org/10.1093/molbev/msaa015>
- Montanucci RR (1973) Systematics and evolution of the Andean lizard genus *Pholidobolus* (Sauria: Teiidae). *Miscellaneous Publication* 59: 1–52. [University of Kansas Natural History Museum]
- O'Shaughnessy A (1879) Descriptions of new species of lizards in the collection of the British Museum. *Annals & Magazine of Natural History* 4(22): 295–303. <https://doi.org/10.1080/00222937908679832>
- Padial JM, Miralles A, De la Riva I, Vences M (2010) The integrative future of taxonomy. *Frontiers in Zoology* 7: 1–16. <https://doi.org/10.1186/1742-9994-7-16>
- Parra V, Torres-Carvajal O, Nunes PMS (2020) Systematics of *Pholidobolus* lizards (Squamata, Gymnophthalmidae) from southern Ecuador, with descriptions of four new species. *ZooKeys* 954: 109–156. <https://doi.org/10.3897/zookeys.954.50667>
- Ruthven AG (1921) Description of an apparently new lizard from Colombia. *Occasional Papers of the Museum of Zoology, University of Michigan* 103: 1–4.
- Ruxton GD, Sherratt TN, Speed M (2004) *Avoiding Attack*. OUP Oxford. <https://doi.org/10.1093/acprof:oso/9780198528609.001.0001>
- Ruxton GD, Franks DW, Balogh ACV, Leimar O (2008) Evolutionary implications of the form of predator generalization for aposematic signals and mimicry in prey. *Evolution* 62(11): 2913–2921. <https://doi.org/10.1111/j.1558-5646.2008.00485.x>
- Saint KM, Austin CC, Donnellan SC, Hutchinson MN (1998) C-mos, a nuclear marker useful for squamate phylogenetic analysis. *Molecular Phylogenetics and Evolution* 10(2): 259–263. <https://doi.org/10.1006/mpev.1998.0515>
- Santos JC, Coloma LA, Cannatella DC (2003) Multiple, recurring origins of aposematism and diet specialization in poison frogs. *Proceedings of the National Academy of Sciences of the United States of America* 100(22): 12792–12797. <https://doi.org/10.1073/pnas.2133521100>
- Savage JM (1997) On terminology for the description of the hemipenes of squamate reptiles. *The Herpetological Journal* 7: 23–25.
- Schindelin J, Rueden CT, Hiner MC, Eliceiri KW (2015) The ImageJ ecosystem: An open platform for biomedical image analysis. *Molecular Reproduction and Development* 82(7–8): 518–529. <https://doi.org/10.1002/mrd.22489>
- Sites-Jr JW, Marshall JC (2004) Operational criteria for delimiting species. *Annual Review of Ecology, Evolution, and Systematics* 35(1): 199–227. <https://doi.org/10.1146/annurev.ecolsys.35.112202.130128>
- Uzzell T (1973) A revision of the genus *Prionodactylus* with a new genus for *P. leucostictus* and notes on the genus *Euspondylus* (Sauria, Teiidae). *Postilla* 159: 1–67. <https://doi.org/10.5962/bhl.part.11535>

- Venegas PJ, Echevarría LY, Lobos SE, Nunes PMS, Torres-Carvajal O (2016) A new species of Andean microteiid lizard (Gymnophthalmidae: Cercosaurinae: *Pholidobolus*) from Peru, with comments on *P. vertebralis*. *Amphibian & Reptile Conservation* 10: e121.
- Weller H, Schwartz ST, Karan E, Lord NP (2021) Recolorize: A flexible R package for color classification. *Integrative and Comparative Biology* 61: E969–E970. <https://cran.microsoft.com/snapshot/2021-12-31/web/packages/recolorize/recolorize.pdf>

## Supplementary material 1

### Linked data table for primary biodiversity data

Authors: Adolfo Amézquita, Luis A. Mazariegos-H, Santiago Cañaverl, Catalina Orejuela, Leidy Alejandra Barragán-Contreras, Juan M. Daza

Data type: occurrences

Explanation note: Data types and sequenced specimens of *Anadia*, *Macropholidus*, and *Pholidobolus* lizards (Gymnophthalmidae) used to build the phylogenetic hypothesis in this study.

Copyright notice: This dataset is made available under the Open Database License (<http://opendatacommons.org/licenses/odbl/1.0/>). The Open Database License (ODbL) is a license agreement intended to allow users to freely share, modify, and use this Dataset while maintaining this same freedom for others, provided that the original source and author(s) are credited.

Link: <https://doi.org/10.3897/zookeys.1141.94774.suppl1>

## Supplementary material 2

### Detailed phylogenetic tree

Authors: Adolfo Amézquita, Luis A. Mazariegos-H, Santiago Cañaverl, Catalina Orejuela, Leidy Alejandra Barragán-Contreras, Juan M. Daza

Data type: phylogenetic

Explanation note: Phylogenetic hypothesis on the relationships between studied lizards. Each terminal represents an included individual.

Copyright notice: This dataset is made available under the Open Database License (<http://opendatacommons.org/licenses/odbl/1.0/>). The Open Database License (ODbL) is a license agreement intended to allow users to freely share, modify, and use this Dataset while maintaining this same freedom for others, provided that the original source and author(s) are credited.

Link: <https://doi.org/10.3897/zookeys.1141.94774.suppl2>

# Four new species of the genus *Andixius* Emeljanov & Hayashi (Hemiptera, Fulgoromorpha, Cixiidae) from China

Xiao-Ya Wang<sup>1,2</sup>, Yan Zhi<sup>3</sup>, Lin Yang<sup>1,2</sup>, Xiang-Sheng Chen<sup>1,2</sup>

**1** Institute of Entomology, Guizhou University, Guiyang, Guizhou 550025, China **2** The Provincial Special Key Laboratory for Development and Utilization of Insect Resources of Guizhou, Guizhou University, Guiyang, Guizhou, 550025, China **3** Laboratory Animal Center, Guizhou Medical University, Guiyang, Guizhou 550025, China

Corresponding author: Xiang-Sheng Chen ([chenxs3218@163.com](mailto:chenxs3218@163.com))

---

Academic editor: Pavel Stoev | Received 30 March 2022 | Accepted 13 December 2022 | Published 19 January 2023

---

<https://zoobank.org/DDB92C86-E5D6-42B8-9469-A252DC18B9B5>

---

**Citation:** Wang X-Y, Zhi Y, Yang L, Chen X-S (2023) Four new species of the genus *Andixius* Emeljanov & Hayashi (Hemiptera, Fulgoromorpha, Cixiidae) from China. ZooKeys 1141: 149–168. <https://doi.org/10.3897/zookeys.1141.84564>

---

## Abstract

Four new species of the genus *Andixius* Emeljanov & Hayashi, 2007 are described and illustrated from China. These are *A. flagellihamus* Wang & Chen, **sp. nov.**, *A. gracilispinus* Wang & Chen, **sp. nov.**, *A. productus* Wang & Chen, **sp. nov.** and *A. truncatus* Wang & Chen, **sp. nov.** Photographs of the new species and an identification key to all *Andixius* species are provided.

## Keywords

Andini, Fulgoroidea, morphology, taxonomy

## Introduction

The planthopper tribe Andini (Hemiptera, Auchenorrhyncha, Fulgoromorpha, Cixiidae, Cixiinae) consists of 129 species in three genera worldwide (Bourgoin 2022; Wang et al. 2022). Within the tribe Andini, *Andixius* is a small genus established by Emeljanov and Hayashi (2007) with two species, *A. nupta* Emeljanov & Hayashi, 2007 (as its type species) and *A. venustus* (Tsaour & Hsu, 1991) (previously placed in

the genus *Brixia* Stål, 1856). Zhi et al. (2018) added two more species, *A. longispinus* and *A. trifurcus*, to the genus. Later, Wang et al. (2020) described two new species: *A. cultratus* and *A. lingulatus*.

Recent study of some Chinese specimens has found four new species, *A. flagellihamus* Wang & Chen, sp. nov., *A. gracilispinus* Wang & Chen, sp. nov., *A. productus* Wang & Chen, sp. nov. and *A. truncatus* Wang & Chen, sp. nov., which are described here. Hence, the number of *Andixius* species is now 10, with nine species occurring in China.

## Materials and methods

The morphological terminology follows Bourgoïn (1987) and Bourgoïn et al. (2015). The morphological terminology of female genitalia follows Bourgoïn (1993). Dry specimens were used for the descriptions and illustrations. Body length was measured from the apex of the vertex to the tip of the forewing; vertex length was measured at the median length of the vertex (from the apical transverse carina to the tip of the basal emargination). Observations and drawings of external morphology were made with the aid of a Leica MZ 12.5 stereomicroscope. Photographs of the types were taken with the Keyence VHX-1000 system. Illustrations were scanned with a CanoScan LiDE 200 scanner and imported into Adobe Photoshop CS7 for labelling and plate composition. The dissected male genitalia are preserved in glycerine in small plastic tubes pinned together with the specimens.

The type specimens are deposited in the Institute of Entomology, Guizhou University, Guiyang, Guizhou Province, China (IEGU).

## Taxonomy

### *Andixius* Emeljanov & Hayashi, 2007

*Andixius* Emeljanov & Hayashi, 2007: 127; Zhi et al. 2018: 56; Wang et al. 2020: 441.

**Type species.** *Andixius nupta* Emeljanov & Hayashi, 2007, original designation.

**Diagnosis.** The distinctive characters proposed by Zhi et al. (2018) are modified as follows: head including eyes distinctly narrower than pronotum. Lateral carinae of frons and postclypeus foliate. Rostrum long, extended considerably beyond hind coxae. Forewings without trifid branching of ScP+R and MP near basal cell, ScP+R (ScP+RA and RP) forming a short common stalk. Legs simple, fore coxae without angular apical lobe, hind tibia with several small lateral spines.

**Distribution.** China (Guangdong, Guangxi, Taiwan, Xizang, Yunnan), Japan (Ryukyu Islands).

Checklist and distributions of species of *Andixius* Emeljanov & Hayashi

- A. cultratus* Wang, Zhi & Chen, 2020; China (Guangdong).  
*A. flagellihamus* Wang & Chen, sp. nov.; China (Xizang).  
*A. gracilispinus* Wang & Chen, sp. nov.; China (Xizang).  
*A. lingulatus* Wang, Zhi & Chen, 2020; China (Guangxi).  
*A. longispinus* Zhi & Chen, 2018; China (Yunnan).  
*A. nupta* Emeljanov & Hayashi, 2007; Japan (Ryukyus).  
*A. productus* Wang & Chen, sp. nov.; China (Xizang).  
*A. trifurcus* Zhi & Chen, 2018; China (Yunnan).  
*A. truncatus* Wang & Chen, sp. nov.; (Guangxi).  
*A. venustus* (Tsaour & Hsu, 1991); China (Taiwan).

Key to species of *Andixius* (males) Emeljanov & Hayashi

- 1 Anal segment symmetrical dorsally ..... 2  
 – Anal segment asymmetrical dorsally ..... 7  
 2 Apical right side of periandrium with a large linguiform laminal process (Wang et al. 2020: figs 31–34) ..... ***A. lingulatus***  
 – Apical right side of periandrium without linguiform laminal process ..... 3  
 3 Ventral margin of periandrium with a projection, of which basal 1/3 longitudinally and 2/3 horizontally extended, endosoma with two simple processes, not bifurcate (Zhi et al. 2018: figs 13–16) ..... ***A. longispinus***  
 – Periandrium without above spinose process ..... 4  
 4 Periandrium with an expanded semi-enclosed structure around the left side and ventral margin of periandrium (Zhi et al. 2018: figs 25–28) ..... ***A. trifurcus***  
 – Periandrium without expanded semi-enclosed structure ..... 5  
 5 Left side of periandrium with a bifurcate process (Emeljanov and Hayashi 2007: figs 11–13) ..... ***A. nupta***  
 – Left side of periandrium without process or process on left side of periandrium not bifurcated ..... 6  
 6 Dorsal margin of endosoma with a large spinose process (Wang et al. 2020: figs 10–13) ..... ***A. cultratus***  
 – Right side of endosoma with a bifurcated production (Tsaour et al. 1991: fig. 33D–F) ..... ***A. venustus***  
 7 Endosoma of aedeagus with a hooked spinose process apically (Fig. 3F) ..... ***A. flagellihamus* sp. nov.**  
 – Endosoma of aedeagus without above spinose process ..... 8  
 8 Middle dorsal margin of periandrium with a slightly stout and long spinose process (Fig. 7E–H) ..... ***A. productus* sp. nov.**  
 – Middle dorsal margin of periandrium without spinose process ..... 9

- 9 Left apical side of ventral margin of periandrium with a triangular laminal process, of which middle right side concaved heavily, forming two large processes (Fig. 5F).....*A. gracilispinus* sp. nov.
- Ventral margin of periandrium with a broad laminal process, apex slightly truncate (Fig. 10E, F) .....*A. truncatus* sp. nov.

***Andixius flagellihamus* Wang & Chen, sp. nov.**

<https://zoobank.org/5BB7E534-9C4C-4507-8FA5-CA5C1D3D5646>

Figs 1A, B, 2A–C, 3A–H

**Type material.** *Holotype*: ♂, CHINA: Xizang Province, Medog County, Beibeng Town (29.2483°N, 95.1819°E), 15 August 2020, Yongjin Sui leg.; *Paratypes*: ♂, same data as holotype.

**Description.** Body length: male 6.65–7.00 mm ( $n = 2$ ).

**Coloration.** General color light yellowish brown (Figs 1A, B, 2A, B). Eyes black-brown, ocelli faint yellowish brown, semitranslucent. Lateral margin of frons yellowish brown, behind eyes with two brown spots. Antenna, vertex, face, and rostrum generally yellowish brown. Pronotum and mesonotum yellowish brown. Forewing semitranslucent, with veins and stigma yellowish brown, tubercles black-brown; costal vein, slightly in front of and behind stigma and near claval fork with an irregular puce spot. Hind tibiae yellowish brown. Ventral abdomen brown.

**Head and thorax.** Vertex (Figs 1A, 2A) 1.14 times longer than wide; anterior and posterior margin slightly recessed, lateral carinae developed, median carina absent. Frons (Fig. 2B) claviform, 2.58 times as long as wide. Pronotum (Figs 1A, 2A) as long as vertex. Mesonotum 1.40 times longer than pronotum and vertex combined, lateral carinae curved outwards. Forewing (Figs 1B, 2C) 2.28 times longer than wide, with 12 apical cells and six subapical cells; RP 3 branches, MP with five terminals: MP<sub>11</sub>, MP<sub>12</sub>, MP<sub>2</sub>, MP<sub>3</sub>, and MP<sub>4</sub>, fork MP<sub>1</sub>+MP<sub>2</sub> basad of fork MP<sub>3</sub>+MP<sub>4</sub>. Hind tibia with three lateral spines; chaetotaxy of hind tarsi 6/7.

**Male genitalia.** Pygofer (Fig. 3A, C) symmetrical. Medioventral process rounded protruding in ventral view. Anal segment (Fig. 3A, D) asymmetrical, apical margin expanded downwards in lateral view; 2.28 times longer than wide in dorsal view; anal style strap-shaped, not beyond anal segment. Gonostyli (Fig. 3B, C) symmetrical ventrally; in inner lateral view, base slender, apex enlarged. Aedeagus (Fig. 3E–H) with five processes. In left side view, basal ventral margin of periandrium protruding; in right side view, base of periandrium with a U-shaped spinose process, directed cephalad; in ventral view, near base of periandrium with a long spinose process, apex curved upwards, forming a hooked process, directed cephalad. Endosoma somewhat long, apex with a hooked spinose process.

**Distribution.** China (Xizang) (Fig. 12).

**Etymology.** The specific name is derived from the Latin adjective *flagellihamus*, referring to the 1-hooked spinose process arising from the apex of the endosoma.

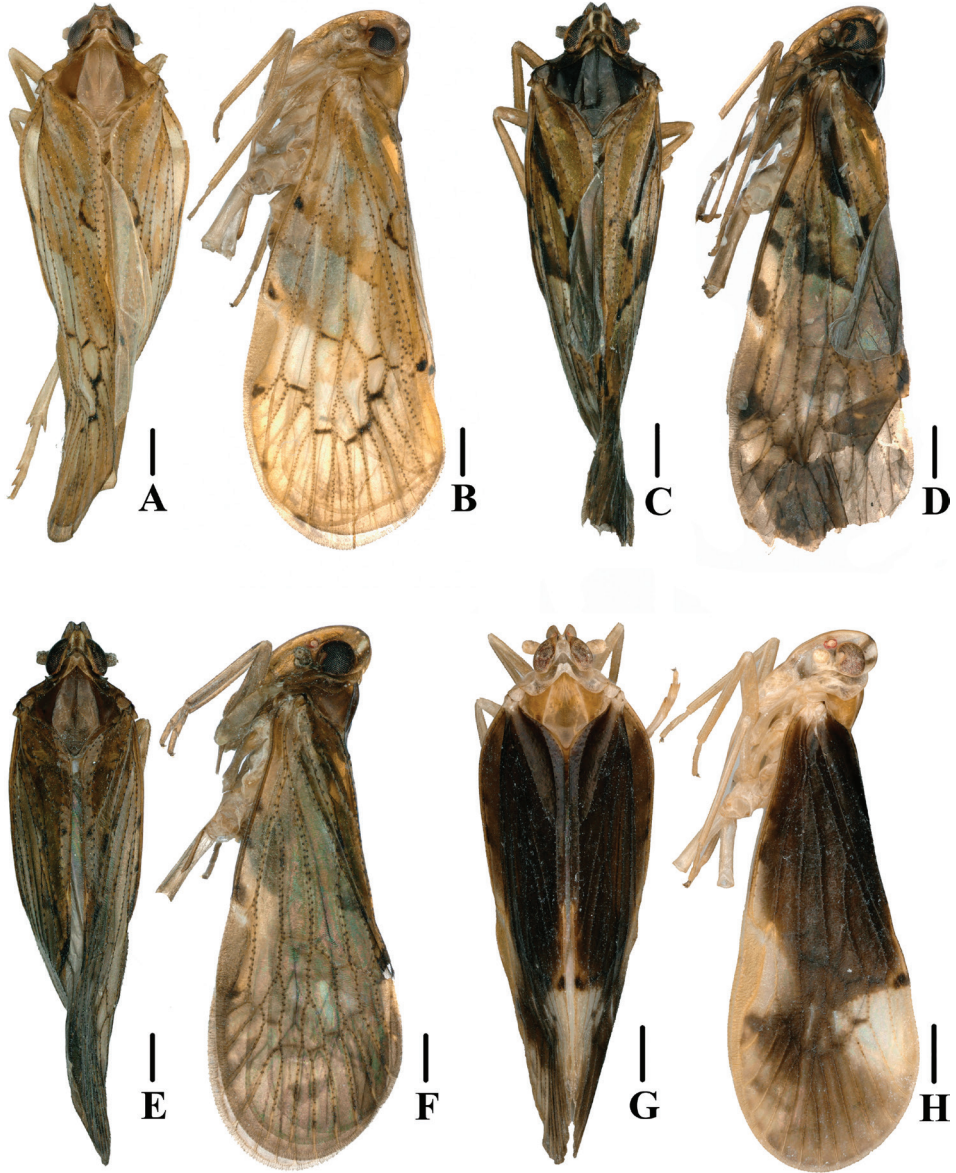


**Figure 1.** New species of *Andixius* **A, B** *A. flagellibamus* sp. nov., male **A** dorsal view **B** lateral view **C, D** *A. gracilispinus* sp. nov., male **C** dorsal view **D** lateral view **E, F** *A. productus* sp. nov., male **E** dorsal view **F** lateral view **G, H** *A. truncatus* sp. nov., male **G** dorsal view **H** lateral view. Scale bars: 0.5 mm.

**Remarks.** This species can be distinguished from the other species of the genus by the following characters: basal right side of periandrium with a U-shaped spinose process; basal ventral margin of periandrium with a long spinose process, apex curved upwards, forming a hooked process; apex of endosoma with a hooked spinose process.

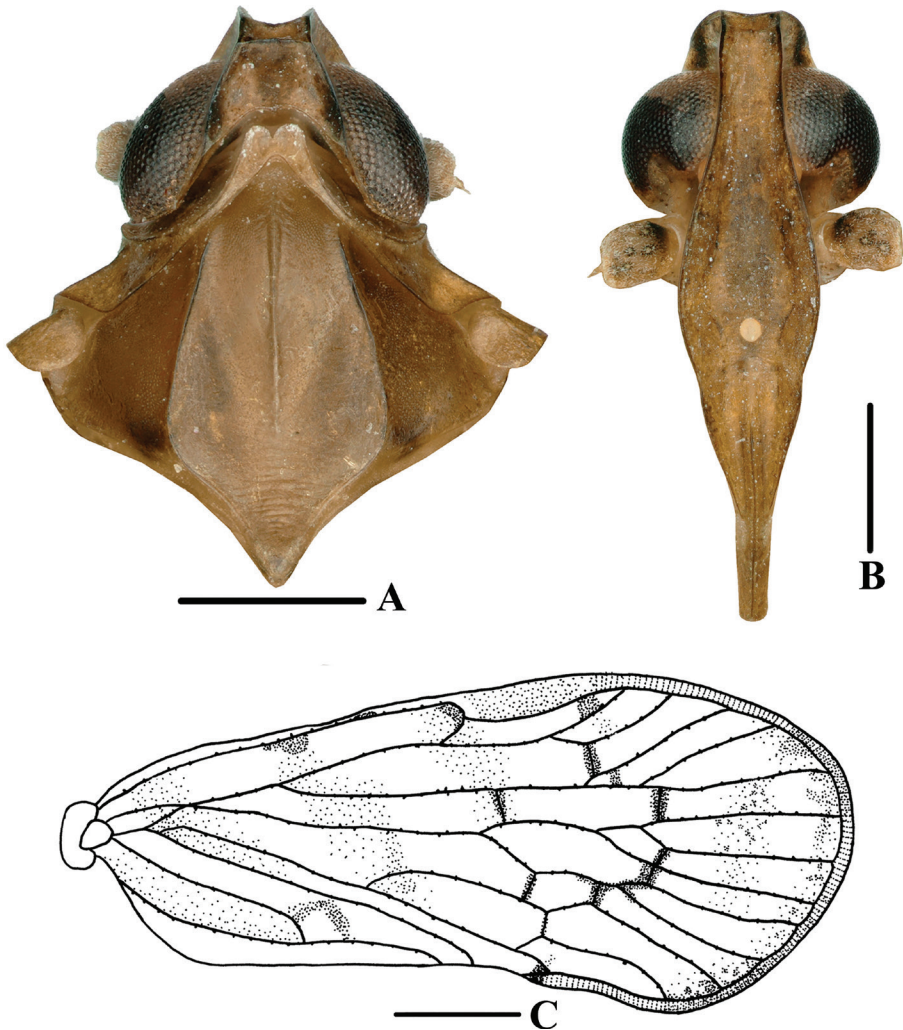


**Figure 2.** *Andixius flagellibamus* sp. nov., male **A** head and thorax, dorsal view **B** face, ventral view **C** forewing. Scale bars: 0.5 mm (**A**, **B**); 1.0 mm (**C**).

***Andixius gracilispinus* Wang & Chen, sp. nov.**

<https://zoobank.org/4CF579B2-3F5B-4926-99D8-59E7F8E16E85>

Figs 1C, D, 4A–C, 5A–H

**Type material.** *Holotype*: ♂, CHINA: Xizang Province, Bomê County, Yigong Town, Tongmai Village (30.1071°N, 95.0867°E), 18–20 August 2020, Yongjin Sui leg.;

*Paratypes*: ♂, same data as holotype.

**Description.** Body length: male 5.63–5.82 mm ( $n = 2$ ).

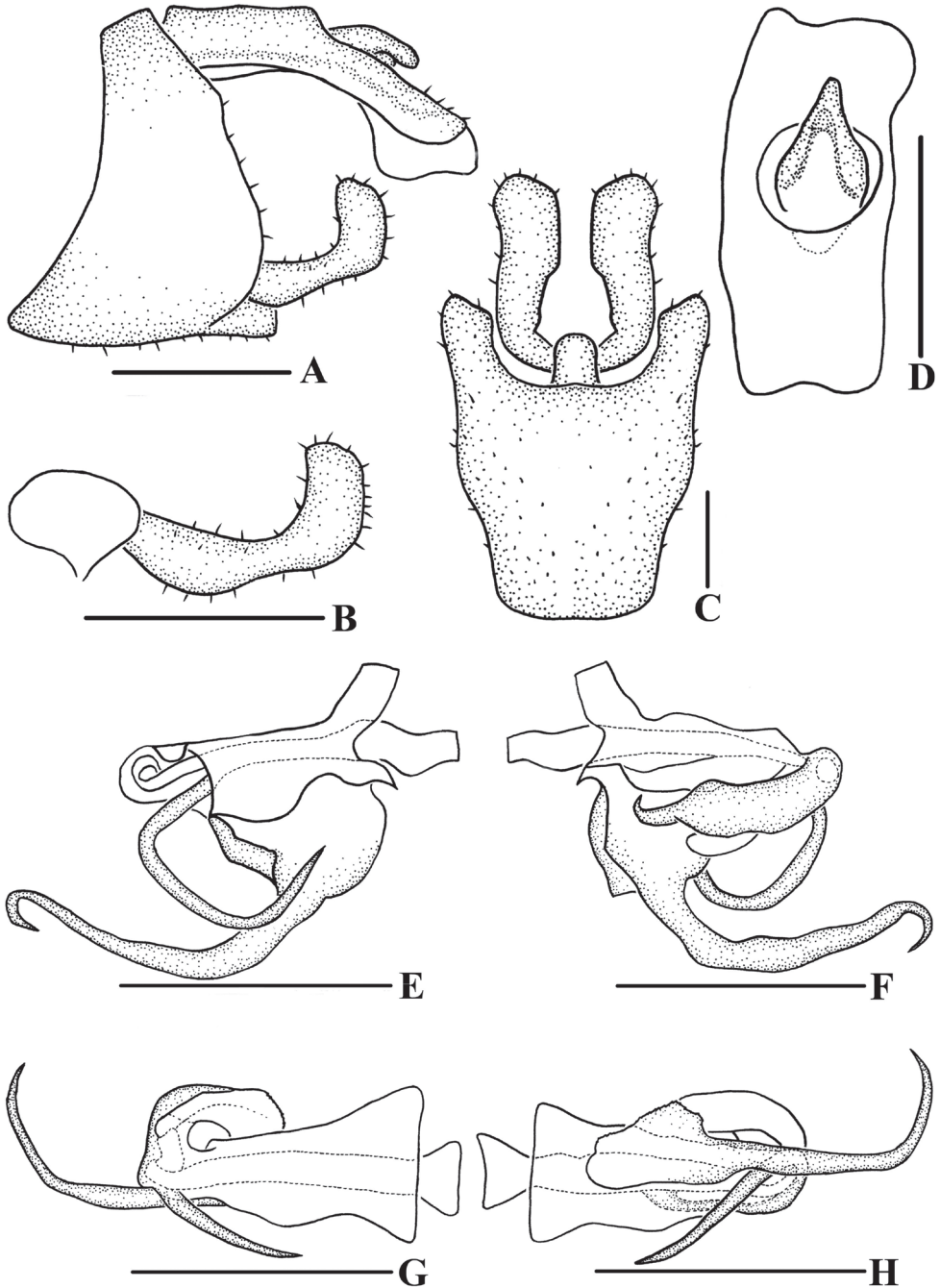


**Figure 3.** *Andixius flagellihamus* sp. nov., male **A** genitalia, lateral view **B** gonostyli, lateral view **C** pygofer and gonostyli, ventral view **D** anal segment, dorsal view **E** aedeagus, right side **F** aedeagus, left side **G** aedeagus, dorsal view **H** aedeagus, ventral view. Scale bars: 0.5 mm.

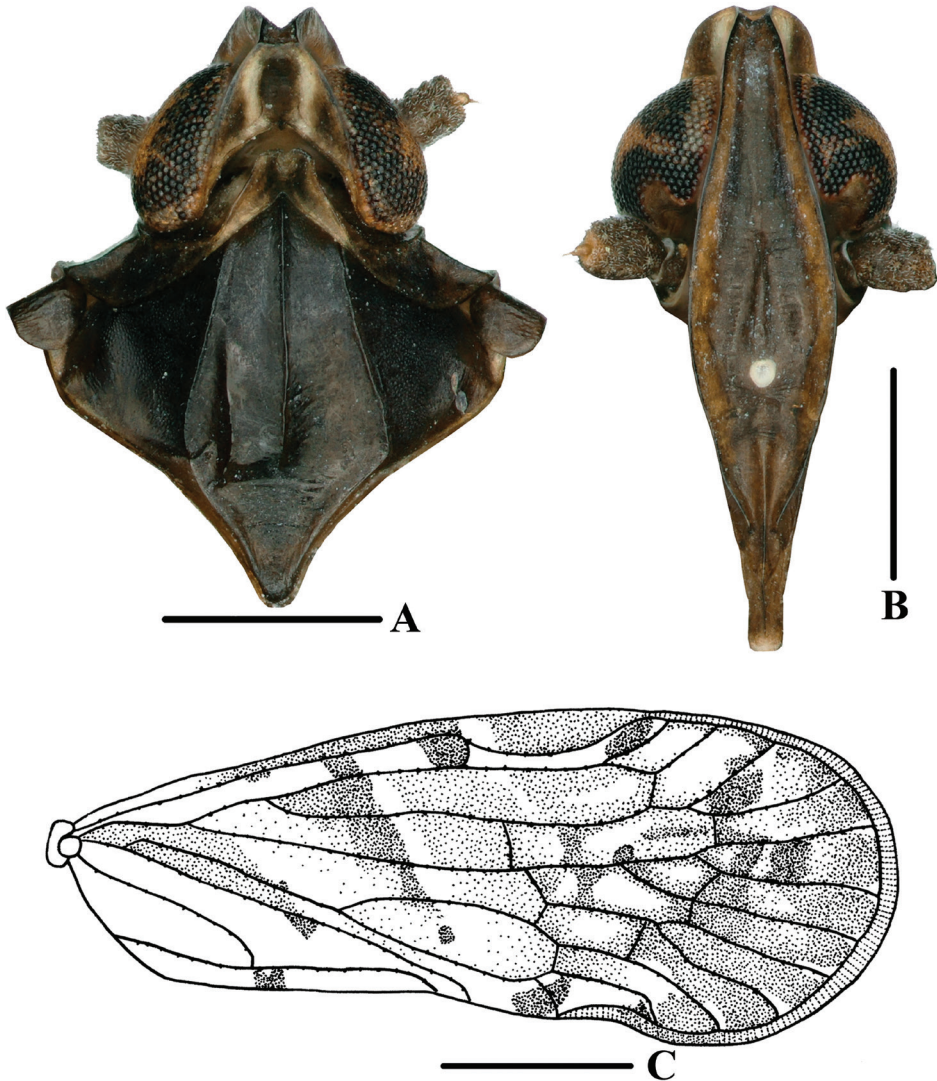


**Figure 4.** *Andixius gracilispinus* sp. nov., male **A** head and thorax, dorsal view **B** face, ventral view **C** forewing. Scale bars: 0.5 mm (**A, B**); 1.0 mm (**C**).

**Coloration.** General color yellowish brown (Figs 1C, D, 4A, B). Eyes black-brown, ocelli faint light yellowish brown, semitranslucent. Lateral margin of frons yellowish brown, behind eyes with an off-white spot. Antenna and vertex yellowish brown. Face and rostrum dark fawn. Pronotum and mesonotum black. Forewing semitranslucent, with veins, stigma, and tubercles black-brown; basal and middle part of forewings with an inner oblique stripe; base and lateral margin black-brown; in front of fork  $CuA_1+CuA_2$  with a pale spot; costal vein with three small, spaced, dark brown spots; behind stigma and near claval fork with an irregular puce spot; apical half of wing with brown patches. Hind tibiae light brown. Ventral abdomen brown.

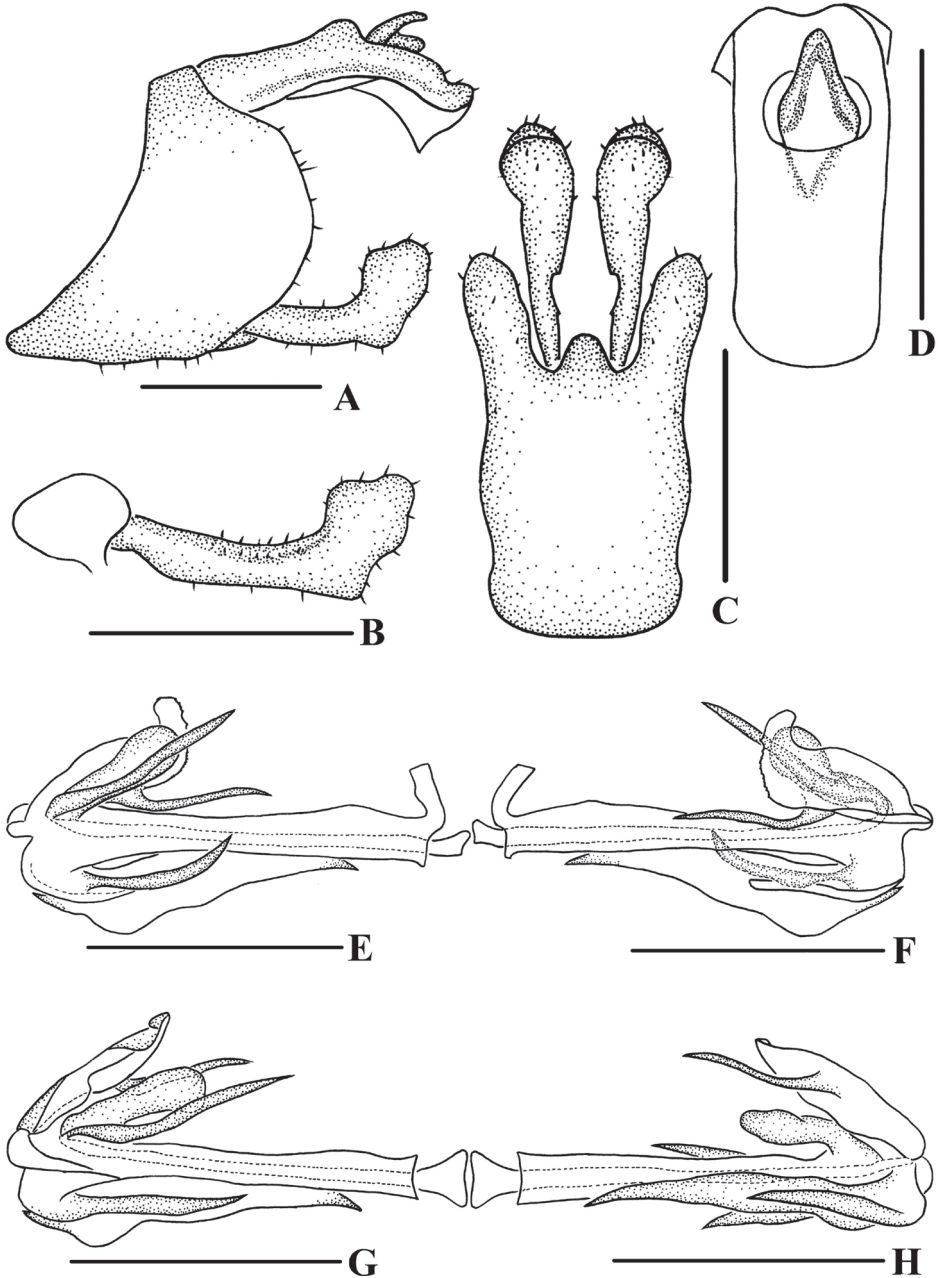


**Figure 5.** *Andixius gracilispinus* sp. nov., male **A** genitalia, lateral view **B** gonostyli, lateral view **C** pygofer and gonostyli, ventral view **D** anal segment, dorsal view **E** aedeagus, right side **F** aedeagus, left side **G** aedeagus, dorsal view **H** aedeagus, ventral view. Scale bars: 0.5 mm.

**Head and thorax.** Vertex (Figs 1C, 4A) 1.37 times longer than wide; anterior margin slightly curved, recessed; posterior margin V-shaped, recessed; lateral carinae developed; median carina absent. Frons (Fig. 4 B) claviform, 2.85 times as long as wide. Pronotum

(Figs 1C, 4A) slightly shorter than vertex. Mesonotum 1.34 times longer than pronotum and vertex combined, lateral carinae curved outwards. Forewing (Figs 1D, 4C) 2.57 times longer than wide, with 11 apical cells and six subapical cells; RP 3 branches, MP with five terminals:  $MP_{11}$ ,  $MP_{12}$ ,  $MP_2$ ,  $MP_3$ , and  $MP_4$ , fork  $MP_1+MP_2$  basad of fork  $MP_3+MP_4$ . Hind tibia with five lateral spines; chaetotaxy of hind tarsi 6/6.

**Male genitalia.** Pygofer (Fig. 5A, C) symmetrical. Medioventral process rounded protruding in ventral view. Anal segment (Fig. 5A, D) asymmetrical, left lobe larger than right lobe, dorsal margin almost straight, apical margin slightly expanded downwards in lateral view; 2.44 times longer than wide in dorsal view; anal style strap-shaped, not beyond anal segment. Gonostyli (Fig. 5B, C) ventrally symmetrical; in inner lateral view, middle part slender but base and apex enlarged. Aedeagus (Fig. 5E–H) with three processes. In left side view, basal ventral margin of periandrium with a triangular laminal process, of which middle right side concaved heavily, forming two large processes, one directed cephalad, another directed caudad, basal dorsal margin of periandrium with a laminal process, of which near apex of dorsal margin recessed, apex convex, left side of margin dentate; in right side view, apical ventral margin of periandrium projecting, near apex with a long spinose process, curved upwards, directed dorsocephalad; in dorsal view, laminal process grooved, arising at left side of basal dorsal margin of periandrium, left side convex, apical right side rolling, middle part concave in a right angle, apex of periandrium with a long spinose process, slightly curved, directed cephalad; in ventral view, near apex of grooved laminal process with a long spinose process, slightly curved, directed cephalad. Endosoma slightly sclerotized, without process.

**Distribution.** China (Xizang) (Fig. 12).

**Etymology.** The specific name is derived from the Latin adjective *gracilispinus*, referring to the one long spinose process arising from the apical right side of the ventral margin of the periandrium.

**Remarks.** Male genitalia of *A. gracilispinus* sp. nov. are similar to *A. venustus* Tsaur & Hsu, 1991 in appearance, but differs in: (1) basal left side of ventral margin of periandrium with a triangular laminal process, of which middle right side concaved heavily, forming two large processes (*A. venustus* with a spinose process in the same position); (2) near apical right side of ventral margin of periandrium with a long spinose process, slightly curved (right side of ventral margin of periandrium without spinose process in *A. venustus*); (3) basal dorsal margin of periandrium with a grooved laminal process (without process in *A. venustus*).

### ***Andixius productus* Wang & Chen, sp. nov.**

<https://zoobank.org/AE3FAE97-597C-41D8-92B8-7C8A2CCB5464>

Figs 1E, F, 6A–C, 7A–H, 8A–H

**Type material.** *Holotype*: ♂, CHINA: Xizang Province, Medog County, Damu Town, 80K (29.6237°N, 95.4888°E), 18 August 2020, Yongjin Sui leg.; *Paratypes*: 6♂♂ 2♀♀, same data as holotype.

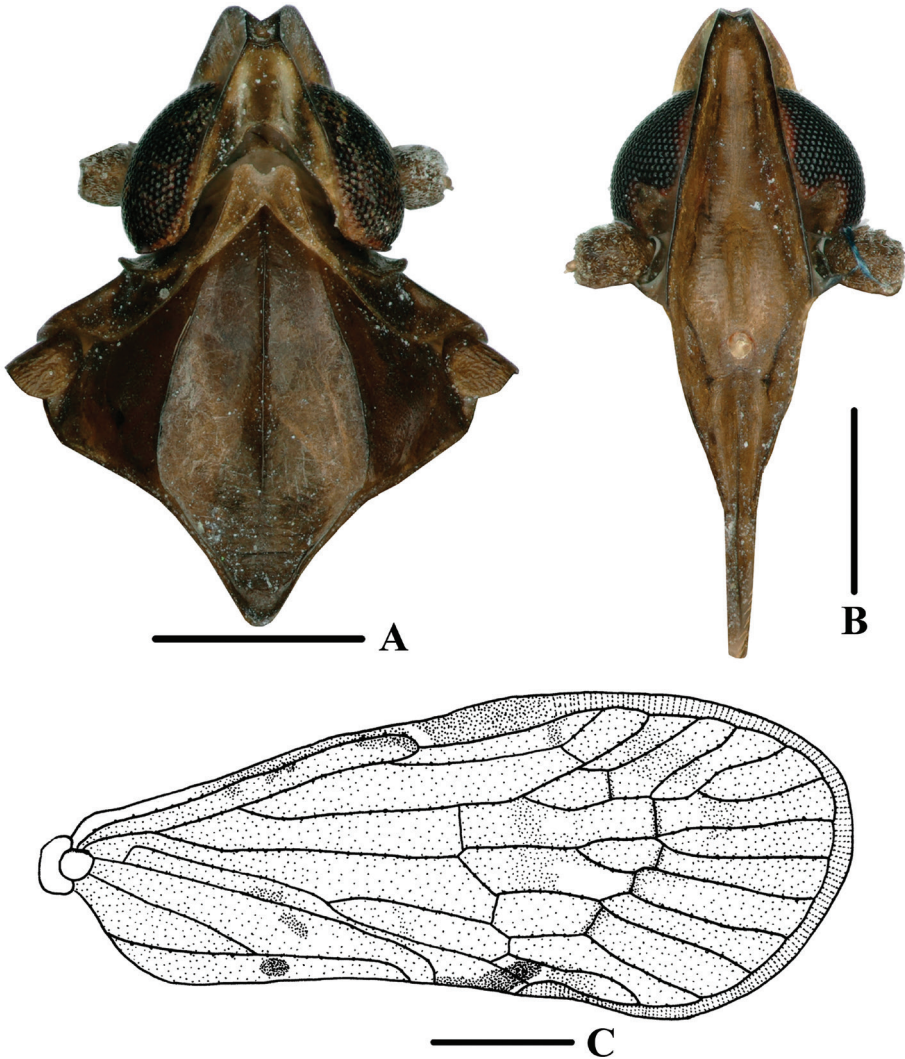


**Figure 6.** *Andixius productus* sp. nov., male **A** head and thorax, dorsal view **B** face, ventral view **C** forewing. Scale bars: 0.5 mm (**A, B**); 1.0 mm (**C**).

**Description.** Body length: male 5.71–6.90 mm ( $n = 7$ ), female 7.78–7.90 mm ( $n = 2$ ).

**Coloration.** General color black-brown (Figs 1E, F, 6A, B). Eyes black-brown, ocelli faint yellowish brown, semitranslucent. Lateral margin of frons yellowish brown, behind eyes with an off-white spot. Antenna and vertex black-brown. Face and rostrum dark fawn. Pronotum and mesonotum black-brown. Forewing semitranslucent, generally black-brown, veins and stigma yellowish brown, tubercles black-brown; costal vein, in the middle of, behind and near claval fork with deep-brown spots. Hind tibiae light brown. Ventral abdomen brown.

**Head and thorax.** Vertex (Figs 1E, 6A) 1.65 times longer than wide; anterior margin slightly curved, recessed; posterior margin V-shaped, recessed; lateral carinae developed; median carina absent. Frons (Fig. 6B) claviform, 2.90 times as long as wide. Pronotum (Figs 1E, 6A) as long as vertex. Mesonotum 1.21 times longer than pronotum and vertex combined, lateral carinae curved outwards. Forewing (Figs 1F, 6C) 2.49 times longer than wide, with 13 apical cells and seven subapical cells; RP 3 branches, MP with five terminals:  $MP_{11}$ ,  $MP_{12}$ ,  $MP_2$ ,  $MP_3$ , and  $MP_4$ , fork  $MP_1+MP_2$  basad of fork  $MP_3+MP_4$ . Hind tibia with five lateral spines; chaetotaxy of hind tarsi 6/5.

**Male genitalia.** Pygofer (Fig. 7A, C) symmetrical. Medioventral process rounded protruding in ventral view. Anal segment (Fig. 7A, D) long, tubular, with dorsal margin almost straight and apical margin slightly expanded downwards in lateral view; 2.67 times longer than wide in dorsal view; anal style strap-shaped, not beyond anal segment. Gonostyli (Fig. 7B, C) symmetrical ventrally, inner margin with a small spinose process near base, apex enlarged; in lateral view, near apex bending upwards. Aedeagus (Fig. 7E–H) with seven processes. In left side view, periandrium with an expanded laminal process around the left side and dorsal margin of periandrium; ventral margin of the expanded structure with two spinose processes, upper one slender, slightly curved, directed ventrocephalad, lower one small, directed ventrad; in right side view, apical ventral margin of periandrium projecting, the process expanded downwards, apex bifurcated, forming two spinose processes, the dorsal one long, another short, directed cephalad, the right side of the process with a long spinose process, bending around the periandrium, directed left-dorsocephalad, apical dorsal margin of periandrium with a long spinose process, near apex slightly curved upwards, directed dorsocephalad; in dorsal view, laminal process covering dorsal margin, middle part of periandrium with a thick, long spinose process, slightly curved, directed cephalad. Endosoma short, slightly sclerotized, without process.

**Female genitalia.** Tergite IX (Fig. 8A, B, D) moderately sclerotized, with a large nearly elliptical wax plate. Anal segment (Fig. 8C) rectangular, 2.43 times longer than wide in dorsal view, anal style linguiform. Gonapophysis IX (Fig. 8F) with one middle tooth; distance ratio between middle tooth to apex and length of denticulate portion is 1.98. Gonoplac (Fig. 8G) rod-like, 4.44 times longer than wide in lateral view. Posterior vagina pattern as shown in Fig. 8H.

**Distribution.** China (Xizang) (Fig. 12).

**Etymology.** The specific name is derived from the Latin adjective *productus*, referring to the one long spinose process arising from the apical ventral margin of the periandrium.

**Remarks.** Male genitalia of *A. productus* sp. nov. are similar to *A. trifurcus* Zhi & Chen, 2018, but differs in: (1) periandrium with an expanded laminal process around the left side and dorsal margin of periandrium (laminal process around the left side, dorsal margin and ventral margin in *A. trifurcus*); (2) basal ventral margin of periandrium with laminal process, of which ventral margin with two processes (*A. trifurcus*

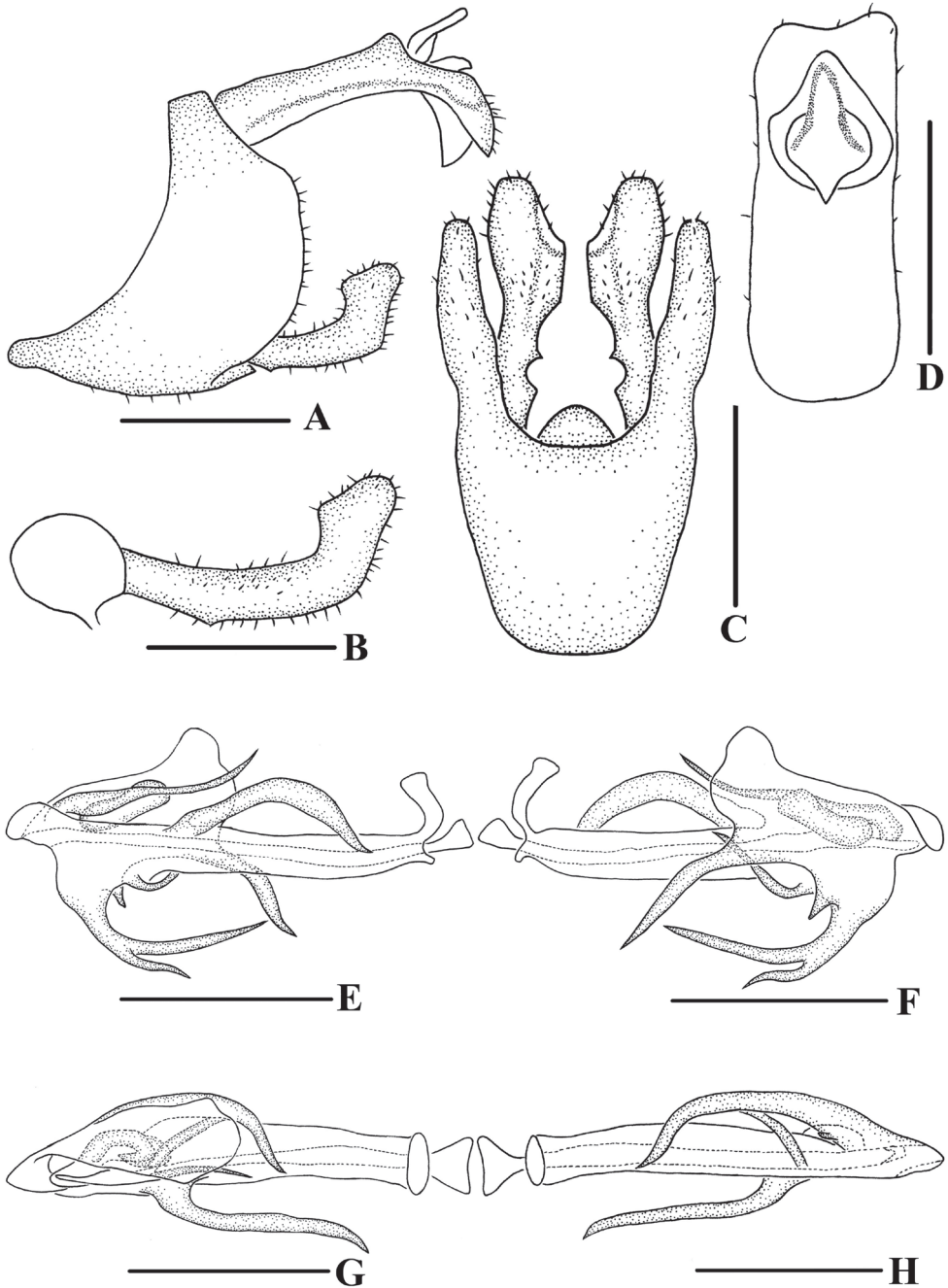


**Figure 7.** *Andixius productus* sp. nov., male **A** genitalia, lateral view **B** gonostyli, lateral view **C** pygofer and gonostyli, ventral view **D** anal segment, dorsal view **E** aedeagus, right side **F** aedeagus, left side **G** aedeagus, dorsal view **H** aedeagus, ventral view. Scale bars: 0.5 mm.

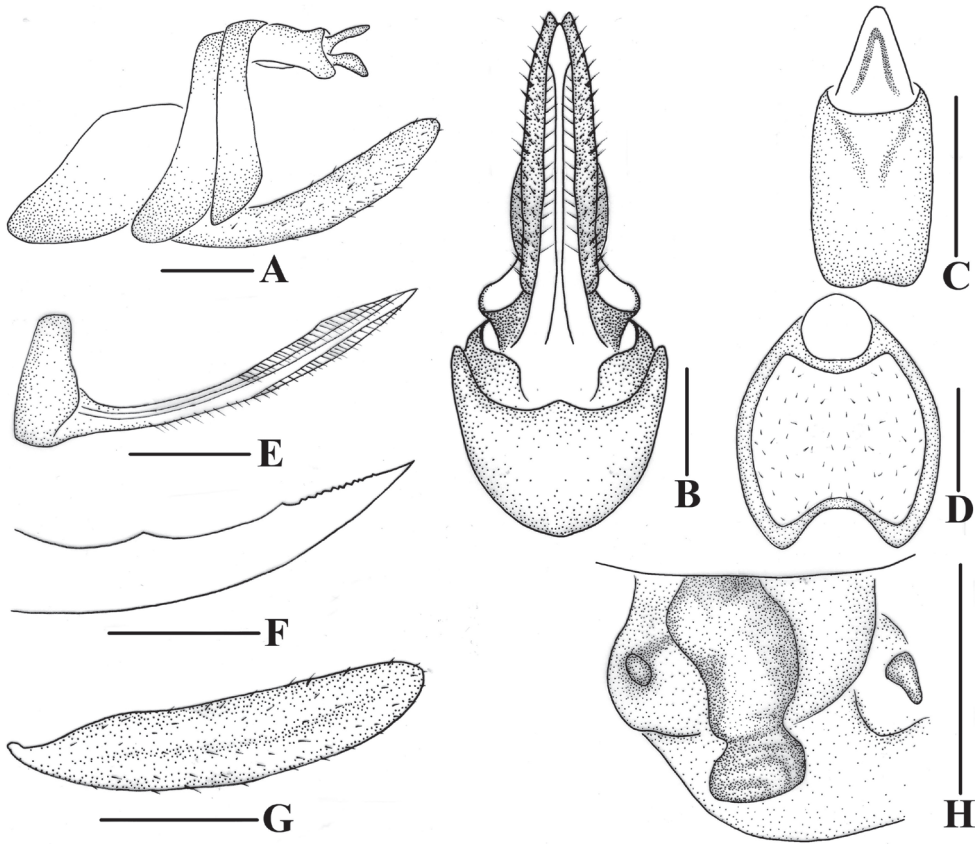


**Figure 8.** *Andixius productus* sp. nov., female **A** genitalia, lateral view **B** genitalia, ventral view **C** anal segment, dorsal view **D** tergite IX, caudal view **E** gonapophysis VIII and gonocoxa VIII, dorsal view **F** gonapophysis IX, lateral view **G** gonoplac, inner lateral view **H** posterior vagina, ventral view. Scale bars: 0.5 mm.

with three long spinose processes in the same position); (3) right side of ventral margin of perianthrium with three spinose processes (right side of middle part of perianthrium with a spinose process in *A. trifurcus*); (4) middle part of perianthrium with a thick and long spinose process (without process in *A. trifurcus*).

***Andixius truncatus* Wang & Chen, sp. nov.**

<https://zoobank.org/1EE35403-E65B-43C5-B171-54C7CC313B23>

Figs 1G, H, 9A–C, 10A–H, 11A–H

**Type material.** *Holotype*: ♂, CHINA: Guangxi Province, Longsheng County, Huaping National Natural Reserve (25.6046°N, 109.9417°E), 18 July 2020, Xiaoya Wang, Yongjin Sui, Zhicheng Zhou and Jing Wang leg.; *Paratypes*: 9♂♂ 5♀♀, same data as holotype.

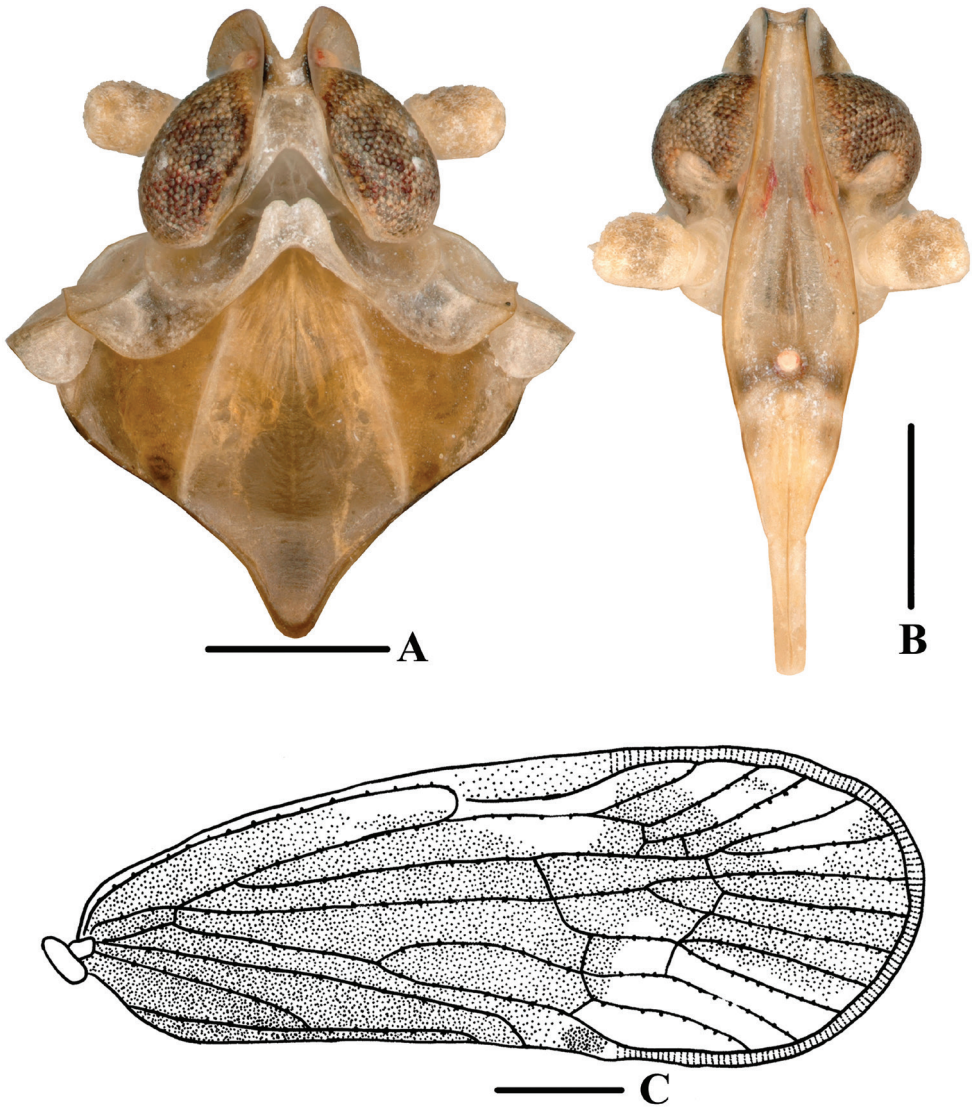


**Figure 9.** *Andixius truncatus* sp. nov., male **A** head and thorax, dorsal view **B** face, ventral view **C** forewing. Scale bars: 0.5 mm (**A**, **B**); 1.0 mm (**C**).

**Description.** Body length: male 6.56–7.20 mm ( $n = 10$ ), female 7.25–8.86 mm ( $n = 5$ ).

**Coloration.** General color black-brown (Figs 1G, H, 9A, B). Eyes yellowish brown, ocelli faintly yellow, semitranslucent. Lateral margin of frons yellowish white, behind eyes with two brown spots. Antenna, vertex, face, and rostrum fawn. Pronotum fawn. Mesonotum yellowish brown. Forewing semitranslucent, generally black-brown; stigma fawn; veins and tubercles the same color as the wing surface; slightly below

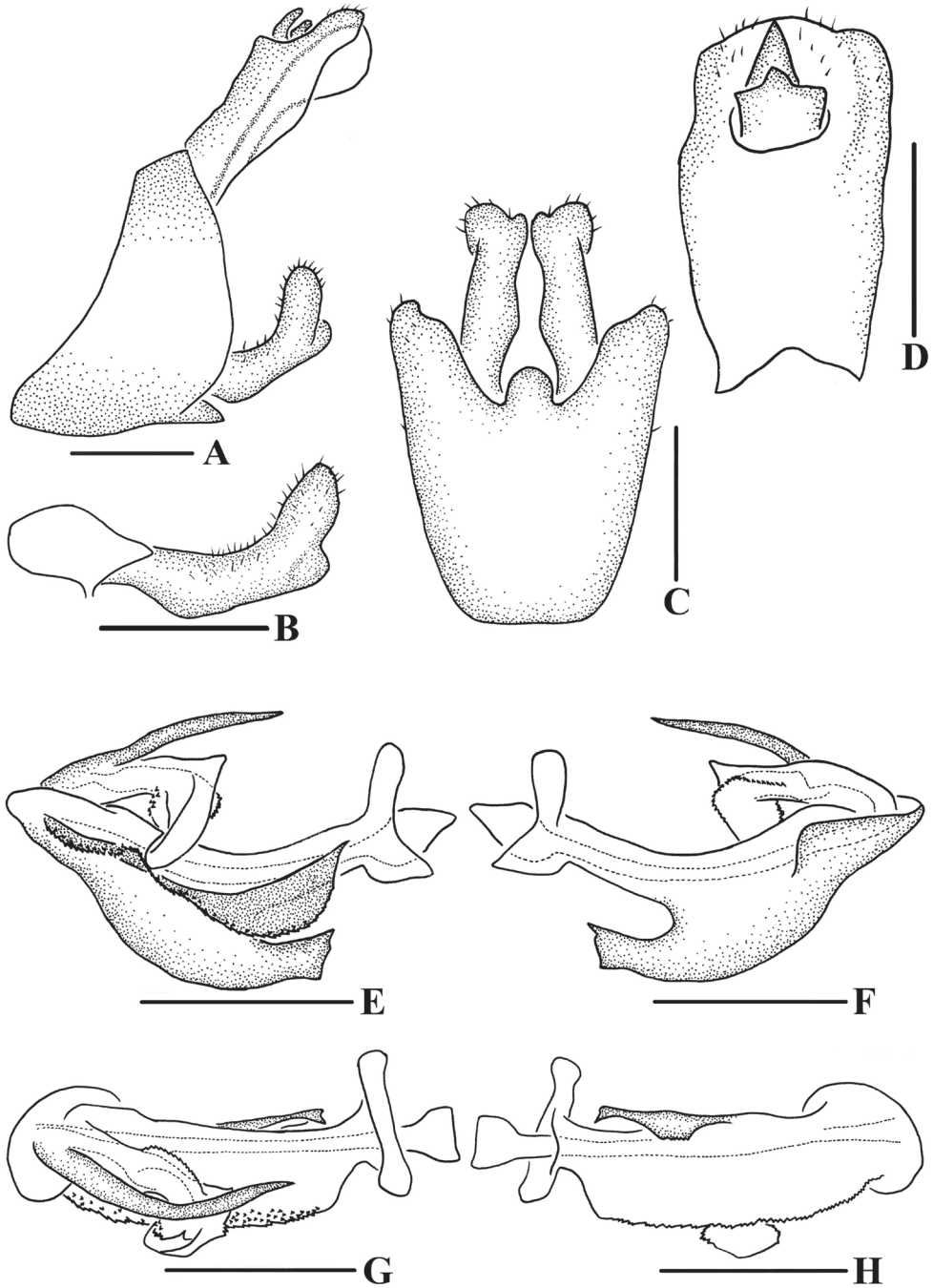


**Figure 10.** *Andixius truncatus* sp. nov., male **A** genitalia, lateral view **B** gonostyli, lateral view **C** pygofer and gonostyli, ventral view **D** anal segment, dorsal view **E** aedeagus, right side **F** aedeagus, left side **G** aedeagus, dorsal view **H** aedeagus, ventral view. Scale bars: 0.5 mm.

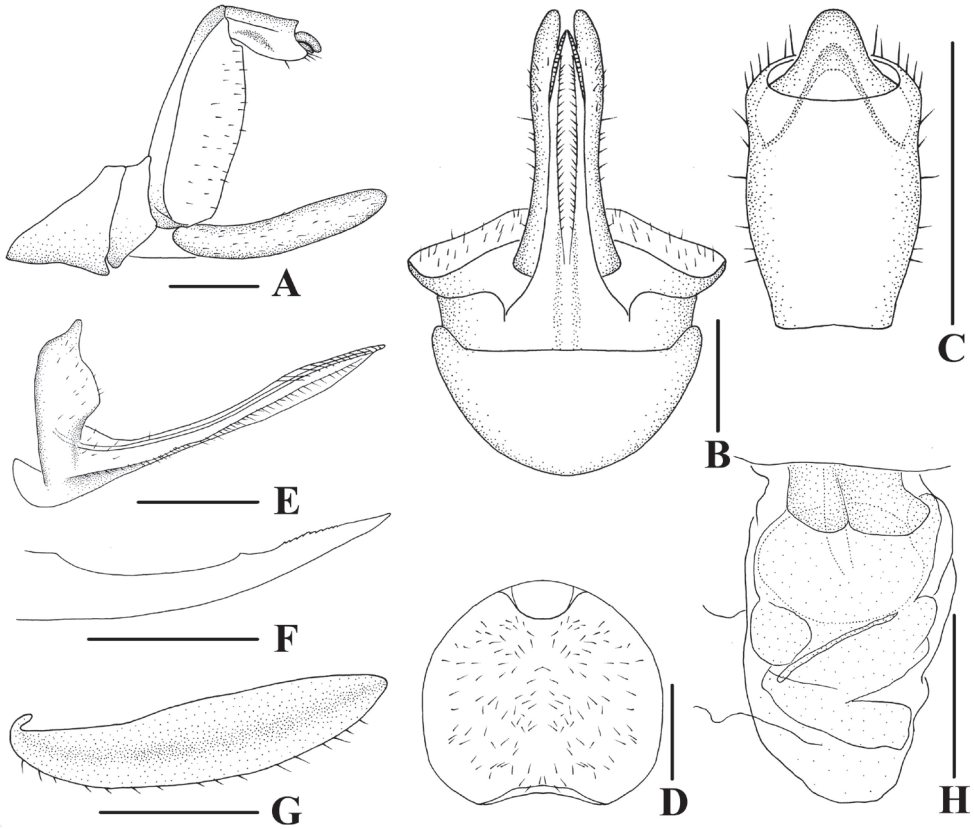


**Figure 11.** *Andixius truncatus* sp. nov., female **A** genitalia, lateral view **B** genitalia, ventral view **C** anal segment, dorsal view **D** tergite IX, caudal view **E** gonapophysis VIII and gonocoxa VIII, dorsal view **F** gonapophysis IX, lateral view **G** gonoplac, inner lateral view **H** posterior vagina, ventral view. Scale bars: 0.5 mm.

stigma and near claval fork with an irregular, yellowish-white spot; apical half of wing light brown. Hind tibiae yellowish brown. Ventral abdomen yellowish brown.

**Head and thorax.** Vertex (Figs 1G, 9A) 2.76 times longer than wide; anterior margin slightly curved recessed, posterior margin U-shaped, recessed; lateral carinae developed; median carina absent. Frons (Fig. 9B) claviform, 3.00 times as long as wide. Pronotum (Figs 1G, 9A) slightly shorter than vertex. Mesonotum 1.08 times slightly longer than pronotum and vertex combined, lateral carinae curved outwards. Forewing (Figs 1H, 9C) 2.74 times longer than wide, with 12 apical cells and seven subapical cells; RP 3 branches, MP with five terminals:  $MP_{11}$ ,  $MP_{12}$ ,  $MP_2$ ,  $MP_3$ , and  $MP_4$ , fork  $MP_1+MP_2$  basad of fork  $MP_3+MP_4$ . Hind tibia with four lateral spines; chaetotaxy of hind tarsi 8/8.

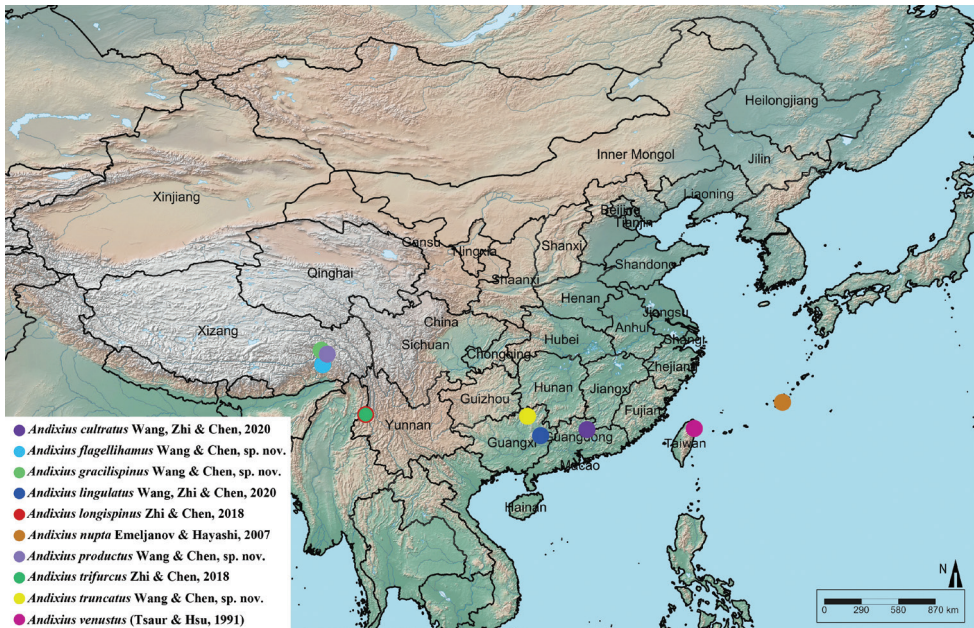


**Figure 12.** Geographic distribution of *Andixius* species.

**Male genitalia.** Pygofer (Fig. 10A, C) symmetrical. Medioventral process rounded protruding in ventral view. Anal segment (Fig. 10A, D) tubular, dorsal margin almost straight, ventral margin slightly curved, right lobe larger than left lobe in lateral view; 1.81 times longer than wide in dorsal view; anal style strap-shaped, not beyond anal segment. Gonostyli (Fig. 10B, C) symmetrical ventrally, inner margin with a small process near base; in lateral view, apex enlarged and foot-shaped. Aedeagus (Fig. 10E–H) with three processes. In left side view, apex of periandrium with laminal process, apex rounded; in right side view, ventral margin of periandrium with a long, broad laminal process, apex truncated, margin with small teeth, directed cephalad, with endosoma curving ventrally at a right angle; in dorsal view, base of endosoma with a long spinose process, slightly curved, directed dorsocephalad.

**Female genitalia.** Tergite IX (Fig. 11A, B, D) moderately sclerotized, with a large, nearly circular wax plate. Anal segment (Fig. 11C) rectangular, 1.60 times longer than wide in dorsal view, anal style linguiform. Gonapophysis IX (Fig. 11F) with one middle tooth; distance ratio between middle tooth to apex and length of denticulate portion is 2.70. Gonoplac (Fig. 11G) rod-like, 4.3 times longer than wide in lateral view. Posterior vagina pattern as shown in Fig. 11H.

**Distribution.** China (Guangxi) (Fig. 12).

**Etymology.** The specific name is derived from the Latin adjective *truncatus*, referring to the ventral margin of periandrium with a long, broad laminal process having a truncated apex.

**Remarks.** This species can be distinguished from the other *Andixius* species by the following characters: forewing general black-brown, with an irregular yellowish-white spot slightly below stigma and near claval fork; ventral margin of periandrium with a long and broad laminal process, apex truncated, margin with small teeth; endosoma curving ventrally in right angle, base of dorsal margin with a long spinose process.

## Discussion

The present discovery of four new species in the genus *Andixius* once again emphasizes the need for further study on the group based on male genitalia whenever possible (Zhi et al. 2018; Wang et al. 2020). Five species of this genus were previously described from southern China. With expanded collection efforts, our team went to Xizang Province in southwestern China, where it had not been, and there we found three of the new species described in the paper. Xizang Province has a high altitude, but it is rich in species and productive for making collections. Additionally, we found a new species with distinctive coloration in Guangxi Province.

Nine *Andixius* species are now known to occur in China, which can be certainly considered to be an underestimate, as the fauna is far from being well known in this interesting region. Therefore, further investigation should be considered to fill the faunistic gaps, as it is obvious that many more taxa remain to be discovered and described.

Currently the tribe Andini includes 129 species in three genera (*Parandes* Muir, 1925, *Andes* Stål, 1866, and *Andixius*), of which only the latter two genera and 18 species occur in China (Bourgoin 2022; Wang et al. 2022). A comparison of *Andes*, *Andixius*, and *Parandes* shows that species in these genera look rather similar, but these genera can be easily distinguished by the veins and fore coxa. The forewings of *Andixius* are without trifold branching of ScP+R and MP near the basal cell, and ScP+R (ScP+RA and RP) forming a short common stalk, while ScP, RP and MP emerge independently or very close to the basal cell in the other Andini genera. The outer edge of the apical half of the fore coxae is extended and smoothly protruding in *Parandes*, but the outer edge of the apical half of the fore coxae is straight and does not extend in *Andes*.

## Acknowledgements

We are grateful to the collectors of the specimens, especially Yongjin Sui, for their hard work in the field and to an associate researcher Dawa at the Institute of Plateau Biology in Xizang Province, China for his help with the specimen collection. This work was supported by the National Natural Science Foundation of China (grant no. 32060343 and 31472033); the Science and Technology Support Program of Guizhou Province (grant no. 20201Y129); the Program of Excellent Innovation Talents, Guizhou Province (grant no. 20154021).

## References

- Bourgoin T (1987) A new interpretation of the homologies of the Hemiptera male genitalia, illustrated by the Tettigometridae (Hemiptera, Fulgoromorpha). Proceedings 6<sup>th</sup> Auchenorrhyncha Meeting, Turin, Italy, 7–11 September 1987, 113–120.
- Bourgoin T (1993) Female genitalia in Hemiptera Fulgoromorpha, morphological and phylogenetic data. *Annales de la Société Entomologique de France* 29(3): 225–244.
- Bourgoin T (2022) FLOW (Fulgoromorpha Lists on the Web): a world knowledge base dedicated to Fulgoromorpha. <http://hemipteradatabasesorg/flow> [Accessed on: 2022-12-7]
- Bourgoin T, Wang RR, Asche M, Hoch H, Soulier-Perkins A, Stroiński A, Yap S, Szvedo J (2015) From micropterism to hyperpterism: recognition strategy and standardized homology-driven terminology of the forewing venation patterns in planthoppers (Hemiptera: Fulgoromorpha). *Zoomorphology* 134(1): 63–77. <https://doi.org/10.1007/s00435-014-0243-6>
- Emeljanov AF, Hayashi M (2007) New Cixiidae (Hemiptera, Auchenorrhyncha) from the Ryukyus, Japan. *Japanese Journal of Systematic Entomology* 13(1): 127–140.
- Tsaur SC, Hsu TC, Van Stalle J (1991) Cixiidae of Taiwan, part V. Cixiini except *Cixius*. *Journal of Taiwan Museum* 44: 1–78.
- Wang XY, Zhi Y, Chen XS (2020) Key to species of the genus *Andixius* Emeljanov & Hayashi (Hemiptera: Fulgoromorpha: Cixiidae) with descriptions of two new species. *Zootaxa* 4802(3): 440–448. <https://doi.org/10.11646/zootaxa.4802.3.2>
- Wang XY, Zhi Y, Chen XS (2022) Five new species of the genus *Andes* Stål, 1866 from China (Hemiptera, Fulgoromorpha, Cixiidae). *European Journal of Taxonomy* 831: 45–66. <https://doi.org/10.5852/ejt.2022.831.1869>
- Zhi Y, Yang L, Zhang P, Chen XS (2018) Two new species of the genus *Andixius* Emeljanov & Hayashi from China (Hemiptera, Fulgoromorpha, Cixiidae). *ZooKeys* 739: 55–64. <https://doi.org/10.3897/zookeys.739.13043>

# Effects of habitat differences on the scatter-hoarding behaviour of rodents (Mammalia, Rodentia) in temperate forests

Dianwei Li<sup>1,2,3</sup>, Jiahui Liu<sup>2</sup>, Chengzhi Zhang<sup>2</sup>, Yuwei Cao<sup>2</sup>, Ming Gao<sup>2</sup>,  
Zhimin Jin<sup>2</sup>, Hongjia Shan<sup>2</sup>, Hongwei Ni<sup>1</sup>

**1** Heilongjiang Academy of Forestry, No. 134 Haping Road, Harbin, Heilongjiang 150081, China **2** College of Life Sciences and Technology, Mudanjiang Normal University, No. 191 Wenhua Road, Mudanjiang, Heilongjiang 157011, China **3** College of Wildlife and Protected Area, Northeast Forestry University, No. 26 Hexing Road, Harbin 150040, China

Corresponding authors: Dianwei Li ([lidianwei@mdjnu.edu.cn](mailto:lidianwei@mdjnu.edu.cn)); Hongwei Ni ([nihongwei2000@163.com](mailto:nihongwei2000@163.com))

Academic editor: N. Nedyalkov | Received 2 November 2022 | Accepted 20 December 2022 | Published 20 January 2023

<https://zoobank.org/57CBDF36-7A60-494D-9B9A-8ABDB8C90635>

**Citation:** Li D, Liu J, Zhang C, Cao Y, Gao M, Jin Z, Shan H, Ni H (2023) Effects of habitat differences on the scatter-hoarding behaviour of rodents (Mammalia, Rodentia) in temperate forests. ZooKeys 1141: 169–183. <https://doi.org/10.3897/zookeys.1141.96883>

## Abstract

To discover the differences in hoarding strategies of rodents for different seeds in different habitats, we labelled and released three different types of seeds, including *Pinus koraiensis*, *Corylus mandshurica*, and *Quercus mongolica*, in temperate forests of northeastern China and investigated the fate of seeds in four different habitats that included a broad-leaved forest, mixed-forest edge, mixed forest, and artificial larch forest. Our research showed that the hoarding strategy of rodents was found to vary substantially in different habitats. The survival curves of seeds from different habitats showed the same trend, but the rates of consumption in different habitats varied. More than 50% of the seeds in the four habitats were consumed by the tenth day. It took 20 days to consume more than 70% of the seeds. The rate of consumption of *P. koraiensis* seeds reached 96.70%; 99.09% of the *C. mandshurica* seeds were consumed, and 93.07% of the *Q. mongolica* seeds were consumed. The seeds were consumed most quickly in the artificial larch forest. In general, most of the early seeds were quickly devoured. After day 20, the consumption gradually decreased. Rodents found the seeds in the artificial larch forest in a shorter average time than those in the other types of forests. The average earliest discovery time was  $1.4 \pm 0.9$  d (1–3 d). The average earliest discovery time in all the other three habitats exceeded 7 d. The median removal times (MRT) was distributed around the seeds at  $14.24 \pm 10.53$  d (1–60 d). There were significant differences in the MRT among different habitats. It was shortest in the artificial larch forest at  $7.67 \pm 6.80$  d (1–28 d). In contrast, the MRT in the broad-leaved forest was the longest at  $17.52 \pm 12.91$  d (4–60 d). There were significant

differences in the MRT between the artificial larch forest and the other habitats. There was less predation of the three types of seeds at the mixed-forest edge, and the most seeds were dispersed. The rates of predation of the *P. koraiensis*, *C. mandshurica*, and *Q. mongolica* seeds were 28.33%, 15.83%, and 44.0%, and 59.17%, 84.17%, and 48.0% of the seeds were dispersed, respectively. The average dispersal distances of all the seeds were less than 6 m, and the longest distance recorded was 18.66 m. The dispersal distances and burial depths differed significantly among the four types of habitats. The distance of seed dispersal was primarily distributed in 1–6 m.

### Keywords

Habitat, rodents, scatter-hoarding, seed fate

## Introduction

Food hoarding behaviour is a type of exceptional feeding activity of the rodents. It is regarded as a strategy to adapt to the periodic fluctuation of food resources, as well as the environment. (Vander Wall 1990, 2001; Lichti et al. 2015; Li et al. 2020). This benefits the rodent by rationally allocating limited food resources to manage food distribution and richness with the changes in time and space. Alternatively, triumphant hoarding is key for the survival and reproductive fitness of many types of species during periods of food scarcity (Vander Wall 2001; Lu and Zhang 2005; Lichti et al. 2015; Luna et al. 2016). In addition, in the forest ecosystem, many plants rely on animals as a manner of dispersing their seeds. The set of behaviours of hoarding animals, including the harvest, transport, and storage, affects the success of both seed germination and the survival of seedlings in a direct way (Vander Wall 2001; Lichti et al. 2015). The hoarding behaviour of rodents is one of the crucial processes that affects the dynamics, structure, spatial distribution, natural selection, and species diversity of plant populations and communities (Willson and Whelan 1990; Vander Wall 2001; Vander Wall and Beck 2011; Li et al. 2018).

A co-evolutionary reciprocity exists between many plants with large seeds and hoarding animals (Vander Wall 1990, 2001; Li and Zhang 2003). Some of the characteristics or habits of both parties contribute to the adaptation and strengthening of the mutualistic relationship during evolution. The hoarding behaviour is influenced by a variety of factors, which include the specialties of plant seeds, yield, distribution, temporal and spatial changes of food resources, and changes in environmental factors, such as climate and habitat structure (Preston and Jacobs 2005; Jenkins 2011; Lichti et al. 2015; Li et al. 2021). The temporal and spatial dependence of hoarding animals could be influenced by such factors as variation in the vegetation and the rhythm of activity of animals. Therefore, rodent behaviour can better reflect its adaptation to habitat selection and environmental changes.

The study site was located in the ecological region of the Zhangguangcai Mountains in north-eastern China. It is located at the northern end of Changbai Mountain. This zone is rich in forest vegetation resources, which is an important resource of species and seed bank. There are abundant types and quantities of rodents in forests.

Rodents not only destroy forest resources by feeding on vegetation and seeds but also promote the regeneration of vegetation by dispersing and hoarding food (Vander Wall 2001, 2003; Lichti et al. 2015).

To further understand these issues to provide theoretical and practical guidance to explore the interaction between rodents and many large-seeded plants, this study labelled and released the seeds of *Pinus koraiensis*, *Corylus mandshurica*, and *Quercus mongolica* in four different habitat types. They included a broad-leaved forest, mixed-forest edge, mixed forest, and artificial larch forest. The fate of seeds, predation, dispersal, and storage of the seeds by rodents were investigated, and the rules of utilization of the seeds by rodents and the habitat differences in natural environment were also investigated. The seeds were regularly investigated to understand the following: (1) the survival curves and consumption time of different habitat types; (2) the selection characteristics of different seeds in the same region; (3) the fate of released seeds; and (4) the characteristics of dispersal distance and burial depth of seeds. The results of this research should increase the theoretical basis to understand the influence of rodents on forest-tree seeds and provide a scientific basis for the renewal and protection of forest vegetation.

## Site and methods

### Study area and research site selection

The research was conducted in a forested area of the Sandao forest farm (44°40'N–44°45'N, 129°24'E–129°32'E, elevation 380–550 m a.s.l.), Mudanjiang City, from April to November 2019. The research area is located at the north end of Changbai Mountain in northeastern China at the east vein of the main ridge of Zhangguangcai Mountain. The climate is temperate and has a cold continental monsoon climate, four distinct seasons, and a hot rainy season. The highest temperature recorded here was 37 °C. The lowest temperature recorded was –44.1 °C, and the annual average temperature is 2.3–3.7 °C. Four types of different habitats were selected for research in the field experiment. They included alternative broad-leaved forest plots with less human disturbance, mixed-forest edge, mixed forest, and artificial larch forest. Each plot was spaced more than 2 km from another plot. The composition of small rodents and the vegetation in the sample were investigated before the experiment was initiated. The rodents in forests were highly abundant and diverse. *Apodemus peninsulae*, *A. agrarius*, and *Clethrionomys rufocanus* were the three most abundant seed predators/dispersers in the forest.

### Tagging and tracking of seeds

Healthy seeds of *P. koraiensis*, *C. mandshurica*, and *Q. mongolica* selected in the field study were marked using an electric drill whose bit is 0.5 mm in diameter, and holes were made at one end of the seed. A thin red plastic sheet was cut into a 3 cm × 1 cm rec-

tangular piece, and a small hole was cut in the middle of the short side. The perforated seeds were connected to the plastic plate with a soft steel wire that was 0.3 mm in diameter and 8 cm long. The seed category, sample number, and seed number were marked on each label. This made the seeds easier to locate during research because the tags were exposed when the rodents ate the seeds or buried them in the ground, under dead branches or in shallow holes. The rodents could not bite off the steel wire. Therefore, this tagging method had no significant effect on their seed dispersal (Li et al. 2018, 2021).

## Release and investigation of the seeds

Food release stations in the forest were randomly spaced more than 50 m apart. A total of 20 seeds of each type were released from each planting for a total of 60 seeds. There were six release stations for each type of habitat and 120 seeds for each type, totalling 360 seeds. The studies were performed on days 1, 2, 3, 4, 6, 8, 12, 16, 20, 28, 36, 44, and 60 after release. The fate, characteristics and dispersal distance of the seeds were measured.

## Definition of seed fate

After finding the seeds, the animals chose different seeds based on their preferences and performed different operations, which led to different fates of the seeds. The fate of seeds released in field experiments was defined as previously described (Li et al. 2018, 2021):

- (1) Intact *in situ* (IS): seeds not eaten or removed from the station
- (2) Predation *in situ* (PS): seed kernels eaten at the seed station
- (3) Predation after removal (PR): seed kernels eaten after removal
- (4) Intact after removal (IR): seeds not eaten and abandoned on the surface of ground after removal
- (5) Hoarded after removal (HR): seeds buried in the soil or humus layer after removal
- (6) Missing after removal (MR): seeds removed but not found
- (7) Consumption: with the exception of intact *in situ* seeds, the fate of other seeds is defined as consumption by rodents.
- (8) Predation: predation *in situ* and predation after removal are defined as predation (Predation *in situ* + Predation after removal)
- (9) Dispersal: intact after removal, hoarded after removal, and missing after removal were defined as dispersal. However, there were no data records for the survey indicators of the missing seeds, so they could not be calculated during the inspection and comparison (Intact after removal + Hoarded after removal + Missing after removal)
- (10) Median removal time (MRT) of the seeds: the time at which 50% of the seeds were removed (expressed in days), which was used to compare the rates of seed removal in both types of vegetation.

## Statistical analysis

All statistical analyses were conducted in SPSS 22.0 for Windows (IBM, Inc., Armonk, NY, USA). Before the data analysis, the data was tested for normality and equality of variance using the Kolmogorov–Smirnov and Homogeneity-of-variance tests. Data were treated with respective nonparametric tests depending on they did not meet the assumptions of normality. A Cox regression was used to analyze the seed survival rates, factoring in in different types of habitats and seeds. The Kruskal–Wallis  $H$  test (nonparametric test) was used to compare the significant differences among the different seed species. The Mann–Whitney  $U$  test (nonparametric test) was used to test the differences between the different habitats and different seed species. The data are represented as the mean  $\pm$  SD. The values are considered statistically significant at  $P < 0.05$ .

## Results

### Seed survival curves

The survival of seeds from different habitats was analysed to produce a survival curve. The survival curves of seeds showed the same trend, but the rates of consumption in different habitats varied ( $W = 111.958$ ,  $df = 3$ ,  $P < 0.001$ ). The seeds were consumed the most quickly in the artificial larch forest. The rates of consumption in the other three habitats were very similar, and there were no significant differences in the degrees of differentiation among the seed survival curves ( $W = 3.526$ ,  $df = 2$ ,  $P = 0.172$ ). In general, most of the early seeds were quickly devoured. After day 20, the consumption gradually decreased. Therefore, when the survival rate of the curve approached 20%, the curve became flat, and the trend of seed consumption decreased (Fig. 1).

The survival curves of three different types of seeds in the various habitats were analyzed. Each type of seed in all four habitats differed significantly (*P. koraiensis*:  $W = 88.400$ ,  $df = 3$ ,  $P < 0.001$ ; *C. mandshurica*:  $W = 15.428$ ,  $df = 3$ ,  $P < 0.001$ ; *Q. mongolica*:  $W = 54.848$ ,  $df = 3$ ,  $P < 0.001$ ) (Fig. 1).

The most readily consumed type of seed was that of *P. koraiensis* in the artificial larch forest, followed by the mixed forest, then the broad-leaved forest, and finally, the mixed-forest edge. There were significant degrees of differentiation among the seed survival curves ( $W = 38.838$ ,  $df = 2$ ,  $P < 0.001$ ), and the seed survival curves in different habitats differed significantly from each other ( $df = 1$ ,  $P < 0.001$ ) (Fig. 1).

The rates of consumption of *C. mandshurica* and *Q. mongolica* were also the highest in artificial larch forest. However, there were no significantly different survival curves in the broad-leaved forest, mixed-forest edge and mixed forest (*C. mandshurica*:  $W = 1.090$ ,  $df = 2$ ,  $P = 0.580$ ; *Q. mongolica*:  $W = 2.109$ ,  $df = 2$ ,  $P = 0.348$ ) (Fig. 1).

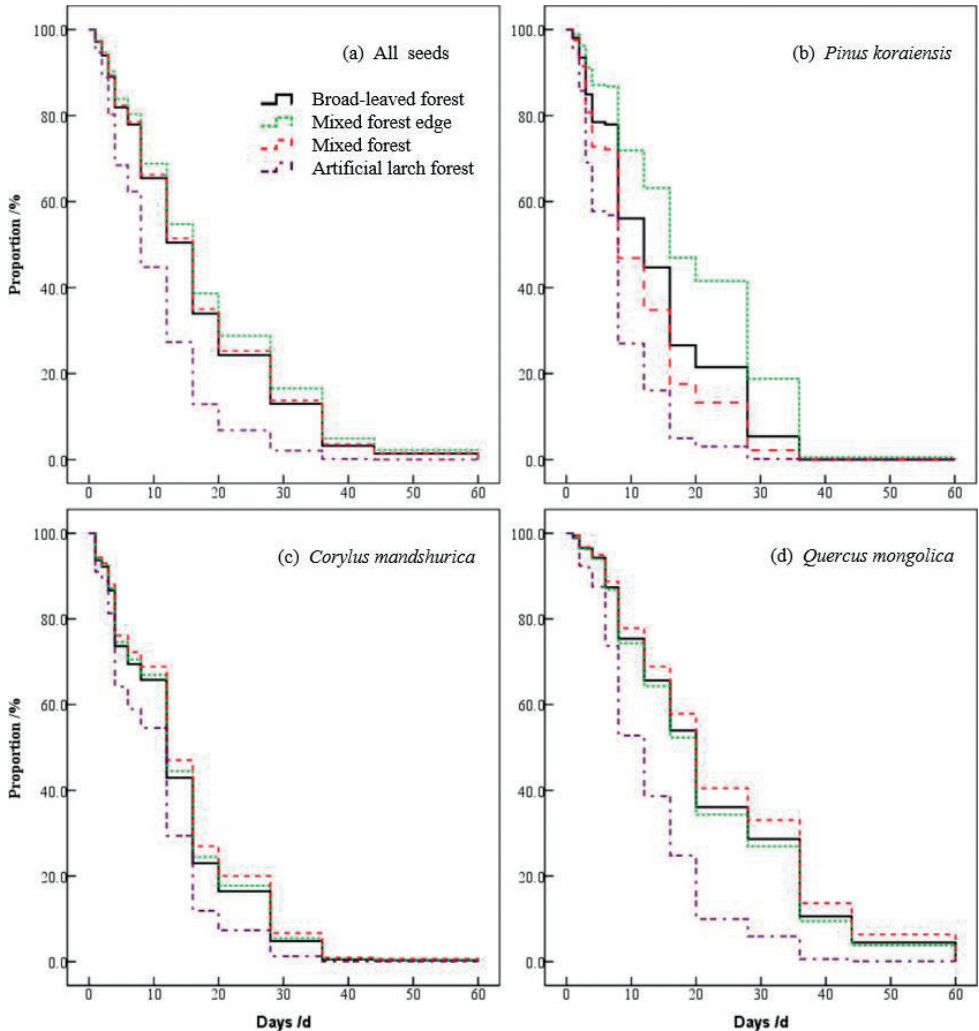


**Figure 1.** The survival curves of three kinds of seeds in different habitats in temperate forests of Northeast China.

### Seed consumption time of the rodents

The seeds were discovered 1 d after they were released in the artificial larch forest and mixed forest. In contrast, the seeds were discovered 3 d after they were released in the secondary broad-leaved forest and mixed-forest edge. Rodents found the seeds in the artificial larch forest in a shorter average time than those in the other types of forests. The average earliest discovery time was  $1.4 \pm 0.9$  d (1–3 d). The average earliest discovery time in all the other three habitats exceeded 7 d,  $7.0 \pm 3.0$  d (3–12 d) in the broad-leaved forest,  $7.5 \pm 5.3$  d (3–16 d) at the mixed-forest edge and  $7.75 \pm 9.4$  d (1–28 d) in the mixed forest. Pairwise comparisons showed that the average time at which the food was first spotted differed significantly between the other habitats ( $Z = -2.363$ ,

$P < 0.05$ ). (Broad leaf forest:  $Z = -2.836$ ,  $P < 0.01$ ; mixed-forest edge:  $Z = -2.723$ ,  $P < 0.05$ ; mixed forest:  $Z = -1.853$ ,  $P < 0.05$ ). However, there was no difference in the average time for the discovery of first food in the other three habitats ( $P > 0.05$ ).

## MRT of the seeds

When the seed species and habitat were not distinguished, the MRT was distributed around the seeds at  $14.24 \pm 10.53$  d (1–60 d). In addition, there were significant differences in the MRT among different habitats ( $\chi^2 = 10.789$ ,  $P < 0.05$ ).

The MRT was shortest in the artificial larch forest at  $7.67 \pm 6.80$  d (1–28 d). In contrast, the MRT in the broad-leaved forest was the longest at  $17.52 \pm 12.91$  d (4–60 d). Pairwise comparisons showed that there were significant differences in the MRT between the artificial larch forest and the other habitats (broad-leaved forest:  $Z = -3.127$ ,  $P < 0.01$ ; mixed-forest edge:  $Z = -2.661$ ,  $P < 0.01$ ; mixed forest:  $Z = -2.459$ ,  $P < 0.05$ ). However, there were no differences in the MRT between the broad-leaved forest and mixed-forest edge ( $Z = -0.210$ ,  $P > 0.05$ ), the broad-leaved forest and mixed forest ( $Z = -0.499$ ,  $P > 0.05$ ), and the mixed-forest edge and mixed forest ( $Z = -0.097$ ,  $P > 0.05$ ) (Table 1).

Analyses of the survival curve of the three types of seeds in the different habitats showed that the fates of different seeds varied (Table 2). The rate of consumption of

**Table 1.** Median removal time of three kinds of seeds in different habitats in temperate forests of north-eastern China.

Habitats	Median removal time (Range; d)			
	All seeds	<i>P. koraiensis</i>	<i>C. mandshurica</i>	<i>Q. mongolica</i>
Broad-leaved forest	17.52 ± 12.91 (4–60)	13.71 ± 7.25 (8–28)	13.43 ± 7.89 (4–28)	25.43 ± 18.21 (6–60)
Mixed-forest edge	15.24 ± 9.35 (3–36)	17.17 ± 10.59 (3–36)	12.67 ± 5.89 (4–20)	16.00 ± 12.25 (6–36)
Mixed forest	14.78 ± 9.61 (1–36)	10.38 ± 9.23 (2–28)	12.63 ± 8.47 (1–28)	22.29 ± 7.61 (12–36)
Artificial larch forest	7.67 ± 6.80 (1–28)	6.00 ± 2.74 (3–8)	6.20 ± 6.06 (1–16)	10.80 ± 9.96 (2–28)

**Table 2.** Statistics of three kinds of seeds with different fates in different habitats in temperate forests of Northeast China (unit: %).

Fate of seeds	Broad-leaved forest			Mixed-forest edge			Mixed forest			Artificial larch forest			All habitats		
	<i>P. koraiensis</i>	<i>C. mandshurica</i>	<i>Q. mongolica</i>	<i>P. koraiensis</i>	<i>C. mandshurica</i>	<i>Q. mongolica</i>	<i>P. koraiensis</i>	<i>C. mandshurica</i>	<i>Q. mongolica</i>	<i>P. koraiensis</i>	<i>C. mandshurica</i>	<i>Q. mongolica</i>	<i>P. koraiensis</i>	<i>C. mandshurica</i>	<i>Q. mongolica</i>
IS	0.71	0	11.43	12.50	0	8.00	0	0.63	4.29	0	3.00	4.00	3.30	0.91	6.93
PS	59.29	22.86	36.43	18.33	2.50	19.00	24.37	7.50	43.57	19.00	3.00	59.00	30.25	8.96	39.50
PR	5.00	10.71	15.00	10.00	13.33	25.00	17.50	14.38	19.29	41.00	19.00	27.00	18.38	14.35	21.57
IR	0	2.14	12.86	0.83	5.00	4.00	1.25	2.50	6.43	4.00	8.00	3.00	1.52	4.41	6.57
HR	14.29	37.86	5.71	3.34	21.67	20.00	25.63	32.50	5.00	11.00	19.00	1.00	13.56	27.76	7.93
MR	20.71	26.43	18.57	55.00	57.50	24.00	31.25	42.50	21.43	25.00	48.00	6.00	32.99	43.61	17.50
Consumption	99.29	87.50	100	100	96.70	100	100	99.38	97.00	90.09	88.57	92.00	95.72	96.00	93.07
Predation	64.29	33.57	51.43	28.33	15.83	44.00	41.87	21.88	62.86	60.00	22.00	86.00	48.63	23.31	61.07
Dispersal	35.00	66.43	37.14	59.17	84.17	48.00	58.13	77.50	32.86	40.00	75.00	10.00	48.07	78.75	32.00

*P. koraiensis* seeds reached 96.70%; 99.09% of the *C. mandshurica* seeds were consumed, and 93.07% of the *Q. mongolica* seeds were consumed. More *Q. mongolica* seeds were intact *in situ* in various habitats, 11.43% in the broad-leaved forest, 8.00% in the mixed-forest edge, 4.29% in the mixed forest and 4.00% in the artificial larch forest.

In contrast to the other habitats, there was less predation of the three types of seeds at the mixed-forest edge, and the most seeds were dispersal. The rates of predation of the *P. koraiensis*, *C. mandshurica*, and *Q. mongolica* seeds were 28.33%, 15.83%, and 44.00%, respectively, and 59.17%, 84.17%, and 48.00% of the seeds were dispersed, respectively.

In the broad-leaved forest and artificial larch forest, the rates of predation of the *P. koraiensis* seeds exceeded 60% and were higher than the dispersal rates, which were 35.00% and 40.00%, respectively. In contrast, the results were the opposite in the mixed-forest edge and mixed forest with the rate of dispersal of the *P. koraiensis* seeds exceeding 60%, which was much higher than the rates of predation of 28.33% and 41.83%, respectively (Fig. 2).

The dispersal rates of *C. mandshurica* were higher than the predation rates in all the habitats. The dispersal rate was the lowest in the broad-leaved forest (66.43%) and the largest at the mixed-forest edge (84.17%) (Fig. 2).

The predation rate of *Q. mongolica* was 44.00% in the mixed-forest edge, while it exceeded 50.0% in the other three types of habitats. It reached 86% in the artificial larch forest. However, the dispersal rate was only 10.00% in the artificial larch forest and approximately 35.00% in the other three types of habitats (Fig. 2).

When the habitats were not distinguished, the rate of predation of *P. koraiensis*, *C. mandshurica*, and *Q. mongolica* was 48.62%, 23.32%, and 61.07%, respectively. The dispersal rate was 48.07%, 75.78%, and 32.00%, respectively (Fig. 3).

## Dispersal of the seeds

The average dispersal distances of all the seeds were less than 6 m, and the longest distance recorded was 18.66 m. The dispersal distances and burial depths differed significantly among the four types of habitats (distance:  $\chi^2 = 24.149$ ,  $P < 0.001$ ; depth:  $\chi^2 = 24.334$ ,  $P < 0.001$ ) (Table 3). The distance of seed dispersal was primarily distributed within 1–6 m. Analyses of the statistical frequency indicated that the dispersal

**Table 3.** Dispersal distance and depth of burial of the seeds in different habitats in temperate forests of northeastern China.

Habitats	Dispersal distance (m)				Burial depth (cm)			
	All seeds	<i>P. koraiensis</i>	<i>C. mandshurica</i>	<i>Q. mongolica</i>	All seeds	<i>P. koraiensis</i>	<i>C. mandshurica</i>	<i>Q. mongolica</i>
Broad-leaved forest	4.10 ± 3.83	7.19 ± 6.06	3.38 ± 2.30	3.31 ± 3.38	1.53 ± 0.45	1.40 ± 0.31	1.61 ± 0.47	1.10 ± 0.42
Mixed-forest edge	5.31 ± 4.12	4.98 ± 1.48	4.89 ± 4.19	6.11 ± 4.81	1.18 ± 0.48	1.17 ± 0.29	0.94 ± 0.34	1.39 ± 0.52
Mixed forest	5.47 ± 3.55	6.09 ± 4.24	5.29 ± 2.90	1.80 ± 1.60	1.31 ± 0.36	1.23 ± 0.36	1.36 ± 0.35	–
Artificial larch forest	3.39 ± 3.12	3.40 ± 3.88	3.61 ± 2.98	2.13 ± 1.36	1.77 ± 0.68	1.00 ± 0.23	2.17 ± 0.48	1.50 ± 0.31

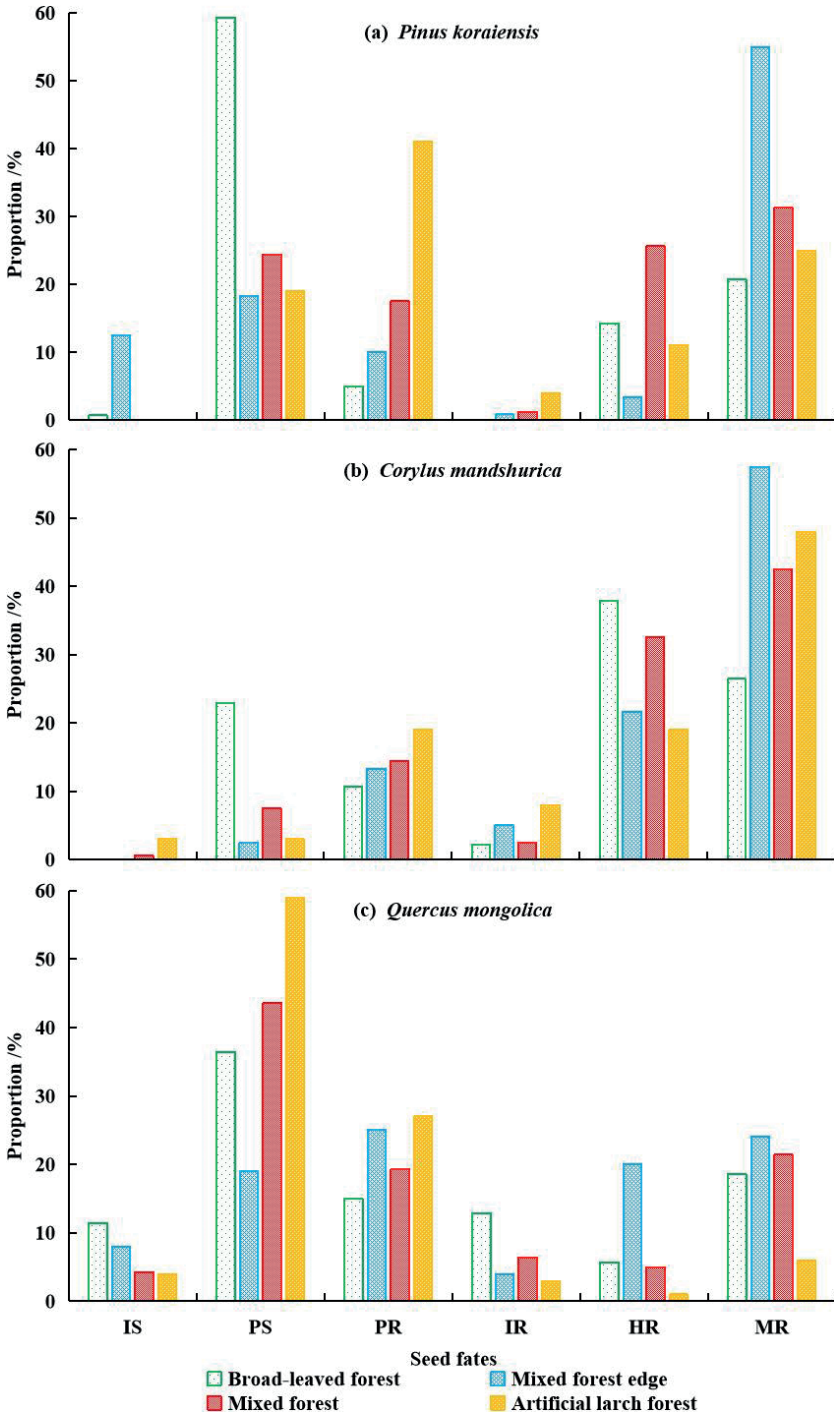


**Figure 2.** Statistics on the fate of three kinds of seeds in different habitats in temperate forests of North-east China. Abbreviations: IS-Intact in situ, PS-Predation in situ, PR-Predation after removal, IR-Intact after removal, HR-Hoarded after removal, MR-Missing after removal.

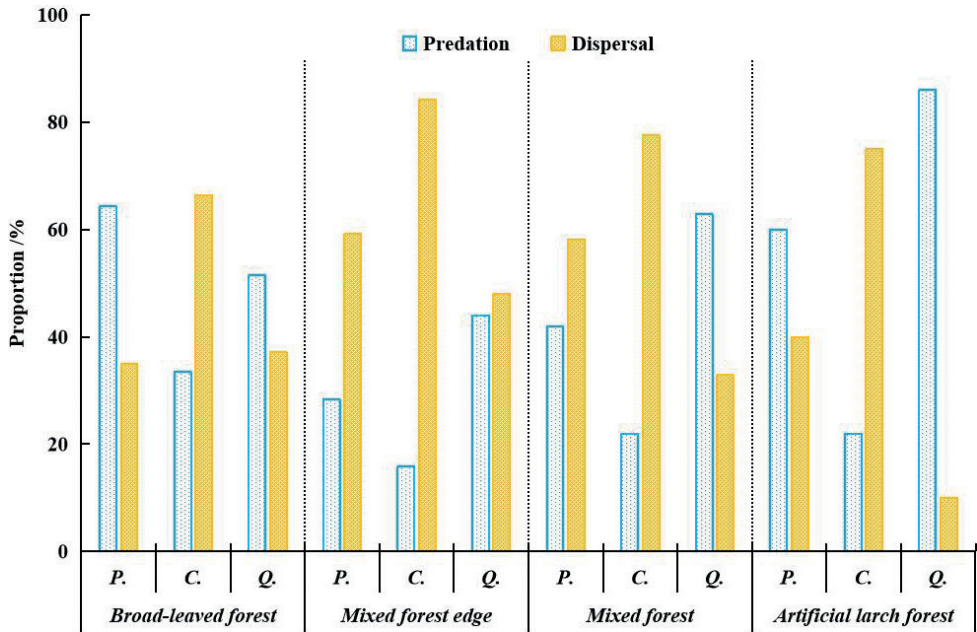


**Figure 3.** Predation rate and dispersal rate of three kinds of seeds in different habitats in temperate forests of Northeast China. Abbreviations: P.- *Pinus koraiensis*, C.- *Corylus mandshurica*, Q.- *Quercus mongolica*.

distances of seeds in the broad-leaved forest were consistent with those in the artificial larch forest. Approximately 44% of the seeds were dispersed within 1–3 m, while approximately 28% of the seeds were dispersed within 3–6 m. In the artificial larch forest, 16.22% were dispersed less than 1 m, and 10.58% were dispersed within 6–9 m in the broad-leaved forests. The rest of the distances were less than 10%.

The dispersal distances of seeds at the mixed-forest edge were consistent with those in the mixed forest. All showed the largest proportion of distances between 3 and 6 m, which accounted for approximately 44%. Dispersal distances of 1–3 m were close to accounting for 17%, while the distance of 6–9 m accounted for 20.83% in the mixed forest, and 12.12% at the mixed-forest edge. The proportion of distances greater than 9 m was less than 10% in both habitats (Fig. 4).

There were significant differences in the dispersal distance between the broad-leaved forest and mixed-forest edge (distance:  $Z = -2.566$ ,  $P < 0.001$ ; depth:  $Z = -3.589$ ,  $P < 0.001$ ), between the broad-leaved forest and mixed forest (distance:  $Z = -3.949$ ,  $P < 0.001$ ; distance:  $Z = -3.341$ ,  $P < 0.001$ ), and between the mixed forest and artificial larch forest (distance:  $Z = -3.811$ ,  $P < 0.001$ ; depth:  $Z = -3.077$ ,  $P < 0.001$ ). The differences in separate comparisons among the other habitats were found to lack significance according to the Mann–Whitney  $U$  test.

There was no significant difference in the dispersal distances of *P. koraiensis* in the four habitats. There were significant differences in the burial depth of *P. koraiensis* in the four habitats (distance:  $\chi^2 = 6.895$ ,  $P = 0.075$ ; depth:  $\chi^2 = 10.151$ ,  $P < 0.05$ ). Both

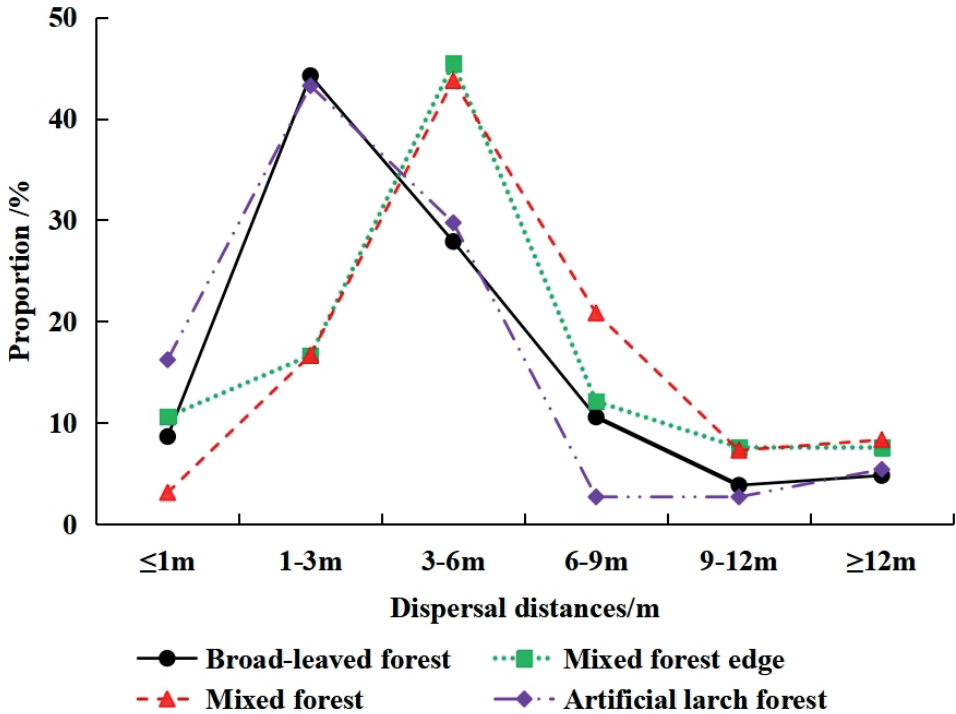


**Figure 4.** Dispersal distance of the seeds in different habitats.

the dispersal distances and burial depth of *C. mandshurica* differed significantly in the four habitats (distance:  $\chi^2 = 16.353$ ,  $P < 0.001$ ; depth:  $\chi^2 = 45.863$ ,  $P < 0.001$ ). The dispersal distances of *Q. mongolica* varied significantly in different habitats, but the difference in burial depth was not significant (distance:  $\chi^2 = 10.306$ ,  $P < 0.05$ ; depth:  $\chi^2 = 1.543$ ,  $P = 0.462$ ).

The burial depth of *C. mandshurica* and the dispersal distances of *Q. mongolica* differed significantly between the broad-leaved forest and mixed-forest edge (*C. mandshurica*:  $Z = -4.413$ ,  $P < 0.001$ ; *Q. mongolica*:  $Z = -2.430$ ,  $P < 0.05$ ).

A comparison of the broad-leaved forest and mixed forest indicated that the burial depth of *P. koraiensis* and the dispersal distance and burial depth of *C. mandshurica* differed significantly (depth of *P. koraiensis*:  $Z = -2.060$ ,  $P < 0.05$ ; distance of *C. mandshurica*:  $Z = -3.985$ ,  $P < 0.001$ ; depth of *C. mandshurica*:  $Z = -2.910$ ,  $P < 0.05$ ).

The broad-leaved forest and the artificial larch forest showed significant differences in the dispersal distance and burial depth of *P. koraiensis*. The burial depth of *C. mandshurica* showed significant differences (distance of *P. koraiensis*:  $Z = -2.314$ ,  $P < 0.05$ ; depth of *P. koraiensis*:  $Z = -2.892$ ,  $P < 0.01$ ; depth of *C. mandshurica*:  $Z = -2.910$ ,  $P < 0.05$ ).

There were significant differences in the dispersal distance of the *P. koraiensis* seeds between the mixed-forest edge and the artificial larch forest and the burial depth of *C. mandshurica* and dispersal distance of *Q. mongolica* (distance of *P. koraiensis*:

$Z = -2.056$ ,  $P < 0.05$ ; depth of *C. mandshurica*:  $Z = -4.833$ ,  $P < 0.01$ ; distance of *Q. mongolica*:  $Z = -2.204$ ,  $P < 0.05$ ).

Comparing the dispersal distance of *P. koraiensis* with that of *C. mandshurica* indicated that there were significant differences. In addition, there were differences in the burial depth of *C. mandshurica* between the mixed forest and the artificial larch forest (distance of *P. koraiensis*:  $Z = -2.401$ ,  $P < 0.05$ ; distance of *C. mandshurica*:  $Z = -2.770$ ,  $P < 0.01$ ; depth of *C. mandshurica*:  $Z = -5.046$ ,  $P < 0.001$ ).

## Discussion

### Factors that influence the rodent feeding strategies

The food availability of rodents in natural environments not only depends on their own feeding input but is also affected by various factors in the habitat (Vander Wall 2001; Lichti et al. 2015; Li et al. 2018, 2021). The availability of food resources (amount and form of distribution) is a central factor that influences the feeding strategy of rodents, which is an adaptation to the changes in food resources. The amount of food available to the rodents depends on the probability of encountering it, and the rodents adjust their feeding strategy by weighing the costs, such as time invested and search range, and the benefits in search for food based on the potential abundance and distribution of food resources in the environment (Vander Wall 2010; Wang et al. 2012). The niche breadth theory postulates that the width of ecological niche increases and generalizes that when there are few available resources, the animal decreases its search for the current resource and specializes where there are abundant available resources (Yang et al. 2011). Thus, foragers shift from selective to opportunistic feeding behaviour as the availability of food decreases.

### Habitat differences in rodent storage strategies

Different habitats have varying characteristics, and the differences in habitat characteristics affect the composition and structure of plant communities, spatial and temporal patterns, seclusion conditions, and food resources in the habitat (Xiao et al. 2005, 2006; Chang et al. 2008; Vander Wall 2010), which all affect the odds of animals encountering seeds. The amount of food resources and their distribution in the habitat leads to differences in the time and energy required to search for and process food, and animals will change their range of activity depending on the availability of food resources. Habitat heterogeneity also alters intra- or interspecific competition patterns by affecting the density and distribution of rodents, which, in turn, affects the ability of rodent to feed on and disperse seeds (Cao et al. 2016; Zhang et al. 2017).

The results showed that there was a significant difference in when the food was first discovered and the rate and time of consumption of rodents in the four habitats,

which reflects the influence of different habitat characteristics. The ratio of feeding to dispersal is the result of the trade-off between the food availability, competition, or predation risk of rodents and the result of optimizing resource acquisition. The results of this study suggest that the habitat characteristics of the mixed-forest edge and larch plantation seem to be relatively special. They appear to be quite different from most forest habitats in vegetation composition and structure, community appearance, and understory microhabitat characteristics, so there are many obvious differences in the study results.

The seed residuals were higher; fewer seeds were taken; the rate of dispersal was the highest, and the consumption time was the slowest in mixed-forest edge habitats. This could be owing to the effects of high species diversity and interspecific competition in the community edge effect, and the low number of trees that result in poorly concealed open habitats and a high risk of predation. Animals adopt strategies to carry stored seeds to reduce the competition and risk of predation, and at a higher risk of predation, they adjust their behavioural strategies, such as becoming increasingly vigilant and reducing foraging (Jonsson et al. 2000; Jansen et al. 2006; Randall and Boltas 2011). It is definitely a sound strategy to sacrifice some food resources to ensure safety.

In the artificial larch forest, not only do animals meet seeds at the earliest, but 50% of the consumption time is significantly shorter. Thus, it takes only approximately half the time of other habitats to find food. Since the vegetation species is single and dense with high cover, the branches are interspersed and good at concealing the rodents. However, the food resources are not abundant, and rapid feeding or dispersal is an effective way to occupy more resources. Such a feeding response is consistent with the rapid isolation hypothesis.

The slowest rate of *Q. mongolica* depletion in the broad-leaved forest could be mostly owing to the fact that *Q. mongolica* is the dominant species in the habitat vegetation, and the seed resources are abundant on the scattered surface. Thus, the animals prefer these seeds when there are multiple seeds that are equally available.

## Conclusions

Rodent feeding and storage strategies differ significantly between habitats. Different habitats are significantly heterogeneous, which leads to significantly different strategies for seed consumption in rodents. The quickest consumption occurs in the artificial larch forest, the slowest at the mixed-forest edge, and the rate of consumption in the broad-leaved forest and mixed forest are close to that of the mixed-forest edge.

Rodents can identify different seed properties of the sympatric distribution and form distinct feeding preferences. Rodents adopt different feeding or storage methods, causing the seeds to have different fates. The seeds of *Q. mongolica* are the mostly strongly preferred for consumption. More seeds of *P. koraiensis* are eaten and stored, and the seeds of *C. mandshurica* are stored the most frequently.

## Acknowledgements

This research was funded by the Natural Science Foundation of Heilongjiang Province of China (SS2021C006), the Science Research Project of Mudanjiang Normal University (GP2021006), and the Science Research Project of the Education Department of Heilongjiang Province (1451PT007). We are grateful to the people who helped collect behavioural data in Sandao forest farm. We thank the anonymous reviewers for their constructive comments on the manuscript. We thank Zhulin Han, Man Jiang, and LEXIS (Scientific editorial experts, United States, LEXIS Academic Service, LLC) for its linguistic assistance during the preparation of this manuscript.

## References

- Cao L, Guo C, Chen J (2016) Fluctuation in seed abundance has contrasting effects on the fate of seeds from two rapidly germinating tree species in an Asian tropical forest. *Integrative Zoology* 12(1): 2–11. <https://doi.org/10.1111/1749-4877.12213>
- Chang G, Xiao Z, Zhang Z (2008) Effect of seed size on hoarding behavior of Edward's long-tailed rats (*Leopoldamys edwardsi*). *Acta Theriologica Sinica* 28: 37–41. <https://doi.org/10.1098/rstb.2009.0205> [in Chinese]
- Jansen PA, Bongers F, Prins H (2006) Tropical rodents change rapidly germinating seeds into long-term food Supplies. *Oikos* 113: 449–458. <https://doi.org/10.1111/j.2006.0030-1299.14461.x>
- Jenkins SH (2011) Sex differences in repeatability of food-hoarding behaviour of kangaroo rats. *Animal Behaviour* 81(6): 1155–1162. <https://doi.org/10.1016/j.anbehav.2011.02.021>
- Jonsson P, Koskela E, Mappes T (2000) Does risk of predation by mammalian predators affect the spacing behaviour of rodents? Two large-scale experiments. *Oecologia* 122(4): 487–492. <https://doi.org/10.1007/s004420050970>
- Li HJ, Zhang ZB (2003) Effect of rodents on acorn dispersal and survival of the Liaodong oak (*Quercus liaotungensis* Koidz.). *Forest Ecology and Management* 176(1–3): 387–396. [https://doi.org/10.1016/S0378-1127\(02\)00286-4](https://doi.org/10.1016/S0378-1127(02)00286-4)
- Li DW, Jin ZM, Yang CY, Yang CW, Zhang MH (2018) Scatter-hoarding the seeds of sympatric forest trees by *Apodemus peninsulae* in a temperate forest in northeast China. *Polish Journal of Ecology* 66(4): 382–394. <https://doi.org/10.3161/15052249PJE2018.66.4.006>
- Li DW, Hao JW, Yao X, Liu Y, Peng T, Jin ZM, Meng FX (2020) Observations of the foraging behavior and activity patterns of the Korean wood mouse, *Apodemus peninsulae*, in China, using infra-red cameras. *ZooKeys* 992: 139–155. <https://doi.org/10.3897/zookeys.992.57028>
- Li DW, Liu Y, Shan HJ, Li N, Hao JW, Yang BB, Peng T, Jin ZM (2021) Effects of season and food on the scatter-hoarding behavior of rodents in temperate forests of Northeast China. *ZooKeys* 1025: 73–89. <https://doi.org/10.3897/zookeys.1025.60972>
- Lichti NI, Steele MA, Swihart RK (2015) Seed fate and decision-making processes in scatterhoarding rodents. *Biological Reviews of the Cambridge Philosophical Society* 92(1): 474–504. <https://doi.org/10.1111/brv.12240>

- Lu J, Zhang Z (2005) Food hoarding behaviour of large field mouse *Apodemus peninsulae*. *Acta Theriologica* 50(1): 51–58. <https://doi.org/10.1007/BF03192618>
- Luna CA, Loayza AP, Squeo FA (2016) Fruit size determines the role of three scatter-hoarding rodents as dispersers or seed predators of a fleshy-fruited Atacama Desert Shrub. *PLoS ONE* 11(11): e0166824. <https://doi.org/10.1371/journal.pone.0166824>
- Preston SD, Jacobs LF (2005) Cache decision making: The effects of competition on cache decisions in Merriam's kangaroo rat (*Dipodomys merriami*). *Journal of Comparative Psychology* 119(2): 187–196. <https://doi.org/10.1037/0735-7036.119.2.187>
- Randall JA, Boltas KD (2001) Assessment and defence of solitary kangaroo rats under risk of predation by snakes. *Animal Behaviour* 61(3): 579–587. <https://doi.org/10.1006/anbe.2000.1643>
- Vander Wall SB (1990) *Food Hoarding in Animals*. University of Chicago Press, Chicago, 445 pp.
- Vander Wall SB (2001) The evolutionary ecology of nut dispersal. *Botanical Review* 67(1): 74–117. <https://doi.org/10.1007/BF02857850>
- Vander Wall SB (2003) Effects of seed size of wind-dispersed pines (*Pinus*) on secondary seed dispersal and the caching behavior of rodents. *Oikos* 100(1): 25–34. <https://doi.org/10.1034/j.1600-0706.2003.11973.x>
- Vander Wall SB (2010) How plants manipulate the scatter-hoarding behaviour of seed-dispersing animals. *Philosophical Transactions of the Royal Society of London* 365(1542): 989–997. <https://doi.org/10.1098/rstb.2009.0205>
- Vander Wall SB, Beck MJ (2011) A comparison of frugivory and scatter-hoarding seed-dispersal syndromes. *Botanical Review* 78(1): 10–31. <https://doi.org/10.1007/s12229-011-9093-9>
- Wang B, Ye C-X, Cannon CH, Chen J (2012) Dissecting the decision making process of scatter-hoarding rodents. *Oikos* 122(7): 1027–1034. <https://doi.org/10.1111/j.1600-0706.2012.20823.x>
- Willson MF, Whelan CJ (1990) Variation in postdispersal survival of vertebrate-dispersed seeds: Effects of density, habitat, location, season, and species. *Oikos* 57(2): 191–198. <https://doi.org/10.2307/3565939>
- Xiao Z, Zhang Z, Wang Y (2005) Effects of seed size on dispersal distance in five rodent-dispersed fagaceous species. *Acta Oecologica* 28(3): 221–229. <https://doi.org/10.1016/j.actao.2005.04.006>
- Xiao Z, Wang Y, Harris M, Zhang Z (2006) Spatial and temporal variation of seed predation and removal of sympatric large-seeded species in relation to innate seed traits in a subtropical forest, Southwest China. *Forest Ecology and Management* 222(1–3): 46–54. <https://doi.org/10.1016/j.foreco.2005.10.020>
- Yang Y, Yi X, Yu F (2011) Repeated radicle pruning of *Quercus mongolica* acorns as a cache management tactic of Siberian chipmunks. *Acta Ethologica* 15(1): 9–14. <https://doi.org/10.1007/s10211-011-0102-0>
- Zhang H, Chu W, Zhang Z (2017) Cultivated walnut trees showed earlier but not final advantage over its wild relatives in competing for seed dispersers. *Integrative Zoology* 12(1): 12–25. <https://doi.org/10.1111/1749-4877.12242>



# A new species of the genus *Cephalodella* (Rotifera, Monogononta) from Korea, with reports of four additional cephalodellid species

Hee-Min Yang<sup>1</sup>, Gi-Sik Min<sup>1</sup>

<sup>1</sup> Department of Biological Sciences and Bioengineering, Inha University, Incheon 22212, Republic of Korea

Corresponding author: Gi-Sik Min ([mingisik@inha.ac.kr](mailto:mingisik@inha.ac.kr))

---

Academic editor: Pavel Stoev | Received 2 August 2022 | Accepted 30 December 2022 | Published 23 January 2023

---

<https://zoobank.org/22AFCBD8-6E4B-4C03-B525-1643237FE073>

---

**Citation:** Yang H-M, Min G-S (2023) A new species of the genus *Cephalodella* (Rotifera, Monogononta) from Korea, with reports of four additional cephalodellid species. ZooKeys 1141: 185–199. <https://doi.org/10.3897/zookeys.1141.91147>

---

## Abstract

A new monogonont rotifer, *Cephalodella binoculata* **sp. nov.**, was described from a soil sample collected in Korea. The new species is morphologically similar to *C. carina* but is distinguished by having two frontal eyespots, a vitellarium with eight nuclei, and the shape of its fulcrum. We also described four other cephalodellid species collected in Korea; *Cephalodella auriculata*, *C. catellina*, *C. gracilis*, and *C. tinca*. Of these four species, *C. gracilis* and *C. tinca* were newly recorded in Korea. We provided the morphological characteristics of the five *Cephalodella* species along with photographs of trophi observed with a scanning electron microscope. Furthermore, we provided the mitochondrial cytochrome *c* oxidase subunit I gene sequences of the five species.

## Keywords

COI, morphology, new records, Notommatidae, rotifers, SEM, taxonomy

## Introduction

The genus *Cephalodella* Bory de St. Vincent, 1826 is one of the most species-rich taxa in the phylum Rotifera Cuvier, 1817, containing 171 species worldwide (Segers 2007; Jersabek and Leitner 2013). This taxon is easily found in various environments but is difficult to distinguish due to its morphological similarity and fragile external characteristics (Jersabek et al. 2011). Like other taxa of Rotifera, *Cephalodella* has been mainly studied in Europe,

and their biology, ecology, and variability are not well known because of the lack of research (Nogrady and Pourriot 1995).

In Korea, a total of seven cephalodellid species have been recorded: *Cephalodella auriculata* (Müller, 1773), *C. catellina* (Müller, 1786), *C. forficula* (Ehrenberg, 1838), *C. gibba* (Ehrenberg, 1830), *C. hoodii* (Gosse, 1886), *C. innesi* Myers, 1924, and *C. ventripes* (Dixon-Nuttall, 1901) (Yamamoto 1953; Turner 1986; Song and Jin 2000; Song 2014; Song 2018; National Institute of Biological Resources 2022). Including the genus *Cephalodella*, studies on the species diversity of the family Notommatidae Hudson & Gosse, 1886 in Korea are insufficient. More than 250 species of notommatid rotifers have been recorded worldwide, but in Korea, only 16 species have been recorded so far (Song and Jin 2000; National Institute of Biological Resources 2022). Korea has a diverse climate and habitat compared to its territorial size; thus, it is expected that many notommatid rotifers will be discovered through continuous study (Republic of Korea 2014).

In this study, we identified five cephalodellid rotifers, one of which was a new species. Two species, *Cephalodella gracilis* (Ehrenberg, 1830) and *C. tinca* Wulfert, 1937 were newly recorded in Korea and two others, *C. auriculata* and *C. catellina*, have previously been recorded in Korea. However, since the first reported paper on rotifers in Korea (Turner, 1986) did not include descriptions for these two species, we have described the two Korean specimens in this study. Here, we provide the morphological characteristics of the five species along with the photographs of trophi observed with scanning electron microscope (SEM). In addition, we deciphered the mitochondrial cytochrome *c* oxidase subunit I (COI) gene sequences of the five species.

## Materials and methods

Specimens were collected and isolated from a pond, reservoir and soil samples (Fig. 1). The rotifers inhabiting pond and reservoir were collected using a 50- $\mu$ m mesh plankton net and transferred to the laboratory alive. In case of soil sample treatment, we dried the soil samples at room temperature for several weeks and rewetted them using mineral water in a plant culture dish (310100, SPL Life Science, Korea). After hatching of the rotifers, they were isolated in a new plant culture dish under a stereo microscope (SZX7, Olympus, Japan) and stored in an incubator at 20 °C. Before the observation and preservation of living rotifers, a few drops of 1% bupivacaine solution (B5274, Sigma-Aldrich, USA) were used for anesthesia. The specimens were then observed under an optical microscope (DM2500, Leica, Germany) at magnifications of  $\times$ 400–1000. Photographs and videos of the specimens were obtained using a digital camera (EOS 6D Mark II, Canon, Japan) mounted on an optical microscope. Trophi were isolated using commercial bleach containing 4–5% NaClO (Yuhan-Clorox, Korea) and prepared for SEM following the methods of De Smet (1998). Two SEM instruments, SU8010 and S-4300SE (Hitachi, Japan), were used for observation at an accelerating voltage of 7–10 kV. External characteristics and trophi elements were measured using ImageJ 1.53k (<https://imagej.nih.gov/ij/>) (Abràmoff et al. 2004).



**Figure 1.** Map showing the collection sites of the rotifers in this study 1 *Cephalodella auriculata* (Müller, 1773) 2 *C. binocolata* sp. nov. 3 *C. tinca* Wulfert, 1937 4 *C. gracilis* (Ehrenberg, 1830) 5 *C. catellina* (Müller, 1786).

Morphological identification of rotifers was based on descriptions of Koste (1978), Nogrady and Pourriot (1995), and Jersabek and Leitner (2013). All specimens described in this study were deposited at the National Institute of Biological Resources (NIBR), Korea.

Genomic DNA was extracted using a LaboPass™ Tissue Genomic DNA Isolation Kit Mini (Cosmo Genetech, Korea). Partial COI gene was amplified using the 30F/885R primers (Zhang et al. 2021). The PCR amplifications were conducted in a final volume of 25µL under the following conditions: 2 min at 95 °C for the initial denaturation, followed by 40 cycles of 95 °C for 15 s, 51 °C for 30 s, 72 °C for 1 min, and a final extension

at 72 °C for 5 min. In the case of *C. auriculata* and *C. tinca*, the primer sets mlCOIintF/jgHCO2198 (Leray et al. 2013) and LCO1490/HCO2198 (Folmer et al. 1994) were used at an annealing temperature of 45 °C. PCR products were visualized by 1% agarose gel electrophoresis, and purified using a LaboPass™ PCR Purification Kit (Cosmo Genetech). DNA sequencing was performed at Macrogen (Korea), and the sequences were trimmed and aligned using Geneious ver. 8.1.9 (<https://www.geneious.com>). Genetic distance was calculated using MEGA ver. 11 with the Kimura 2-parameter model (K2P) (Tamura et al. 2021). All the extracted DNAs of the five species were deposited at the NIBR, and COI sequences were uploaded to GenBank.

The maximum-likelihood (ML) tree was inferred based on the partial COI gene sequences of 11 notommatid species and one euchlanid species (Table 1). The ML tree was constructed using IQ-TREE ver. 1.6.12, with the GTR+I+G model and 1000 replicates (Nguyen et al. 2015; Kalyaanamoorthy et al. 2017).

**Table 1.** List of species for which COI sequence data was used for molecular analysis.

Family	Species	GenBank No.	Reference
Notommatidae	<i>Cephalodella binoculata</i> sp. nov.	ON898529 (759 bp)	This study
	<i>Cephalodella auriculata</i> (Müller, 1773)	ON898533 (315 bp)	
	<i>Cephalodella catellina</i> (Müller, 1786)	ON898532 (759 bp)	
	<i>Cephalodella gracilis</i> (Ehrenberg, 1830)	ON898535 (759 bp)	
	<i>Cephalodella tinca</i> Wulfert, 1937	ON898534 (660 bp)	
	<i>Cephalodella</i> cf. <i>gibba</i> (Ehrenberg, 1830)	JX216594 (661 bp)	García-Morales and Elías-Gutiérrez (2013)
	<i>Eothimia elongata</i> (Ehrenberg, 1832)	DQ079964 (660 bp)	Sørensen et al. (2006)
	<i>Eospora ehrenbergi</i> Weber, 1918	HQ444173 (646 bp)	Curini-Galletti et al. (2012)
	<i>Notommata allantois</i> Wulfert, 1935	MT521624 (661 bp)	Fontaneto et al. (2021)
	<i>Notommata codonella</i> Harring & Myers, 1924	DQ297785 (660 bp)	Sørensen and Giribet (2006)
Euchlanidae (Outgroup)	<i>Pleurotrocha petromyzon</i> Ehrenberg, 1830	EU499803 (583 bp)	Swanstrom et al. (2011)
	<i>Euchlanis dilatata</i> Ehrenberg, 1830	JX216599 (661 bp)	García-Morales and Elías-Gutiérrez (2013)

## Results and discussion

In the present study, we identified five cephalodellid species in Korea; *C. auriculata*, *C. binoculata* sp. nov., *C. catellina*, *C. gracilis*, and *C. tinca*. The new species, *C. binoculata* sp. nov., was distinguished from other cephalodellid species by a combination of the following characteristics: two distinct frontal eyespots, short tail and toes, vitellarium with eight nuclei, and the shape of the trophi components. Two species, *C. gracilis* and *C. tinca* were newly recorded in Korea. *Cephalodella gracilis* is a common species worldwide. However, the morphological characteristics of *C. gracilis* have been reported to exhibit high morphological variation (Nogrady and Pourriot 1995), and it is necessary to re-examine these characteristics through morphological redescription and molecular analysis. *Cephalodella tinca* is probably a cosmopolitan species and has been recorded in the Australian, Neotropical, Oriental, and Palearctic regions (Segers 2007). The remaining two species, *C. auriculata* and *C. catellina* were recorded in Korea by Turner (1986) as a species list without description. Therefore, we

described the Korean specimens of the two species and provided photographs of the trophi observed using SEM.

In this study, we obtained partial COI sequences from each of the five species and constructed an ML tree using the sequences of 11 notommatid rotifers and one euchlanid rotifer. The sequence of *Euchlanis dilatata* Ehrenberg, 1830 was used as the outgroup. The final length of the sequence alignment was 561 bp, and the genetic distance between the notommatid species was 0.172–0.412 (Table 2). The species in the genus *Cephalodella* formed a monophyletic group, with a support value of 100 (Fig. 7). The new species, *C. binocolata* sp. nov., formed a clade with *C. auriculata* and *C. gracilis* and was located closest to *C. auriculata*. However, the phylogenetic relationships between species within the *Cephalodella* was not clearly revealed when compared using morphological characteristics. Although more than 170 morphospecies of the genus *Cephalodella* have been recorded worldwide (Nogrady and Pourriot 1995; Segers 2007; Jersabek and Leitner 2013), only seven sequences from two species, *C. forficula* and *C. gibba*, have been registered in GenBank. For the phylogenetic study of cephalodellid rotifer species, further acquisition and analysis of the COI sequences and nuclear gene sequences such as 18S ribosomal RNA or internal transcribed spacer (ITS), is required.

## Systematic account

**Phylum Rotifera Cuvier, 1817**

**Class Eurotatoria De Ridder, 1957**

**Subclass Monogononta Plate, 1889**

**Order Ploima Hudson & Gosse, 1886**

**Family Notommatidae Hudson & Gosse, 1886**

**Genus *Cephalodella* Bory de St. Vincent, 1826**

***Cephalodella binocolata* sp. nov.**

<https://zoobank.org/D9C8E9C8-55AD-4E49-A7A7-713E3B413D78>

**Material examined. Type locality.** Soil from Incheon, Republic of Korea (37°24.788'N, 126°44.738'E), 19 Jun. 2019, Kyu-Seok Chae leg. **Holotype.** 1 female, glycerol permanent slide, NIBRIV0000896982. **Paratype.** 2 female, glycerol permanent slides, NIBRIV0000896983, NIBRIV0000896984; trophi preparation for SEM, NIBRIV0000896985.

**Differential diagnosis.** *Cephalodella binocolata* sp. nov. was most similar to *C. carina* Wulfert, 1959 in terms of frontal eyes, type B virgate trophi, dorsally curved toes, total length/toe length ratio, and short tail. The new species, however, was distinguished from *C. carina* by the following characteristics: (1) the new species has two distinct eyespots, whereas *C. carina* has one small eyespot; (2) the vitellarium of the new species contains eight nuclei, while that of *C. carina* contains six; and (3) the fulcrum of the new species is straight and without extension at the distal end, while the fulcrum of *C. carina* is thicker at the distal end.

**Table 2.** Genetic distance of notommatid species and outgroup (K2P distance).

Species	GenBank No.	1	2	3	4	5	6	7	8	9	10
<i>Cephalodella binoculata</i> sp. nov.	ON898529										
<i>Cephalodella auriculata</i>	ON898533	0.251									
<i>Cephalodella catellina</i>	ON898532	0.274	0.335								
<i>Cephalodella gracilis</i>	ON898535	0.229	0.312	0.282							
<i>Cephalodella tinca</i>	ON898534	0.243	0.321	0.267	0.293						
<i>Cephalodella</i> cf. <i>gibba</i>	JX216594	0.297	0.412	0.323	0.289	0.293					
<i>Eothinia elongata</i>	DQ079964	0.293	0.374	0.349	0.363	0.331	0.373				
<i>Eosphora ehrenbergi</i>	HQ444173	0.321	0.386	0.327	0.306	0.319	0.351	0.309			
<i>Notommata allantois</i>	MT521624	0.235	0.385	0.312	0.307	0.296	0.340	0.262	0.207		
<i>Notommata codonella</i>	DQ297785	0.237	0.347	0.324	0.313	0.283	0.346	0.310	0.229	0.172	
<i>Pleurotrocha petromyzon</i>	EU499803	0.327	0.369	0.364	0.345	0.374	0.363	0.303	0.301	0.278	0.317

The new species also resembles *C. gibboides* Wulfert, 1951 and *C. graciosa* Wulfert, 1956. However, it is distinguished from *C. gibboides* by the shape of its manubrium and tail length. The manubrium of *C. gibboides* has a bump in the middle with no basal lamellae, whereas the new species has basal lamellae in the manubrium and no bumps in the middle. The shape of the distal end of the manubrium also differed between the two species. The tail of *C. gibboides* covers the foot, whereas that of the new species is short. The new species is distinguished from *C. graciosa* in several morphological characteristics as follows: (1) the trophi of the new species is symmetrical, while that of *C. graciosa* is asymmetrical; (2) the manubrium of the new species has basal lamellae, while that of *C. graciosa* does not; (3) the new species has two eyespots, while *C. graciosa* has one eyespot; and (4) the new species has eight nuclei in the vitellarium, while *C. graciosa* has six.

**Description. Female.** Body moderately elongated and not laterally compressed (Figs 2, 3A, B). Dorsal and ventral margins slightly convex; posterior third of trunk gradually tapered to the foot. Lorica soft, transparent, and comprised of three body plates. Dorsal and ventral plates separated by narrow lateral sulci. Tail short and rounded. Head large, almost one-quarter of the total length. Head and trunk clearly distinguished by the neck fold. Corona oblique, convex, without lips. Dorsal antenna located near the junction of the head and trunk. Foot trapezoidal shape and moderate size, approximately 15% of the total length. Foot widest at the front and narrowed toward the back. Caudal setae absent. Short tail covered only part of the foot. Toes symmetrical and short, accounting for 16–17% of the total length. Toes smoothly tapered to posterior end, without any spines. In the lateral view, toes curved dorsally. In the dorsal view, toes always curved outwards. Saccate large brain extending over the neck fold. No retrocerebral organ. Two distinct red eyespots located in front of the head (Fig. 3C). Distance between the two eyespots far and clear. Mastax large, with elongated salivary gland. Esophagus thin, passing between the brain and mastax. Gastric glands large, oval shaped, containing round granules, and located in the antero-dorsal part of the stomach (Fig. 3D). Stomach colorless and indistinctly separated from the intestine. Anus located near the posterior end of the foot. Bladder round and large when fully

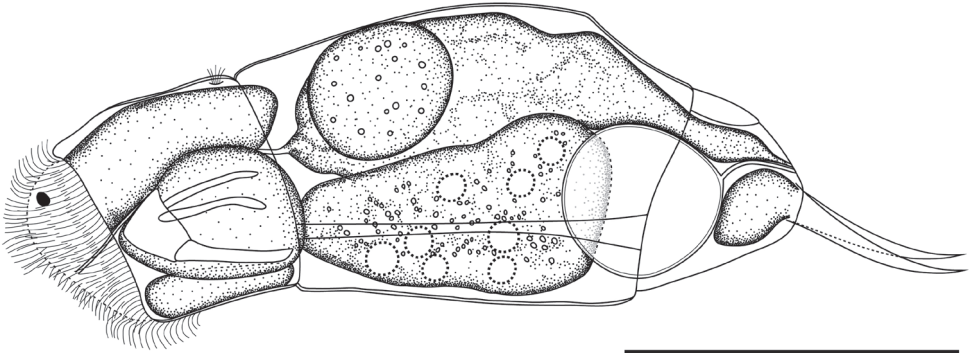


**Figure 2.** Line drawing of *Cephalodella binocolata* sp. nov., lateral view. Scale bar: 50  $\mu$ m.

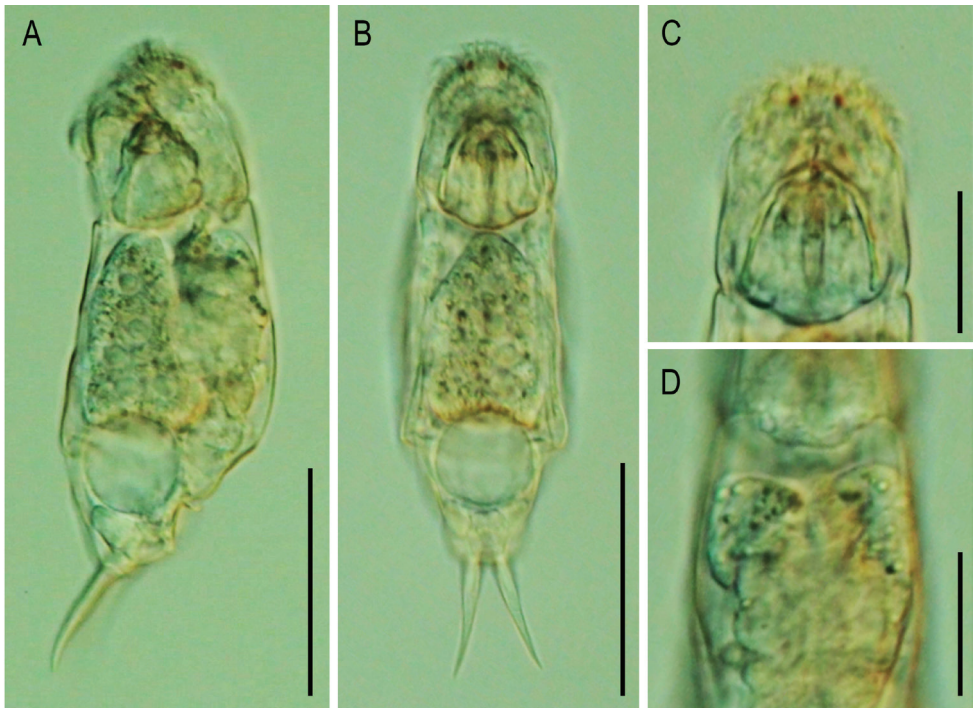


**Figure 3.** Live specimen of *Cephalodella binocolata* sp. nov. observed under the optical microscope **A** lateral view **B** ventral view **C** eyespots **D** neck region and gastric glands, dorsal view. Scale bars: 50  $\mu$ m (**A, B**); 20  $\mu$ m (**C, D**).

filled. Vitellarium large with eight nuclei. Pedal glands short, sac-shaped. Trophi virgate, type B (see Fischer and Ahlrichs 2011), almost symmetrical (Fig. 4A). Rami with no alulae on posterior end (Fig. 4C). Basal chamber of rami wide, left side relatively larger than right at distal end. Shape of the subbasal chamber foramina also slightly asymmetrical; both foramina oval shaped, but the right foramen larger in length. Inner

margin of rami with two distinct teeth and several comb-like teeth (Fig. 4C). Fulcrum long and straight in the ventral view (Fig. 4A). Terminal end of fulcrum simple, without any thickening or expanded shape. In the lateral view, the ventral margin straight and relatively thick (Fig. 4B). No basal apophysis on fulcrum. Uncus with a large, single tooth. Manubria symmetrical. Each manubrium with a basal lamella, the length of which was approximately half of that of the manubrium (Fig. 4D). Middle part of the manubrium with oblong-shaped foramina. Shaft of the manubrium thick and straight in lateral view; while terminal end curved inward in ventral view. Terminal end crutch-shaped, dorsal side stubby, ventral side pointed and curved upwards (Fig. 4B, D).

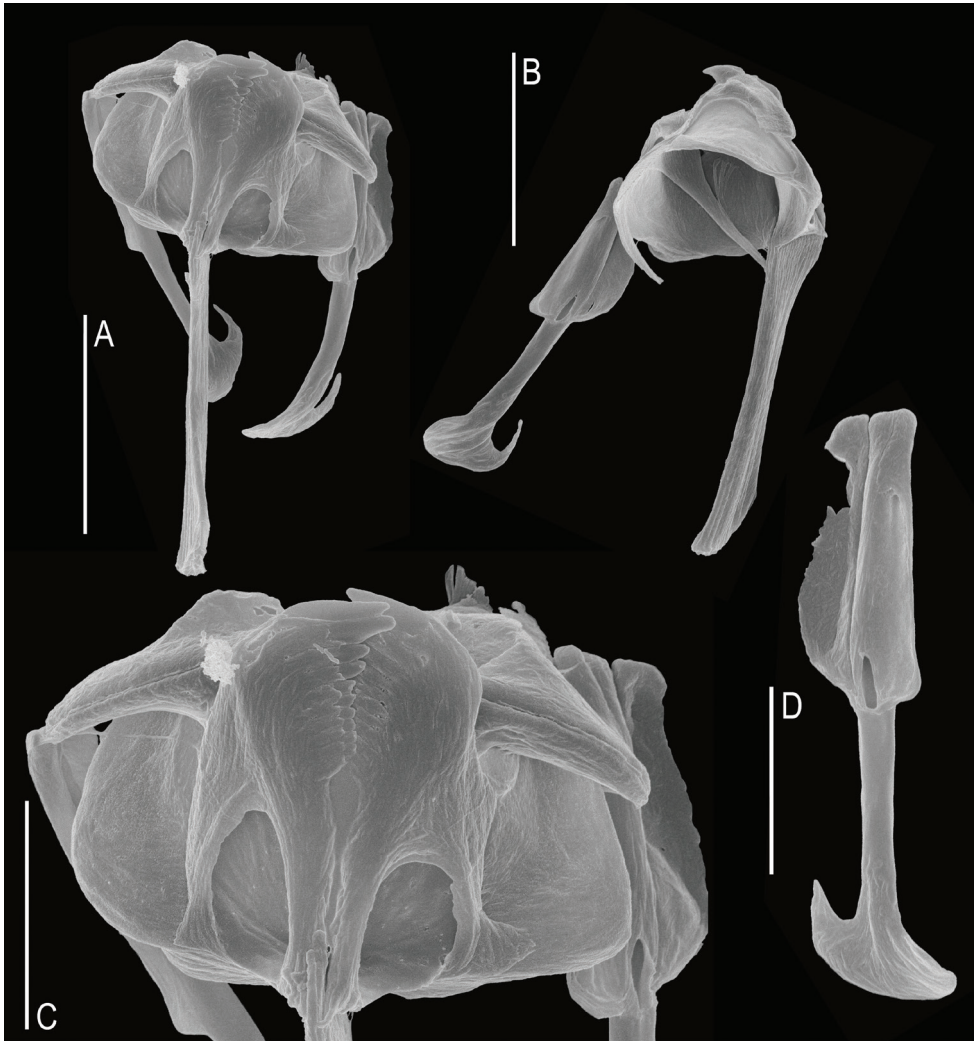


**Figure 4.** SEM image of the trophi of *Cephalodella binocolata* sp. nov. **A** ventral view **B** dorsolateral view **C** detail rami and unci, ventral view **D** detail manubrium, lateral view. Scale bars: 10  $\mu\text{m}$  (**A**, **B**); 5  $\mu\text{m}$  (**C**, **D**).

Characteristics of male and eggs remain unknown.

**Measurement.** Total length 134–155  $\mu\text{m}$ , toe 26–29  $\mu\text{m}$ , trophi 24–28  $\mu\text{m}$ , ramus 8–9  $\mu\text{m}$ , fulcrum 15–17  $\mu\text{m}$ , manubrium 14–17  $\mu\text{m}$ .

**Etymology.** The specific name, *binoculata*, derived from the Latin word *bi*, meaning “two” and *oculata*, meaning “eyed”.

**Molecular data.** Partial COI sequences were obtained from three specimens of *C. binoculata* sp. nov. (NIBR deposit numbers, NIBRGR0000649735–NIBRGR0000649737; GenBank accession numbers, ON898529–ON898531).

### *Cephalodella auriculata* (Müller, 1773)

**Material examined.** Pond in Incheon Metropolitan City, Republic of Korea (37°27.020'N, 126°39.345'E), 2 Dec. 2021, Hee-Min Yang leg. NIBRIV0000896986, 1 female, glycerol permanent slide.

**Remarks.** The morphological characteristics of the Korean specimens generally corresponded to those reported in a previous study (Nogrady and Pourriot 1995). The body was soft and stout, 110–130  $\mu\text{m}$  in length (Fig. 5C). The head was large and as wide as the body. Foot was short and wide. The toes were short, 23–28  $\mu\text{m}$  in length. The two toes were equal in length and curved ventrally. One red cerebral eye was located at the posterior end of the saccate brain. The vitellarium had eight nuclei. Trophi was symmetrical and virgate type A, 30  $\mu\text{m}$  in length (Fig. 6A). The fulcrum was long and straight. The manubrium was thin and curved. The rami of Korean specimen had blunt teeth at the apical part, whereas the specimens of previous studies had no teeth at the apical part (Koste and Shiel 1991; Nogrady and Pourriot 1995).

**Molecular data.** Partial COI sequence was obtained from one Korean specimen (NIBR deposit number, NIBRGR0000649738; GenBank accession number, ON898533).

### *Cephalodella catellina* (Müller, 1786)

**Material examined.** Reservoir in Wanju-gun, Jeollabuk-do, Republic of Korea (35°50.196'N, 127°00.975'E), 27 Mar. 2022, Hee-Min Yang leg. NIBRIV0000896987, 1 female, glycerol permanent slide.

**Remarks.** Korean specimens of *C. catellina* had morphological characteristics that were generally consistent with those reported in previous studies (Koste and Shiel 1991; Nogrady and Pourriot 1995). The body was short and stout, and 100  $\mu\text{m}$  in length (Fig. 5D). The posterior end of the body bulging. The head was large and approximately one-third of its total length. The foot and toes were located ventrally. The two toes were short and symmetrical, 12–16  $\mu\text{m}$  in length (Fig. 6C). The two frontal eyes were red. The vitellarium had eight nuclei. The salivary glands were located under the mastax. Trophi was asymmetrical, virgate type C, and 25  $\mu\text{m}$  in length. The fulcrum was

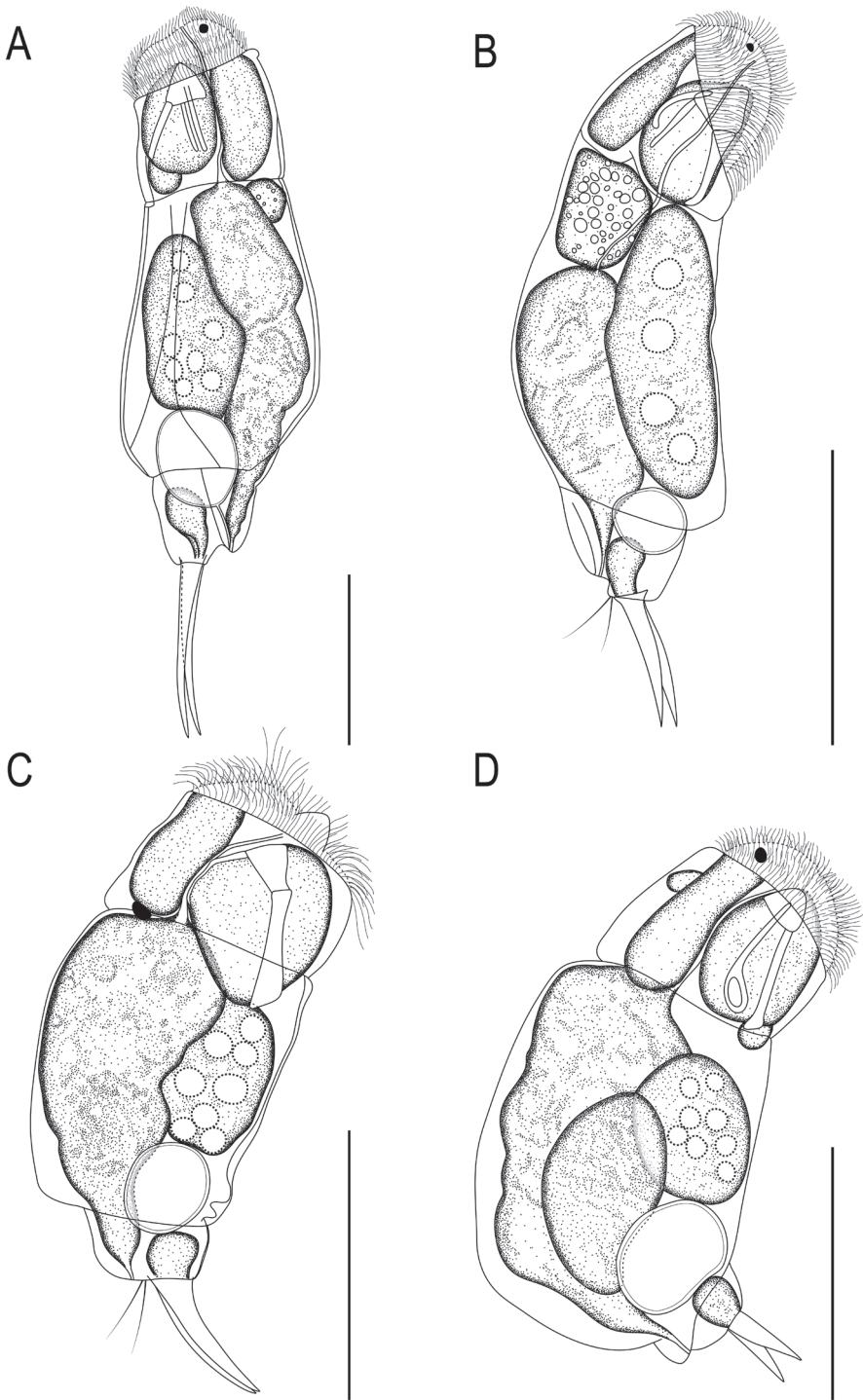


**Figure 5.** Line drawing of cephalodellid rotifers **A** *Cephalodella tinca* Wulfert, 1937 **B** *C. gracilis* (Ehrenberg, 1830) **C** *C. auriculata* (Müller, 1773) **D** *C. catellina* (Müller, 1786). Scale bars: 50  $\mu\text{m}$ .

straight and long, with a slightly expanded distal end. The manubria were asymmetrical and curved inward. The right manubrium was larger than left manubrium. Distal ends of both manubria had incomplete loop. The right ramus had tooth-like alula.

**Molecular data.** Partial COI sequence was obtained from one Korean specimen (NIBR deposit number, NIBRGR0000649739; GenBank accession number, ON898532).

### *Cephalodella gracilis* (Ehrenberg, 1830)

**Material examined.** Soil from Cheonan-si, Chungcheongnam-do, Republic of Korea (36°54.095'N, 127°12.380'E), 22 Jun. 2019, Hee-Min Yang leg. NIBRIV0000879592, 1 female, glycerol permanent slide.

**Remarks.** The body size of the Korean specimens was 120–125 µm in length (Fig. 5B). The soft body was elongated and compressed laterally. The head was clearly distinguished from the body by a neck fold. The foot was conical in shape, short, and half the length of the toes. The length of the toes was 20–25 µm, less than one-fifth of the total length. The two toes were equal in length and slightly curved dorsally. One red eye was located at the front of the head. The vitellarium was large and contained four nuclei. The large trophi was symmetrical, virgate type B, and had a length of 20 µm (Fig. 6B). The fulcrum was long and straight without expansion at the end. The manubrium was long and crutched, with a bulge in the middle. The uncus had one tooth and was less than half the length of the manubrium. The rami were denticulated.

*Cephalodella gracilis* has been reported to have high morphological variation in the shape of the toes and trophi. The Korean specimen had dorsally curved toes that gradually tapered toward the end. The trophi shape of the Korean specimen did not correspond to a specific specimen but was most similar to that described by Jersabek et al. (2003) in that it had a straight, slender fulcrum without expansion and a crutched manubrium end. However, this species can be regarded as a species complex, based on its morphological diversity and cosmopolitan distribution. Therefore, it is necessary to re-examine it through morphological redescription and molecular analysis.

**Molecular data.** Partial COI sequences were obtained from two Korean specimens (NIBR deposit numbers, NIBRGR0000649741, NIBRGR0000649742; GenBank accession numbers, ON898535, ON898536).

### *Cephalodella tinca* Wulfert, 1937

**Material examined.** Soil from Yeosu-si, Gyeonggi-do, Republic of Korea (37°18.483'N, 127°41.067'E), 26 Sep. 2019, Kyu-Seok Chae leg. NIBRIV0000895434, 1 female, glycerol permanent slide.

**Remarks.** The body was 200–220 µm long, elongated, and laterally compressed (Fig. 5A). The dorsal and ventral margins were slightly bulbous in the lateral view. The

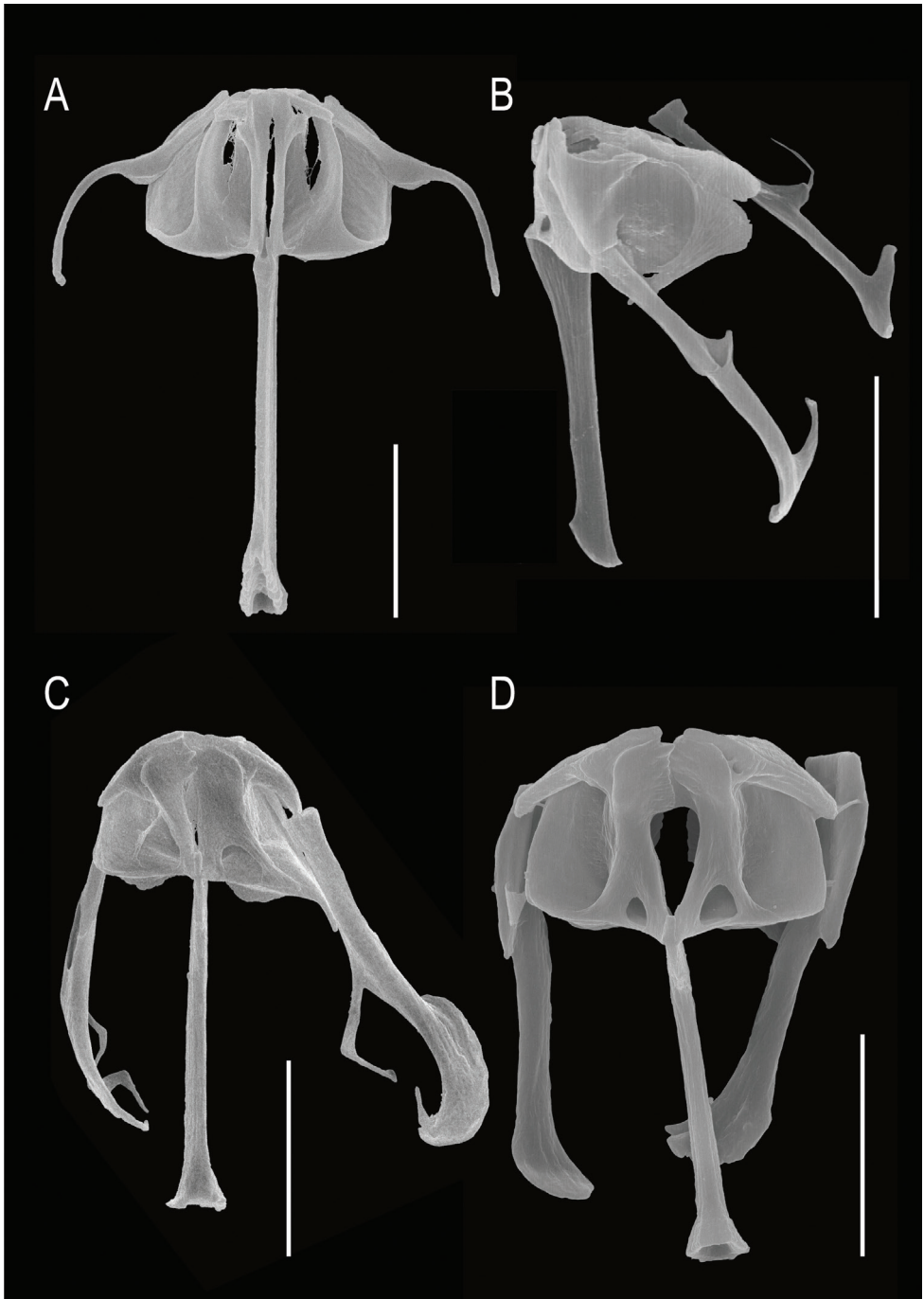


**Figure 6.** SEM image of the trophi of cephalodellid rotifers **A** *Cephalodella auriculata* (Müller, 1773) **B** *C. gracilis* (Ehrenberg, 1830) **C** *C. catellina* (Müller, 1786) **D** *C. tinca* Wulfert, 1937. Scale bars: 10  $\mu\text{m}$ .

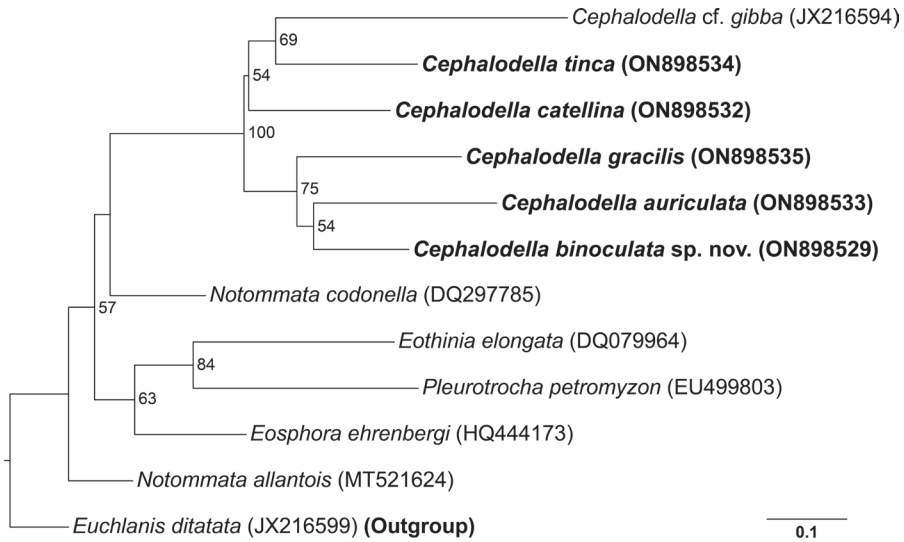


**Figure 7.** Maximum-likelihood (ML) phylogenetic tree based on COI sequences. Numbers on nodes indicate bootstrap value (BV). Only BV over 50% are shown. Scale bar indicates number of nucleotides substitutions per site.

lorica was flexible and transparent. The head was large, approximately one-fourth of the total length, and clearly distinguished from the body by the neck fold. The tail was rounded and as long as the foot. The toes were equal in length, slightly curved dorsally, and approximately one-fourth of the total length. A pair of red eyes was located at the front of the head. The mastax was large and had a salivary gland. The gastric glands were round and contained several granules. The vitellarium was large and had eight nuclei. The trophi was virgate type D, and symmetrical (Fig. 6D). The fulcrum was straight and slightly spatulated at the posterior end. The manubrium was thick and had basal lamellae. The tip of the manubrium expanded and curved inward. The uncus had one large tooth.

Morphological characteristics of Korean *C. tinca* specimens corresponded well to the original description except for the size of body length. The body length of the Korean specimen was 200–220  $\mu\text{m}$ , which was slightly smaller than the original description (260–280  $\mu\text{m}$ ) (Wulfert 1937).

**Molecular data.** Partial COI sequence was obtained from one Korean specimen (NIBR deposit number, NIBRGR0000649740; GenBank accession number, ON898534).

## Acknowledgements

This study was supported by a grant from the National Institute of Biological Resources (NIBR), funded by the Ministry of Environment (MOE) of the Republic of Korea (NIBR202002204, NIBR202102203, NIBR202203204). This study was also supported by Inha University.

## References

- Abràmoff MD, Magalhães PJ, Ram SJ (2004) Image processing with ImageJ. *Biophotonics International* 11(7): 36–42.
- Curini-Galletti M, Artois T, Delogu V, De Smet WH, Fontaneto D, Jondelius U, Leasi F, Martínez A, Meyer-Wachsmuth I, Nilsson KS, Tongiorgi P, Worsaae K, Todaro MA (2012) Patterns of diversity in soft-bodied meiofauna: Dispersal ability and body size matter. *PLoS ONE* 7(3): e33801. <https://doi.org/10.1371/journal.pone.0033801>
- De Smet WH (1998) Preparation of rotifer trophi for light and scanning electron microscopy. *Hydrobiologia* 387(387): 117–121. <https://doi.org/10.1023/A:1017053518665>
- Fischer C, Ahlrichs WH (2011) Revisiting the *Cephalodella* trophi types. *Hydrobiologia* 662(1): 205–209. <https://doi.org/10.1007/s10750-010-0497-z>
- Folmer O, Black M, Hoeh W, Lutz R, Vrijenhoek R (1994) DNA primers for amplification of mitochondrial cytochrome *c* oxidase subunit I from diverse metazoan invertebrates. *Molecular Marine Biology and Biotechnology* 3(5): 294–299.
- Fontaneto D, Rodríguez-Gijón A, Garlaschè G (2021) A survey of Azorean rotifers. *Acoreana* (supplement 11): 79–84.
- García-Morales AE, Elías-Gutiérrez M (2013) DNA barcoding of freshwater Rotifera in Mexico: Evidence of cryptic speciation in common rotifers. *Molecular Ecology Resources* 13(6): 1097–1107. <https://doi.org/10.1111/1755-0998.12080>
- Jersabek CD, Leitner MF (2013) The Rotifer World Catalog. <http://www.rotifera.hausderna-tur.at/> [accessed 23 May 2022]
- Jersabek CD, Segers H, Dingmann BJ (2003) The Frank J. Myers Rotifera collection. The whole collection in digital images. (CD-ROM). The Academy of Natural Sciences of Philadelphia, Special Publication 20.
- Jersabek CD, Weithoff G, Weisse T (2011) *Cephalodella acidophila* n. sp. (Monogononta: Notommatidae), a new rotifer species from highly acidic mining lakes. *Zootaxa* 2939(1): 50–58. <https://doi.org/10.11646/zootaxa.2939.1.2>
- Kalyaanamoorthy S, Minh BQ, Wong TKF, von Haeseler A, Jermiin LS (2017) ModelFinder: Fast model selection for accurate phylogenetic estimates. *Nature Methods* 14(6): 587–589. <https://doi.org/10.1038/nmeth.4285>
- Koste W (1978) Rotatoria. Die Rädertier Mitteleuropas. Ein Bestimmungswerk, begründet von Max Voigt. Überordnung Monogononta. 2. Auflage. I. Textband. Gebrüder Borntraeger, Berlin, Stuttgart, 673 pp.
- Koste W, Shiel RJ (1991) Rotifera from Australian inland waters. VII. Notommatidae (Rotifera: Monogononta). *Transactions of the Royal Society of South Australia* 115(3): 111–159.
- Leray M, Yang JY, Meyer CP, Mills SC, Agudelo N, Ranwez V, Boehm JT, Machida RJ (2013) A new versatile primer set targeting a short fragment of the mitochondrial COI region for metabarcoding metazoan diversity: Application for characterizing coral reef fish gut contents. *Frontiers in Zoology* 10(1): 34. <https://doi.org/10.1186/1742-9994-10-34>
- National Institute of Biological Resources (2022) National species list of Korea. National Institute of Biological Resources, Incheon, Korea. <http://kbr.go.kr/> [accessed 23 May 2022] [in Korean]

- Nguyen LT, Schmidt HA, von Haeseler A, Minh BQ (2015) IQ-TREE: A fast and effective stochastic algorithm for estimating maximum-likelihood phylogenies. *Molecular Biology and Evolution* 32(1): 268–274. <https://doi.org/10.1093/molbev/msu300>
- Nogrody T, Pourriot R (1995) Family Notommatidae. In: Nogrody T, Dumont HJ (Eds) *Guides to the identification of the microinvertebrates of the continental waters of the world. Rotifera. Vol. 3: Notommatidae and Scaridiidae*. SPB Academic Publishing, Amsterdam, 1–229.
- Republic of Korea (2014) Fifth national report. Convention on Biology Diversity, Montreal. <https://www.cbd.int/reports/nr5/>
- Segers H (2007) Annotated checklist of the rotifers (Phylum Rotifera), with notes on nomenclature, taxonomy and distribution. *Zootaxa* 1564(1): 1–104. <https://doi.org/10.11646/zootaxa.1564.1.1>
- Song MO (2014) Eight new records of monogonont and bdelloid rotifers from Korea. *Journal of Species Research* 3(1): 53–62. <https://doi.org/10.12651/JSR.2014.3.1.053>
- Song MO (2018) Five new records of monogonont rotifers from Korea. *Journal of Species Research* 7(4): 333–339.
- Song MO, Jin DH (2000) Rotifer fauna of natal streams of Chum salmon (Oshipcheon). *Journal of Fisheries Science and Technology* 3(2): 71–77.
- Sørensen MV, Giribet G (2006) A modern approach to rotiferan phylogeny: Combining morphological and molecular data. *Molecular Phylogenetics and Evolution* 40(2): 585–608. <https://doi.org/10.1016/j.ympev.2006.04.001>
- Sørensen MV, Sterrer W, Giribet G (2006) Gnathostomulid phylogeny inferred from a combined approach of four molecular loci and morphology. *Cladistics* 22(1): 32–58. <https://doi.org/10.1111/j.1096-0031.2006.00085.x>
- Swanstrom J, Chen K, Castillo K, Barraclough TG, Fontaneto D (2011) Testing for evidence of inefficient selection in bdelloid rotifers: Do sample size and heterogeneity matter? *Hydrobiologia* 662(1): 19–25. <https://doi.org/10.1007/s10750-010-0480-8>
- Tamura K, Stecher G, Kumar S (2021) MEGA 11: Molecular evolutionary genetics analysis version 11. *Molecular Biology and Evolution* 38(7): 3022–3027. <https://doi.org/10.1093/molbev/msab120>
- Turner PN (1986) Some rotifers from Republic of Korea. *Hydrobiologia* 137(1): 3–7. <https://doi.org/10.1007/BF00004166>
- Wulfert K (1937) Beiträge zur Kenntnis der Rädertierfauna Deutschlands. Teil III. *Archiv für Hydrobiologie* 31: 592–635.
- Yamamoto K (1953) Preliminary studies on the rotatorian fauna of Korea. *Pacific Science* 7(2): 151–164.
- Zhang Y, Xu S, Sun C, Dumont H, Han BP (2021) A new set of highly efficient primers for COI amplification in rotifers. *Mitochondrial DNA. Part B, Resources* 6(2): 636–640. <https://doi.org/10.1080/23802359.2021.1878951>

